2001

Mass Transfer of 2,4,6-Trinitrotoluene and Lower Chlorinated Benzenes From Sediment Into Water.

Marti Charleen Blad
Louisiana State University and Agricultural & Mechanical College

INFORMATION TO USERS

This manuscript has been reproduced from the microfilm master. UMI films the text directly from the original or copy submitted. Thus, some thesis and dissertation copies are in typewriter face, while others may be from any type of computer printer.

The quality of this reproduction is dependent upon the quality of the copy submitted. Broken or indistinct print, colored or poor quality illustrations and photographs, print bleedthrough, substandard margins, and improper alignment can adversely affect reproduction.

In the unlikely event that the author did not send UMI a complete manuscript and there are missing pages, these will be noted. Also, if unauthorized copyright material had to be removed, a note will indicate the deletion.

Oversize materials (e.g., maps, drawings, charts) are reproduced by sectioning the original, beginning at the upper left-hand corner and continuing from left to right in equal sections with small overlaps.

Photographs included in the original manuscript have been reproduced xerographically in this copy. Higher quality 6" x 9" black and white photographic prints are available for any photographs or illustrations appearing in this copy for an additional charge. Contact UMI directly to order.

ProQuest Information and Learning
300 North Zeeb Road, Ann Arbor, MI 48106-1346 USA
800-521-0600

MASS TRANSFER OF 2,4,6-TRINITROTOLUENE AND LOWER CHLORINATED BENZENES FROM SEDIMENT INTO WATER

A Dissertation

Submitted to the Graduate Faculty of the
Louisiana State University and
Agricultural and Mechanical College
in partial fulfillment of the
requirements for the degree of
Doctor of Philosophy

in

The Department of Civil and Environmental Engineering

by
Marti Charleen Blad
B.S., St. Mary's College, 1990
M.S., Louisiana State University, 1994
August 2001

DEDICATION

In loving memory of my father, Wayne Allen Blad.

May 13, 1945 - May 30, 2000

ACKNOWLEDGEMENTS

I would like to thank Dr. David Constant for believing in my dream to be an engineer, even though I was a biologist. I appreciate your guidance, encouragement and support on the long path of the dissertation. I am grateful for Dr. K.T. Valsaraj, Dr. Ralph Portier, Dr. Dean Adrian, Dr. John Pardue, Dr. Danny Reible and Dr. Donald Baltz for serving on my committee. Thank you all for your time and imparted knowledge throughout my graduate tenure. Each of you has taught me more than what was in a book and I am appreciative.

I believe it takes a community to raise a child and it took the entire LSU community to produce this Ph.D. There are many people who shaped my experience at LSU and I wish I could list them all. I am grateful to the department of Civil and Environmental Engineering, especially Dr. Macari, Dr. Avent, Janet Labatut, and Jane Crawford. I would like to acknowledge the staff and resources of the HSRC. Thanks to Cheryl Guillory, Nedra Davis Korevec, Margaret Brewer, Chris Schwehm and all of the HSRC student workers. Thank you to Donna Schlotzhauer, Donna Abernathy, Michael Ellis, Jenny Vosburg Hebert, Ben Hebert, Brian Owens, Le Nguyen, Tammy Webb Gray, Nathan Myers, Danielle Domingue, Haley Plaisance, Jason Price, and Melissa Collins. I am grateful to these students who worked in 2226 by my side and endured my learning experience.

I wish to thank the other graduate students who have participated in keeping me sane. The special mentions are Dr. Raghava Kommelapati, Dr. Pradeep Chapfalkar, Dr. Andrew Jackson, Dr. Dean Muirhead, Dr. Henry Lamousin, Dr. Mark Ford, Amy Armstrong, Janet Lippich, Kristi Trail, Beth Hamilton, Denise Rousseau

Ford, Dana Scott, Jonathan Scott, Jonathan Hird, Brian Cunningham, Chad Cristina (extra thanks for the Mathcad help), Sangjin Lee, Jason House, Will Norman, Felipe Martinez, and my office mate, Brent Jones.

I would like to thank Emily Hyfield for the assistance in preparation of this manuscript. I am also grateful for my exercise buddies, Emily Hyfield, Claudia Agnaz, Joy Johnson, Karen Daigle, Manuela Bosschart and Mr. John Drew at the Student Recreational Sports Center for showing me constructive ways to channel stress. I would like to express my gratitude to Dr. Chuck Kulpa and Dr. Ramaraj Boopathy for introducing me to the science of research and starting me on this path.

Most importantly, I want to thank my family. I am grateful and humbled by their continuous encouragement and sacrifices on my behalf. Thank you to my nurturing grandparents, wise parents, loving siblings for supporting my education.

TABLE OF CONTENTS

LIST OF TABLES

LIST OF FIGURES

ABSTRACT

Bioremediation and phytoremediation are in their infancy and this research addresses concerns for application of these technologies. This laboratory and mathematical modeling effort predicts the pollutant flux from soils and sediments to the overlying waters. Little work has been done on transport in surface waters such as the slow moving and stagnant areas of the southern U.S.. Mass transfer is a proposed rate limiting factor for biological transformation when using phytoremediation or natural attenuation. The research quantified mass transport of two different contaminants, TNT and chlorinated benzenes, under different advective conditions.

The TNT study was part of a "riffle-bed reactor" of the TNT leaching unit and the plant catalyzed (hydroponic) reactor. The contaminant flux rates to the biological reactor were quantified for successful use of the riffle bed system. Experimental flux rates were calculated based on overlying bulk water concentrations. Static diffusion flux rates were determined for the TNT system. Different flow regimes were tested to increase leaching efficiency for TNT. The experimental flux rates were compared to published diffusion models for predictability.

The chlorinated benzene site underwent remedial activities including natural attenuation. Initial experiments were performed with a single individual contaminant, chlorobenzene or 1,3 dichlorobenzene. Experiments were also performed utilizing a mixture of: chlorobenzene, 1,2-dichlorobenzene, 1,3-dichlorobenzene, and 1,2,4-trichlorobenzene because natural systems rarely contain one pollutant. The impact of multiple contaminants on desorption and dissolution were quantified via flux rates in dynamic stream systems. The continuous flow regimes followed characteristic

exponential decay while the cyclic flow regime demonstrated spikes of higher flux when the flow rate changed, yielding a higher overall average flux rate. Thus demonstrating the pulsed flow regimes prevented equilibrium conditions thereby increasing leaching efficiency. The core results support the removal of contaminants from sediment due to leaching.

The experimental flux was used to calibrate published diffusion models. Once calibrated, tortuosity and effective diffusivity were determined to be system descriptors. The two descriptors were then validated by comparing flux rates from the slow flow and cyclic flow to model predicted flux rates. Models adequately described and predicted chemical transport based on root mean squared error and correlation coefficient.

CHAPTER 1. BACKGROUND AND LITERATURE REVIEW

1.1. INTRODUCTION

Clean water is essential for human existence. The most important resource to humans is potable water as there is no survival without it. Contamination of both surface waters and ground waters is a chronic problem and a concern of the public. The movement of pollutants needs to be understood and quantified to protect our water resources for the future. Subsurface migration of chemicals detrimentally affects groundwater quality. This means pollutants end up in aquifers and drinking water sources. Once pollutants reach water supplies, then receptor populations can be impacted by the toxicological effects of the chemicals. The degree of adverse impact is dependent on several factors: the particular compounds present, the concentration of the compounds, the persistence of the compounds, and the transport of compounds within and out of environmental compartments, including the biota. Study and quantification of chemical transport is a valid pursuit and an increasing concern.

In 1976, there were 2 million anthropogenic organic compounds and that number is growing at a rate of about 300-500 new formulations annually. It was estimated that up to 1/3 of the total produced synthetic organic compounds eventually enter the biosphere (Freeze and Cherry, 1979). More than 1200 individual anthropogenic substances have been identified in drinking water supplies and that number is increasing as more ground water contamination is investigated (Freeze and Cherry, 1979). For the protection of ground and surface waters, and to mitigate these problems, scientists and engineers must identify the mechanisms by which pollutants can enter groundwater flow systems and develop predictive models for the transport.

These predictive models can only be as accurate as the mathematical descriptions of the process. The equations are based on laboratory or field observations which indicate that multiple and competing chemical reactions impact transport processes of environmental pollutants. Each class of environmental pollutants (petroleum hydrocarbons, pesticides, explosives, or chlorinated solvents for example) have different reactions and mass transfer components to consider.

For effective risk assessment in the active remediation, and for the natural attenuation of contaminants, understanding diffusive and advective mechanisms is critical. The focus here is on primarily two contaminant problems: TNT and lower chlorinated benzenes. Many authors have proposed models (Valsaraj et al., 1996; Choy and Rieble, 2000; Mackay et al., 1996) for static and steady state systems. However, it is the dynamic system that is most often found in both natural and augmented natural systems such as streams and sheet flow (riffle bed) reactors. Both systems exhibit departure from equilibrium due to 1) rainfall events in nature (streams) and 2) the concept of extending this perturbation to reactor systems to enhance flux of contaminants for treatment.

1.1.2 Pump and Treat Technology

At sites where significant levels of ground water contamination exists, pump and treat (P and T) technologies are frequently considered and utilized. Pump and treat technologies can include or combine several remedial methods in a treatment train. One goal of these technologies can be hydraulic containment, which prevents the movement of ground water off site. Another strategy is actual clean up, where the contaminant is pumped to the surface and treated with physical, chemical or biological

systems. One of the limitations of P and T is the long time to achieve acceptable clean up levels. Soil is a complex microcosm composed of multiple organic and inorganic substrates, sething with micro and meso, flora and fauna affecting the local soil conditions. There can be many channels and small pores where contaminants can migrate and be trapped changing it's availability. Pollutants can precipitate or sorb in small or tortuous spaces, then slowly desorb or dissolve in the soil water and ground water as local equilibrium changes. In such cases, the chemicals are not easily removed. This slow sorption/desorption behavior is seen as an asymptotic decrease in contaminant concentration, called tailing. The movement of soluble/mobile contaminants into less permeable zones is a deviation from the theoretical removal rate (U.S.E.P.A., 1990). These desorption processes may be the rate limiting step in transport (Mackay et al., 1996). Pump and treat remediation can be rate limited by desorption of pollutant into bulk water and therefore quantifying the effective diffusivity can be a useful parameter for predictive transport models.

Pump and treat systems can operate at a continuous rate thereby maintaining a hydraulic gradient or it can be pulsed for an efficient extraction at a maximum concentration (U.S.E.P.A., 1990). Switching from continuous to pulsed flow was shown to improve contaminate recovery because the non-pumping time allows for local equilibrium to be reached. When the pump is off, the chemicals can diffuse out of less permeable zones until equilibrium is established. However, mathematical and laboratory models quantifying these dynamic systems in surface soils and sediments are scarce in the literature.

1.1.3 Biological Technologies

Successful biotransformation by landfarming, composting, and engineered bioreactors have remediated both soil and water utilizing microorganisms. The implementation of bioremediation requires the contaminant to be present in the aqueous phase to be accessible. Current research is examining the use of plants as remedial alternatives (Schnoor, 1997, 1996; Gomez, 2000; Jones. 2001, 2000). Phytoremediation is the use of plants for remediation and shows promise for uptake and possible treatment of contaminants. However, the mass transfer limitations of this process require further investigation for phytoremediation to be a widespread technology.

1.2 SOIL PROPERTIES

1.2.1 Tortuosity

Diffusion in saturated sediment is impacted by the texture of the solid media, its porosity and tortuosity (Lerman, 1978). Generally, smaller pore sizes and greater tortuosity decrease diffusional flux. Small pore sizes constrain the random movements of molecules in solution. Tortuosity is the estimate for the winding path between two points within porous material, as opposed to a straight line (Lerman, 1978). The molecule traveled in a straight line when tortuosity equals one. Tortuosity is estimated by using the porosity as shown in equation 1.1.

$$\tau = \varepsilon^{\frac{1}{3}} \qquad (1.1)$$

Therefore, the impeded molecular diffusion is termed effective diffusivity, D_e, to account for the tortuous path the molecule traveled represented by

$$D_e = D_w * \left(\frac{\varepsilon}{\tau}\right) \qquad (1.2)$$

The greater the tortuosity, the slower the molecule traveled, and the smaller the effective diffusivity. Likewise, the smaller tortuosity will yield a higher effective diffusivity indicating the molecule is traveling in a straighter path.

1.2.2 Porosity

Porosity, ε, is the ratio of the pore volume to the total volume which is calculated using the bulk density. Conceptually, porosity is the space not taken by a solid. If a jar is filled with soil, some of the soil pores will be irregularly shaped, small and not easily accessible to flowing water, so the term effective porosity is given to the interstices that are readily available to flowing water. Water saturation is the percent of the total porosity occupied by water. If some spaces are not filled by water, the medium is considered unsaturated. The porosity is an important parameter in saturated soils as pores are assumed filled by water. In reality, the soil matrix contains many cavities of different sizes, shapes, tortuosity, and continuities, which are impossible to characterize. Porosity is one of the model inputs as seen in the retardation factor.

1.2.3 Partition Coefficient

The partition coefficient, K_d, is the equilibrium concentration of a chemical in the soil (mg/kg) divided by the concentration of the chemical in the water (mg/L). This ratio has units of L/kg. If chemicals are strongly sorbed onto the soil matrix, they are less likely to leach off as seen by the soil / water partition coefficient, K_d. Soil

water partition coefficient is dependent on the fraction of organic carbon, f_{oc}, and the organic carbon partition coefficient, K_{oc} by the equation (Watts, 1997):

$$K_{oc} = K_d / f_{oc} \qquad (1.3)$$

K_{oc} is an indicator of how much organic material is present for binding of other organic material. If soil or chemical properties change, then K_d changes.

1.2.4 Particle Size

A key difference between soil and sediment is the particle size composition. Karickhoff et al. (1979) states sediments are eroded soils that are continually re-dispersed and fractionated with the hydrologic cycle. Due to this process, a given system will contain predominately particles of similar size. If contaminant partitioning is highly correlated to particle size, sorption will vary within the sediment and watershed at large. Within a given particle size category, the partition coefficient were directly related to organic carbon content in different sediments. Therefore, the sediment particle size is important in sorption behavior (Deane et al., 1999). Colloids are particle with diameters ranging from 0.001 to 0.45 μm derived from detrital material. Colloids are relatively stable, have the ability to bind hydrophobic organics, and may facilitate the transport of contaminants (Valsaraj et al., 1996). That research proposes advective processes may increase the flux of pollutants due to colloidal releases. The presence of colloids and colloid-sorbed contaminants in supernatant may indicate the measured partition coefficient, K_{pm}, may be different than the true partition coefficient, K_d.

1.2.5 Organic Matter

It has been proposed that the adsorption of pollutants is associated with 1) humic material also called organic matter, 2) clay content, 3) mineral surfaces (Hassett and Anderson, 1979). These materials affect the partitioning between bound and dissolved chemical forms indicating soil properties play an important role in chemical transport. It is known that humic material can be qualitatively and quantitatively impacted by changing oxidation- reduction conditions. Therefore, changing the chemical properties of the humic material may also affect adsorption of hydrophobic organics.

Research indicates organic matter content to be one of the most important soil parameters affecting adsorption (Hassett and Anderson, 1979; Deane et al., 1999). Dissolved organic matter is also an important transport mechanism by increasing solubility of hydrophobic organics (Gauthier et al., 1987; Hassett and Anderson, 1979; Valsaraj et al., 1993). Mackay et al. (1996) indicates the high organic carbon soil had a slower loss of chlorobenzene than the low organic carbon soil. Depending on the origin of the humic material, K_{oc} varies by as much as one order of magnitude (Gauthier et al., 1987). Valsaraj et al. proposes a mathematical model to describe transport of colloids with high organic properties (1993). Gauthier et al., (1987) states the "quality" of the carbon in the sorbent should be considered such as aromaticity. He points out there are many equations relating K_{oc} with K_{ow} suggesting that some other parameter is missing. Like in many other investigations, the prediction of partition coefficients is on the basis of solubility or octanol/water partition coefficients in this study (Jepsen and Lick, 1999).

1.2.6 Mineral Surfaces

Mineral surfaces are involved in sorption along with organic matter. Valsaraj et al., (1999) proposes a 2 phase model to determine the contributions of both the organic carbon and mineral matter. Mayer (1994) supports a monolayer of organic carbon (OC) adsorbed on mineral surfaces and proposes the "monolayer equivalent" zone to explain the relationship between OC concentrations and surface area in sediments from continental shelf regions located away from major sediment- carrying rivers like the Mississippi. McCarthy and Zachara (1989) found the detrital colloidal material a function of the mineral composition as well as the depositional environment. Research has also indicated in soils with low organic matter content, oxalate extractable Mn and Ca may play a significant role in adsorption. The soil has binding sites on both the organic portion and the mineral portion, although, depending on concentration, one or the other may be controlling.

Environmental modeling efforts are widespread and are increasing our understanding of how chemicals are transported and their fates. Models incorporate both chemical and soil properties in an attempt to describe transport of chemicals, specifically from sediment to the overlying water column. Mackay et al. (1996) present the equilibrium criterion evaluative model (EQC) and uses chlorobenzene as example. Currently models are being developed for sediment quality criteria (SQC) for use in determining "how clean is clean". The pollutant concentration in water is a consequence of the concentration in the sediment. The U.S.E.P.A.'s sediment quality criteria (SQC) are calculated as:

$$SQC = f_{oc} * K_{oc} * FCV \qquad (1.4)$$

where f_{oc} is the fraction of organic carbon, K_{oc} is the organic carbon partition coefficient and FCV is the final chronic water quality criteria values assuming equilibrium partitioning (McGroddy and Farrington, 1995). The final chronic water quality criteria values (FCVs) were chosen so as to not detrimentally impact receptor populations.

Thus, many factors are involved in pollutant transport, most notably the soil properties and the chemical properties. McGroddy and Farrington (1995) state clearly " the mobility and bioavailabilty of organic contaminants associated with sediment beds depend on the concentration of these compounds in the porewater."

1.3 CHEMICAL PROPERTIES

Knowledge of the chemical properties of the pollutants are required for an understanding of their migration. Chemical structure determines chemical behavior such as 1) aqueous solubility, 2) Henry's law constant, 3) density, 4) K_{ow}, 5) K_{oc}, 6) biodegradability (U.S.E.P.A., 1990). Usually high aqueous solubility indicates decreased sorption; Henry's coefficient is important for volatilization in dilute solutions; the density of chemical in relation to water indicates how it will behave once it contacts the water table. If the chemical is denser than water, e.g., dichlorobenzene, it will sink in the water column and spread along bottom if not miscible. Hydrophobic partitioning will predominate if the pollutants have a high octanol water partition coefficient, K_{ow}. Chemicals with large octanol-water partition coefficients by their nature stay sorbed onto soil organic matter (Deane et al., 1999).

1.3.1 Age of Contaminant

The impact of aging on pollutant removal can be significant in terms of transport and bioavailability. Hatzinger and Alexander (1995) indicate pollutants may become progressively less toxic with time due to the aging. They present evidence that the chemical is initially rapidly sorbed to the surface, then over time the available fraction decreases as molecules are sequestered inside the particle, in internal micropores. This concept is important for risk assessment purposes. The age of the contaminant on the soil influences the extractable fraction, and therefore the bioavailable fraction. In these cases, not all of a contaminant is available for diffusion.

1.3.2 Retardation Factor

The retardation factor can be defined as the amount by which the contaminant is held back by the soil in comparison to the groundwater velocity. That is, how much the flow of one compound is "retarded" compared to flow of the ground water. Chemicals sorbed to soils are either slowly exchanged by diffusion with flowing water in large pores or migrate at slower velocities found in smaller pores (U.S.E.P.A., 1990). This retardation of movement is relative to the movement of ground water and quantified by a retardation factor, R_f, which is a function of porosity, partitioning and bulk density as:

$$R_f = \varepsilon + K_d * \rho_b \qquad (1.5)$$

where ε is the porosity, K_d is the partition coefficient, and ρ_b is the bulk density (Valsaraj et al., 1998). Consequently, the retardation factor is an important modeling descriptor, as this term incorporates both chemical properties and soil properties.

Currently models are being developed for sediment quality criteria (SQC) which are tools used for determining "how clean is clean" in natural systems. The pollutant concentration in water is frequently a consequence of the concentration in the sediment. Pore water concentration, C_{pw}, is assumed to be dependent on the sediment concentration, W, and the K_d as:

$$C_{pw} = W / K_d \qquad (1.6)$$

Some chemical species, like phosphate and ammonia, are generated in the sediments and not totally removed by diffusion because the sediment particles may sorb these compounds as they migrate (Lerman, 1978). Soil properties affect sorption processes which may increase bioavailability and/or mobility. Environmental impact models assume the leached concentration to be the bioavailable fraction.

1.4 THEORY

1.4.1 Advection - Dispersion Equation

One of the fundamental principles in environmental engineering is the mass balance concept. This concept can be explained by using a control volume and examining what goes into and out of a delineated volume. This theory is validated by the Conservation of Matter – since matter is not created or destroyed in typical systems. In other words, what goes in must come out and if not, then the difference has to be explained by a reaction or an accumulation in the delineated volume. The movement of mass through the control volume is termed flux has units of mg/cm^2*hr. Transport into and out of the control volume is principally due to two phenomena: advection and dispersion. Advection is best understood as the bulk transport mechanism or the flow of fluid through the control volume. Advection usually has

one predominate direction in systems such as shallow rivers or ground water. The observed spreading and dilution of a solute plume as it passes through soils in generally termed dispersion. Dispersion can be subdivided into mechanical dispersion and molecular diffusion. The mechanical dispersion is movement around the media or due to turbulence. Dispersion is the tortuous path a molecule may take through the subsurface or around other molecules. On the other hand, molecular diffusion is due to the Brownian movement of molecules from a high concentration to a lower one. Molecular diffusion is a slow process due to its dependence on the random movement of molecules (Lerman, 1978). Molecular transport of all chemical species across the sediment water interface is due to the concentration differences that develop on the two sides of the interface. It is this increase or decrease in concentration in the pore water compared to the overlying water which establishes the gradient for diffusional flux, ($\partial C/\partial x$), as seen in Fick's First Law (Lerman, 1978). Diffusion as a random process can be modeled using statistical approaches (Karni and Bar-Ziv, 1991).

1.4.2 Adsorption and Desorption

Soils and surface sediments are by their nature heterogeneous and make understanding the impact of changes in soil properties difficult. In the environment, one of the controlling factors in determining the fate of pollutants is the adsorption and desorption of chemicals from soils and sediments. Adsorption is the accumulation of solutes at an interface and is considered to be reversible (McGrath, 1995). At residual concentrations, reversibility is lost with the isotherms exhibiting a fast and slowly desorbed fraction (Valsaraj et al., 1999). The opposite of adsorption is desorption; meaning mass is released back into the environment. Adsorption is the main

mechanism retarding contaminants from moving into surface water and aquifer systems from the land surface/subsurface. Desorption determines the concentration to which receptor populations are exposed and provides a measure of bioavailability. Adsorption and desorption are key to chemical movement and successful remediation strategies when contaminants are bound to particles in a matrix.

Generally, for any reactions to take place the chemical must be in the aqueous phase and this preliminary step is controlled by desorption and dissolution rates of the pollutant. In risk assessment, the risk is directly related to the concentrations to which sensitive receptor organisms are exposed. Natural attenuation and bio-kinetic models require input of the pollutant's concentration, that to which the microorganisms are exposed. Current research is examining the capability of plants to catalyze degradation or attenuate migration, but again, requires uptake of contaminants from an aqueous environment. The presented laboratory and mathematical modeling is an effort to predict the pollutant concentrations leaching off of soil and sediments to the overlying water which would then be fed into plant reactor systems. Modeling is a cost effective and valuable tool to evaluate the complex and changing parameters inherent in the remediation of hazardous site. The advantage of models is the ease of changing input values to determine the ramifications and the ability to identify which parameters have the most impact on the system in question.

Multiple sorption mechanisms may be involved in natural systems due to the plethora of possible substrates such as humic material, organic and inorganic colloids, metal-oxyhydroxides, and microbial mucopolysaccharides (McCarty and Zachara, 1989; McGrath, 1995). Transport and sorption behavior is also affected by soil

processes: plant exudates, bioturbation, mycorrhizal enzymes and many abiotic reactions. Bioturbation (movement of meso and meiofauna in sediments) has been shown to increase hydrocarbon flux rates by decreasing diffusion paths (Reible et al., 1991; Thibodeaux, 1996).

The systems in this study is predominately composed solely of surface sediments and water, thereby invoking the assumption of saturated media. Molecular diffusion through isotropic media can be then described by Fick's law:

$$\text{Flux} = - D_{AB} * A * (\partial C / \partial x) \qquad (1.7)$$

where D_{AB} is the molecular diffusivity of chemical A, in solution B. For steady state conditions, the derivative may be replaced by a finite change in concentration along a finite distance of the change. The steady state situation allows D_{AB} to be calculated. This is in the ideal situation of one chemical in a dilute solution. Dispersion coefficients are the sum of both the mechanical dispersion coefficient and the molecular diffusion coefficient if both are present and relevant. Generally, dispersion flux rates are one or more orders of magnitude smaller than the advection flux rates. The mass balance equation can be described verbally as rate of mass (M) accumulating within a control volume being equal to the flux (F) of mass into the system minus the flux of mass out of the system ± any reactions, sinks or sources inside the system. Based on the Principle of Conservation of Mass, this can be shown in the equation:

$$\partial M / \partial t = \partial F_x / \partial x + \partial F_y / \partial y + \partial F_z / \partial z \pm \text{Rxns} \qquad (1.8)$$

where x,y, and z indicate direction. While transformation reactions may take place inside the system, as seen by the +/- reaction (Rxns) term, they are not considered

here. Fick's Second Law describes the changing concentration with respect to time along the x axis due to diffusion and is frequently written as:

$$(\partial C/\partial t) = D\,[\partial^2 C/\partial x^2] \qquad (1.9)$$

Simplifying equation 1.8 to only one direction and substituting in equation 1.7 yields the advection-dispersion equation. The advection-dispersion equation, which describes how the concentration in the control volume is changing over time, is commonly written as:

$$\partial C/\partial t = D\,(\partial^2 C/\partial x^2) - v\,(\partial C/\partial x) \qquad (1.10)$$

where x indicates direction, C is again concentration of chemical, v is velocity and, D is the diffusivity of the chemical. The negative sign is used to indicate direction or the movement. The first term describes pollutant movement due to diffusion whereas the second term addresses the advection component. For subsurface systems there is a retardation factor, as discussed previously, seen in the advection-dispersion equation below:

$$\partial C/\partial t = D_e/R_f * (\partial^2 C/\partial x^2) - v/R_f * (\partial C/\partial x) \qquad (1.11)$$

The effective diffusivity, D_e, (Welty, et al., 1984; Choy and Reible, 2000) may be estimated by using the diffusivity of the compound in water (D_w) and the porosity (ε) as:

$$D_e = D_w * \varepsilon^{(4/3)} \qquad (1.12)$$

Diffusion is slowed by the partitioning from pore wall to pore water and the tortuous path from the soil particle surface (Hatzinger and Alexander, 1995). If there is no flow, then the second term of the advection dispersion equation is deleted and transport is solely due to diffusion.

1.4.3 Water Side Mass Transfer Coefficient

Film theory describes transport by the presence of a thin film surrounding particles or surfaces. This film creates resistance to mass transport and can be modeled as the water side mass transfer resistance in aqueous systems. The soil side mass transfer resistance comes from the tortuous path molecules take to get to or from a sorption site within the soil particle. The internal movement at the interface of soil particle pore and pore water is described by the equilibrium partition coefficient, K_d, which was discussed earlier.

1.4.4 Surface Mass Transfer Coefficient

In an attempt to separate processes, both the water and the soil may present a resistance to transport. The soil side mass transfer resistance comes from the tortuous path molecules take to get to or from a sorption site within the soil particle. This can be approximated from boundary layer theory in the laminar flow range as:

$$K_a = 0.664 * R_e^{0.5} * S_c^{1/3} * (D_w / H_z) \qquad (1.13)$$

where R_e is the Reynolds number, S_c is the Schmidt number, D_w is the diffusivity of the chemical in water, and H_z is the depth of the contaminated layer. In a sensitivity analysis, Mackay et al. (1996) indicates the mass transfer coefficients "profoundly affect the source concentration in the water".

1.4.5 Overall Mass Transfer Coefficient

The overall mass transfer coefficient takes into account both resistances, water side and soil side mass transfer resistances. Resistances in series are summed. The following equation is proposed for determining the overall mass transfer coefficient:

$$1/K_L = 1/k + 1/(D_e * R_f/\pi * t)^{1/2} \qquad (1.14)$$

where K_L is the overall mass transfer coefficient, k is the water side resistance, D_e is effective diffusivity, R_f is the retardation factor, and t is time (Valsaraj et al., 1996). An overall mass transfer coefficient, K_L, is frequently used when all the individual processes are lumped into one parameter. This can be seen in the differential equation describing the change in water concentration with time as:

$$\frac{dC}{dt} = K_L * (C_{pw} - C_s) \qquad (1.15)$$

where C_{pw} term describes the pore water concentration, and C_s describes the water saturation concentration. The second term is the driving force or the concentration gradient driving diffusion. These lumped parameters are useful when all the internal resistances cannot be quantified or when pore water concentrations cannot be measured separately. The bulk water concentration is used for U.S.E.P.A.'s sediment quality criteria to determine clean up endpoints. In the lab, it is possible to measure bulk water concentration but difficult to measure pore water, although pore water is what drives the transport equation (C_b - C_{pw}).

1.4.6 Model Development

Integration of the advection dispersion equation can be found in a number of transport phenomena texts and will not be necessary in this study. Solving the advection dispersion equation requires an understanding of boundary conditions present in the modeled system. Assumptions for the model in this study include constant density of the media, constant viscosity of the fluid phase, incompressible flow, and isotropic and saturated media. The advectively enhanced diffusion models employed assumes a finite layer of sediment in contact with the overlying water.

Finite indicates that the contaminant is depleted over time in the z direction. Semi-infinite means the processes occurring far below the sediment water interface do not affect the fluxes at the interface during the short time scale of the experiment. The infinite assumption dictates that the processes at the interface or near the sediment surface never impact the concentration far below the sediment interface (at $z = \infty$) (Lerman, 1978; Welty et al., 1984). Simple diffusion in a semi-infinite is utilized to see baseline diffusion values for the nitroaromatic studies.

It is also assumed that adsorption is linear, i.e., $S=K_d*C$, where S is adsorbed concentration, C is the aqueous concentration and K_d is the partition coefficient. This is an ideal sorption model. Traditional ground water models employ local equilibrium assumption (LEA). This means that flow past the particle is slow relative to any transport at the particle such as desorption/dissolution. The linear isotherm is based on 1) sorption is reversible, 2) system at equilibrium, 3) K_d is independent of concentration, 4) each solute adsorbs independently, and 5) the reactions are fast (McGrath, 1995; Deane et al., 1999). Historically, sorption rates were thought to be fast so that the assumption of equilibrium was valid. Recent work proposes sorption rates may be slow and the equilibrium times may be weeks depending on the hydrophobicity of the organic chemical, the size of the suspended particles/floc, and the amount of organic matter in the sediment (Deane et al., 1999, Tye et al., 1999).

These assumptions may not be valid in all cases, but will be considered applicable in modeling the SFLB. Deane et al. (1999) points out that hydrophobic organic chemicals (HOCs) exhibit slow equilibrium times and sorption rates. Invoking the LEA simplifies the mathematical description but tends to underestimate

cleanup times (McGrath, 1995). However, laboratory experiments help to calibrate models for specific sites and situations. Since these processes are so complex, an estimate of the effective diffusivity and/or mass transfer coefficient are lumped parameters. The effective diffusivities presented in Valsaraj et al. (1998) indicate the mass transfer may be rate limiting in applied biological systems.

1.4.7 System Being Evaluated

This dissertation analyzes diffusive transport of two classes of contaminants in a laboratory soil system to simulate natural processes. A static bed and a sheet flow leaching bed (SFLB) were used to investigate transport from sediment to the water column and to validate a simple diffusion and an advective enhanced diffusion vignette models with experimental results utilizing Mathcad ® to obtain a solution. The research compares the appropriate advection dispersion solution to experimental fluxes for two different chemical classes: explosives and chlorinated benzenes. The explosives containing soil were field aged whereas the chlorinated benzene studies utilized lab contaminated sediments. This study examines diffusive mass transfer in a quiescent or static system first, then in a sheet flow leaching bed (SFLB), which is advectively enhanced. The effect of different flow regimes on the transport of chemicals was assessed by quantifying the flux of contaminants and deriving the effective diffusivity.

Since both the soil and water can contribute resistance to the transport, the controlling resistance may depend on the contaminant load present on the soil / sediment or the water solubility of the contaminant. Quantification of chemical movement was done by determination of pollutant flux rates. The SFLB effluent

concentrations were used to calculate the flux rate of contaminant at the soil-water interface. The experimentally calculated flux was fitted to the solution for the advection dispersion equation using Mathcad® to determine the effective diffusivity (Choy and Reible, 2000).

1.5 CURRENT RESEARCH RATIONALE

The following studies examine mass transport of two different contaminants, under different flow conditions. The TNT study was part of a larger project to validate the feasibility of a unique, low cost, two-stage reactor system. This design was called a riffle-bed reactor and was proposed for TNT remediation as an alternative to conventional extraction beds. As stated, the riffle-bed is composed on two parts; the first is a TNT leaching unit and the other is a plant catalyzed (hydroponic) reactor. The research examines diffusion flux rates for TNT from a bed of site soil. Experimental flux rates were calculated based on concentrations in the overlying bulk water. The experimental flux rates were compared to diffusion models using the commercially available program, Mathcad®. Using this model, the effective diffusivity will be used to quantify pollutant movement in different soils under quiescent conditions. The diffusion studies described herein utilize previously described models to fit experimental data. Once baseline diffusion rates were known, the preliminary leaching experiments began. The overall thrust was to match contaminant flux rates to the biological reaction rates to optimize the riffle bed reactor system.

The second study was also part of a larger study evaluating chlorinated solvent remediation in steam sediment and wetland areas. The initial experiments were performed with a single individual contaminant, chlorobenzene and 1,3

dichlorobenzene, in order to better understand the transport of a single compound in the environment. Because natural systems rarely contain one pollutant, later experiments were performed utilizing a mixture of four components: chlorobenzene (MCB), 1,2-dichlorobenzene (1,2-DCB), 1,3-dichlorobenzene (1,3-DCB), and 1,2,4-trichlorobenzene (TCB). One aspect of the chlorinated benzene studies was the impact of multiple contaminants on desorption and dissolution via flux rates in a dynamic stream system. Experimental data from the aqueous phase were fitted to a previously described model (Choy and Reible, 2000) in order to determine the effective diffusivity utilizing Mathcad®. The effective diffusivity (D_e) here is a lumped parameter to describe the transport of lower chlorinated benzenes.

Initially, the TNT study investigated transport in a man-made reactor system. As knowledge was gained on the system, and project work was completed, the remedial work evolved to natural processes due, in many cases, to high cost of very active remediation at sites. Thus, the active remedial TNT effort was redirected to toward natural remedies for chlorinated benzene contaminants. Similar models and methods were utilized in the chlorinated benzene study to quantify flux rates and determine the effective diffusivity.

This work investigates the applicability of published models to predict flux rates of chemicals in two different systems. It is hypothesized here that in the dynamic SFLB system, the flux observed in cyclic flow regime will yield a higher flux than expected from either low or high flow rates due to displacement from equilibrium. Also, the input of mixtures on such systems is thought to increase mobility of the contaminants due to changes in partitioning when compared to single component

systems and will be examined. Herein, all experiments are conducted in saturated porous media for modeling purposes. Local equilibrium between the sediment and pore water is assumed.

1.6 REFERENCES

Choy, Bruce and Danny D. Reible. 2000. Diffusion Models of Environmental Transport. Lewis Publishers, Boca Raton, Fl.

Deane, G., Z. Chroneer, and W. Lick. 1999. Diffusion and Sorption of Hexachlorobenzene in Sediments and Saturated Soils. Journal of Environmental Engineering, Vol. 125, No. 8., 689-696.

Freeze, R.A. and J.A. Cherry. 1979. Groundwater. Prentice-Hall, Inc., Englewood Cliffs, NJ.

Gauthier, T.D., W.R. Seltz, and C.L. Grant. 1987. Effects of Structural and Compositional Variations of Dissolved Humic Materials on Pyrene K_{oc} Values. Environmental Science and Technology Vol. 21, No. 3, 243-248.

Gomez, Caesar. 2000. Personal Communication.

Hassett, J.P., and M.A. Anderson. 1979. Association of Hydrophobic Organic Compounds with Dissolved Organic Matter in Aquatic Systems. Environmental Science and Technology Vol. 13, No. 12, 1526-1529.

Hatzinger, Paul B., and M. Alexander. 1995. Effect of Aging of Chemicals in Soil on Their Biodefradability and Extractability. Environmental Science and Technology 29, (2): 537-545.

Jepsen, R. and W. Lick. 1999. Nonlinear and Interactive effects in the Sorption of Hydrophobic Organic Chemicals by Sediments. Environmental Toxicology and Chemistry, Vol. 18, No. 8, 1627-1636.

Jones, P.B. 2000. Personal communication.

Jones, P.B. 2001. Phytobuffering of Lower Chlorinate Benzene Contamination via Willows at the PPI Superfund Site: Laboratory and model results. (In Press)

Karickhoff, S.W., D.S. Brown, T.A. Scott. 1979. Sorption of Hydrophobic Pollutants on Natural Sediments. Water Research 13: 241-248.

Karni, Y. and E. Bar-Ziv. 1991. Stochastic Coalescence – Redispersion Model for Molecular Diffusion and Chemical Reactions. 1. Methodology. The Journal of Physical Chemistry Vol. 95, No. 8, 3012-3016.

Lerman, A. 1978. Chemical Exchange Across Sediment-Water Interface. Annual Review Earth Planet Science 6:281-303.

Mackay D., A. Di Guardo, S. Paterson, G. Kicsi, D.E. Dowan, and D.M. Kane. 1996. Assessment of Chemical Fate in the Environment Using Evaluative, Regional and Local-scale Models: Illustrative Application to Chlorobenzene and Linear Alkylbenzene Sulfonates. Environmental Toxicology and Chemistry vol. 15 no. 9, 1638-1648.

Mayer, Lawrence M. 1994. Relationships Between Mineral Surfaces and Organic Carbon Concentrations in Soils and Sediments. Chemical Geology 114:347-363.

McCarthy, J.F., and J.M. Zachara. 1989. Subsurface Transport of Contaminants: Mobile Colloids in the Subsurface Environment May Alter the Transport of Contaminants. Environmental Science and Technology Vol. 23, No. 5, 496-502.

McGrath, C. J. 1995. Review of Formulations for Processes Affecting the Subsurface Transport of Explosives. Technical Report IRRP-95-2, U.S. Army Engineer Waterways Experimental Station, Vicksburg, MS.

McGroddy S.E., and J.W. Farrington. 1995. Sediment Porewater Partitioning of Polycyclic Aromatic Hydrocarbons in Three Cores from Boston Harbor, Massachusetts. Environmental Science and Technology Vol. 29, No. 6, 1542-1550.

Reible, D.D., K.T. Valsaraj, and L.J. Thibodeaux. 1991. Chemodynamic Models of Contaminant Transport from Bed Sediments. In *The Handbook of Envrionmental Chemistr, Vol. 2.* [Ed] O. Hutzinger. Springer-Verlag, Germany.

Schnoor, J.L. 1996. Environmental Modeling: Fate and Transport of Pollutants in Water, Air and Soil. John Wiley and Sons, Inc. New York, New York.

Schnoor, J.L. 1997. Phytoremediation. Ground-Water Remediation Technologies Analysis Center (GWRTAC) Technology Evaluation Report TE-98-01. Pittsburgh, PA.

Thibodeauz, Louis, J. 1996. Environmental Chemodynamics: Movement of chemicals in Air, Water, and Soil. John Wiley and Sons, Inc. New York, New York.

Tye, R., R. Jepsen and W. Lick. 1996. Effects of colloids, Flocculation, Particle Size, and Organic Matter on the Adsorption of Hexachlorobenzene to Sediments. Environmental Toxicology and Chemistry, Vol. 15, No. 5, 643-651.

U.S.E.P.A. 1990. Basics of Pump-andTreat Ground-Water Remediation Technology, EPA-600/8-90/003. Mercer, J.W., D.C. Skipp and D.Giffin. Robert S. Kerr. Environmental Research Laboratory, Ada, OK.

Valsaraj, K.T., R.R. Kommalapati, E.D. Robertson, and W.D. Constant. 1999. Partition Constants and Adsorption/Desorption Hysteresis for Volatile Organic Compounds on Soil from a Louisiana Superfund Site. Environmental Monitoring and Assessment 58: 225-241.

Valsaraj, K.T., K.M. Qaisi, W.D. Constant, L.J. Thibodeaux, and K.S. Ro. 1998. Diffusive Transport of 2,4,6-trinitrotoluene (TNT) from Contaminated Soil to Overlying water. Journal of Hazardous Materials 59: 1-12.

Valsaraj, K.T., S. Verma, I. Sojitra, D.D. Reible and L.J. Thibodeaux. 1996. Diffusive Transport of Organic Colloids from Sediment Beds. Journal of Environmental Engineering Vol. 122, No. 8, 722-729.

Valsaraj, K.T., G.J. Thoma, C.L. Porter, D.D. Reible and L.J. Thibodeaux. 1993. Transport of Dissolved Organic Carbon-derived Natural Colloids from Bed Sediments to Overlying Water: Laboratory Simulations. Water Science and Technology Vol. 28, No. 8-9, 139-147.

Watts, Richard, J. 1997. Hazardous Wastes: Sources, Pathways, Receptors. John Wiley and Sons, Inc. New York, New York.

Welty, J.R., C.E. Wicks, and R. E. Wilson. 1984. Fundamentals of Momentum, Heat, and Mass Transfer. Third edition. John Wiley and Sons, Inc. New York, New York.

CHAPTER 2. 2,4,6-TRINITROTOLUENE (TNT) DIFFUSION STUDIES

2.1 INTRODUCTION

2.1.1 Scope of Problem

There have been numerous sites contaminated with munitions from the early forties to the seventies. Explosives, and 2,4,6-trinitrotoluene (TNT) specifically, have contaminated soils from a variety of sources such as packing or warehouse facilities, solid waste destruction facilities and production facilities (McGrath, 1995). Ground water contamination has been primarily due to wastewater lagoons and leach pits at these aforementioned facilities (McGrath, 1995; Kaplan and Kaplan, 1982). Although 2,4,6-trinitrotoluene is historically the most widely used high explosive, other isomers are formed during production but are undesirable and removed, contributing to the waste problem. The dinitro isomers are also commonly found in wastes. The pollutant source is a mixture of crystalline and microcrystalline explosives. These crystals are unintentionally released to the soil during normal operations. The packing of explosives required large volumes of water for washing explosives from the shells which was then stored in lagoons on site. (McGrath, 1995; U.S. Army, 1994). Other explosives, Hexahydro-1,3,5-trinitro-1,3,5-triazine (RDX) and octahydro-1,3,5,7-tetranitro-1,3,5,7-tetrazocine (HMX) are also present at many sites but have such low water solubilities that they were not seen at concentrations as high as TNT. Other TNT related compounds, which are typically present or tested for include; 1,3,5-trinitrobenzene, 1,3-dinitrobenzene, 2-amino-4,6-dinitrotoluene, 4-amino-2,6-dinitrotoluene, and N,2,4,6-tetranitro-N-methylaniline (Tetryl).

2.1.2 Objective

The goal of this research is to quantify diffusion flux rates of TNT from a bed of soil obtained from a contaminated site. Experimental flux rates were calculated based on concentrations in the overlying water. The TNT diffusion studies were aimed at modeling flux rates for input to plant bioreactor systems. Baseline diffusion rates from quiescent saturated beds were determined first. Enhancement by advection could then be assessed in the dynamic bed studies. The experimental flux rates were compared to diffusion models using the commercially available software program called Mathcad®. The model is derived from the advection dispersion equation using a semi-infinite assumption with no advection term. The diffusion studies described herein utilize previously described models to fit experimental data. Using this approach, the effective diffusivity was used to quantify pollutant movement in different soils. The effective diffusivity was iteratively calculated by setting the sum squared error (SSE) equal to zero in the Mathcad® program. Correlation coefficients can be returned by the program's ability to linearize the data and will be shown to indicate goodness of fit for experimental data to model. The flux of TNT from site soils will be compared to degradation rates in a related study to determine the rate limiting processes for phytoremediation.

2.1.3 Riffle Bed Reactor for TNT Bioremediation

The following study was part of a larger project to validate the feasibility of a unique, low cost, two stage reactor system. This design is called a "riffle-bed reactor" and was proposed for TNT remediation as an alternative to conventional extraction beds (Qaisi et al., 1996a; Qaisi et al., 1996b; Valsaraj et al., 1998). The riffle-bed is

composed on two parts; the first is a TNT leaching unit and the other is a plant catalyzed (hydroponic) reactor. The field leaching bed contains the TNT contaminated material and water is sprayed onto the soil bed. The water will flow over and through the bed picking up contaminants flowing into the plant pool where the degradation reactions occur. The treated pool water can then be recycled continuously or intermittently as reaction rates dictate (Qaisi et al., 1996). Experiments were designed to imitate the first part of the reactor when contaminants are leached from soil into water.

2.1.4 Chemicals

Many of the explosive pollutants are nitro aromatics or nitroamides with methyl and nitro functional groups. These compounds have fairly low molecular weights, ranging from 168 g/mol for dinitrobenzene to 296 g/mol for HMX. The positions of the nitro groups were reported to affect biotransformation. The para position is most susceptible to degradation whereas the meta positions are the most stable (Chou and Spanggord, 1981). Nitroaromatics are considered to be recalcitrant as indicated by their continued presence at field sites. Table 2.1 shows the relevant physical and chemical properties for TNT.

2.1.5 Toxicity/Health

TNT has been shown to cause liver damage and anemia in humans and animals (Sax, 1963; Dilley et al., 1982). Kaplan and Kaplan (1982) indicated TNT is mutagenic in the Ames assay. Won et al. (1976) indicated TNT is highly toxic to freshwater unicellular green algae, tidepool copepods, and oyster larvae. Intense TNT exposure can result in pancytopenia, which is a decrease in platelets, reticulocytes and

Table 2.1. TNT physical and chemical properties

Parameter	Value	Reference
CAS RN	118-96-7	CRC Handbook
Empirical formula	$C_7H_5N_3O_6$	CRC Handbook
Molecular Mass	227.13 g/mol	CRC Handbook
Henry's Law constant, K_h	$1.1E^{-8}$ $atm*m^3*mol^{-1}$	Rosenblatt et al. (1989)
Density	1.654 $g*cm^{-3}$	CRC Handbook
Melting Point	80.1 C	CRC Handbook
Solubility (25C)	100 mg/L 85 mg/L 150 mg/L	Merck (1983), Venogopal, (1996), Ro et al. (1996) Urbanski (1964)
EPA Drinking water Standard	0.020 mg/L	Rosenblatt et al. 1989
Octanol-Water Partition Coeffiecient, log K_{ow}	1.86 2.06	Jenkins (1989) Rosenblatt et al. (1989)
Organic Carbon Partition Coefficient, log K_{oc}	2.72	Rosenblatt (1986)
Soil-Water Partition Coefficient, K_d	53 +\- 20 ml/g 2-12 L/kg 2.91 L/kg	Chou and Spanggord (1981) Pennington (1988) Valsaraj et al. (1998)
Diffusion coefficient (25C)	6.71 E^{-6} cm/s	Rosenblatt et al. (1989)
Toxicity	Possible human carcinogen	Rosenblatt et al. (1989

leukocytes (blood elements) due to damage to bone marrow (Caserett and Doull, 1991). Based on limited data, TNT has been classified as a possible human carcinogen (Gordon and Hartley, 1989). Nitroaromatic compounds are problematic due to these aforementioned health effects.

2.1.6 Biological Transformation

Microbial transformation of nitroaromatic compounds has been fairly well studied although mineralization to CO_2 is rarely observed (McCormick et al., 1976; Funk et al., 1993; Boopathy et al., 1993; Boopathy et al., 1994; Bradley et al., 1994). The major microbial metabolites of a pseudomonad – like organism were found to be nontoxic and non-mutagenic indicating their potential use in bioremediation as a safe clean up alternative for TNT contaminated sites (Manning et al., 1995; Manning et al., 1996). Other types of bacteria and fungi are capable of degrading TNT and its related products (dinitrotoluenes) to triaminotoluene (TAT). Fungi are reported to perform ring cleavage but reports of biological reductive deamination are scarce (Spiker et al., 1992; Fernando et al., 1990). Aquatic plants have shown promise of TNT biotransformation capabilities and may other plants have demonstrated successful treatment of a variety of pollutants (Pavlosthasis et al., 1998; Bhadra et al., 1999; Schnoor, 1996, 1997; Gomez, 2000; Jones, 2000). The success of any bioremediation plan is dependent on the contaminant being present in the aqueous phase so it can be acquired or accessed by the necessary microbes. Phytoremediation may be dependent on desorption and diffusion limitations.

2.2 SITE HISTORY

The Alabama Army Ammunition Plant (AAAP) is located in Talladega County near Childersburg, in the east-central part of Alabama. Originally on 13,233 acres, the plant was built in 1941 and operated during WWII as a government owned /contactor operated facility. In 1945 the manufacturing operations ceased and the site was on standby similar to many ammunition manufacturing and packing plants found throughout the country after WWII. The site was included in the EPA National Priorities List in 1987. The site has several areas with different contaminants, two being TNT manufacturing areas and of interest in this study. During operation the small natural ditches were enlarged and channelized to provide drainage from the manufacturing areas. The surface runoff predominately drains to the Coosa River. A man-made channel called "the red water ditch" also carried liquid industrial wastes from the explosives manufacturing operations to the Coosa River. Remedial action followed in 1994 due to Comprehensive Environmental Response, Compensation, and Liability Act (CERCLA) and Superfund Amendments and Reauthorization Act (SARA). The contaminated soils and sediments were excavated and incinerated if the contaminant concentration was above 647 ppm for TNT (U.S. Army, 1994).

All of the soils used for this research were samples from TNT contaminated areas at the AAAP. The nitroaromatic soils used were site contaminated soils meaning the soil were not spiked in the laboratory but contained multiple contaminants aged in the field. Current research indicates contaminant binding properties change due to aging which effects contaminant transport and mobility (Hatzinger and Alexander, 1995). Most of the models assume single solute in sample

aqueous systems but natural systems involve multiple contaminants and complex sorbents (McGrath, 1995). Movement of pollutants from surface soils and sediments via water contact may be described by diffusion.

2.3 MATERIALS AND METHODS

2.3.1 Soil Characterization

Representative soil samples were sent for characterization by the Department of Agronomy Laboratory in Sturgis Hall at LSU. The soil characterization parameters for four different buckets of soil were performed. Results are to be presented in the following section.

2.3.2 Sample Collection

One of the soils used in this study was excavated a "hot spot" at the Alabama Army Arsenal Plant (AAAP) in Childersburg, Alabama by Marti Blad. Samples were collected from different depths in the "hot spot. These samples were collected and stored in glass sterile 1 kg jars with Teflon lined lids and refrigerated at 4°C in the dark until utilized. The labels indicated the location and depth of sample: surface soil, 0-6", 6-12", 12-18", 18-24".

A second soil was collected at the AAAP site and used in diffusion studies. In a collaborative venture with AAAP, Georgia Institute of Technology (GIT), Rice University and LSU in the Hazardous Substance Research Center/South and Southwest, multiple 55-gallon drums were filled with soil from the incineration staging area. This soil had low TNT contamination levels (1-60 mg/kg) and was the mix that was fed into the on-site incinerator in remediation. In the results this soil was labeled GIT soil.

A third soil was received from the Vicksburg Waterways Experimental Station (WES) and graciously donated by Dr. D. Dean Adrian. This (WES) soil was highly contaminated (10,000-25,000 mg/kg) and visibly different from the AAAP soil. Each soil had multiple sample preparations as described below. Initial experiments done with the GIT soil indicated the soil load was too low for a long-term study. Later experiments mixed GIT soils with WES soil and homogenized to yield the desired concentration.

2.3.3 Culture Collection

All soil and water samples from the AAAP were cultured for TNT tolerant bacteria. Approximately 10 aerobic and 25 anaerobic consortia were isolated by standard enrichment technique of three transfers to heterotrophic media.

2.3.4 Soil Preparation

Following appropriate safety measures, soil buckets were unsealed, large twigs and debris removed by hand while pouring soil into tray. Generally, each bucket was prepared sequentially. Soil was sieved through #10 mesh (US std) to remove hard clumps, rocks and small pieces of debris. The sieved soil was ground in grinder as a final homogenization step. All TNT contaminated soil was kept stable and in the dark until used. All soils were kept sealed until prepared. Sieved dry low TNT concentration soil was stored in clean five gallon buckets until used. High concentration soil was kept damp until use to avoid any explosion hazard.

2.3.5 Bulk Density, Particle Density and Porosity Determination

These parameters were determined in the lab following the standard methods for each (SSSA, 1986). Bulk density is the ratio of the mass of dry solids to the bulk

volume of the soil, including the pore space whereas the particle density excludes the pore space. The bulk density is simply the mass of dry packed soil in a 10 ml volumetric flask. The data is given units of g/cm^3 by convention.

Particle density is calculated by the difference in weights and utilizing the density of water. The volumetric flask is weighed empty, that is, full of air. Then soil is added to the volumetric flask, approximately 10 grams for the weight of flask with soil. Lastly, degassed water is added to the flask with the soil but not to the fill line. The soil and water mixture will frequently have gases or hydrophobic particles that require mixing to homogenize. Once the mixture is uniform the flask may be filled and weighed, because now all spaces are filled by either water or soil. The flask is then emptied and cleaned to remove all soil particles. The clean flask is filled with water and weighed one last time.

The equation to calculate the particle density is shown below:

$$\rho_p = \rho_w(W_s - W_a) / (W_s - W_a) - (W_{sw} - W_w) \qquad (2.1)$$

where ρ_w is the density of water, W_s is the weight of flask with soil only, W_a is the weight of the flask with air only, W_{sw} is the weight of the soil and water mixture, W_w is the weight of the water only.

Porosity is the fraction of soil that is not solid relative to the total volume. This is generally written as a percent. The equation for porosity is one minus the ratio of bulk density over particle density.

$$\varepsilon = \{1 - (\rho_b / \rho_p)\} * 100 \qquad (2.2)$$

2.3.6 Static Bed Diffusion Experimental Set up

Dry sieved soil was weighed and poured into 1000 ml borosilicate glass beakers. The soil column in the beaker was 8-10 cms high leaving 4-5 cms space to the top of the beaker lip. The soil was wetted drop wise with distilled water to saturation in order to prevent disturbance of the soil and to allow for all pore volumes to fill with water to establish an initial equilibrium. Approximately 100 mls of water was left on the top surface of the soil overnight to allow the soil to settle. The following day is designated day 0, the head volume of water was removed and replaced, which is added dropwise by running the water down the side of the beaker so the soil surface is not disturbed. This is the experimental starting time when the initial surface water is removed and replaced. The contaminated head volume was thus removed and an aliquot was saved for analysis as described in chemical analysis section.

2.3.7 Flow Regime

Two "flow rates" were tested. The surface headwater was replaced to provide a concentration gradient. In the calculation of flux in the results section, the removal of the head volume was averaged over the whole day yielding a "flow rate". The majority of experiments utilized a 50 ml head volume replaced daily for a "flow rate" of 2 mls per hour. Replacing the 50 ml head volume twice a day was examined to evaluate the effect of doubling the "flow rate" from 2 mls per hour to 4 mls per hour.

2.3.8 Sample Collection

The static beds were run for 3-4 months or until the surface water analysis indicated no TNT present. All beakers were kept in an environmental chamber of

constant temperature, humidity and in the dark for the duration of the experiment. TNT and related explosives are photosensitive and therefore all samples were shielded from UV light. Samples were collected by pipet, into glass scintillation vials with foil-lined caps and transported in sealed boxes.

2.3.9 Sample Preparation for HPLC

An aliquot of the removed head volume was analyzed by high pressure liquid chromatography (HPLC) for RDX, HMX, and TNT with its breakdown products. An aliquot of aqueous sample was mixed with equal volume HPLC grade acetonitrile in a scintillation vial. The mixture was swirled to homogenize. Using a 5 cc syringe, 5 mls of mixture was filtered thru 0.2 micron PTFE syringe filter. The first 2mls were wasted back into scintillation vial while the remaining solution went into the glass 1.8 ml crimp capped vial for HPLC analysis. This wastage was to prevent error due to contaminant binding on filters. The lid was sealed on the HPLC vial using a crimper and stored in refrigerator until analysis.

This initial static diffusion models were run only for TNT, as it was most prevalent in the samples. RDX, HMX, and Tetryl were present in very low concentrations so could not be consistently quantified.

2.3.10 Chemical Analysis

The concentration of contaminants, namely TNT, RDX, HMX and the dinitrotoluene isomers were monitored using high pressure liquid chromatography (HPLC) following EPA SW-846 method 8330 modified to a flow rate of 0.9 ml/min and 50/50 water /methanol mobile phase. The analytical column was a Hewlett Packard 5 um ODS Hypersil 4.6 mm X 25 cm cartridge column on a Hewlett Packard

1090 series II chromatograph using HP ChemStation software with photodiode array detector at 254 nm. Standards (TNT with 20% water, Sigma Chemical) were made every two months and the calibration curve regenerated. Daily HPLC runs had standards at beginning and end to validate the current standard curve.

2.3.11 Mass Balance

2.3.11.1 Core Procedure

The beakers were cored at the end of each leaching experiment to determine the concentration of contaminants that remained on the soil. Wax paper was wrapped around a 60 cc syringe barrel and taped to retain its shape. This cylinder was gently pressed into the damp soil until the bottom was touched. The cores were allowed to dry in place in order to ease their removal while maintaining the soil integrity. The cores were cut into 1 cm slices and placed into 60 ml amber borosilicate jars. The core samples were extracted by sonication with methanol as the solvent as described below.

2.3.11.2 Sonication Extraction

Into 60 ml amber bottle, approximately 10 g or 1/2 cm of soil core was weighed. One problem with sonication can be the loss of solvent or contaminant due to volatilization or evaporation from heat. To prevent this loss, the sonicator must have flow thru capabilities or ice addition. The temperature of the water inside the sonicating bath was maintained cool to the touch. After the bottle was removed from the bath it was allowed to settle to allow the finer particles to fall out. Removal of the liquid phase was performed while not disturbing the soil surface using a Pasteur pipet. After the liquid was removed, the bottle was refilled with 20 mls and sonication

continued (Repeat steps 1-4 six more times). Sonication was for a total time of 6 hours, in one-hour cycles. The liquid was filtered, diluted, and analyzed by HPLC as described previously.

2.3.11.3 Experimental Flux Calculation

The experimental flux (mg/cm^2*hr) can be calculated by:

$$Flux = Q * C / (A) \quad (2.3)$$

where Q is the volumetric flow rate (L/hr), C is concentration (mg/L), A is area of the bed surface (cm^2). This flux rate will be graphed as experimental fluxes and discussed in the results section.

2.3.11.4 Theoretical Flux Determination

The effluent mass values in the mass balance were calculated by two methods. The first method was the simple back calculation as:

$$M = F * A * \Delta T \quad (2.4)$$

where M is mass of TNT, F is the calculated flux rate from equation 2.3, and delta t is the time between sample n and sample n+1.

The other method is labeled trapezoid. This method follows the basic principles of forming a trapezoid using the two time values and their respective flux values. By utilizing the "trapezoid" method, the total is the sum of a series of averages. These 'trapezoids' were summed to determine removal per unit area and will be discussed in the results section.

2.3.12 Data Analysis

Graphing and calculations of flux were performed utilizing the Microsoft Excel® spreadsheet software in Microsoft Office 2000®. Spreadsheets were

constructed to calculate the flux rates and mass balances from the reported concentrations. Graphs and tables were constructed from these spreadsheets and will be shown in results section.

2.3.13 Development of Semi Infinite Diffusion Model

The purpose of these models is to explore the diffusive transport processes involved in pollutant release from site soil and to provide a starting point for estimation of pollutant release rates. Quantification of chemical movement was done by determination of pollutant flux rates. By using the effluent concentrations to calculate the flux rate of contaminant at the soil-water interface, experimentally calculated flux data from the aqueous phase was fitted to the solution for the advection dispersion equation using Mathcad® to determine the effective diffusivity (Choy and Reible, 2000).

$$\text{Flux} = C_o \cdot \sqrt{\frac{D_e \cdot R_f}{\pi \cdot t}} \qquad (2.5)$$

where C_o is the initial pore water concentration, D_e is the fitted parameter effective diffusivity, R_f is the retardation factor and t is time.

Local equilibrium and linear partitioning for the contaminant between soil particles and the aqueous phase are assumed. Initial experiments assumed a semi-infinite source with uniform initial concentration and zero concentration at the surface as boundary conditions. Flux from the base was assumed to be zero due to the experimental apparatus. Static bed experiments were utilized to quantify the flux of material into the overlying water, or head volume. Different sampling regimes were

evaluated for their impact on flux rates. The experimental flux was fit to equation 2.5 to obtain a model derived effective diffusivity under quiescent conditions.

2.3.14 Model Analysis

Mathcad 2000 Professional® software was utilized for higher math functions. Most importantly, an effective diffusivity was calculated to quantify the contaminant transport and compare movement of pollutants in different soils. By setting the sum of squared error equal to zero, Mathcad® is able to iteratively calculate an effective diffusivity which allows the model to fit experimental data. Correlation coefficients were returned by the programs ability to linearize data and will be used to demonstrate goodness of fit. Dimensionless parameters were also calculated utilizing Mathcad® in order to validate the model application.

2.4 RESULTS FOR NITROAROMATIC STUDIES

2.4.1 Soil Characteristics

The soil was analyzed by the Department of Agromomy Soils Laboratory in Sturgis Hall on the LSU campus. Values for % organic matter (OM), pH, and other soil parameters are shown in Table 2.2. The results show the variation in the samples, which is an indicator of the homogeneity of the AAAP site itself. The values for bulk density, particle density and porosity, were determined and are shown in Table 2.3.

A supplementary soil analysis was graciously provided by Dr. Thomas Junk indicating the mineral portion was 46% Kaolinite, 33% Illite, 10% each of Chlorite and Quartz with the remaining t1% as Smectite. Sediment size analysis indicated 56.6% silt, and 1% clay with the remaining as sand. The sand portion was composed of fine sand and very fine sand at 19.4 % and 13.5% respectively. Medium sand was

Table 2.2. Soil characteristics for all TNT soils

					Alabama Army Ammunition Plant hot spot horizons											
Parameter	GIT Soil I	GIT Soil II	Surface I	Surface II	0" - 6"	0" - 6"	6" - 12"	6" - 12"	12" - 18"	12" - 18"	18" - 24"	18" - 24"	Red Water Ditch	Red Water Ditch	WES soil	WES soil
pH	6.5	6.6	6.9	6.2	4.8	4.9	4.8	4.9	4.9	4.9	4.7	4.7	4.8	4.7	5.7	5.6
Na	20	15	12	8	11	7	12	10	37	12	12	12	18	16	7	10
Mg	105	103	128	123	100	102	91	83	120	103	98	96	117	103	118	125
Ca	1273	1231	1469	784	363	361	210	206	230	163	87	80	555	465	797	812
P	32	42	69	29	14	14	10	11	9	16	17	11	18	22	14	13
K	64	65	114	76	97	97	83	72	98	94	96	95	60	58	53	61
%OM	1.78	1.61	0	0	0	0	0	0	0	0	0	0	0	0	0	0
Sum Bases	7.5	7.2	8.7	5.2	2.9	2.9	2.1	1.9	2.5	2	1.5	1.5	4	3.4	5.1	5.3

Table 2.3. AAAP soil particle density, bulk density and porosity

Replicate	Particle density	Bulk density	Porosity
Sample 1	2.590	1.397	0.461
Sample 2	2.564	1.368	0.466
Sample 3	2.570	1.382	0.462
Average	2.57	1.38	0.46

9.1% while coarse sand was only 0.4% of the total. The x-ray diffraction indicated this was typical A horizon type soil with sparse clay. Clays typically leach from the A horizon to reform in the B horizon.

2.4.2 Experimental Measurements for TNT in Static Beds

The first soil studied had low concentrations of contaminants and was designated as GIT in the aforementioned sample collection section. As previously mentioned, the aqueous samples were analyzed for the TNT concentration and the flux was calculated by Equation 2.4. For simplicity, only one graph of concentration vs. time is shown in Figure 2.1 for the low concentration (GIT). Figure 2.1 exhibits the typical shape of diffusion curves, with initially higher concentrations rapidly decreases to a concentration termed steady state indicated by the flattening of the line. In Figure 2.2 the flux curve is shown for the data in Figure 2.1 and therefore looks very similar to the concentration curve Figure 2.1 as would be expected from equation 4. The difference to note between graphs is how fast the steady state concentration is reached and at what concentration steady state is obtained. The concentration and flux line shown in Figures 2.1 and 2.2 are the average of four replicates. The initial concentration values are very low and the steady state values were non detectable after 250 hours, with the final concentration values hovering around 0.05 mg/L.

To show the variation among samples, Figure 2.3 follows four replicates utilized in Figure 2.2. In can be seen there is only a slight variation between samples. This steady state flux value is approximately 1.5 E 10^{-6} mg/cm^2*hr to correspond with the concentration value of 0.05 mg/L. The flux for each beaker continues to decrease over time as shown in Figure 2.3 for the low contaminant loaded soil. As

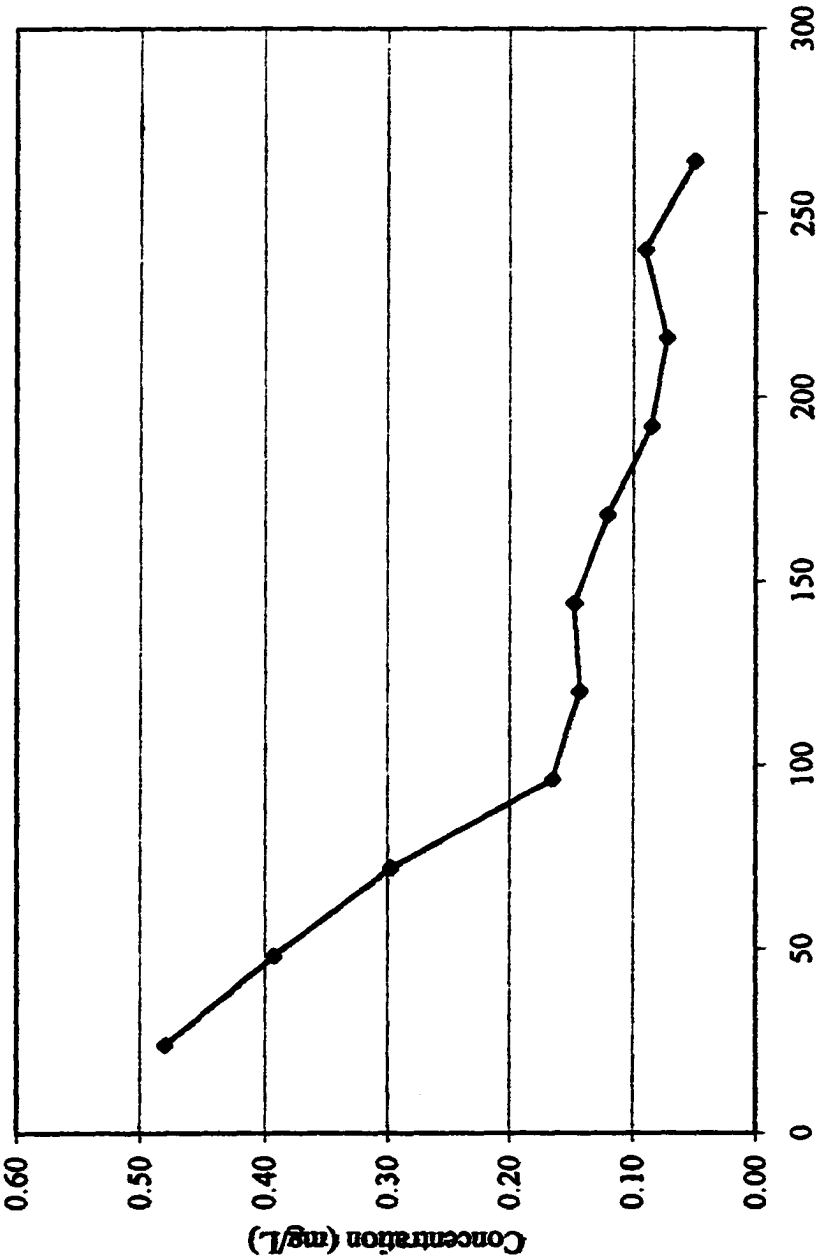

Figure 2.1. Average static concentration from GIT soil

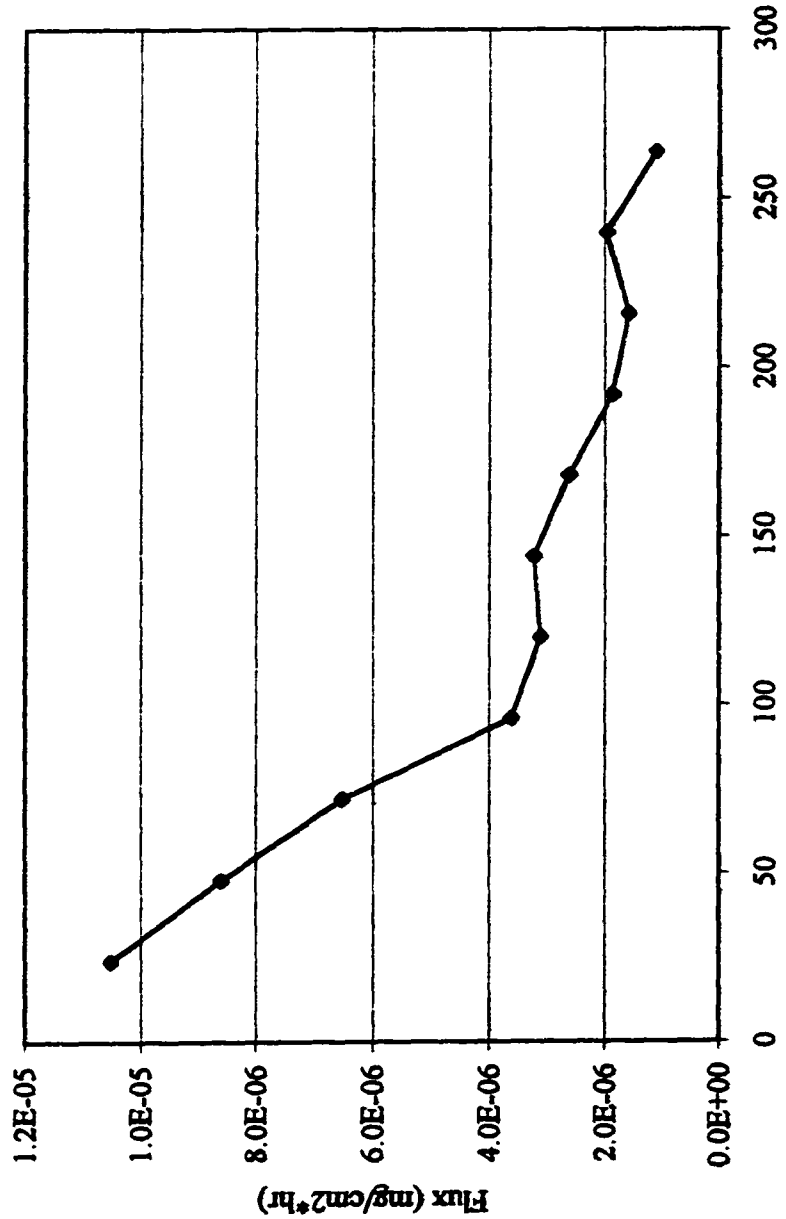

Figure 2.2. Average static flux from GIT soil

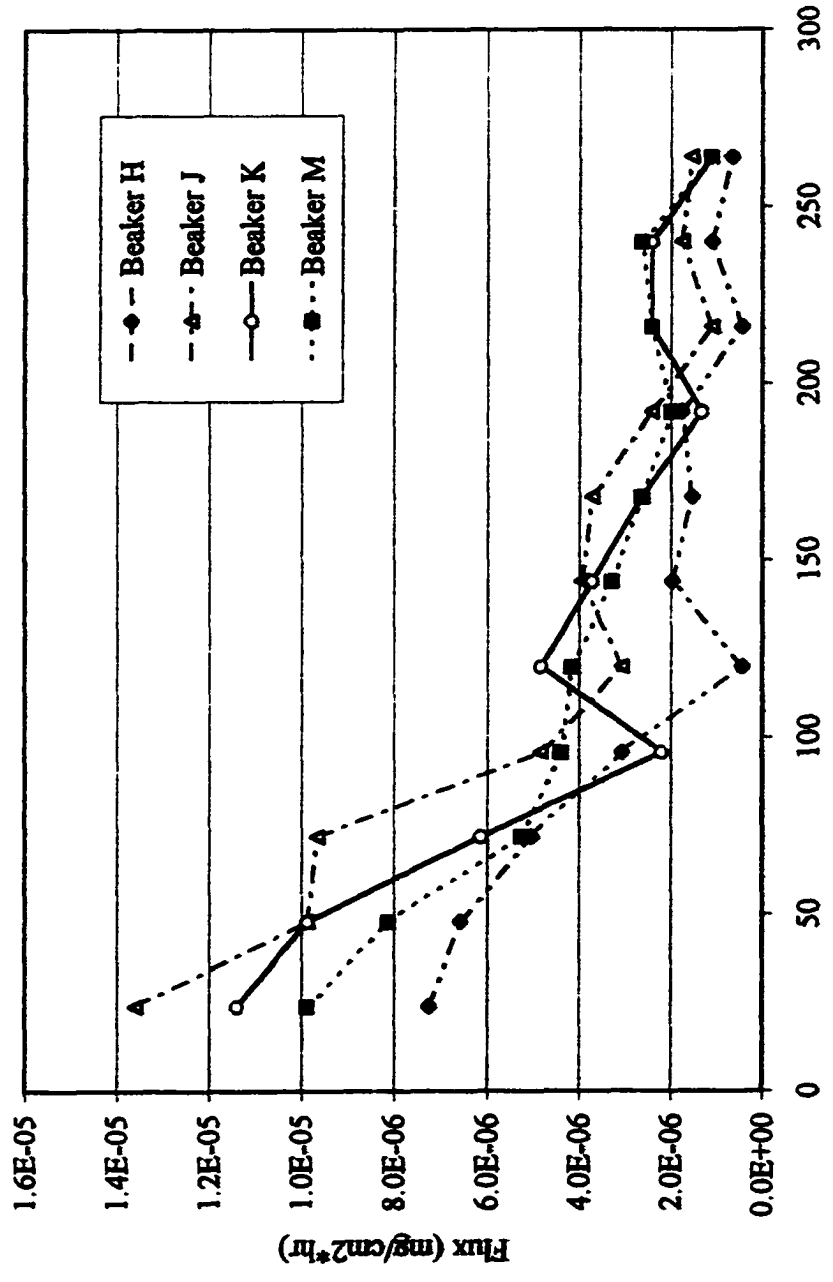

Figure 2.3. Individual static fluxes from GIT soil

shown in all the previous figures, TNT contaminated soil diffuses pollutants to the overlying water with decreasing concentration over time.

The following set of figures describes the behavior of TNT in different soil horizons at the AAAP site. Figures 2.4 follows the experimental flux for the surface soil from the AAAP. Figure 2.5 demonstrates the model fit to the experimental results shown in Figure 2.4. Figure 2.6 shows the TNT flux from the 0" – 6" AAAP soil horizon. Figure 2.7 examines the model fit to the experimental flux.

Figure 2.8 presents the experimental flux from the soil horizon of 6"- 12" inches deep at the AAAP "hot spot". The model fits the experimental data well as can be seen in Figure 2.9. Figure 2.10 follows the experimental flux for the 12"-18" soil from the AAAP. Figure 2.11 demonstrates the model fit to the experimental results shown in Figure 2.10. The deepest horizon sampled was 18" – 24" from the surface and the flux of TNT from that soil is shown in Figure 2.12 with the corresponding model comparison shown in Figure 2.13. Figure 2.14 shows the TNT flux from the AAAP location called red water ditch. Figure 2.15 examines the model fit to the experimental flux at that site.

2.4.3 Results from Mathcad Modeling

Experimental flux data from the beaker head volume concentration was calculated and fitted to a simple diffusion model (Choy and Reible, 2000) in order to determine the effective diffusivity. The derived solution is given by

$$\text{Flux} = C_o * [(De * R_f)/(\pi * t)]^{1/2} \qquad (2.6)$$

where C_o is the initial concentration, R_f is retardation factor, t is time, D_e is the effective diffusivity, which is the only parameter to fit. The purpose of this model is

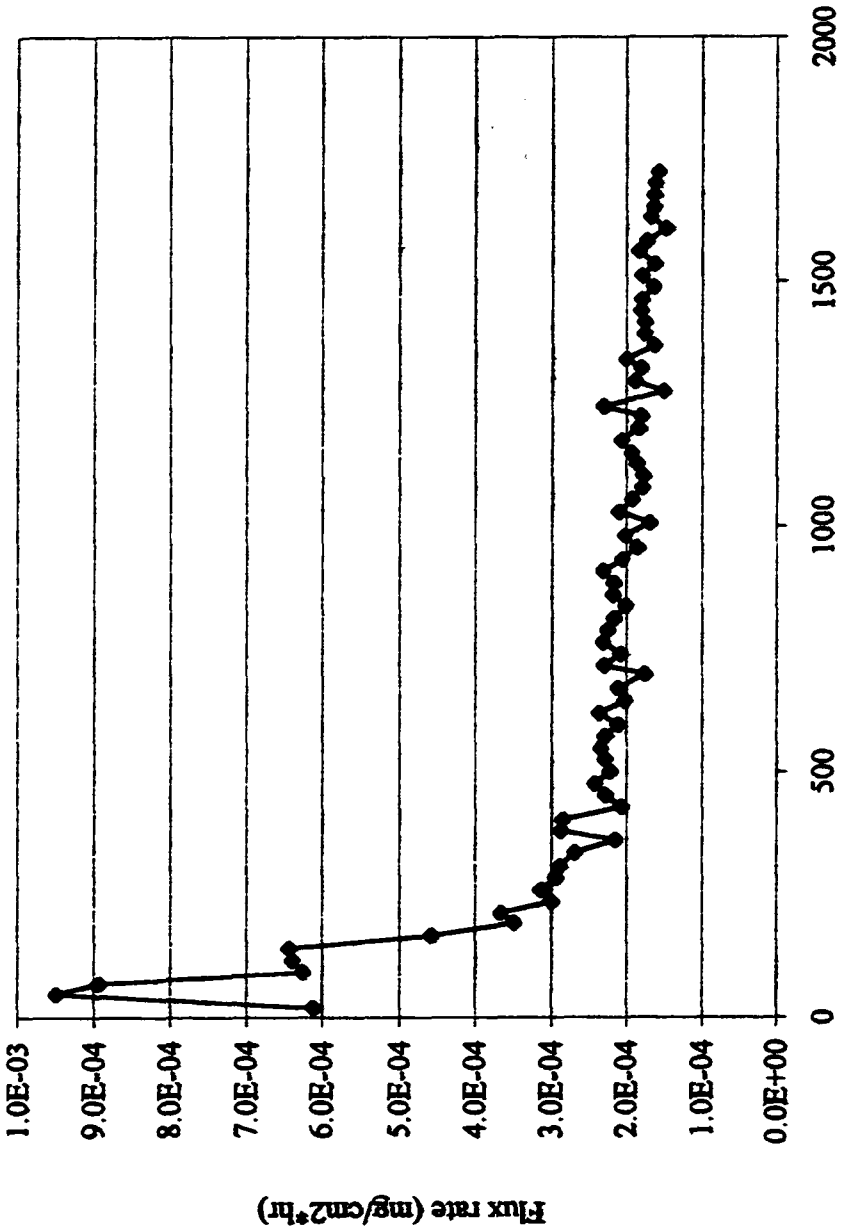

Figure 2.4. TNT static flux from AAAP surface soil

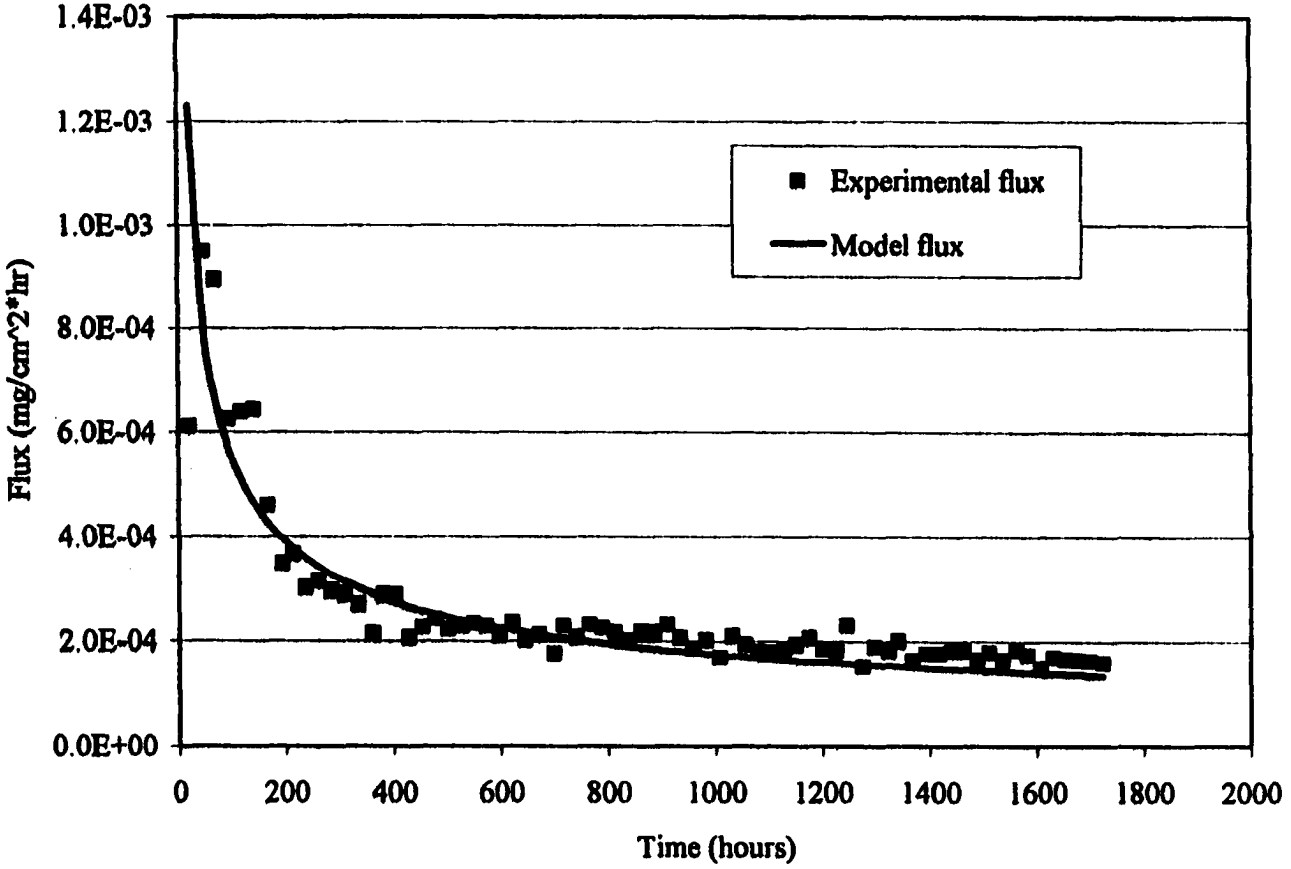

Figure 2.5. Model vs. experimental flux from AAAP surface soil

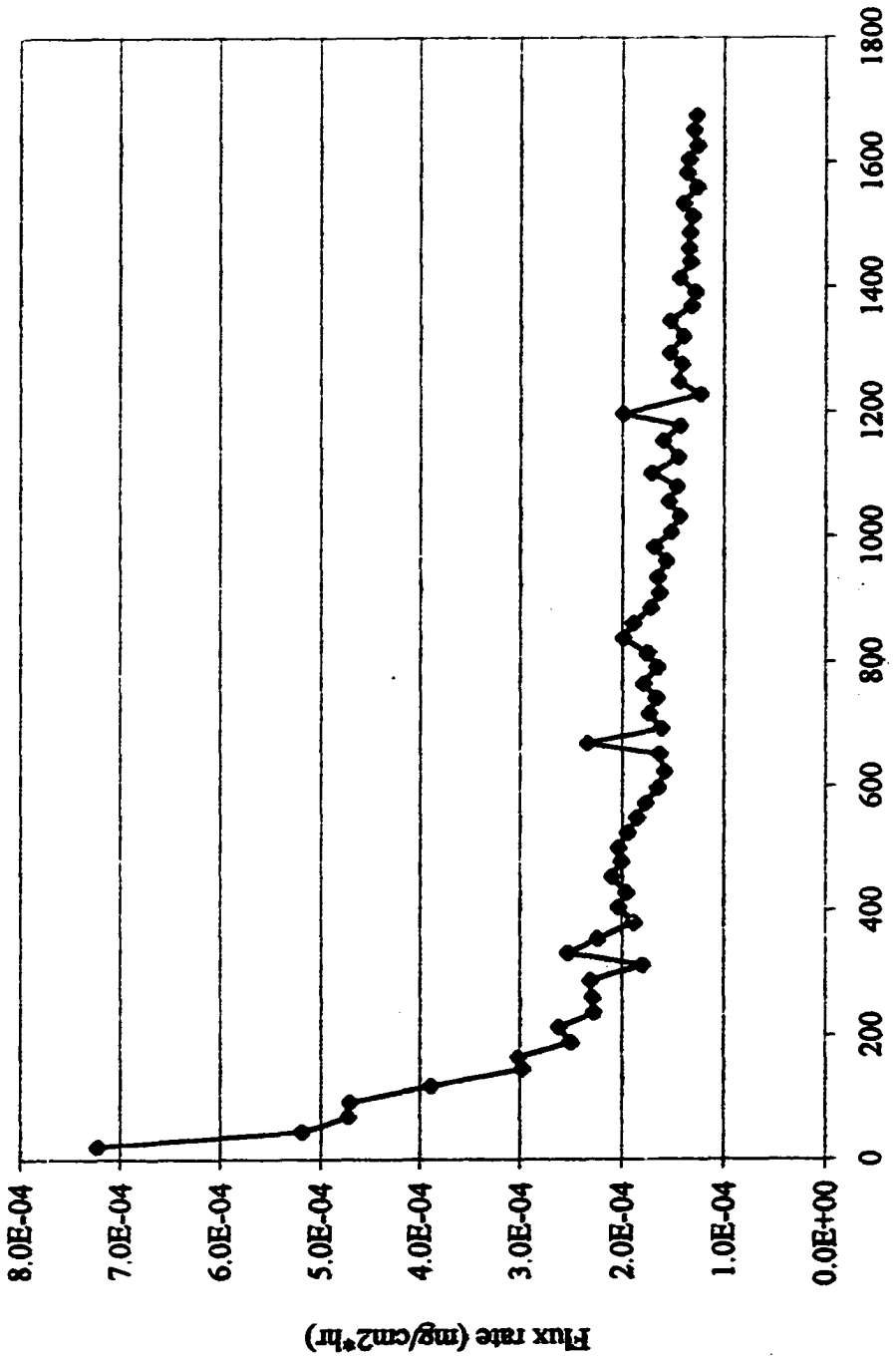

Figure 2.6. TNT static flux from AAAP 0"- 6" soil

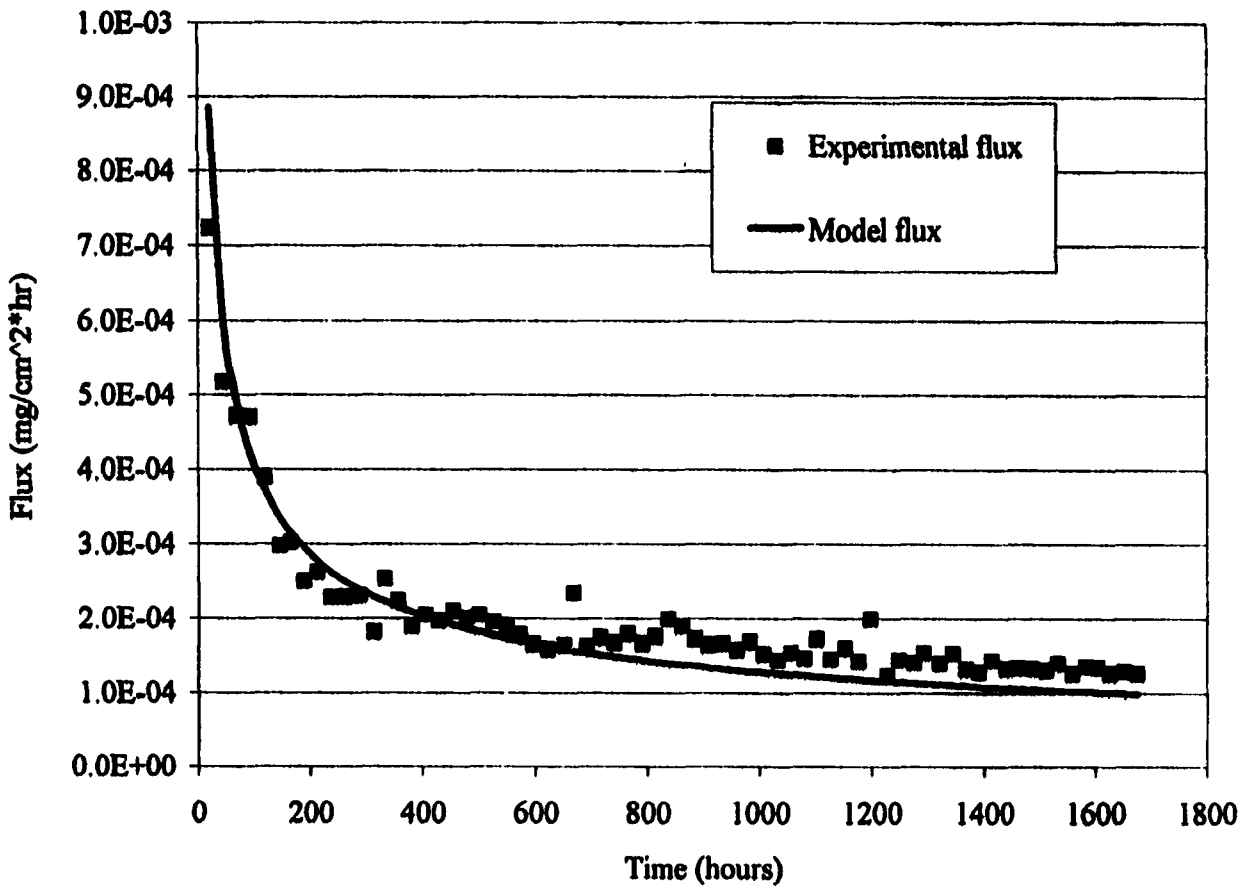

Figure 2.7. Model vs. experimental flux from AAAP 0"-6" soil

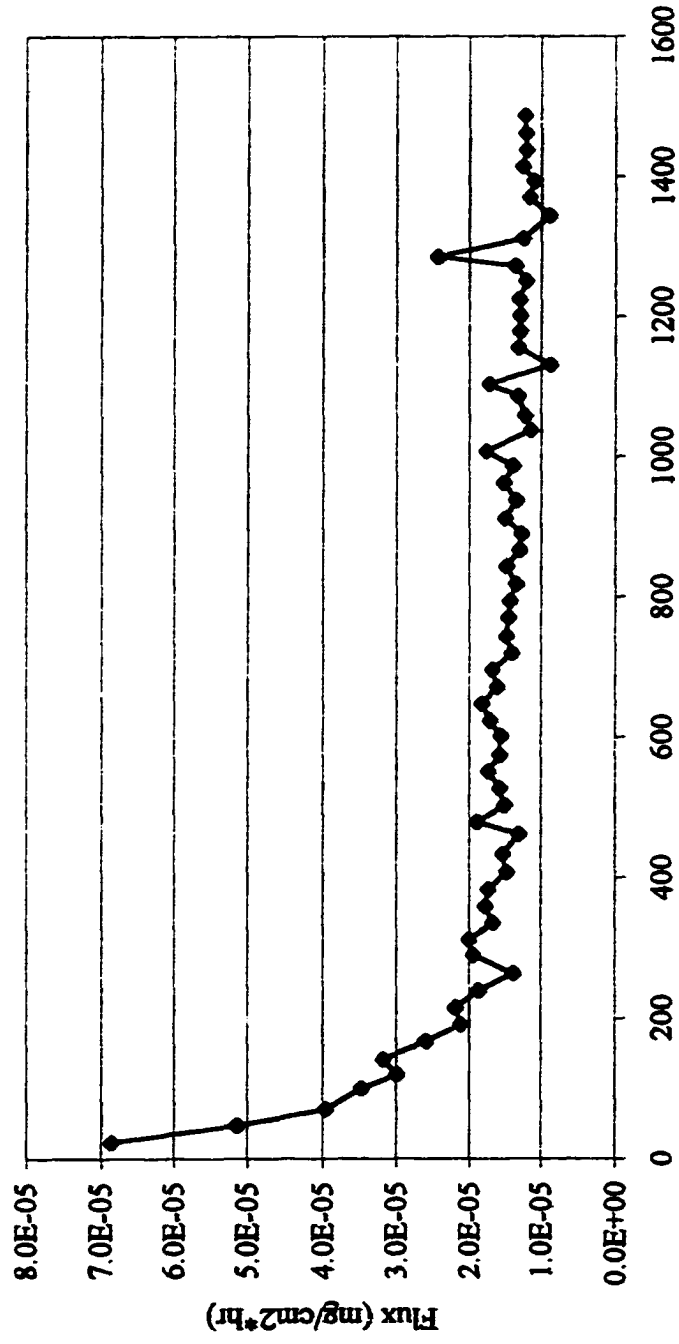

Figure 2.8. TNT static flux from AAAP 6" - 12" soil

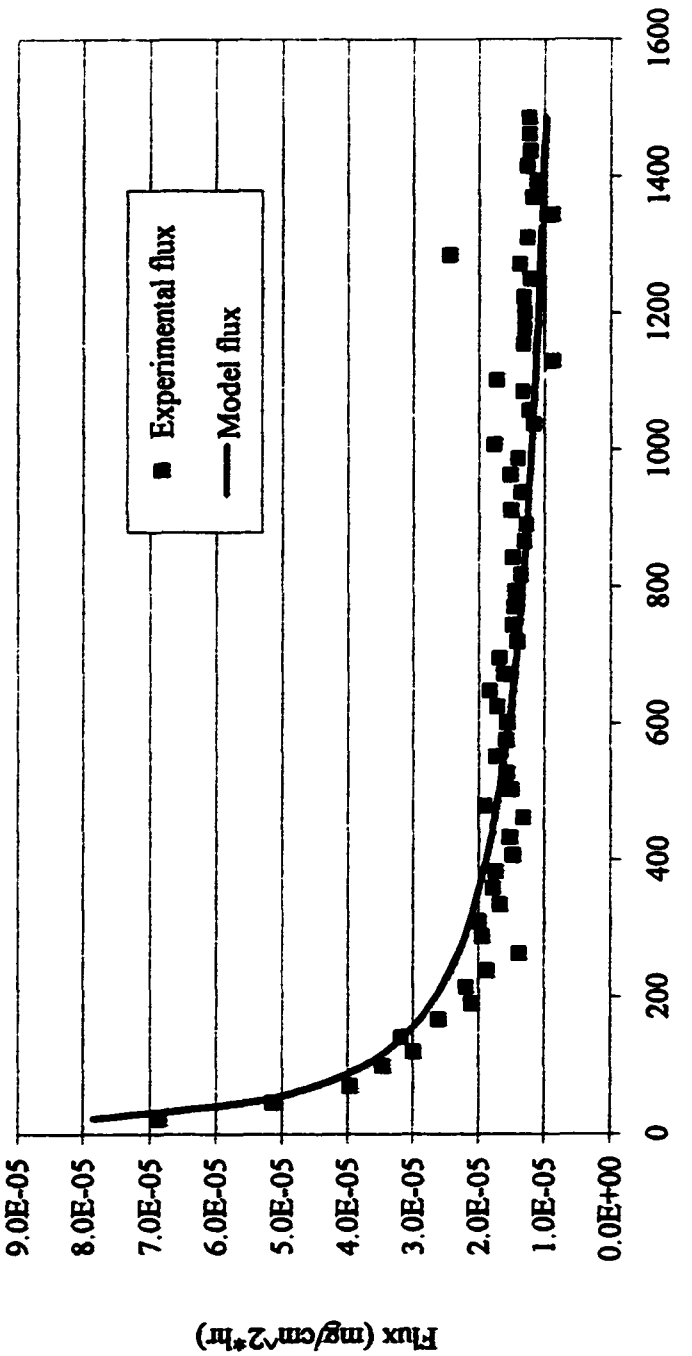

Figure 2.9. Model vs. experimental flux from AAAP 6"-12"soil

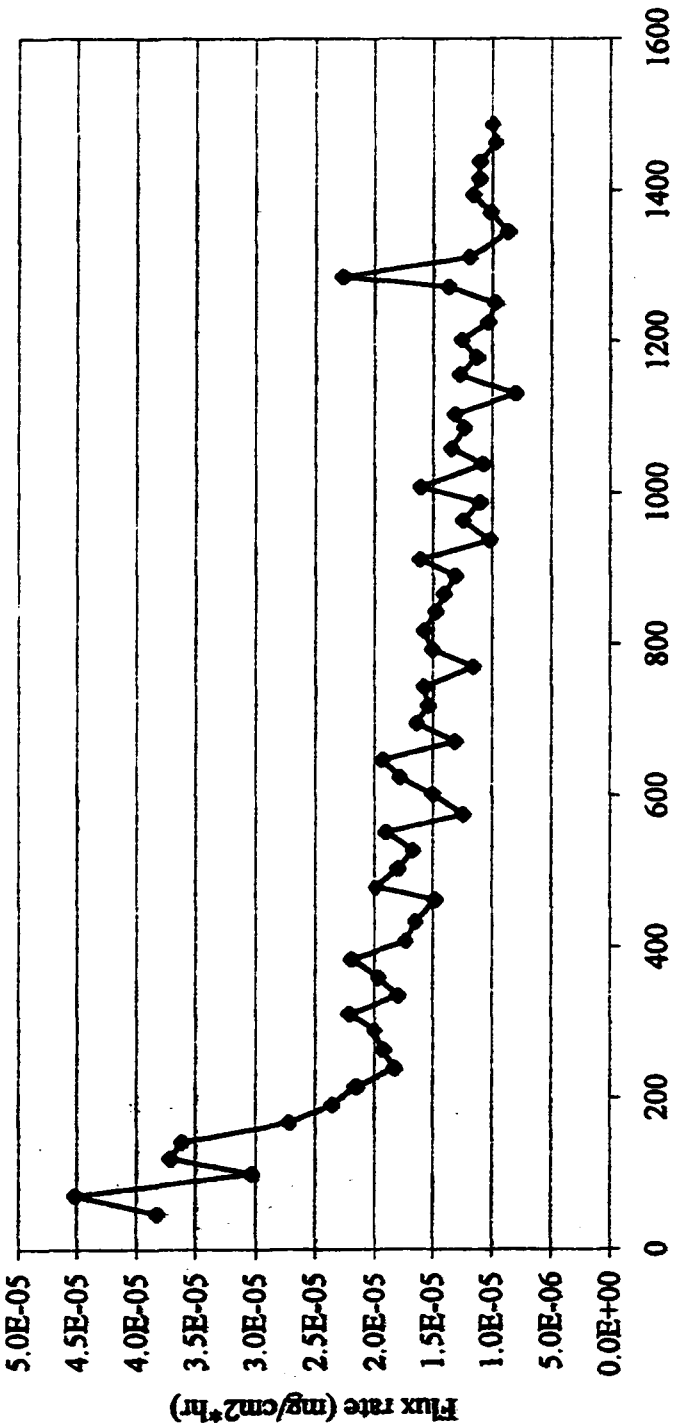

Figure 2.10. TNT static flux from 12"- 18" AAAP soil

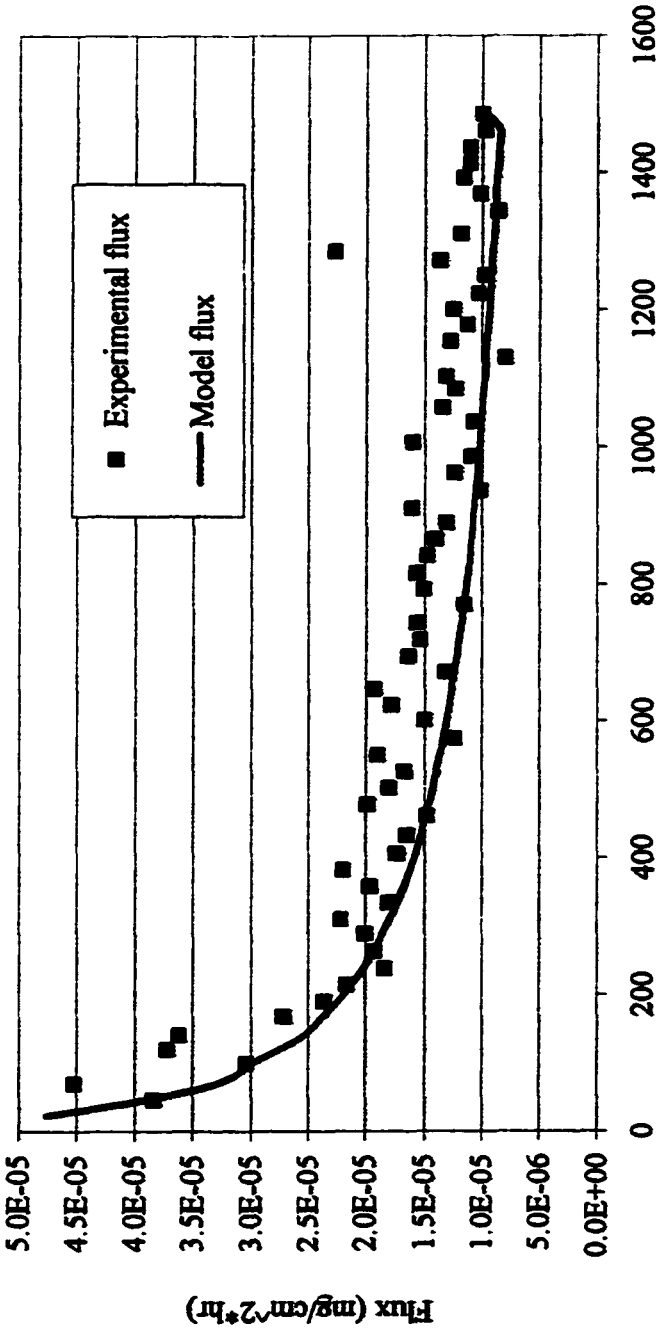

Figure 2.11. Model vs. experimental flux from AAAP 12" - 18" soil

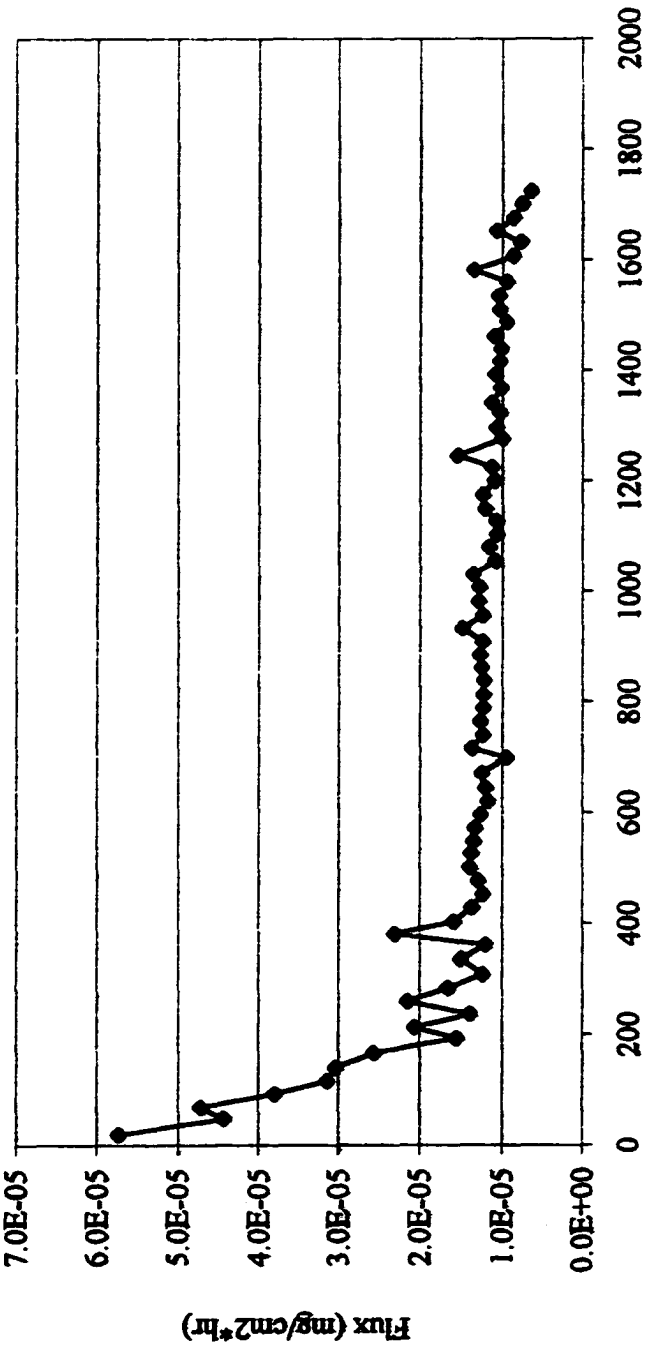

Figure 2.12. TNT static flux from AAAP 18" - 24" soil

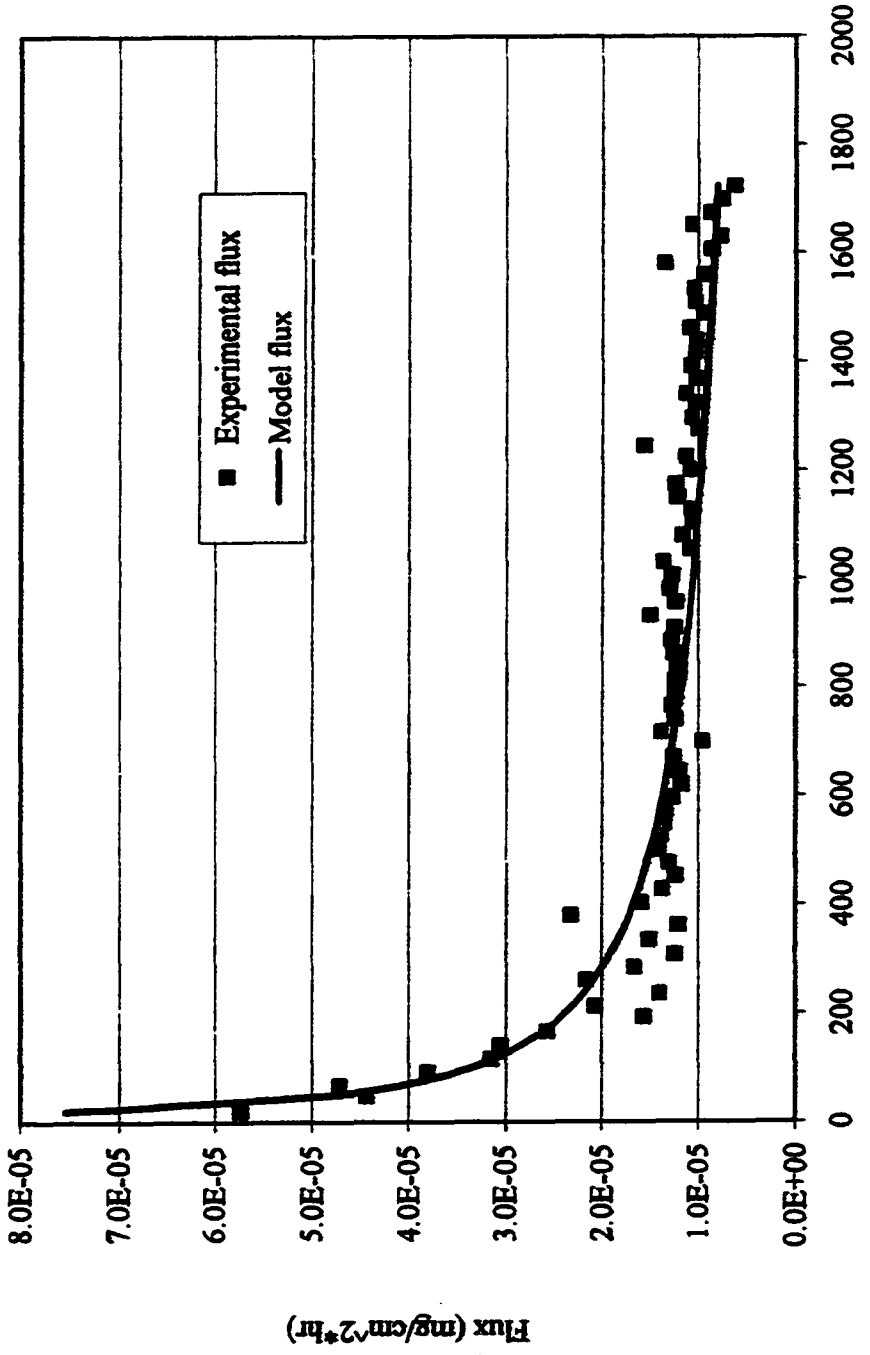

Figure 2.13. Model vs. experimental flux from the AAAP 18"-24"

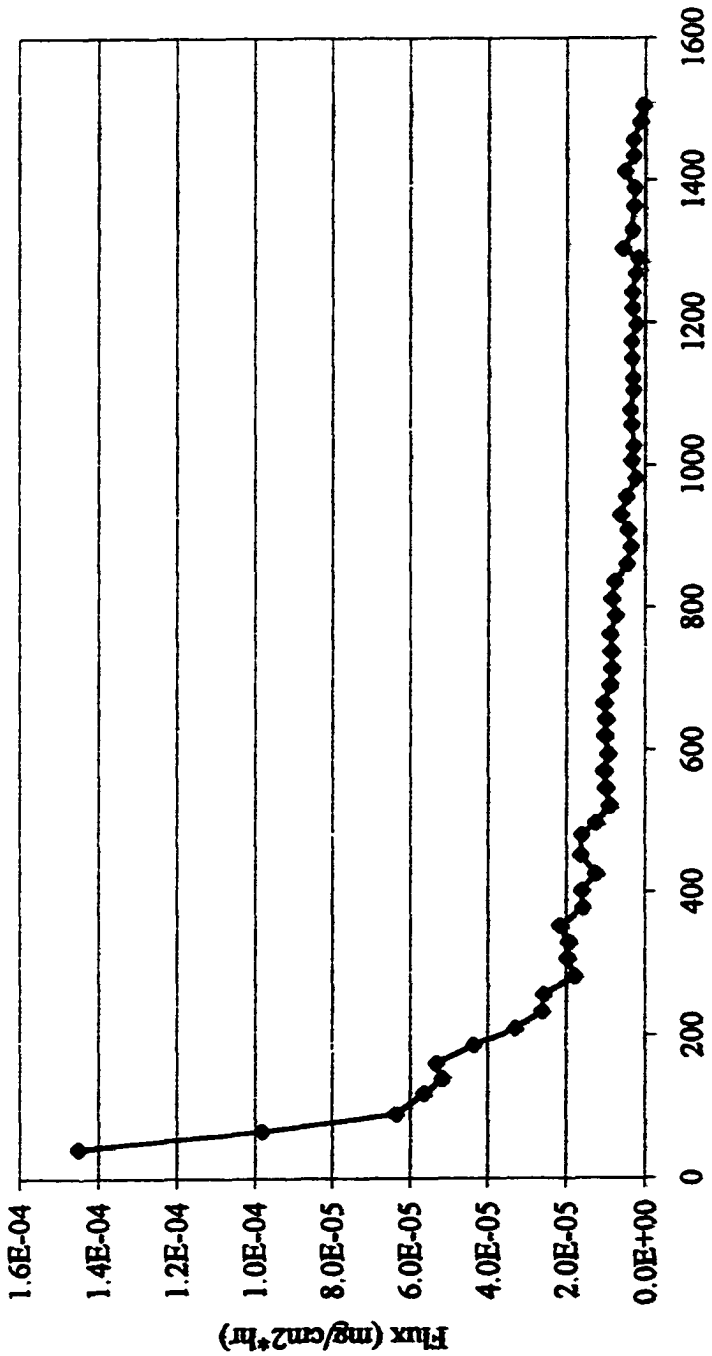

Figure 2.14. TNT static flux from AAAP Red Water Ditch sediment

Figure 2.15. Model vs. experimental flux from AAAP Red Water ditch sediment

to quantify the diffusive transport process involved in TNT release from soil and sediment to provide a starting point for estimation of pollutant release rates. Table 2.4 presents the model effective diffusivity and the correlation coefficient to indicate how closely the model fit the experimental flux data.

The presented data for the AAAP soil indicates simple diffusion adequately represents the major transport process for TNT under quiescent conditions. The simple diffusion model gives good fit to experimental flux from AAAP soil as indicated by correlation coefficients between 0.84 and 0.98. The fastest transport is indicated by the largest effective diffusivity; therefore, the surface soils behave differently than the lower layer in the vertical direction as seen in Table 2.4. Of interest is the difference in D_e as depth changes, with surface soils allowing rapid flux of contaminants. The effective diffusivity decreases as samples get deeper indicating contaminants move away from the soil more slowly. This may be related to the presence of colloids or changing particle size at the surface due to weathering. This supports the hypothesis that TNT diffusion can be faster in some soils and slower in other soils depending on soil characteristics and contaminant load.

2.4.4 Core Results

After the diffusion experiments were completed, the soil was cored, and core samples sonication extracted and analyzed by HPLC as described previously. This data indicates the amount of pollutant remaining on the soil and is termed the residual soil load. The soil core slices are numbered starting at the bottom of the beaker so the larger the number the closer to the surface. The top layer of soil, which is closest to the

Table 2.4. Model results

Location (depth)	Fitted effective diffusivity (cm^2/s)		Correlation coefficient, r
Surface I	6.69E-05	+/- 0.23	0.859
0" - 6"	4.26E-05	+/- 0.11	0.978
6" - 12"	3.12E-07	+/- 0.14	0.959
12" - 18"	2.97E-07	+/- 0.18	0.879
18" - 24"	2.50E-07	+/- 0.15	0.947
Red Water Ditch	5.68E-07	+/- 0.24	0.839

overlying water, is 7.7-8 cm in height. The dependent axis is the height from the bottom of the beaker.

Figure 2.16 shows the residual load remaining on the GIT soil for which the flux data is shown in Figure 2.2. The low residual load in the top few centimeters (8.5-9 and 9-9.5) indicates TNT has diffused out of those layers. The middle layers appear to have the highest concentrations because they have the longest diffusion path to the top or the bottom. The bottom layers appear to have more residual load than middle or bottom layers, except the two samples at 4-4.5 cm and 5-5.5 cm depth have very high residual concentration. The remaining contaminant load is expected to decrease with position or as location moves toward the surface of the beaker.

The core profile data shown in Figures 2.17 and 2.18 are from the different AAAP soil horizons. Figure 2.17 indicates a great deal of variation between replicates for the surface soil core residual load. This soil profile correlates to the experiment shown in Figure 2.4, the AAAP soil. Then general trend of more residual load at the bottom of the beaker and less residual load remaining in soils close to the overlying water can be seen. The top centimeter indicates residual loads of less than 10 mg/kg whereas the deeper layers contain much higher concentrations of TNT.

In Figure 2.18 the residual soil load of the two replicate cores and the average is presented. Figure 2.18 residual soil load is the remaining soil load for the experimental flux shown in Figure 2.7, the AAAP 0" – 6" soil horizon. Figure 2.18 shows a similar soil profile to Figure 2.17 although a much lower soil load overall. The differences between the replicates appear to be small in Figure 2.18 unlike the replicates from Figure 2.17.

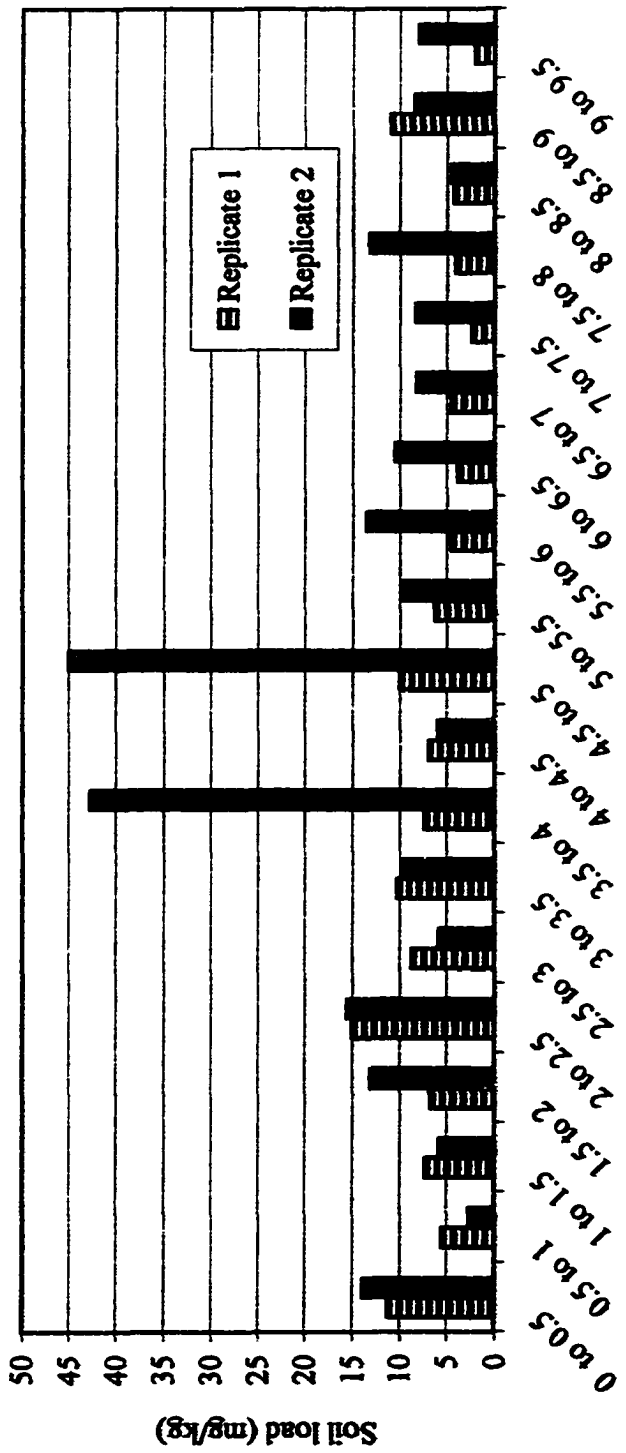

Figure 2.16. Residual soil load for surface soil (GIT)

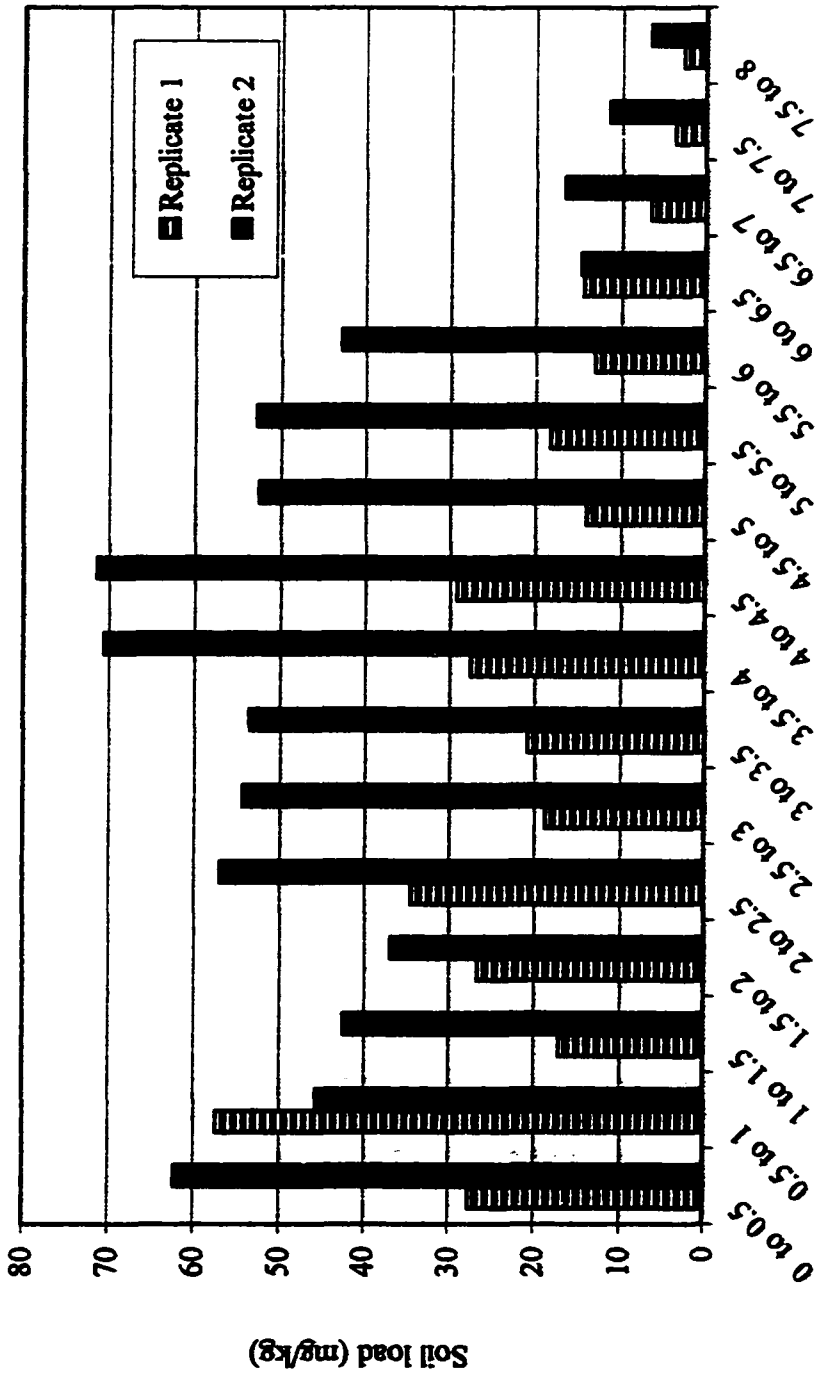

Figure 2.17. Residual soil load for AAAP surface soil

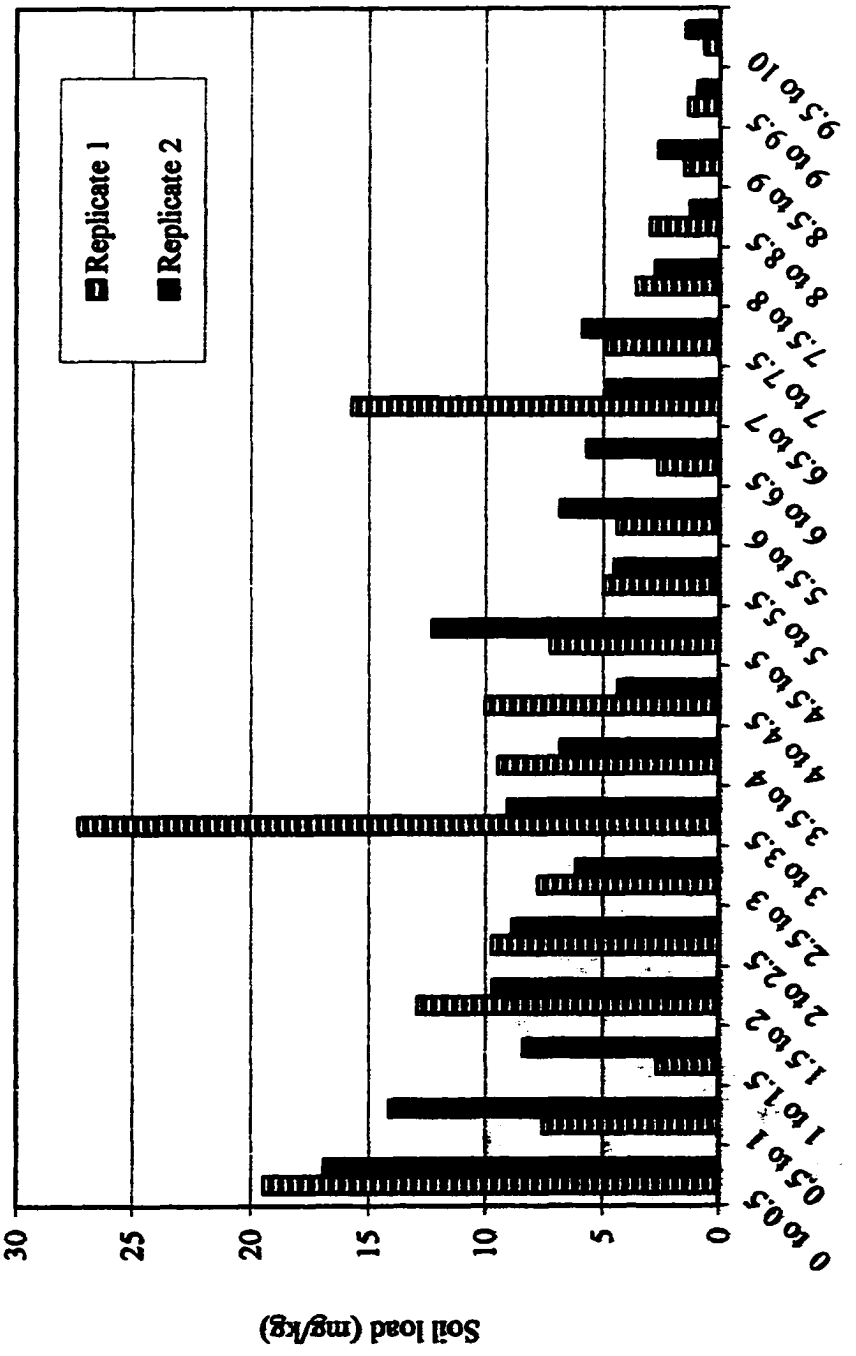

Figure 2.18. Residual soil load for AAAP 0" - 6" soil

Generally, the soil core profiles demonstrate less TNT in the surface layer as would be expected since it has the shortest path to diffuse out of the soil compartment. Utilizing the average values the small differences disappear and the general trend can be seen. The low residual load in the top few centimeters indicates TNT has diffused out of the surface layers. The bottom layers appear to have the highest concentrations because they have the longest diffusion path to the top. A possible explanation for high residual contamination in the middle layers may be that the TNT desorbs from the bottom layer to be re-sorbed in the middle layer. The variation could be attributed to the heterogeneous nature of the soil. This also demonstrates the problem of observed crystals of "neat" TNT that may be present in the soil. Due to the presence of "neat" TNT a different model with a source term could be considered.

2.4.5 Mass Balance

A mass balance was not possible because of the residual soil load appeared to be higher than the initial soil load determinations. The soil cores from the remaining soil horizons gave concentrations below the analytical detection limit and could not be reliably quantified and therefore are not shown.

2.5 CONCLUSIONS FOR LOW CONCENTRATION STATIC DIFFUSION STUDIES

The exponential decay signature shown in the flux curves is characteristic of diffusion curves (Deana et al., 1999). The movement of contaminants by leaching can be quantified by flux rates. The capacity of biological systems to remediate explosives contaminated soil and water is dependent on their ability to tolerate and metabolize under the concentrations presented.

Model goodness of fit for the different soil horizons is indicated by correlation coefficients of .84 or larger. The changing diffusivity indicates there are changing soil characteristics as samples are taken from deeper locations. As seen in Table 2.4 the surface soil had much higher diffusivity in the range of 10^{-5} cm^2/s and therefore TNT can quickly diffuse out of those soils. This value is uncharacteristically high and maybe due to small rocks homogenized into the soil matrix. The deeper soils had slower transport mechanisms as indicated by the smaller effective diffusivities all clustered near 10^{-7} cm^2/s. Only one sediment sample was examined in this study. The red water ditch effective diffusivity was in the range of 10^{-6} cm^2/s.

Effective diffusivity values in the range of 10^{-6} to 10^{-7} cm^2/s are found in the literature. The higher values found in the surface soil indicate this model may not be able to account for all the processes present in the experimental apparatus.

2.5.1 Model Assumptions

The K_d was experimentally determined by Dr. Kamel Qaisi (1996) for the GIT soil and was assumed to be 2.5 L/kg. From the soil characteristics presented in Table 2.2, only the GIT soil had detectable organic matter so K_d could not be correlated with f_{oc} in this study. The initial soil load was assumed to be 25 mg/kg for determination of the pore water concentration by the K_d. The model assumes no water - side resistance which is presumed valid due to the good model fit. The semi-infinite model investigated herein is valid for quantifying the effective diffusivity under quiescent conditions provided the contaminated soil provides an initial pore water concentration below the solubility limit.

2.6 HIGH CONCENTRATION SOIL STUDIES

Static bed diffusion experiments were also conducted using the high concentration soil from WES to determine if similar diffusive behavior would be present in this case. This soil had other contaminants present in detectable concentrations. The experimental apparatus is still a beaker with soil and overlying water but now the head volume is 100 mls and sampling occurred once a day. As seen in Figure 2.19 the flux does not appear to follow the same pattern of decay as previously discussed. Both of the replicates are shown. The flux rate is not exponentially decreasing instead it is more closely resembling a constant rate. The flux vs. time curve shows a saw tooth like pattern and a much higher flux rate of approximately 3 to 4 x 10^{-3} mg/cm^2*hr.

Figures 2.20 compare the flux of the four main detected soil pollutants in the overlying water sampled one time per day. Here, the individual component flux rates are shown to vary. Although the contaminants show overall behavioral similarity, it should be noted that each compound partitions into the water phase differently due to differences in chemical properties such as K_{ow} and solubility. This data will not be modeled by equation 2.5 because the flux rate does not decrease over time. One interesting observation of this experiment was the other contaminant flux rates follow TNT flux rates if they are present in high enough concentrations to be detected.

Figure 2.21 compares the four detectable pollutant flux rates from the same high concentration soil but sampled 2 times per day. It can be seen that chemicals partition according to their individual partition coefficients but follow a similar trend as TNT. The twice a day sampling regime demonstrates even higher spikes in flux

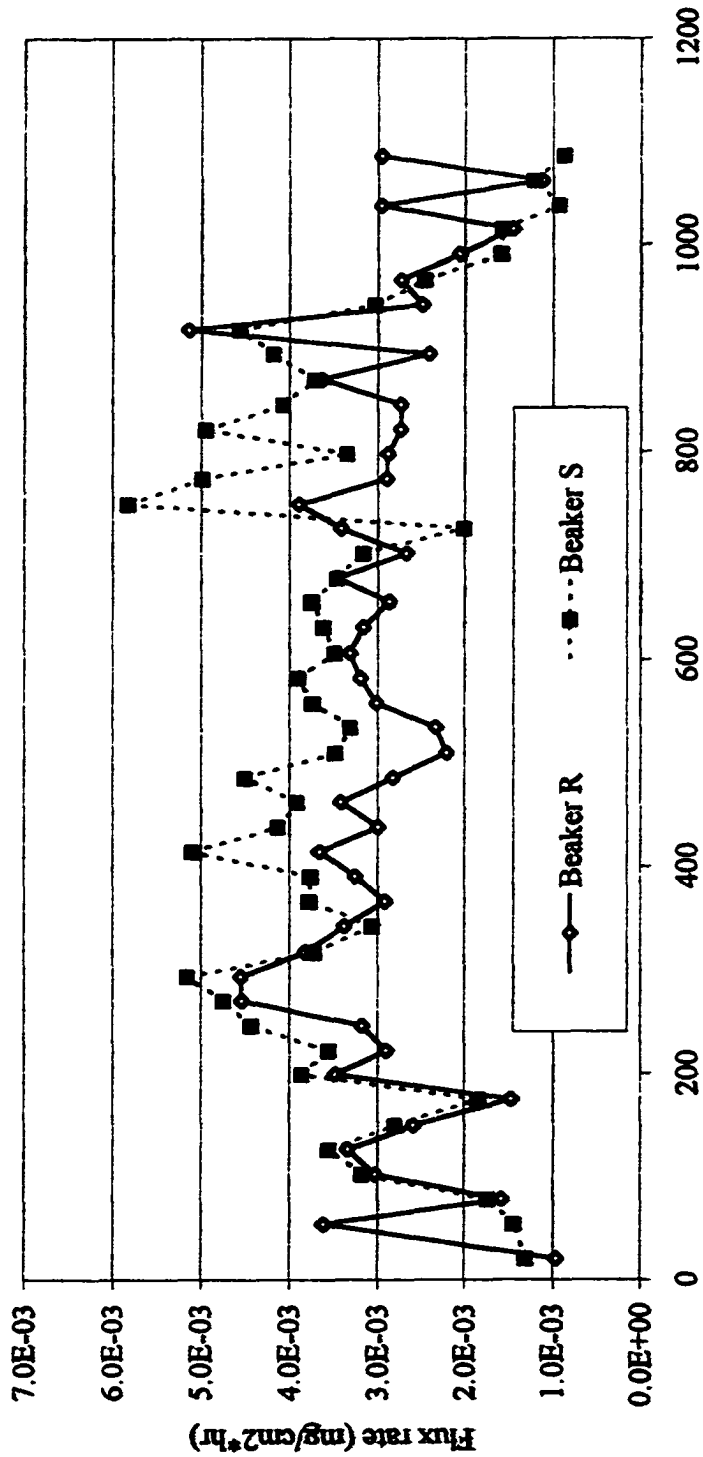

Figure 2.19. TNT static flux from WES soil

Figure 2.20. Static flux of four contaminants from WES soil

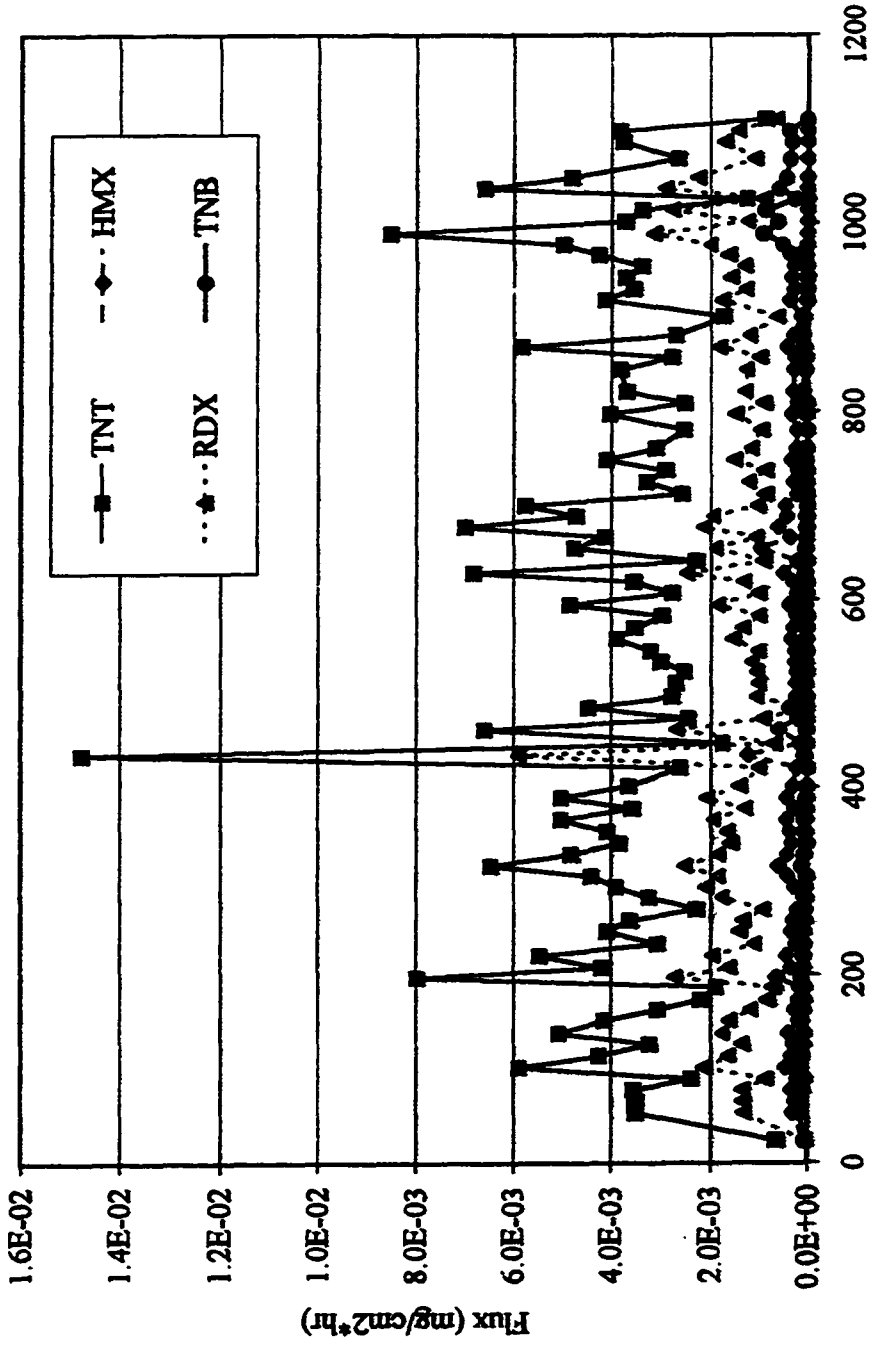

Figure 2.21. Static flux of four contaminants from WES soil: 2 x day

rates than the one time per day sampling regime which is indicative of the affects of perturbing the system from equilibrium. The concentrations from which the flux rates were derived were very close to solubility and thereby indicative of increased water side resistance.

The two different sampling regimes were compared for 3 contaminants in Figures 2.22, 2.23, and 2.24 for TNT, RDX, and HMX respectively. In all cases, the perturbation from equilibrium increased the flux rate. Overall the flux rates appear more constant if averaged over the entire time but more frequent water change provided higher flux rates.

The comparison of sampling scheme results indicate much higher overall flux rates during the twice a day sampling because the driving force is greater, and equilibrium is not achieved. Moreover, the flow rate is basically doubled by the sampling scheme because in one experiment 100 mls head volume was removed in 24 hours whereas the other experiment 100 mls was removed every 12 hours. The increased flux rate in perturbed systems lead to consideration of dynamic systems.

2.6.1 Mass Balance

Soil cores not shown because the initial and final concentration were so high that no significant difference could be demonstrated in the experimental time frame.

2.7 CONCLUSION FOR HIGH CONCENTRATION SOIL STUDIES

Characteristic exponential decay not seen in high concentration soil therefore contaminant behavior was not effectively modeled by the semi-infinite diffusion model. The WES soil demonstrates different transport mechanisms are controlling the movement of pollutants in that soil. It is proposed that due to the high concentration of

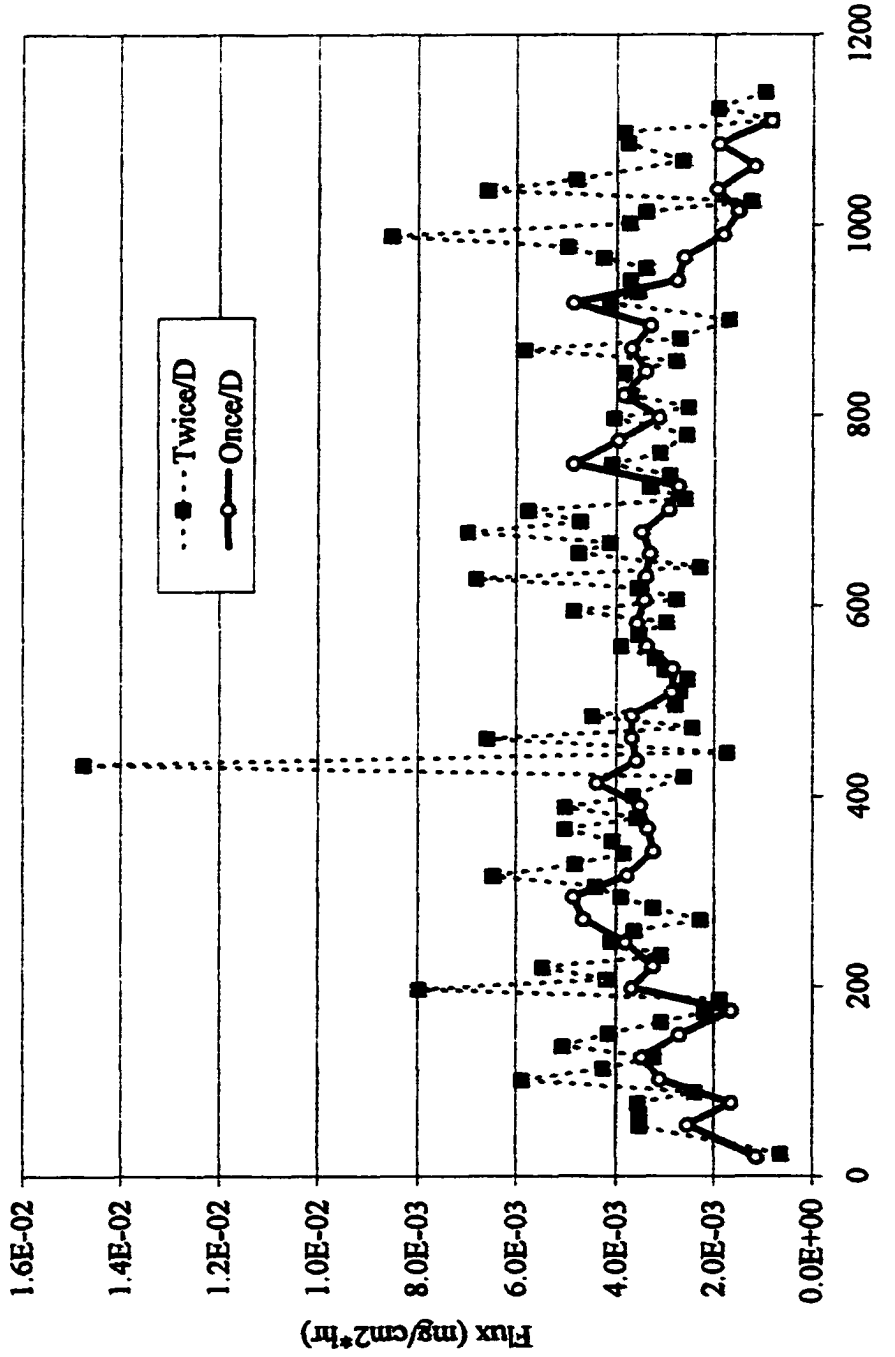

Figure 2.22. TNT static flux comparison

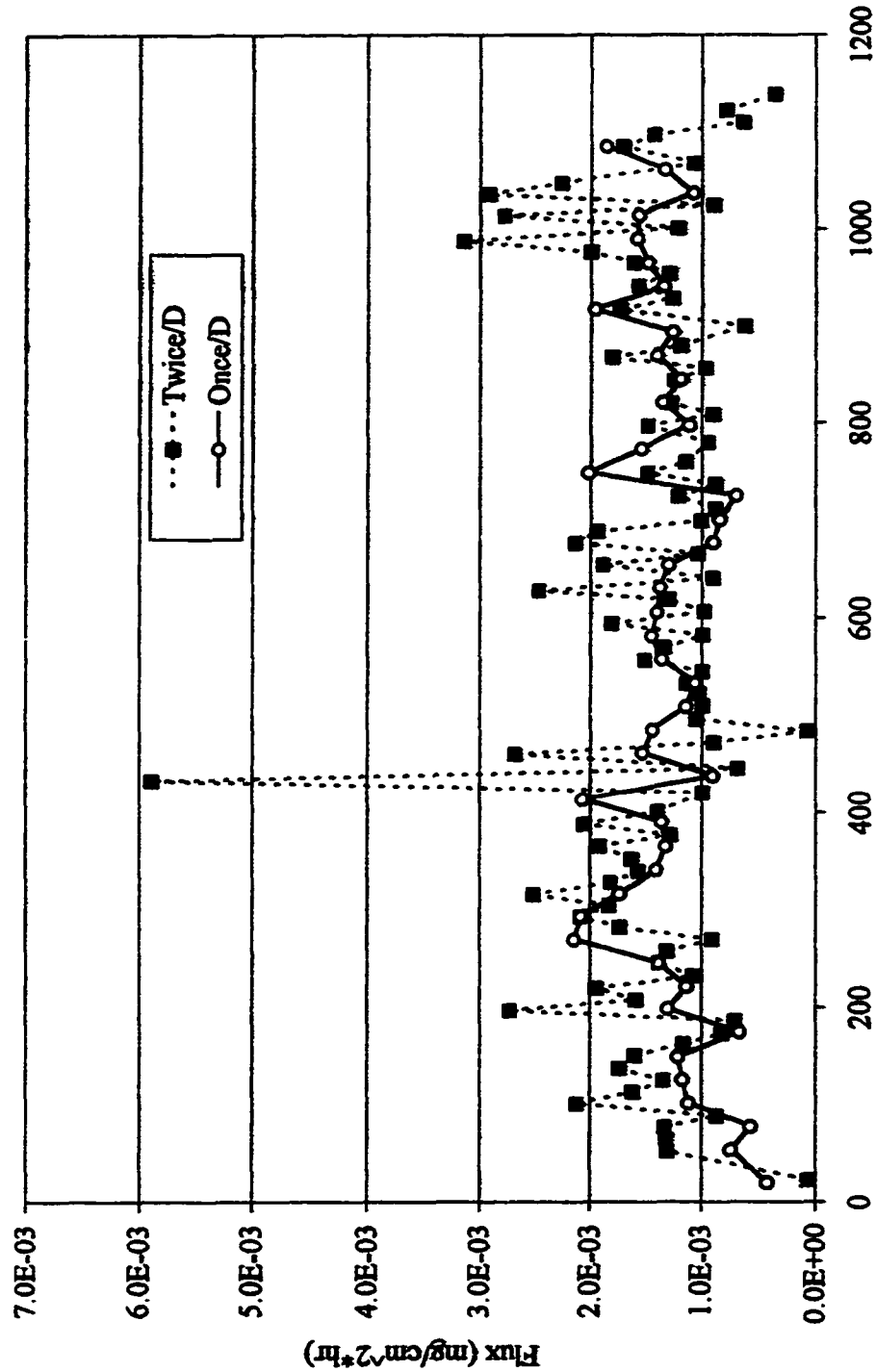

Figure 2.23. RDX static flux comparison

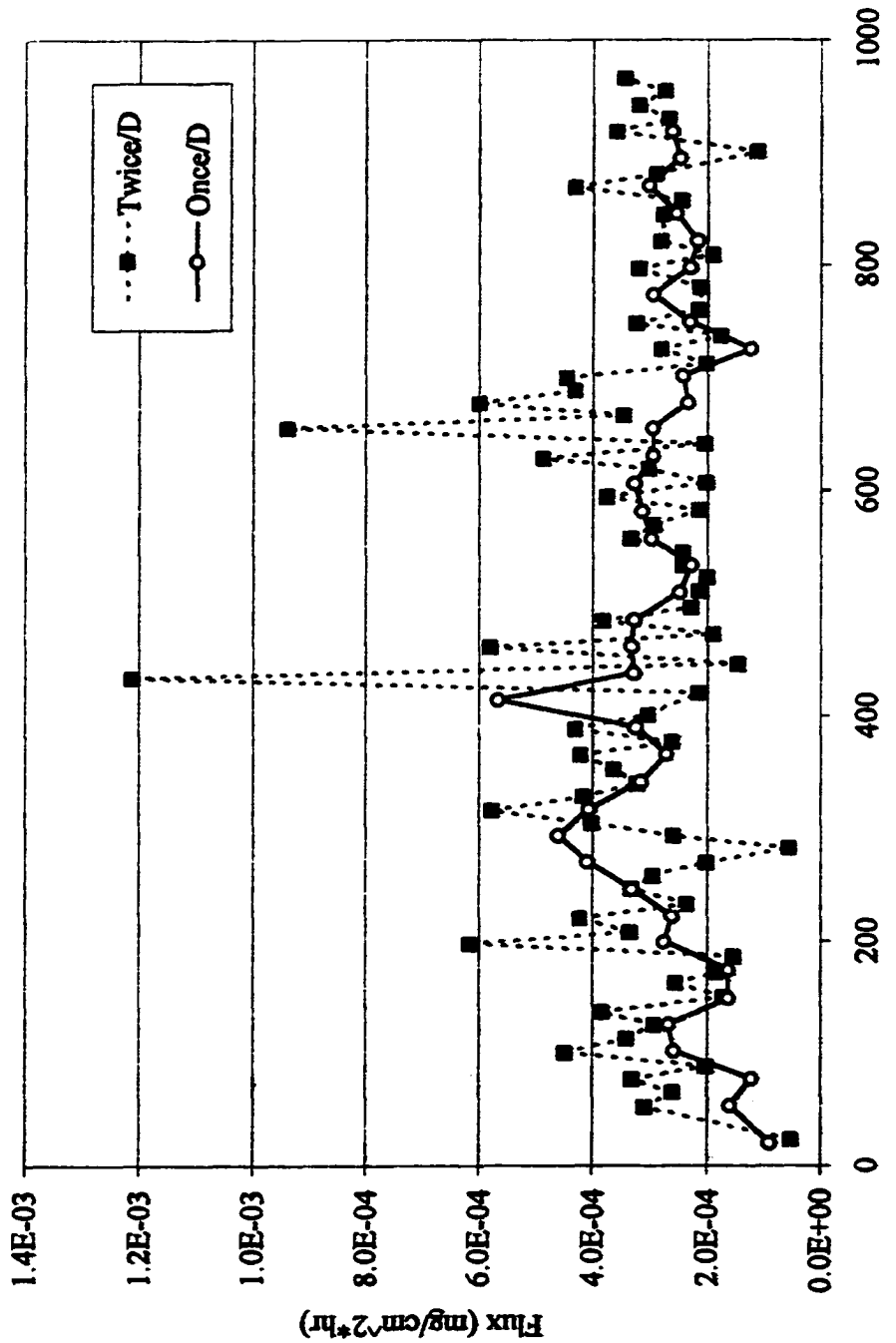

Figure 2.24. HMX static flux comparison

contaminants, the water side resistance is controlling the diffusion rates. The water is saturated with TNT and cannot pick up more contaminant thereby controlling the process.

2.8 DISCUSSION OF STATIC DIFFUSION STUDIES

Soil load is one parameter for determining an applicable diffusion model as can be seen in the two studies presented previously. The partition coefficient describes the ratio of chemical in the soil phase to the chemical in the aqueous phase and is the dominating term in the retardation factor. The initial concentration is a dominant term in the semi infinite diffusion model and is back calculated by dividing soil load by the K_d, again showing the importance of site specific partition coefficients. Therefore chemicals present at levels near their solubility would have an added resistance, which was not addressed in this study. The water side resistance controls the transport in the high concentration soil so cannot be effectively modeled by the semi infinite diffusion model presented here. Simple diffusion models were adequate for long term approximations of contaminant flux rates from static beds into overlying water. This predictive tool assesses the minimum transport rate for biota exposure and uptake.

2.9 ADVECTIVE ENHANCED LEACHING TNT STUDY INTRODUCTION

This research was part of a larger project to validate the feasibility of a unique, low cost, two stage reactor system. This design is called a riffle-bed reactor and was proposed for TNT remediation as an alternative to conventional extraction beds. As stated the riffle-bed is composed on two parts; the first is a TNT leaching unit and the other is a plant catalyzed (hydroponic) bioreactor. Valsaraj et al., (1998) presented

this system previously. Water is sprayed onto the bed and carries contaminants into the plant pool where degradation reactions occurs. Plant exposure concentrations will be dependent on concentrations leached from the bed. Many researchers are examining the uptake and capacity of plants and trees for phytoremediation potential (Pavlostathis et al., 1998; Schnoor, 1997; Jones, 2001; Gomez, 2000). The TNT diffusion studies were aimed at modeling flux rates for input to plant bioreactor systems.

Baseline diffusion rates from quiescent saturated beds were determined first. Simple diffusion models were adequate for long-term approximations of flux rates for contaminants in large areas of contaminated soils and sediments in quiescent conditions. Enhancement by advection could then be assessed in the dynamic bed studies, which were designed to maximize flux rates of contaminants. Quantification of transport processes were examined by fitting experimental flux rates to an appropriate single parameter diffusion model (Choy and Reible, 2000) and deriving an effective diffusivity, D_e, using the commercially available software called Mathcad®.

2.10 MATERIALS AND METHODS

Soil collection and preparation procedure were discussed previously and are the same for the present work.

2.10.1 Sheet Flow Leaching Bed

The experimental apparatus, a sheet flow leaching bed (SFLB), is shown in Figure 2.25. Laboratory scale leaching beds were designed with 5 cm depth by 5 cm width and 50 cm in length. The soil leaching bed holds a shallow layer of contaminated soil approximately 3 cm in depth. Water was pumped into a chamber

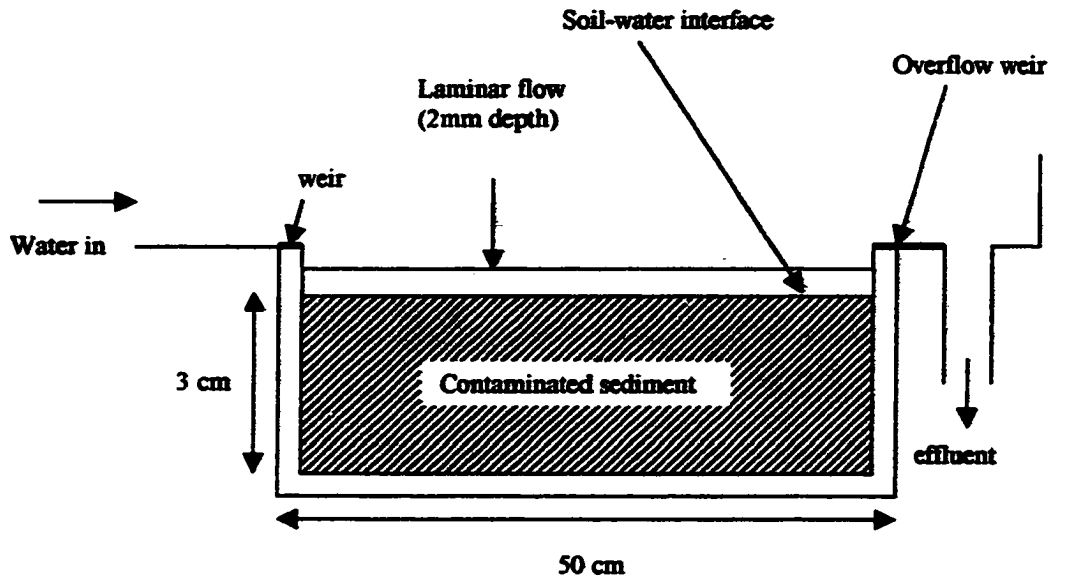

(Side View)

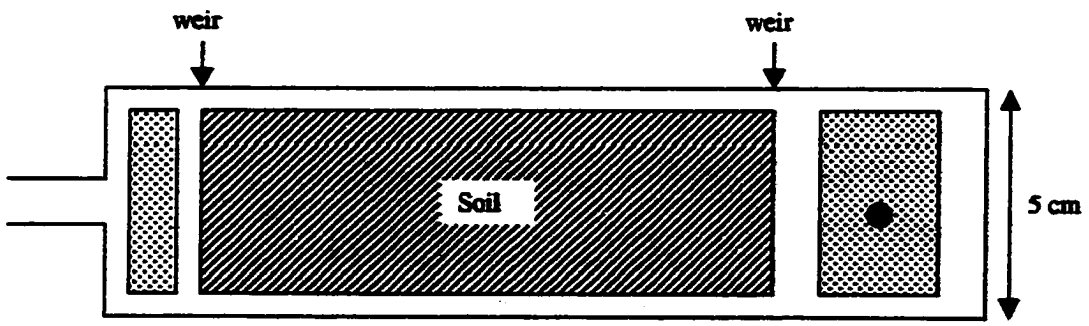

(Top View)

Figure 2.25. TNT sheet flow leaching bed (SFLB)

equipped with a weir at the front of the bed that allowed laminar flow over the surface of the soil. The water layer was 2-3 mm depth across the bed due to an additional weir at the end of the bed. The weirs provided an even flow and prevented soil movement as the water moved over the surface. An outlet chamber located at the end of the bed allowed for sampling without disturbing the water surface.

2.10.2 TNT SFLB Set up

To achieve soil homogeneity, the GIT soil (low concentration) and WES soil (high concentration) were mixed, sieved and ground. The prepared soil was saturated with deionized water overnight in a bucket. The next day the resulting mud was placed into the leaching bed using spoon and spatula. The beds were then "thumped" (dropped from a low height repeatedly) against the table to remove air pockets and settle the soil evenly. Prior to initiation of the experiment, the pump was turned on and water flowed onto the soil until the area between the weirs held 2 mm of water. This water was allowed to remain in contact with the soil for times ranging from 8 to 16 hours before the experiment was initiated to allow soil-water equilibrium to be established. Initial experiments had continuous flow of water, at a rate of approximately 200 ml/hr, to determine a baseline steady state TNT concentration and flux rate. Flow rates were calculated by dividing the measured sample volume by the time required for collection of the sample. The actual flow rates ranged from 100-300 ml/hr. Samples were collected at the effluent outlet in 20 cc amber jars with Teflon lined lid and stored at 5°C until analysis by HPLC.

2.10.3 Flow Regime

The initial dynamic bed experiments examined advective enhanced diffusion with a continuous flow rate. Several studies were performed to model the impact of increased driving force by contaminant removal at the surface of the soil or sediment, termed advective enhanced leaching. Initially, the flow rate was held constant and labeled continuous flow until a "steady state" was achieved.

Following a period of continuous flushing of water across the surface, the pump was shut off for varying periods to perturb the system. Pulsing the flow rate was expected to increase the flux rates by increasing desorption and dissolution of TNT. Two pumping schemes were tested other than simple continuous flow; 1) the pump was turned on and a sample was collected (approximately 10 - 20 minutes) but the pump was turned off immediately after the sample, 2) pump turned on at 6 a.m. and run continuously until 6 p.m. These two regimes are called "pump on-off" and "pump on day-off night," respectively. Samples were taken every few hours during the course of the study. The intent of "pump off" time was to see if flux rates could be enhanced by non-equilibrium conditions expected to occur in cyclic flow systems compared to steady state systems.

2.10.4 Nitroaromatic Sample Preparation for HPLC

From the aqueous effluent sample, an aliquot was mixed with an equal volume HPLC grade acetonitrile in glass scintillation vials. The mixture was then swirled to homogenize. Using a 5 cc syringe, 5 mls of mixture was filtered thru 0.2 micron PTFE syringe filter. The first 2mls were wasted back into scintillation vial while the remaining solution went into the glass 1.8 ml crimp capped vial for HPLC analysis.

This wastage was done to prevent error due to contaminant binding on filters. The lid was sealed on the HPLC vial using a crimper and stored in refrigerator until analysis.

2.10.5 Experimental Flux Calculation

The experimental flux can be calculated by:

$$Flux = (C^* Q)/A \qquad (2.6)$$

where C is concentration (mg/L), Q is the flow rate (L/hr), and A is SFLB area (cm^2) thereby yielding flux units of mg/cm^2*hr. The flux rate is a measure of the mass per area per time and will be used to quantify contaminant movement in this study.

2.10.6 Theoretical Flux Determination

The effluent mass values in the mass balance were calculated by two methods. The first method was the simple back calculation as:

$$M = F * A * \Delta T \qquad (2.7)$$

where M is mass of TNT, F is the calculated flux rate from equation 1, and delta t is the time between sample n and sample n+1. For ease of discussion, the resulting extraction efficiencies are summed in 24 hour increments to compare flow regimes.

2.10.7 Chemical Analysis

Concentrations of contaminants, namely TNT, RDX, HMX and TNB were monitored using high pressure liquid chromatography (HPLC) following EPA SW-846 method 8330 modified to a flow rate of 0.9 ml/min and 50/50 water /methanol mobile phase. The column compartment was maintained at 40°C for a run time of 15 minutes. The column is a Hewlett Packard 5 um ODS Hypersil 4.6 mm X 25 cm cartridge column. This research was conducted on a Hewlett Packard 1090 series II chromatograph using HPChemStation software with photodiode array detector at 254

nm. Standards were made every two months and the calibration curve regenerated. Daily HPLC runs had standards at beginning and end to validate the current standard curve.

2.10.8 Data Analysis

Graphing and calculations of flux were performed utilizing the Microsoft Excel® spreadsheet software in Microsoft Office 2000®. Spreadsheets were constructed to calculate the flux rates and mass balances from the reported concentrations. Graphs and tables were constructed from these spreadsheets and will be shown in results section.

2.10.9 Model Analysis

Quantification of chemical movement was done by determination of pollutant flux rates. The SFLB effluent concentrations were used to calculate the flux rate of contaminant at the soil-water interface. The experimentally calculated flux was fitted to the solution for the advection dispersion equation using Mathcad® to determine the effective diffusivity (Choy and Reible, 2000). The first equation, 2.8 presents the case 2 model which assumed zero contaminant concentration at the surface.

$$\text{Flux} = \frac{2 \cdot D_e \cdot C_o}{H_z} \sum_{n=1}^{\infty} \exp\left(\frac{D_e}{R_f} \cdot \alpha_n^2 \cdot t\right) \qquad (2.8)$$

where D_e is the effective diffusivity, C_o the initial concentration, H_z is the depth of the contaminated layer, R_f is the retardation factor, t is time and α_n is defined as

$$\alpha_n = \frac{\pi}{H_z} * \left(\frac{2n-1}{2}\right) \qquad (2.9)$$

Mathcad 2000 Professional® computer software was utilized for higher math functions. Some parameters used in model are calculated from literature values using Mathcad®, are given in Table 2.5. By setting the sum of squared errors equal to zero, Mathcad® is able to iteratively calculate an effective diffusivity which allows model to fit experimental data. Several different models were tested to evaluate which most accurately described the experimental data. The best fit was determined by the smallest value for total sum squared error (SSE).

2.11 RESULTS FOR NITROAROMATIC STUDIES-SFLB

2.11.1 Flux Measurements for Leaching Beds

Figure 2.26 shows the initial TNT peak concentration which tapers off as an exponential decay curve that asymptotically approaches a steady state concentration when the pump is run continuously at one flow rate. The pump was set at one flow setting although variation in flow rates still occurred. The first few samples had higher concentrations and flux rates because the water was saturated with TNT, due to the fact that the system was allowed to equilibrate over night. Therefore, when flow was initiated, a highly contaminated wave of water can be seen coming off the extraction bed. The results will discuss flux rates, not concentration, since they are inherently related as seen in equation 2.6. The flux rate was used in Mathcad® to derive a baseline effective diffusivity for this advective enhanced condition. Figure 2.27 shows the model fit to the experimental flux, yielding a D_e of 5.95E-8 with a correlation coefficient, r, of 0.914. This indicates an adequate fit to the model so varying flow rate was studied next. Due to the previously shown increase in flux rate due to flow perturbation, the flux rate of TNT was expected to spike with changes in flow rate.

Table 2.5. Symbols and values used in Mathcad

Parameter	Symbol	Value	Reference
Porosity	ε	0.46/0.42	Lab determined
Molecular diffusivity	D_m	6.71×10^{-6} cm^2/s	McGrath (1995); Qaisi (1996)
Effective diffusivity	De	$D_e = D_w * \varepsilon^{4/3}$	Calculated
Flow rate	Q	2 to 4 ml/hr	Lab determined
Bulk density	ρ_b	1.38 - 1.53	Lab determined
Particle density	ρ_p	2.57 – 2.64	Lab determined
Retardation factor	R_f	$\varepsilon + \rho_b * K_d$	Calculated
Water side resistance	k	equation	Choy & Reible (2000)
Partition coefficient	K_d	2 - 12 L/kg	Pennington (1988)
Area of beaker Area of bed	A Area	68 cm^2 258.064 cm^2	Lab determined
Initial concentration	C_o	10 mg/L	Lab determined
Octanol/water partition coefficient	K_{ow}	1.84 2.00	Pennington (1988) Rosenblatt et. al., (1989)
Organic carbon partition coefficient	Koc	2.72	Rosenblatt et. at,. (1989)

Figure 2.26. TNT flux under continuous flow in SFLB

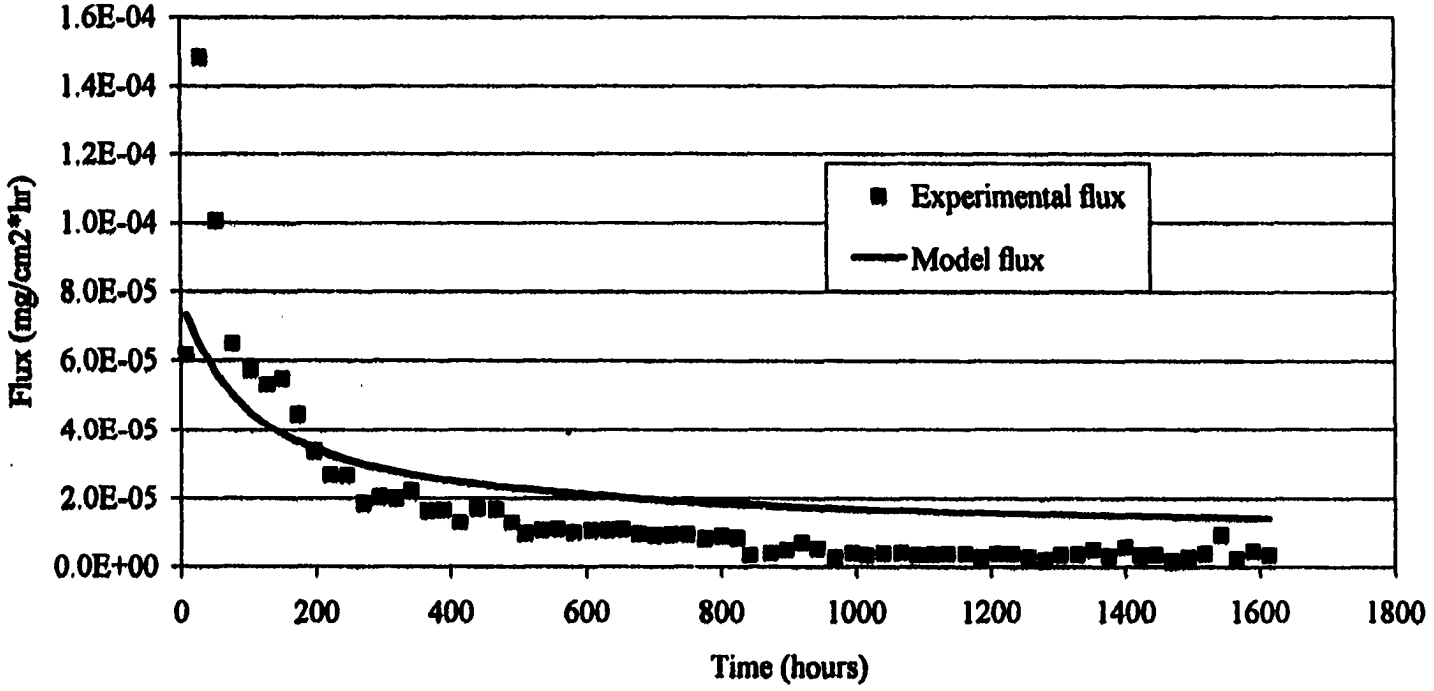

Figure 2.27. TNT experimental flux and model comparison for continuous fast flow

In the following graphs, the flow rate was varied to see the affect on flux. Figure 2.28 and 2.29 show the flow rate and flux rates vs. time for 2 contaminants in the same experiment (TNT and RDX). Both figures clearly indicate the flux dependency on flow. Figure 2.28 presents both flux rate of TNT and flow rate as a function of time to show the dependence of flux on flow. Figure 2.29 examines the behavior of RDX, instead of TNT, in conjunction with varying flow rate. Like TNT, which spiked every time the flow rate spiked, RDX appears to follow that same trend. Figure 2.29 follows the concentration of TNT as the flow regime was changed. This demonstrates the correlation of pulsed flow regime yielding consistently higher flux rates compared with the continuous flow in Figure 2.26.

Figure 2.30 examines three different flow regimes that were tested sequentially. Initially, the flow is continuous but at about 130 hours the flow regime is changed to on in the day but turned off every night. Finally, around 500 hours the flow regime is changed to turning the pump on to take the sample and turning pump off immediately after sampling. This is called "pump on day, off night" and "pump on-off", respectively. Figure 2.30 indicates a pattern of higher contaminant flux rates when the pump was turned off. The flux rates return to the steady state levels as seen in Figure 2.30 in the "pump on day-off night" regime. A saw tooth pattern can be seen in demonstrating the non-equilibrium conditions enhanced flux rates and concentrations. Likewise, the "pump on-off" regime shows spikes of higher flux rates every time a sample was taken but flux rates are not much different than the pump on day-off night regime.

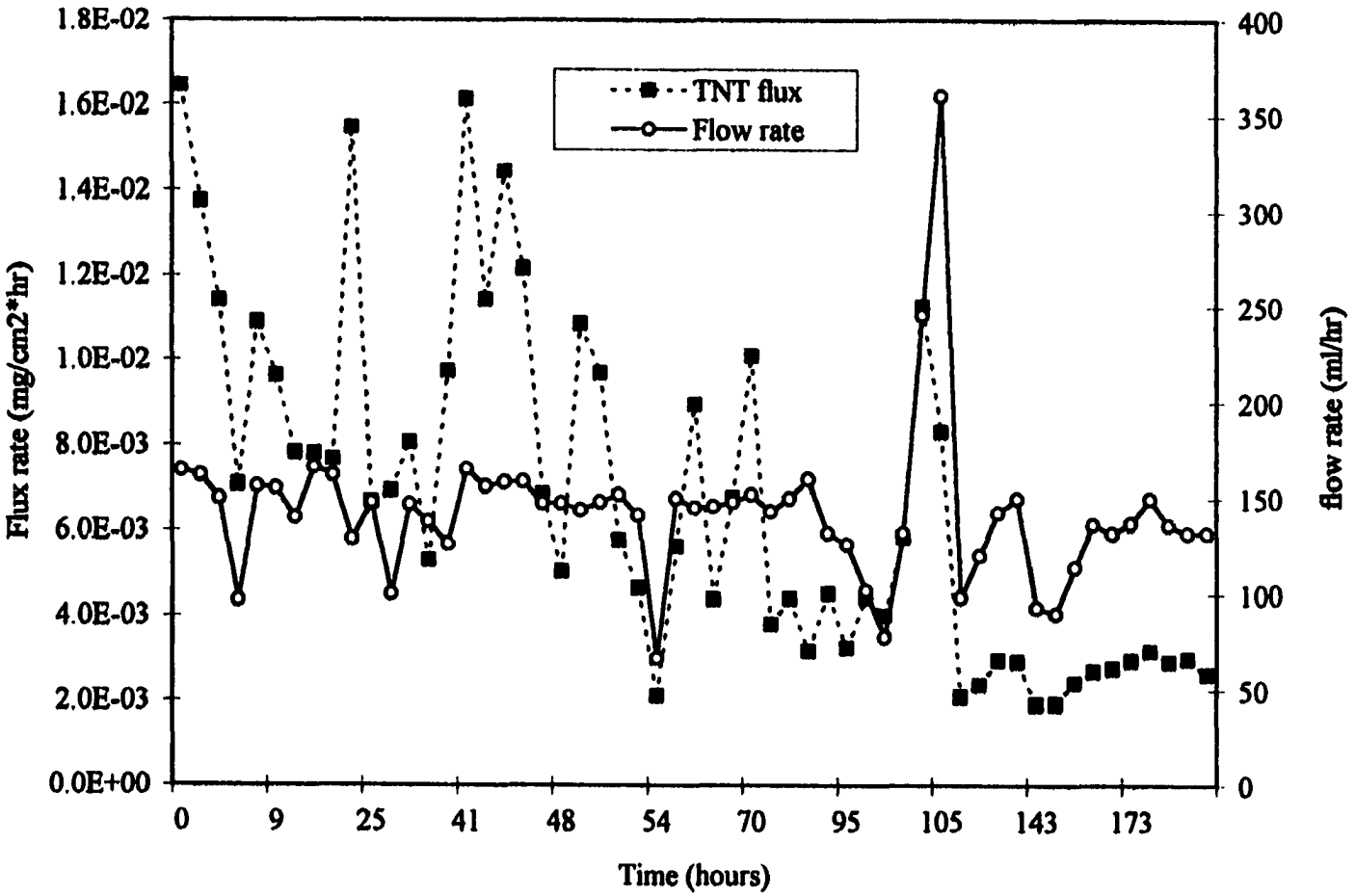

Figure 2.28. TNT experimental flux rate and flow rate from SFLB

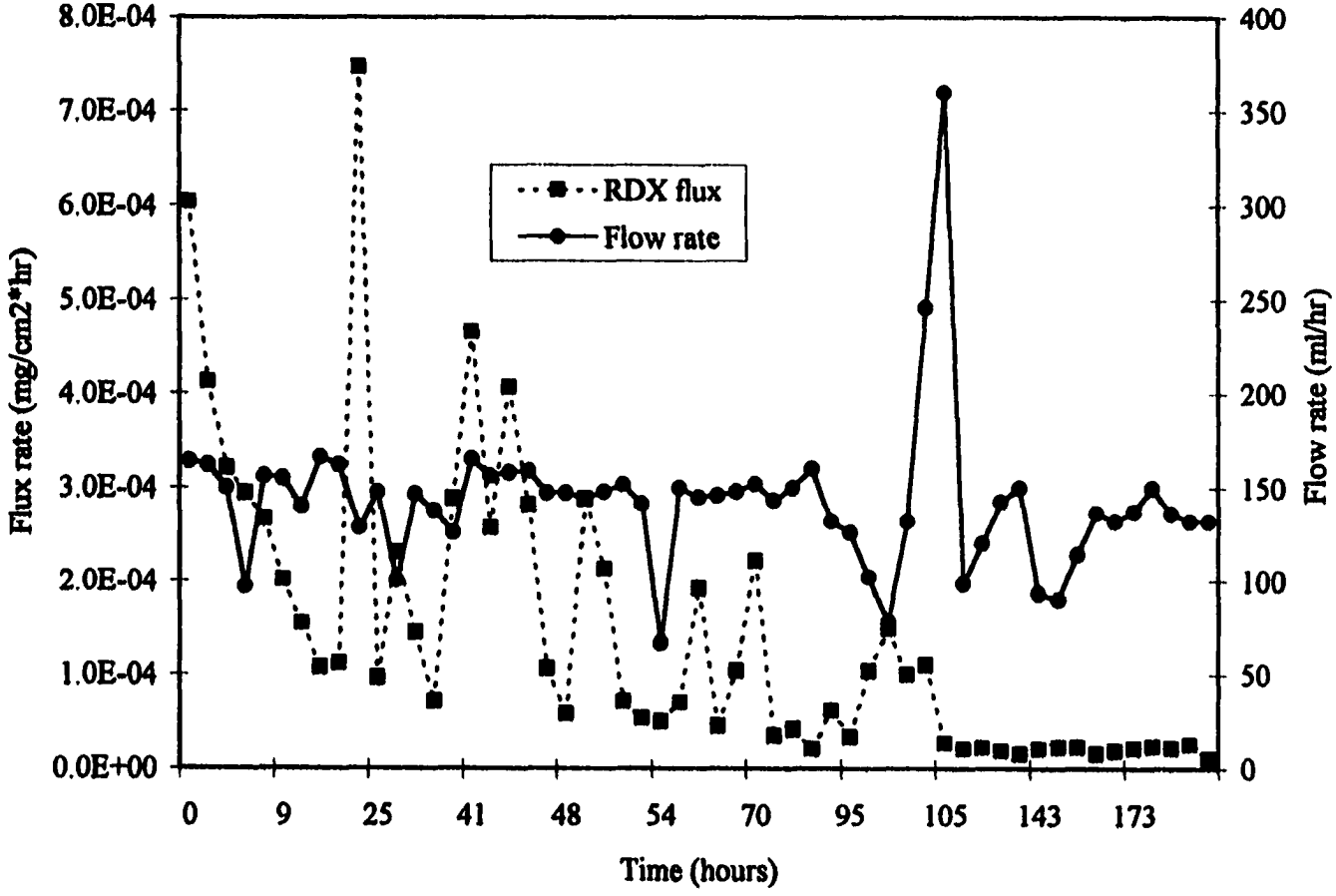

Figure 2.29. RDX experimental flux rate and flow rate from SFLB

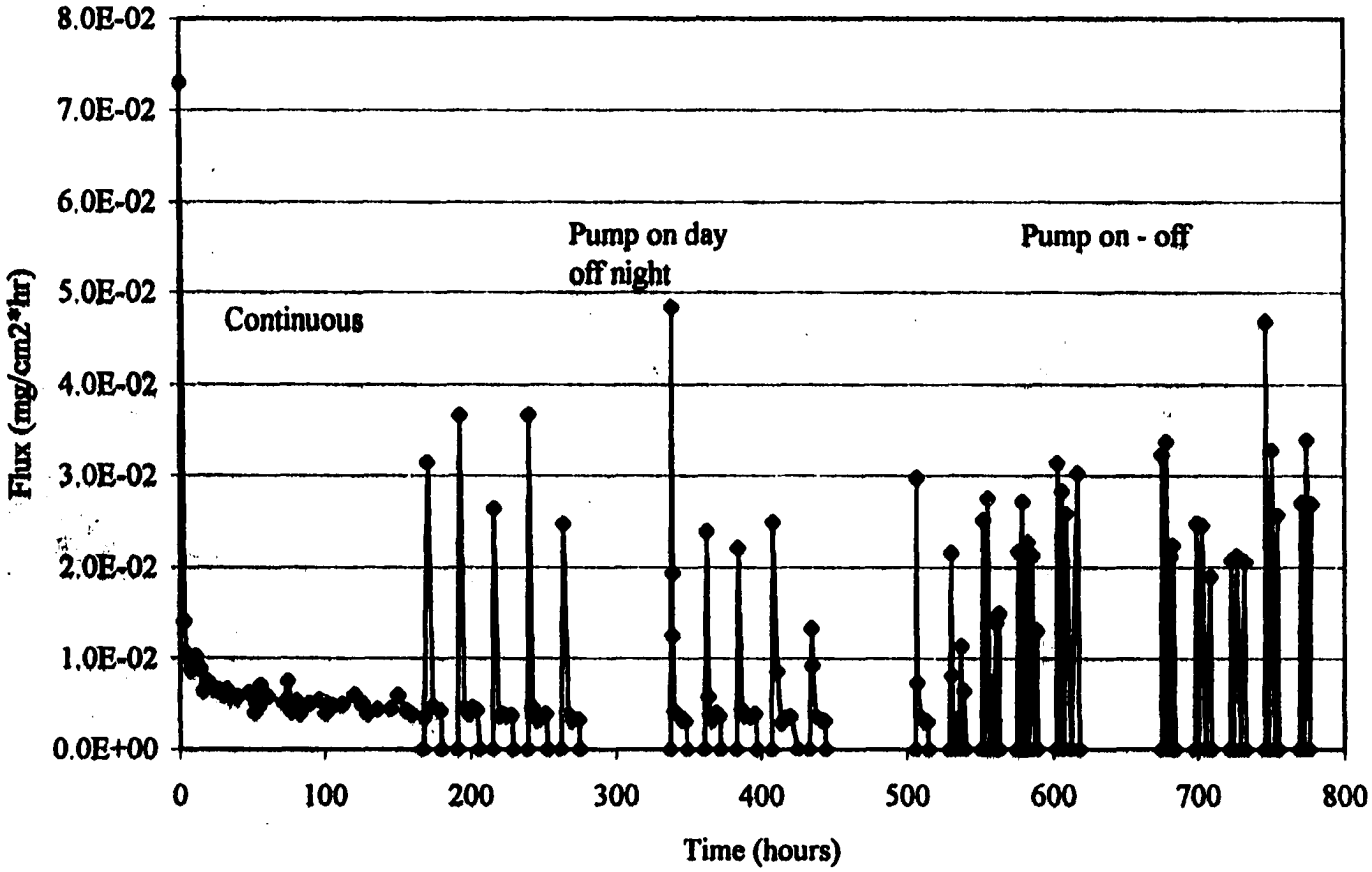

Figure 2.30. TNT experimental flux for all three flow regimes

To determine the effectiveness of the different pumping frequencies the TNT removal rates were compared. Total contaminant removal was determined by calculating the area under the curve. Normally this would involve integrating the curve but because the curve is not a smooth line or known function, the area was approximated using the trapezoid rule numerical method. It subdivides the area of integration into small pieces of known time intervals and approximates the function as a constant function using data points. This approach is valid because the pulsing is a step function and can be adequately approximated by a trapezoid. These 'trapezoids' were summed to determine removal per unit area of leaching bed. Due to the different pumping schemes tested (continuous, on day-off night, on-off), the use a time-based value was not a practical way to compare removal effectiveness. Table 2.6 compares contaminant removal effectiveness in approximately 24 hour intervals (per day) of the different pumping regimes. Table 2.6 indicates a steady state removal rate of 178 - 202 mg TNT/L collected per day. The "pump on day-off night" has an average mg TNT/L removal of 181-185 mg TNT/L collected per day but the "pump on-off" frequency has concentrations of 274-330 mg TNT/L collected per day. It can be inferred from these results that the steady state, i.e., continuous removal efficiency is similar to the "pump on day –off night" regime. The "pump on-off" appears to have the highest TNT removal efficiency and would yield the highest aqueous concentrations. Both extraction beds were shown for the data discussed above in Table 2.6 to indicate the variation among the replicate SFLB's.

No models were found to adequately describe the pulsed flow regimes. One problem is that if the pump is off equation 1 collapses without a flow term. This

Table 2.6. TNT extraction efficiency by flow regime

Flow regime	Time interval (hours)	Efficiency (mg/ml/~d)	Efficiency (mg/ml/~d)
continuous	0 - 24	0.124	0.153
continuous	24 - 48	0.169	0.194
continuous	48 - 72	0.150	0.176
continuous	72 - 96	0.266	0.269
continuous	96 - 120	0.147	0.182
continuous	120 - 150	0.211	0.236
		0.178	0.202
on day, off night	160 - 179	0.310	0.298
on day, off night	180 - 204	0.244	0.198
on day, off night	205 - 229	0.124	0.149
on day, off night	229 - 252	0.152	0.200
on day, off night	253 - 275	0.285	0.251
on day, off night	337 - 348	0.111	0.096
on day, off night	350 - 371	0.136	0.138
on day, off night	372 - 396	0.092	0.161
on day, off night	397 - 420	0.186	0.262
on day, off night	426 - 445	na	0.121
on day, off night	500 - 514	0.214	0.120
		0.185	0.181
pump on-off	529 - 552	0.139	0.098
pump on-off	555 - 579	0.312	0.231
pump on-off	581 - 605	0.417	0.168
pump on-off	602 - 618	0.285	0.403
pump on-off	674 - 699	0.218	0.254
pump on-off	701 - 724	0.281	0.500
pump on-off	726 -749	0.164	0.478
pump on-off	750 - 778	0.374	0.506
		0.274	0.330

system was unable to be modeled but the increased flux rates confirmed that non-equilibrium conditions need to be further examined with varying flow rates.

2.12 CONCLUSIONS

The D_e values determined for the AAAP soil changed with depth. Interestingly the surface soils (within six inches of surface) are between 4-7 E^{-5} cm^2/s, whereas the soil from 6 inches to 2 feet depth has an effective D_e between 2.5-3.5 E^{-7} cm^2/s. The soil from the ditch has an effective diffusivity of 5.68 E^{-7} cm^2/s, indicating the sediment had different characteristics which affect the movement of pollutants. The high concentration soils indicated that models are constrained by physical parameters, i.e., solubility limit of the contaminant due high soil load. Due to the high sorptive capacity of most soils in comparison to the water solubility of TNT, the partition coefficient and contaminant load soil are important site parameters. The static bed studies lead to the dynamic leaching beds with perturbed flow regimes. The spikes in the concentration and therefore flux rates demonstrates the pulsed flow regimes prevented equilibrium conditions, thereby increasing leaching efficiency. Partitioning may be affected by other contaminants present but flow rate impacts dissolution and desorption and therefore important to understand for fate and transport. Increased flux rates could yield increased leaching of contaminants for transport to a receptor, such as trees and plants, which may be utilized in a remedial plan

The purpose of these models was to quantify the diffusive transport processes involved in pollutant release from bed soil and to provide a starting point for estimation of pollutant release rates. Experimental data from the aqueous phase was fitted to a model in order to determine the baseline effective diffusivity in low level

contaminated soil. The modeling results indicate site specific soil properties, particularly the partition coefficient, impact pollutant transport. Once the simple diffusion flux rates were determined, the system was changed to examine varied flow conditions to increase the leaching efficiency. By changing flow regime or initial soil load, the system was not modeled with the simple diffusion solution. The SFLB demonstrated increased flux rates in simulated natural systems. By comparing the pump on day off night to pump on-off, it can be seen that the more frequently the system is perturbed, the more efficient the contaminant removal. The high values seen in the extraction efficiency may be an artifact of how the trapezoids were calculated but are comparable to each other. Colloid enhanced transport may have contributed to the near- solubility extraction efficiency values.

Understanding how variations in flow affect transport processes can be advantageous in a riffle bed system, or engineered plant contact reactors. More work is needed for modeling of these highly unstable systems but the preliminary results indicate the local equilibrium is established quickly. This fact supports the validity of the local equilibrium assumption. The changing flow regimes reflect the impact that rainfall events can have on contaminant transport processes.

2.13 REFERENCES

Bhadra, R., R.J. Spanggord, D.G. Wayment, J.B. Hughes, and J.V. Shanks. 1999. Characterization of Oxidation Products of TNT Metabolism in Aquatic Phytoremediation Systems of Myriophyllum aquaticum. Environmental Science and Technology Vol. 33, No. 19, 3354-3361.

Boopathy, R., M. Blad Wilson, and C.F. Kulpa. 1993. Anaerobic Removal of 2,4,6-Trinitrotoluene (TNT) under Different Electron Accepting Conditions: Laboratory Study. Water Environment Research Vol. 65, No. 3, 271-275.

Boopathy, R. M. Blad Wilson, D.D. Montemagno, J.F. Manning, Jr. and C.F. Kulpa. 1994. Biological Transformation of 2,4,6-Trinitrotoluene (TNT) by Soil Bacteria Isolated from TNT-Contaminated Soil. Bioresource Technology, Vol. 47, 19-24.

Bradley, P.M., F.H. Chapelle, J.E. Landmeyer, and J.G. Schumacher. 1994. Microbial Transformation of Nitroaromatics in Surface Soils and Aquifer Materials. Applied and Environmental Microbiology, Vol. 60, No. 6, 2170-2175.

Caserett and Doull,'s Toxicology: The Basic Science of Poisons, Fourth edition. 1991. Amdur, Doull, and Klaassen [Eds]. Pergamon Press, Inc. N.Y., N.Y.

Chou, T.W., and R.J. Spanggord. 1981. Part A: Biotransformation of Nitroaromatic Compounds as a Function of Structure: Environmental Fate Studies on Certain Munition Wastewater Constitiuents, Phase III, Part. 2, Laboratory studies. Report AD-A133987. R.J. Spanggord, W.R. Mabey, T. Milll, T.W. Chou, J.H. Smith and S. Lee Eds. U.S. Army Medical Research and Development Command, Ft. Detrick, Frederick, MD, 2-20.

CRC Handbook of Chemistry and Physics. 1995. D.R. Lide [Ed]. CRC Press, Boca Raton, Florida.

Deane, G., Z. Chroneer, and W. Lick. 1999. Diffusion and sorption of Hexachlorobenzene in sediments and saturated soils. Journal of Environmental Engineering, Vol. 125, No. 8., 689-696.

Dilley, J.V., C.A. Tyson, R.J. Spanggord, D.P. Sasmore, G.W. Newell and J.C. Dacre. 1982. Short-term Oral Toxicity of 2,4,6-Trinitrolouene in Mice, Rats and Dogs. Journal of Toxicology and Environmental Health Vol. 9, 565-586.

Funk, S.B., D.J. Roberts, D.L. Crawford, and R.L. Crawford. 1993. Initial-phase Optimization for Bioremediation of Munition Compound–Contaminated Soils. Applied and Environmental Microbiology Vol. 59, No. 7, 2171-2177.

Gordon, L. and W.R. Hartley. 1989. Health Advisory on 2,4,6-Trinitrotoluene. U.S. Environmental Protection Agency.

Hatzinger, P. B., and M. Alexander. 1995. Effect of Aging of Chemicals in Soil on Their Biodefradability and Extractability. Environmental Science and Technology 29, (2): 537-545.

Kaplan, D.L., and A.M. Kaplan. 1982. 2,4,6-Trinitrotoluene –Surfactant Complexes, Biodegradability, Mutatgenicity and Soil Leaching Studies, Technical Report NATICK/TR-82/006.

Manning, J.F. Jr., R. Boopathy, and E.R. Breyfogle. 1996. Field Demonstration of Slurry Reactor Biotreatment of Explosives-Contaminated Soils. Report number SFIM-AEC-ET-CR-96178. U.S. Army Environmental Center (USAEC) Aberdeen Proving Ground, MD

Manning, J.F. Jr., R. Boopathy, and C.F. Kulpa. 1995. A Laboratory Study in Support of the Pilot Demonstration of a Biological Soil Slurry Reactor. Report number SFIM-AEC-TS-CR-94038. U.S. Army Environmental Center (USAEC) Aberdeen Proving Ground, MD

McCormick, N.G., J.H. Cornell, and A.M. Kaplan. 1976. Microbial Transformation of 2,4,6-Trinitrotoluene and other Nitroaromatic Compounds. Applied and Environmental Microbiology. Vol. 31, No. 6, 949-58.

McGrath, C. J. 1995. Review of Formulations for Processes Affecting the Subsurface Transport of Explosives. Technical Report IRRP-95-2, U.S. Army Engineer Waterways Experimental Station, Vicksburg, MS.

Merck. 1983. The Merck Index. 10th Ed. Merck and Co.. Rahway, NJ.

Pavlostathis, S.G., K.K. Comstock, M.E. Jacobson, and F.M. Saunders. 1998. Transformation of 2,4,6-Trinitrotoluene by the Aquatic Plant *Myriophyllum spicatum*. Environmental Toxicology and Chemistry, Vol. 17, No. 11, 2266-2273.

Pennington, J.C. 1988. Soil Sorption and Plant Uptake of 2,4,6-Trinitrotoluene: A Dissertation. Louisiana State University, Baton Rouge, Louisiana.

Qaisi, K.M., K.S. Ro, D. Reible, L.J. Thibodeaux, K.T. Valsaraj, and W.D. Constant. 1996. Transport Process of TNT from Flooded Highly Contaminated Surface Soil Bed. Journal of Environmental Science and Health, Part A, Vol. 10, 2515-2532.

Qaisi, K.M., L.J. Thibodeaux, K.S. Ro, K.T. Valsaraj, and D.D. Adrian. 1996. A Proposal for a Field-Scale Pilot Demonstration Unit for Bioremediation of TNT Contaminated soil. Journal of Environmental Science and Health, Part A, Vol. 9, 2287-2294.

Ro, K.S., A. Venugopal, D.D. Adrian, D. Constant, K. Qaisi, K.T. Valsaraj, L.J. Thibodeaux, and D. Roy. 1996. Solubility of 2,4,6-Trinitrotoluene (TNT) in Water. Journal of Chemical Engineering Data Vol. 41, No. 4, 758-761.

Rosenblatt, D.H., Burrows, E.P., Mitchell, W.R., and D.L. Parmer. 1989. Organic Explosives and Related Compounds *In* The Handbook of Environmental Chemistry. O. Hutzinger [Ed]. Springer-Verlag, Germany

Rosenblatt, D.H. 1986. Contaminated soil cleanup objectives for Cornhusker Army Ammunition Plant. Plant Technology Report 8603, U.S. Army Medical Bioengineering Research Development Laboratory, Ft. Detrick, MD.

Sax, N.I. 1963. Dangerous Properties of Industrial Materials, 2nd Edition. Reinhold Publishers, N.Y., N.Y.

Schnoor, J.L. Phytoremediation. 1997. Technology Evaluation Report TE-98-01. Ground-Water Remediation Technologies Analysis Center. Pittsburgh, PA.

Schnoor, Jerald, L. 1996. Environmental Modeling: Fate and Transport of Pollutants in Water, Air and Soil. John Wiley and Sons, Inc. New York, New York.

Soil Science Society of America. 1986. Standard Methods.

Urbanski, T. 1964. Chemistry and Technology of Explosives. MacMillan Publishing Co., N.Y., N.Y.

U.S. Army. 1984. Draft Final Interim Record of Decision for Alabama Army Ammunition Plant, Childersburg, Alabama.

Valsaraj, K.T., K.M. Qaisi, W.D. Constant, L.J. Thibodeaux, and K.S. Ro. 1998. Diffusive Transport of 2,4,6-Trinitrotoluene (TNT) from Contaminated Soil to Overlying Water. Journal of Hazardous Materials 59: 1-12.

Venugopal, A. TNT Dissolution Mass Transfer in Contaminated Sites. A Thesis. Louisiana State University, May, 1996.

Won, W.D., R.J. Heckly, D.J. Gover, and J.C. Hoffsommer. 1974. Metabolic Disposition of 2,4,6-Trinitrotoluene. Applied Microbiology Vol. 27, No. 9, 513-516.

CHAPTER 3. CHLORINATED BENZENE TRANSPORT: LABORATORY MODEL

3.1 INTRODUCTION

Hexachlorobenzene (HCB) is one of the harbinger compounds at the PPI site and its degradation products include chlorobenzene, dichlorobenzenes, and trichlorobenzenes. The initial experiments were performed with a single individual contaminant, chlorobenzene and 1,3 dichlorobenzene, in order to better understand the transport of a single compound in the environment. Because natural systems rarely contain one pollutant, later experiments were performed utilizing a mixture of four components: chlorobenzene (MCB), 1,2-dichlorobenzene, (1,2-DCB) 1,3-dichlorobenzene (1,3-DCB), and 1,2,4-trichlorobenzene (TCB). One aspect of the chlorinated benzene studies was examination of the impact of multiple contaminants on desorption and dissolution in a dynamic system. This research investigates two previously described models with application to experimental data in order to quantify lower chlorinated benzene compound movement from sediment into overlying water under dynamic laboratory flow conditions simulating Baton Rouge Bayou.

The compounds utilized in this study are relatively mobile compared to HCB in sediment/soil systems-as seen by properties in Tables 3.1, 3.2, 3.3 and 3.4. As discussed previously, chemical properties impact mass transport.

If a pollutant is sorbed or bound to sediment particles, it will have a low mobility and will not be transported easily off site nor will it be available for biotransformation. If a pollutant is considered highly mobile, it can easily leave the site and may contaminant surface or ground waters.

Table 3.1. MCB physical and chemical properties

Parameter	Value	Reference
CAS RN	108-90-7	CRC Handbook
Empirical formula	C_6H_5Cl	CRC Handbook
Molecular Mass	112.56g/mol	CRC Handbook
Henry's Law constant, K_h	3.58E-3 $atm*m^3*mol^{-1}$ .0037 $atm*m^3*mol^{-1}$	www.mvp-wc.usace.army.mil Watts, 1979
Density	1.1058 $g*cm^{-3}$	CRC Handbook
Vapor Pressure	8.8E1 mm Hg	www.mvp-wc.usace.army.mil
Boiling Point	131.7 C	CRC Handbook
Melting Point	-45.2 C	CRC Handbook
Water Solubility (25C)	500 mg/L 503 mg/L	www.mvp-wc.usace.army.mil Thibodeaux, 1996
EPA Drinking water Standard	0.1 mg/L	Schnoor, 1996
Octanol-Water Partition Coeffiecient, log K_{ow}	6.9E2 2.71 –2.98	www.mvp-wc.usace.army.mil Watts, 1997
Organic Carbon Partition Coefficient, log K_{oc}	2.46	Thibodeaux, 1996
Diffusion coefficient (25C)	9.09E-6 cm^2/s	Thibodeaux, 1996
Carcinogen	No classification	Watts, 1997
Oral RfD	0.02	Watts, 1997

Table 3.2. 1,3-DCB physical and chemical properties

Parameter	Value	Reference
CAS RN	541-73-1	CRC Handbook
Empirical formula	$C_6H_4Cl_2$	CRC Handbook
Molecular Mass	147.0 g/mol	CRC Handbook
Henry's Law constant, K_h	$2.63E^{-3}$ atm*m^3*mol^{-1} $3.60E^{-3}$ atm*m^3*mol^{-1}	http://esc.syrres.com/interkow Watts, 1979
Density	1.2884 g*cm^{-3}	CRC Handbook
Vapor Pressure	2.15 mm Hg	http://esc.syrres.com/interkow
Boiling Point	173 C	http://esc.syrres.com/interkow
Melting Point	-24.8 C	CRC Handbook
Water Solubility (25C)	125 mg/L	http://esc.syrres.com/interkow
EPA Drinking water Standard	75 ug/L	Schnoor, 1996
Octanol-Water Partition Coefficient, log K_{ow}	3.53 3.38 –3.60	http://esc.syrres.com/interkow Watts, 1997
Organic Carbon Partition Coefficient, log K_{oc}	3.03-3.14	Watts. 1997
Diffusion coefficient (25C)	8.33E-6 cm^2/s	Extrapolated
Carcinogen	No classification	Watts, 1997
Toxicity	Mouse LD_{50} 1062mg/kg	http://ntp-server.niehs.nih.gov/htdocs
Oral RfD	Pending	Watts, 1997

Table 3.3. 1, 2-DCB physical and chemical properties

Parameter	Value	Reference
CAS RN	95-50-1	CRC Handbook
Empirical formula	$C_6H_4Cl_2$	CRC Handbook
Molecular Mass	147.0 g/mol	CRC Handbook
Henry's Law constant, K_h	.0019 atm*m^3*mol^{-1}	Watts, 1997
Density	1.3059 g*cm^{-3}	CRC Handbook
Melting Point	-16.7 C	CRC Handbook
Boiling Point	180.0	CRC Handbook
Water Solubility (25C)	.008396 g/100mL	www.chemfinder.com
EPA Drinking water Standard	0.6 mg/L	Schnoor, 1996
Octanol-Water Partition Coefficient, log K_{ow}	3.38 -3.55	Watts, 1997
Organic Carbon Partition Coefficient, log K_{oc}	2.99 – 3.26	Watts, 1997
Diffusion coefficient (25C)	8.33 E-6 cm^2/s	Extrapolated
Carcinogen	No classification	Watts, 1997
Oral RfD	0.09	Watts, 1997

Table 3.4. 1, 2,4 -TCB physical and chemical properties

Parameter	Value	Reference
CAS RN	120-82-1	CRC Handbook
Empirical formula	$C_6H_3Cl_3$	CRC Handbook
Molecular Mass	181.45 g/mol	CRC Handbook
Henry's Law constant, K_h	0.00232 $atm*m^3*mol^{-1}$	Watts, 1997
Density @ 25 C	1.459 $g*cm^{-3}$	CRC Handbook
Melting Point	17 C	CRC Handbook
Water Solubility (25C)	48.8 mg/L	CRC=insoluble Thibodeaux, 1996
Octanol-Water Partition Coefficient, log K_{ow}	4.10	Thibodeaux, 1996
Organic Carbon Partition Coefficient, log K_{oc}	3.69	Thibodeaux, 1996
Diffusion coefficient (25C)	7.57E-6 cm^2/s	Thibodeaux, 1996
Oral RfD	0.01	Watts, 1997

3.1.1 Chemicals

Chlorobenzene is a priority substance with the Canadian Federal Government. Its major uses are as a solvent in pesticides, adhesives, drugs, and textile dyes, and as an intermediate in the manufacture of other organic chemicals, insecticides, and rubber polymers (Mackay et al., 1996). Incinerators may be a source because chlorobenzene is a product of incomplete combustion. The oral LD_{50} for rat and rabbit were 2290 mg/kg and 2250 mg/kg respectively. Chlorobenzene is considered an experimental teratogen when inhaled and mutagenic in mice and hamsters (NIH). The time weighted average permissible exposure limit (PEL - TWA) is 75 ppm; OSHA indicated this is the concentration to which most workers can be exposed without adverse affect averaged over a normal 8 hour day. The EPA has given chlorobenzene Group D classification meaning 'not classifiable as to human carcinogenicity'. The EPA Office of Groundwater and Drinking Water indicates the maximum contaminant limit, MCL, as 0.1 mg/L. Chlorobenzene is considered harmful if swallowed, inhaled, or absorbed through skin. The Sigma Aldrich library of chemical safety data states, "symptoms of exposure include nausea, dizziness, headache, liver damage and kidney damage". Other symptoms include central nervous system depression, skin irritations, defatting, dermatitis, skin burns, drowsiness, cyanosis, spastic contractions of extremities and loss of consciousness.

1,3-dichlorobenzene is used as a fumigant, an insecticide, and an intermediate in the production of other chemicals. 1,2-dichlorobenzene is a degreasing agent commonly found in dry cleaning. It is used as a solvent for waxes, gums, tars, resins, rubbers, oils, and asphalts, also as an insecticide and fumigant. 1,2-dichlorobenzene

and 1,3-dichlorobenzene have not been adequately tested for mutagenicity and carcinogenicity but 1,2-dichlorobenzene may damage the testes (U.S.E.P.A., 1994). They are both listed as hazardous substances by the DOT and EPA. Exposure to these chemicals can cause headaches, nausea, and irritation of the eyes and throat. Higher exposures may lead to dizziness and loss of consciousness. Chronic exposure may result in damage to the liver and the kidneys. Repeated exposure may damage blood cells and the ability to make blood cells, which can be fatal (Casarett and Doull, 1991). The time weighted average permissible exposure limit (PEL - TWA) is 50 ppm for 1,2-dichlorobenzene; OSHA indicated this is the concentration to which most workers can be exposed without adverse effect averaged over a normal 8 hour day. No information was found on 1,2,4-trichlorobenzene health effects.

3.2 SITE HISTORY: CHLORINATED BENZENES STUDIES

The Petro-Processors of Louisiana, Inc. Superfund site (PPI) is located north of Scotlandville, in East Baton Rouge Parish, Louisiana, approximately ten miles north of the city of Baton Rouge. The site area is about 55 acres and consists of two disposal areas, called Scenic site and Brooklawn site, near Baton Rouge Bayou, Devil's Swamp, and the Mississippi River. The disposal areas were contracted out to hazardous waste generators in the area and raw waste was dumped into unengineered pits, with total waste mass estimated to be 400,000 tons (Constant et al., 1995). The main pollutants are chlorinated organics and polycyclic aromatic hydrocarbons. A US District Court, Middle District of LA judge has ordered a Consent decree allowing the defendants to cleanup the site. The remediation strategy has been hydraulic containment and recovery technologies augmented with monitored natural attenuation.

The nearest community consists of a few houses approximately 1,000 feet from the border of the Scenic site. The closest drinking water well is located 3,000 feet up gradient of the site.

3.2.1 Brooklawn Site

This site is the larger of the two disposal areas and was operational until 1980. As previously mentioned waste was placed in unengineered pits, so contamination is present in sediments, soils, and lagoons. Downstream wells indicate contaminants have leached through the banks of Baton Rouge Bayou and into groundwater. Currently, the remediation strategy is pump and treat for hydraulic containment using 193 recovery wells with installation of another 11 wells pending. An on-site incinerator is used for destruction of organic waste generated.

3.2.2 Scenic Site

Like the Brooklawn site, there are 11 recovery wells to collect the non-aqueous phase liquids (NAPLs) and thirty-four monitoring wells, which monitor natural attenuation of the plume.

Baton Rouge Bayou winds around both Brooklawn and Scenic sites and empties into Devil's Swamp. Therefore understanding and quantifying transport of CBs from BRB will contribute to the clean up of this specific site and potentially help modelers understand the site specific nature of other models.

3.3 MATERIALS AND METHODS

3.3.1 Sediment Collection

All sediments were originally from the site but contaminated in the laboratory. Sediment was taken from the Petro Processors site near the Baton Rouge Bayou. All

sediment for CB studies was kept sealed until prepared. Multiple CB sediment samples can from PPI site and were collected by PPI personnel. All buckets were labeled with location and date, sealed on site, delivered to LSU by NPC Services, Inc. or LSU personnel.

A representative sample was sent for characterization by the Agronomy Laboratory in Sturgis Hall at LSU. The sediment characterization parameters for five different buckets of sediment were performed.

3.3.2 Sediment Preparation

Following appropriate safety measures, sediment buckets were unsealed, large twigs and debris was removed by hand by pouring sediment into tray. Generally, each bucket was prepared sequentially. Initial sediment preparation was placement inside a hood to air dry in flat Nalgene trays (18" X 24" size). During the drying process, the large clumps were broken and debris removed. Sediment was sieved through #10 mesh (US std) to remove hard clumps, rocks and small pieces of debris. The sieved sediment is ground in grinder as a final homogenization step. Sediments were separated, air dried, sieved, and ground in the preparation phase. The sediment was weighed into 1 kg glass jars with Teflon lined lids. Approximately 4.5 kg of sediment was placed into jars and saturated with distilled water.

The desired contamination level for the beds was 10 ppm; the addition of another 5 mg/kg excess contaminant was a safeguard against volatilization during sediment loading, transfer, and mixing. The sediment was loaded by adding a small amount of contaminant solubilized in methanol stock solution into the slurry mixture. A contamination load of 15 mg/kg was desired for the chlorinated benzene studies.

Laboratory spike was calculated to be 15 mg CB/kg sediment to apply a uniform initial concentration assumption. Contaminant levels were verified by analysis both before and after experiments were completed.

3.3.3 Sheet Flow Leaching Bed (SFLB) Set-up

The jars of sediment were placed in a tumbler for approximately 48 hours for even distribution of spiked contamination. After the 48 hours of mixing, the jars were emptied into a large Nalgene® tray and mixed again. The CB contaminated mud was scooped into the two SFLBs, (Figure 3.1) and "thumped" against a table to remove air pockets and help settling. Sediment was added until the surface is even with the weirs at both ends of the beds. The weirs allow 2-3 mm of laminar flow water to form during the experiments. Finally, the sediment was smoothed out to guarantee uniform surface throughout the beds. It is important for the height of the mud not fall above or below the weir because the validity of the experiment relies on the film water concentration. Therefore, the laminar flow film water must be maintained at 2-3 mm thickness. The sheet flow leaching bed holds a shallow layer of contaminated sediment approximately 3 cm in depth as seen in Figure 3.1. Experiments consisted of two beds run simultaneously, designated as bed 1 and bed 2 in experimental data.

Distilled water was pumped from a water reservoir via Tygon flexible plastic tubing with 1/8" inner diameter, 3/16" outer diameter, and 1/32" wall thickness to the SFLB inlet using a multichannel peristaltic pump. Duplicate beds are run simultaneously, using the same water source and the same multicartridge peristaltic pump. The water flows over the sediment in laminar flow, with a thickness of 2-3mm as seen in Figure 3.1. Prior to initiation of the experiment, the pump was turned on

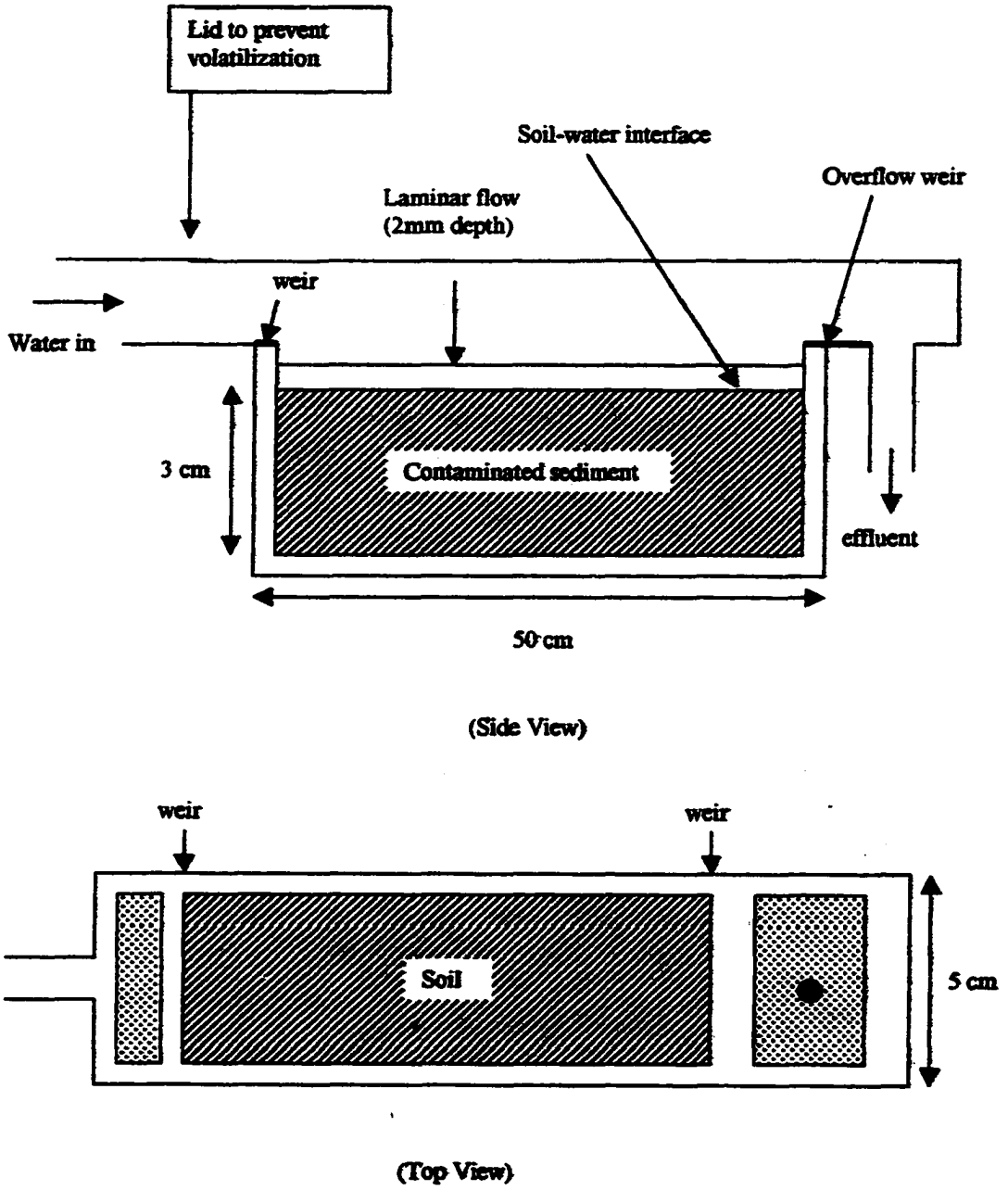

Figure 3.1. Sheet flow leaching bed (SFLB)

and water flowed onto the sediment until the area between the weirs held 2 mm of water. This water was allowed to remain in contact with the sediment for times ranging from 8 to 16 hours before the experiment was initiated to allow sediment-water equilibrium to be established.

The initial dynamic bed experiments examined diffusion with a continuous water flow. Several studies were performed with different flow rates to quantify the contaminant removal. This is called advection enhanced leaching. There were three flow regimes performed in the chlorinated benzene studies; continuous fast flow (Q = 150 ml/hr), continuous slow flow (Q = 50 ml/hr), and cyclic flow where the flow was alternated from fast to slow every 24 hours, i.e., one day fast, one day slow, then back to fast again. These flow rates were selected to simulate typical conditions found in Baton Rouge Bayou, scaled to simulate 150' of the stream in SFLBs, based on retention time. Hypothetically, cyclic flow would prevent the system from achieving equilibrium thereby increasing the mass transfer coefficient when compared to steady state systems. As the water flows across the contaminated sediment, the contaminant diffuses into the water transported at the chosen flow rate thereby simulating desorption and release rates of contaminants which may occur in Baton Rouge Bayou.

Experiments labeled as fast flow had continuous flow at a rate of approximately 150 ml/hr. Those indicated by slow flow had rates of approximately 50 ml/hr. Continuous flow experiments determine a baseline steady state CB concentration and flux rate. Flow rates were calculated by dividing the measured sample volume by the time required for collection of the sample. Actual flow rates will be utilized in flux calculations. During a period of continuous flushing of water

across the surface, samples were taken every few hours during the course of the study. After performing leaching studies at the fast and the slow flow rates, experiments were performed where the flow rate varied between fast and slow every 24 hours. This variation between the two rates was labeled cyclic flow. The intent of cyclic flow was to see if flux could be enhanced by non-equilibrium conditions. The cyclic flow data will be compared to the continuous flow data in order to see how the variation in flow affected the overall mass removal rate.

3.3.4 Sample Preparation for GC/MS

Samples were collected at the effluent outlet in 40 cc Volatile Organic Analysis vials (VOA Vials from Fischer Scientific) were used with Teflon lined septa lids. Blanks were analyzed as a check for glassware contamination. To prevent volatilization losses during the slow flow regime, a rubber stopper was used to hold tubing into vials. The sample vials were filled to have no headspace and refrigerated until analysis. Analyses for VOC's were performed within 7 days of collection.

3.3.5 Experimental Flux Determination

The experimental flux can be calculated by:

$$\text{Flux} = (C^* Q) / A \qquad (3.1)$$

where C is concentration of the effluent (mg/L) and Q is the flow rate (L/hr), A is area (cm^2) of the bed normal to the flux (Figure 3.1), thereby giving units mg/cm^2*hr. The advective enhanced leaching model gives a predicted flux and this is compared to the experimental flux obtained from Equation 3.1.

3.3.6 Theoretical Flux Comparison

The effluent mass values in the mass balance were calculated by two methods. The first method was the simple back calculation as indicated in

$$M = F * A * \Delta T \qquad (3.2)$$

where M is mass of chlorinated benzene, F is the calculated flux rate from equation 1, and delta t is the time between sample n and sample n+1.

The other method is labeled trapezoid. This method follows the basic principles of forming a trapezoid using the two time values and their respective flux values. By utilizing the "trapezoid" method, the total is the sum of a series of averages. These 'trapezoids' were summed to determine removal per unit area of leaching bed in the table. The extraction efficiency can be seen in the column labeled Mass/hour (mg/hr) of the mass balance for each set of experiments in the results section.

3.4 MASS BALANCE

3.4.1 Initial Sediment Load

The initial contaminant load was determined by taking replicate samples out of the sediment as it is loaded into the sheet flow leaching bed. This sediment is extracted flowing the same procedure as the cores, described below.

3.4.2 Core Procedure

Core samples were taken from each bed after the leaching experiment had been terminated to determine the residual concentration of contaminants remaining in the sediment. By cutting the Luerlok® top off a disposable 60 cc syringe, the syringe could be pushed into the sediment while still contained in the experimental apparatus

to take a cylindrical core out of the SFLB. The cut syringe barrel was pushed into bed sediment in three places: front, middle and back in the direction of the water flow as seen in Figure 3.2. These cores were then cut into thirds to get a bottom, middle, and top aliquot of sediment for each of the areas taken, vertically. In this way, every layer of the bed sediment, vertically and horizontally could be examined. This method was implemented after the first MCB sheet flow leaching bed. The preliminary SFLB had only two cores taken, front and back but they were only divided in half; top and bottom. The sediment was placed into 60 ml jars and extracted using the same sample method as the initial samples. The initial sediment and final sediment (core) were tested using sonication extraction.

3.4.3 Sonication Extraction

Methanol was chosen as the solvent in all extraction tests because the CB's are infinitely soluble in it. Amber 60-cc borosilicate jars with Teflon lined lids were labeled and weighed then a section of core was placed inside. Methanol was added to the jars until no headspace was achieved. The jars were weighed again to determine the volume of methanol added. The jars were sonicated for three hours to break up the sediment and left to settle in order to separate the sediment from the methanol. After settling, the methanol was removed from the sediment, diluted, and put into VOA vials. A Pasteur pipet was used to remove liquid phase, while not disturbing the sediment surface. Sample vials were stored in the dark at 4°C until analysis. The extraction process was repeated three times for each individual jar in order to remove all leachable contaminants.

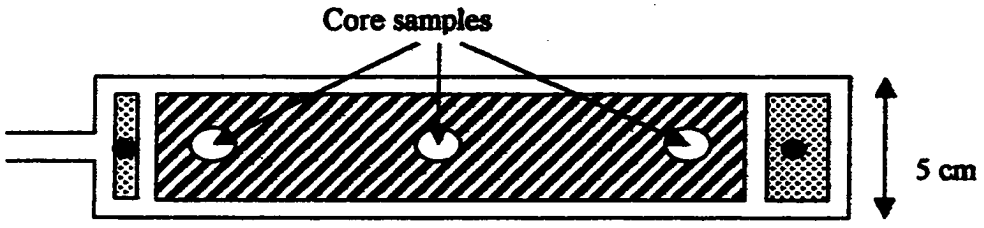

Top view

Figure 3.2. Location of cores, front, middle and back

One aspect of this extraction is the temperature of the water inside sonicating bath must be cool to the touch. One problem with sonication can be the loss of solvent or contaminant due to evaporation from heat. To prevent this loss, the sonicator must have flow thru capabilities or addition of ice to maintain a cool water temperature.

3.4.4 SFLB to Model Devil's Swamp and Baton Rouge Bayou

A schematic of the sheet-flow leaching bed reactor (SFLB) was shown in Figure 3.1 and was described earlier. The SLBR (bed) is a stainless steel bed consisting of a thin film of water flowing over a flat bed of sediment. By setting equal retention times, the extraction beds represent approximately 150 feet of the Baton Rouge Bayou near the Scenic Site, based on data provided by NPC Services, Inc.

3.5 DATA ANALYSIS

3.5.1 Chemical Analysis

The effluent samples were analyzed with a Hewlett Packard 5890 gas chromatograph (GC) equipped with a Hewlett Packard 5971 mass spectrometer detector (MS). The GC/MS system was run by HPChemStation software and utilized a PTA-30 autosampler. Due to the nature of volatile organics, a Tekmar liquid solid sample concentrator (LSC-2) purge and trap was utilized with a purge flow of 40 ml/min. The GC run time is 27 minutes with injector and detector temperatures of 180°C. In accordance with 8260A method parameters, the initial temperature is 45°C for 2 minutes the ramp to 110°C at a rate of 6°C per minute followed by a ramp of 12°C per minute to a final temperature of 210°C, which is held for 5 minutes. The column is a Phenomenex ZB-624 30 m length by 0.25mm diameter. The flow rate to

MS is 1.0 ml/min with an initial 4 minutes solvent delay. Standards of known concentrations are prepared and run before samples for every GC/MS operation. The concentration values of the standards are determined by the expected value of the sample. All standard curves had coefficient of variance above 0.96.

3.5.2 Data Entry

Graphing and calculations of flux were performed utilizing the Microsoft Excel spreadsheet software in Microsoft Office 2000. Spreadsheets were constructed to calculate the flux rates and mass balances from the sample concentrations by the equations previously shown. Graphs and tables were constructed from these spreadsheets and will be shown in the results section.

3.6 RESULTS FOR SINGLE CONTAMINANT CHLORINATED BENZENE STUDIES

3.6.1 Sediment Characteristics

The sediment was analyzed by the Agronomy Laboratory in Sturgis Hall on the LSU campus. Values for the percent organic matter (OM), pH, and other sediment parameters are shown in Table 3.5. The results show the variation in the sediment samples, which is an indicator of the homogeneity of the site itself. The organic matter (OM) is used to calculate the fraction of organic carbon, f_{oc}, which is used in the models to get K_d, the estimated partition coefficient. The average OM was calculated to be 0.33 %. The average f_{oc} was calculated to be 0.00213 and used to initially guess K_d.

Table 3.5. Soil characteristics for chlorinated benzene studies

Parameter	PPI-1	PPI-2	PPI-3	PPI-4	PPI-5
pH	7.8	6.5	7.3	6	7.4
Na	11	33	49	38	29
Mg	50	278	347	285	197
Ca	757	1437	3172	1625	1970
P	55	171	264	220	162
K	29	76	139	78	74
%OM	0.02	0.46	0.55	0.52	0.29
Sum Bases	4.3	9.8	19.3	10.8	11.8

3.6.2 Experimental Measurements for MCB in Single Contaminant Studies

As previously mentioned, the aqueous samples were analyzed for the chlorinated benzene concentration and the flux rate was calculated by Equation 3.1 as shown previously. The concentration of MCB in the effluent during the slow flow over time is shown Figure 3.3. Both of the sheet flow leaching beds are shown to indicate the little variation between the replicates. Notice the rapid decrease in concentration initially and the stable tailing values. The curve is described by the transient initial desorption and advective removal of MCB followed by steady state desorption/dissolution flux rate.

The concentration curve follows the same pattern under the fast flow rate with MCB as the sole contaminant in Figure 3.4. Again, both of the sheet flow leaching beds are shown to indicate the variation between the replicates. The initial concentration of the pollutant is high but rapidly decreases to a concentration termed steady state in this research. The variation seen in the first few days is due to variation in the flow rate. This exponential decay signature is characteristic of diffusion curves (Deana et al., 1999). The difference is how fast the steady state concentration is reached and at what concentration.

Figure 3.5 is the concentration curve of MCB for cyclic flow shows the variation in concentration due to flow regime. Notice the beds give similar results and that the flow rate directly affects the concentration due to the advective dependence of desorption and dissolution. The single contaminant MCB flux and flow rate are graphed together in Figure 3.6 to demonstrate the change in flux rate is dependent on the flow rate.

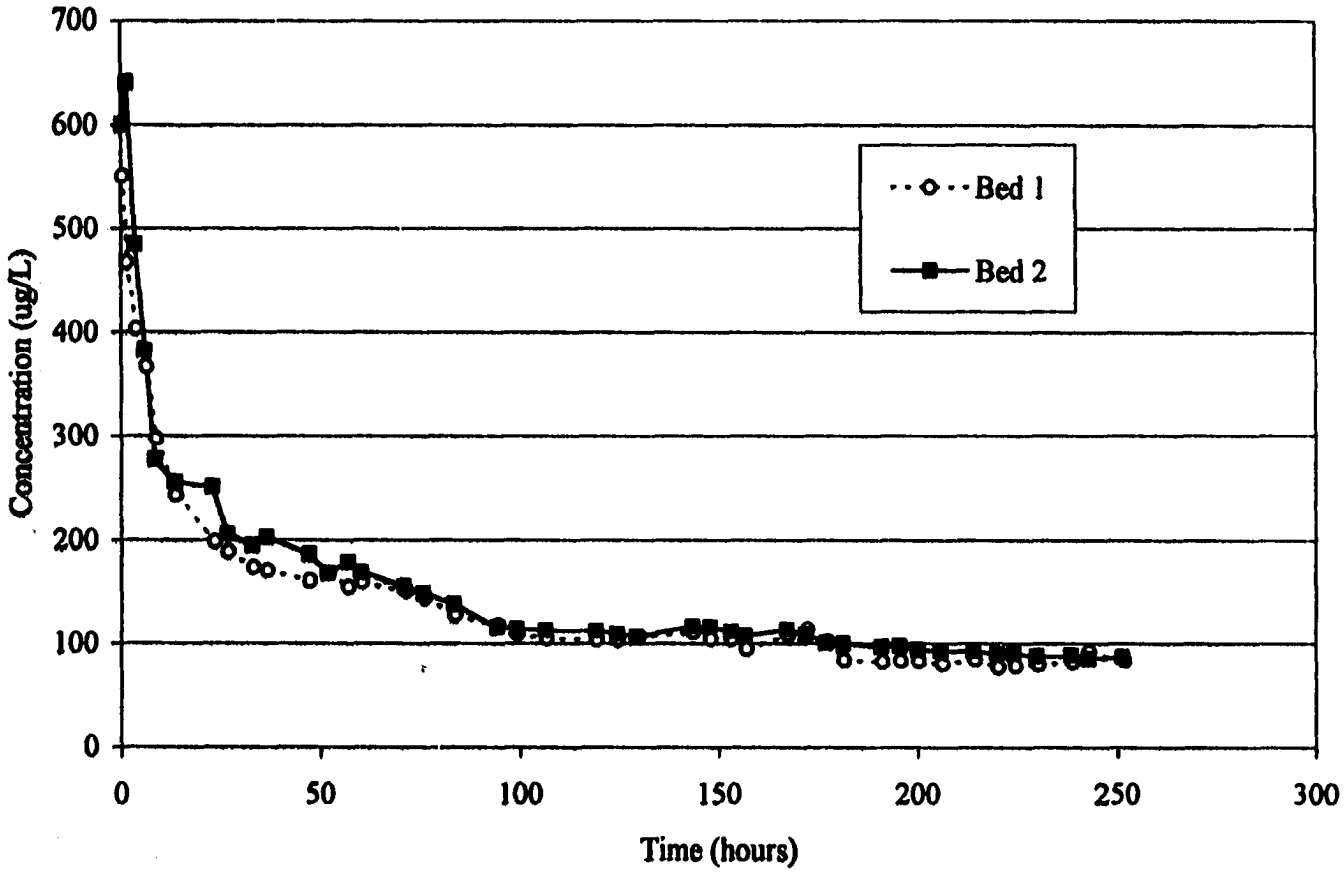

Figure 3.3. MCB single contaminant concentration under slow flow

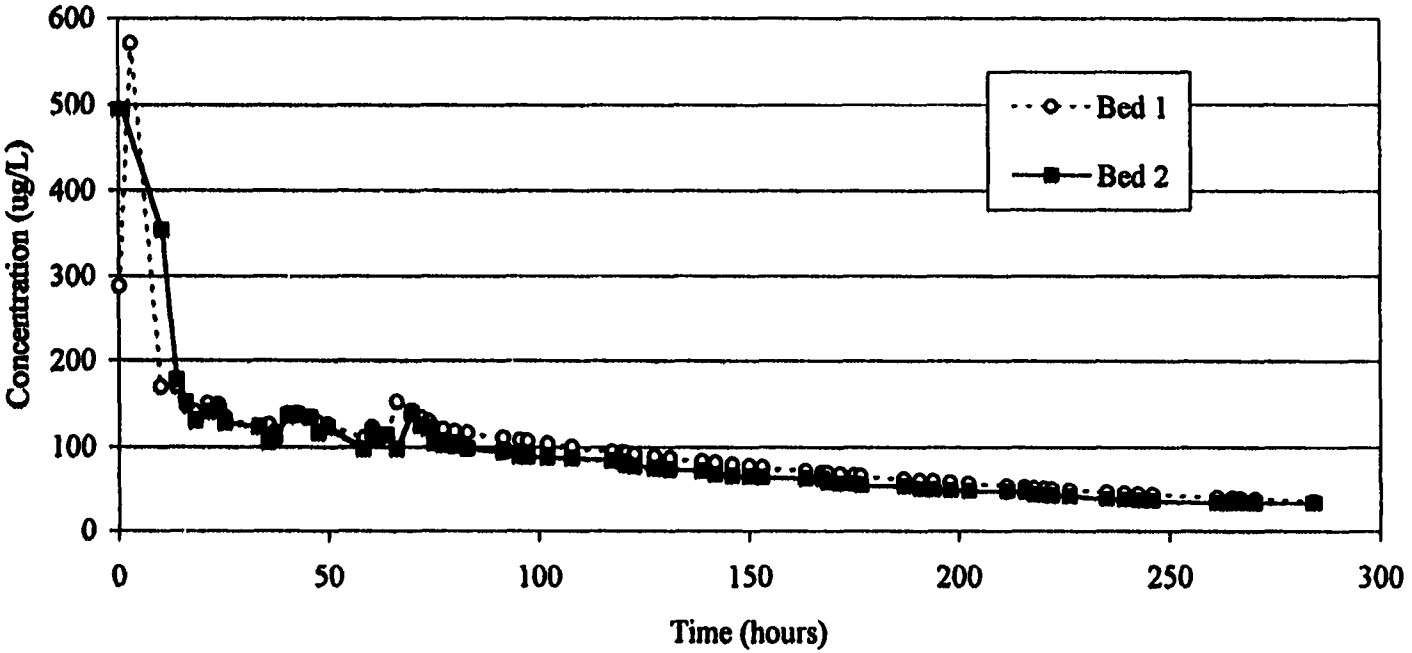

Figure 3.4. MCB single contaminant concentration under fast flow

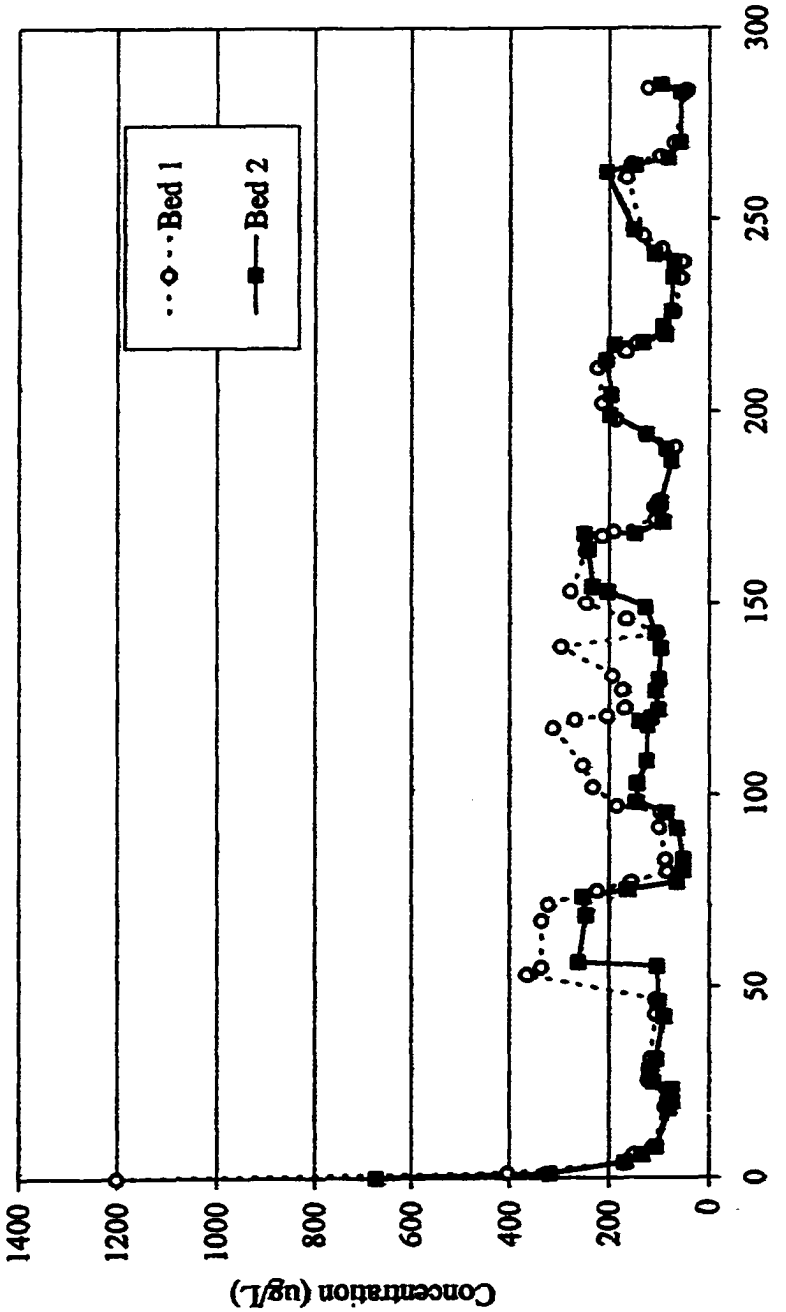

Figure 3.5. MCB single contaminant concentration under cyclic flow

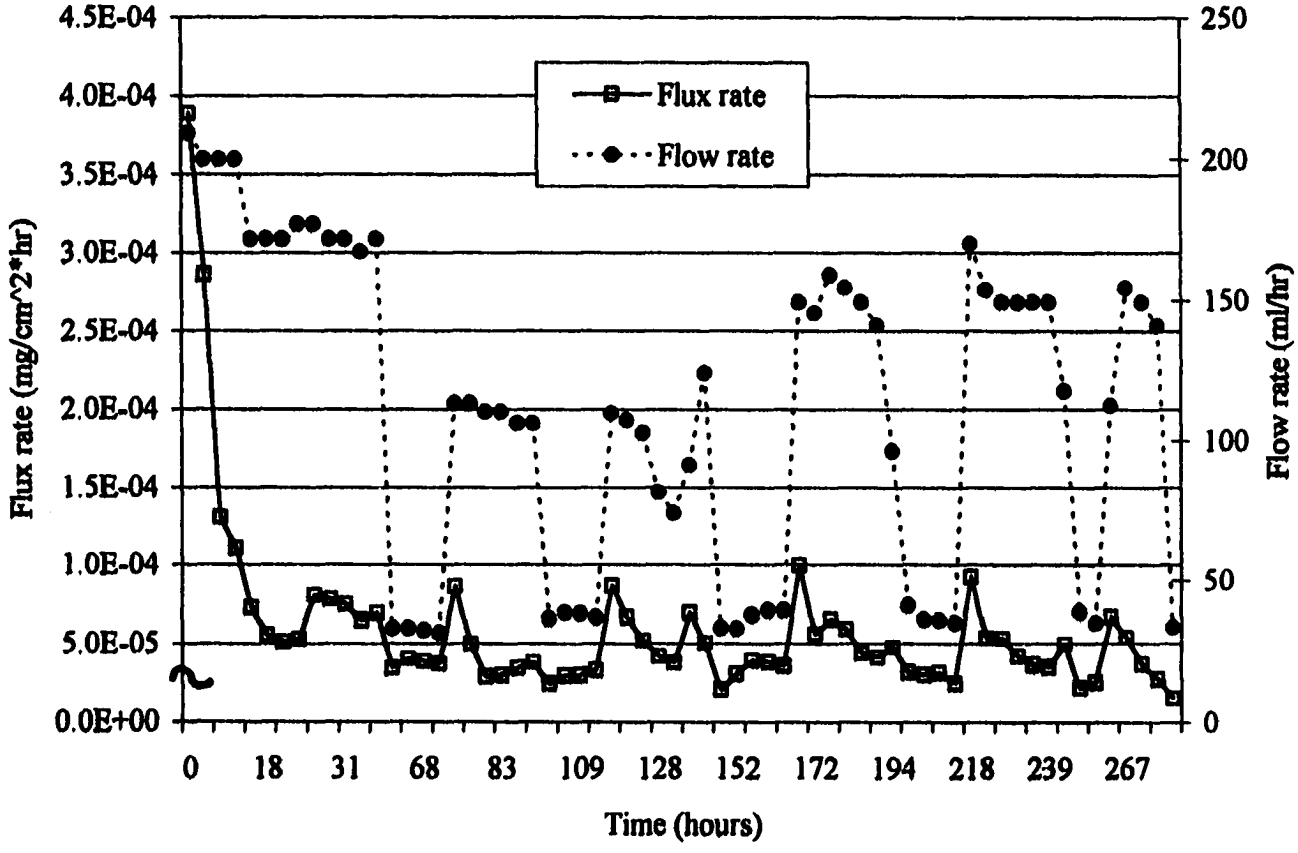

Figure 3.6. MCB single contaminant flux dependent on flux cyclic flow

In Figure 3.7, the comparison of flux rates by all the flow regimes demonstrates the impact different flow rates have on steady state flux rates. It appears the cyclic flow rate may be a more efficient way to leach contaminants out of the sediment due to periodic perturbation from steady state conditions.

3.7 MASS BALANCE FOR MCB SINGLE CONTAMINANT

3.7.1 Initial Contaminant Load

The initial contaminant load on the sediment was determined by taking replicate samples out of the sediment as it is loaded into the sheet flow leaching bed. This sediment is extracted following the same procedure as the cores. There are only two sets of graphs for the initial sediment load of the MCB single contaminant studies; Figure 3.8 shows data from fast and slow flow regimes combined and Figure 3.9 is from the cyclic flow regime. The fast and slow flow initial average sediment load was 11.90 mg/kg as determined from the three replicates shown. The average sediment load is 10.11 mg/kg for the cyclic flow bed runs. Both initial load graphs show a great deal of variability, which is a problematic with sediment media. As mentioned previously the sediment was laboratory contaminated to be in the range of 10-15 mg/kg. The initial sediment load results indicate the contamination procedure was successful.

3.7.2 Core Results

After the diffusion experiments were completed, the sediment was cored to determine the amount of contaminant remaining in place. This remaining amount is termed the residual sediment load. The remaining contaminant load varied spatially inside of the leaching bed as can be seen from the core profiles. In the first

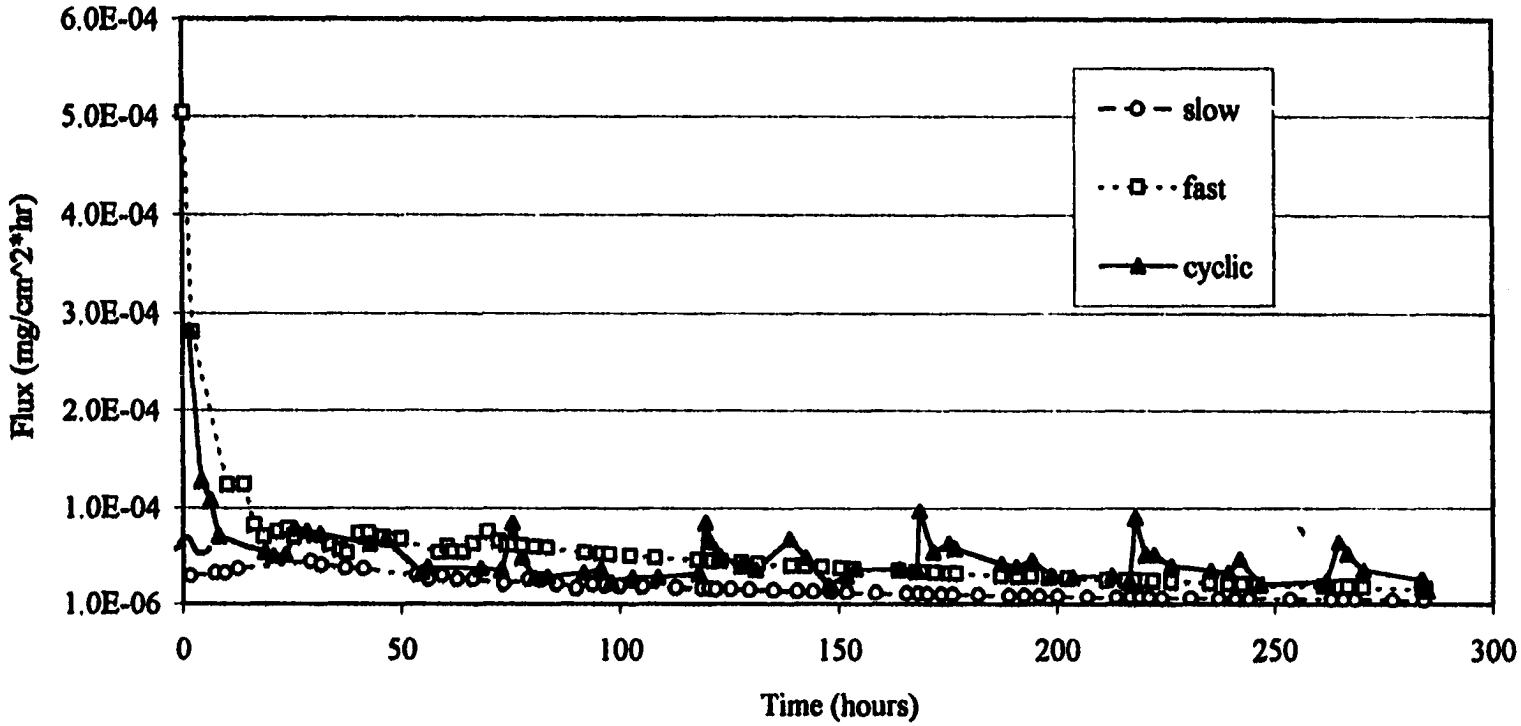

Figure 3.7. MCB flux comparison by flow rate

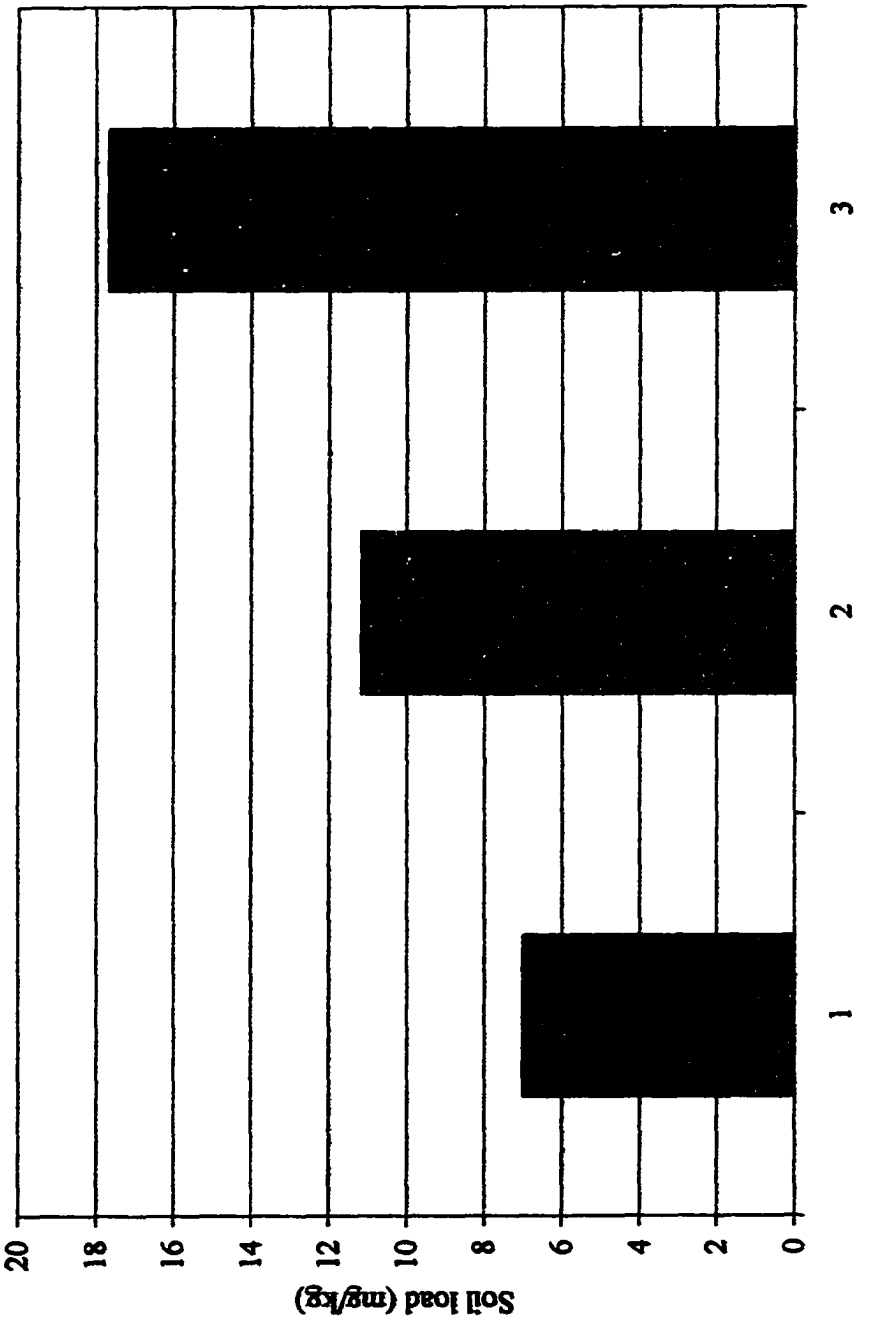

Figure 3.8 Single contaminant MCB initial soil load for slow and fast flow

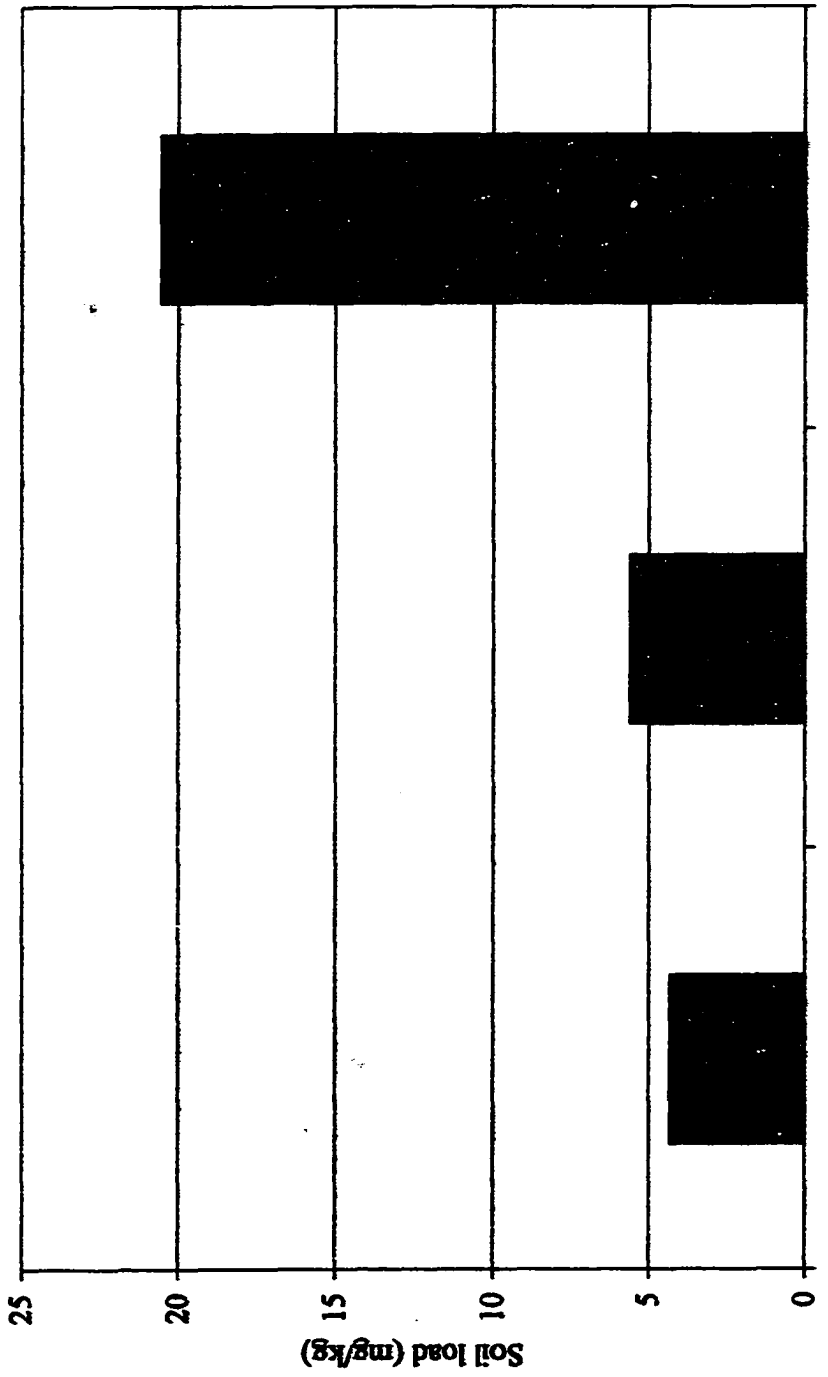

Figure 3.9. Single contaminant MCB initial soil load for cyclic flow

experiment, one less core was taken as seen when comparing the two sets of core results. The replicates of each bed are not shown, only the average of the two beds will be shown for simplicity. Recall, the fast and slow flow runs were combined and very little MCB appears to be remaining on the sediment in Figure 3.10. The initial sediment load was nearly 11 mg/kg and the residual left on the sediment is approximately 3 mg/kg. The front top section appears to have less remaining sediment load as expected due to its contact with clean water.

The cyclic flow experiment was cored as described previously. Figure 3.11 shows lower residual load in the top layers indicating the CB has diffused out of those layers in the cores, as would be predicted by the advective flow at the surface. The middle layers appear to have the highest concentrations. The bottom cores are not very clear as to what is happening. This may be an artifact of the experimental apparatus allowing diffusion along the bottom and sides or a variation in concentration due to residual heterogeneity of the sediment mixture.

Generally, the sediment core profiles demonstrate less CB's in the surface layer as would be expected since it has the shortest path to diffuse out of the soil compartment. Overall, the top layers indicate the least amount of contaminant left on the sediment as expected in cores. One of the interesting observations in examining the experimental sediment core is the middle both vertically and horizontally, appears to have the highest remaining sediment load. Recall that several different sediments were obtained from the site. Both experimental runs indicate the middle horizon has slower transport therefore a higher concentration of the contaminant would be expected. Again, this could be attributed to the heterogeneous nature of the matrix or

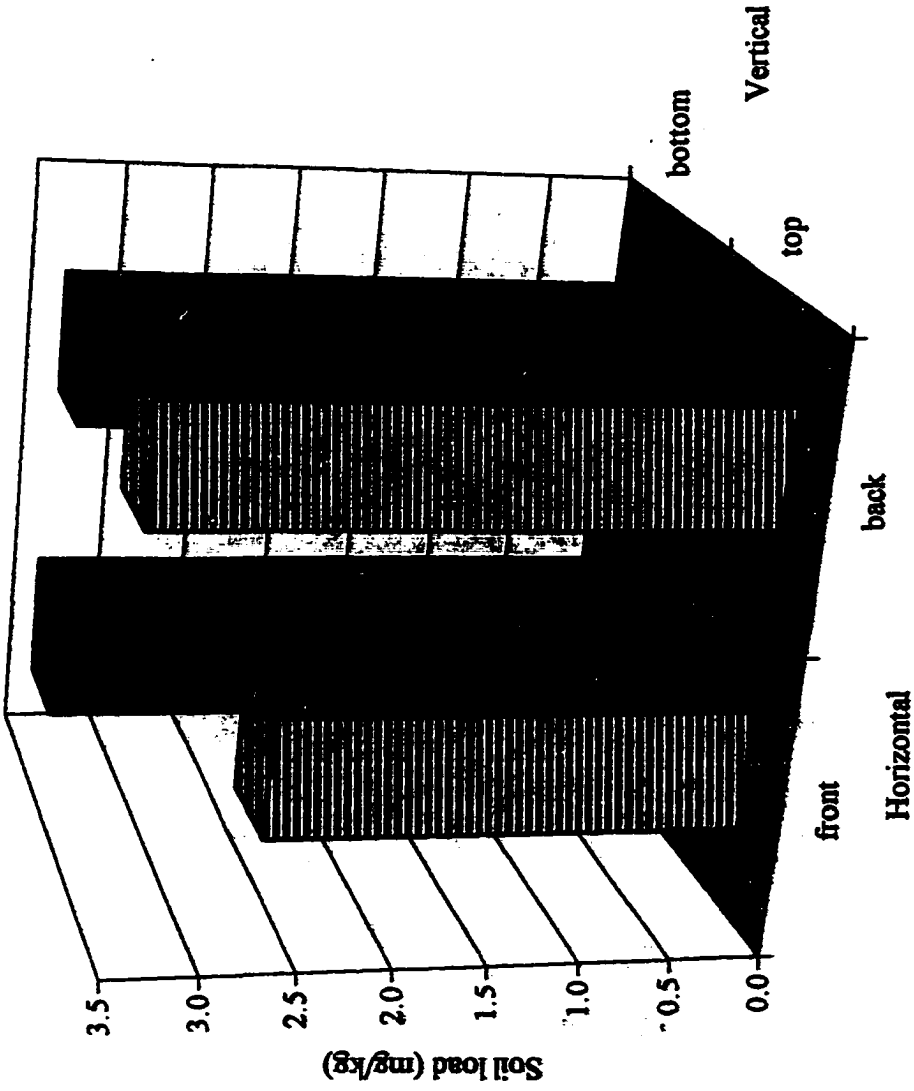

Figure 3.10. MCB single contaminant fast and slow flow core

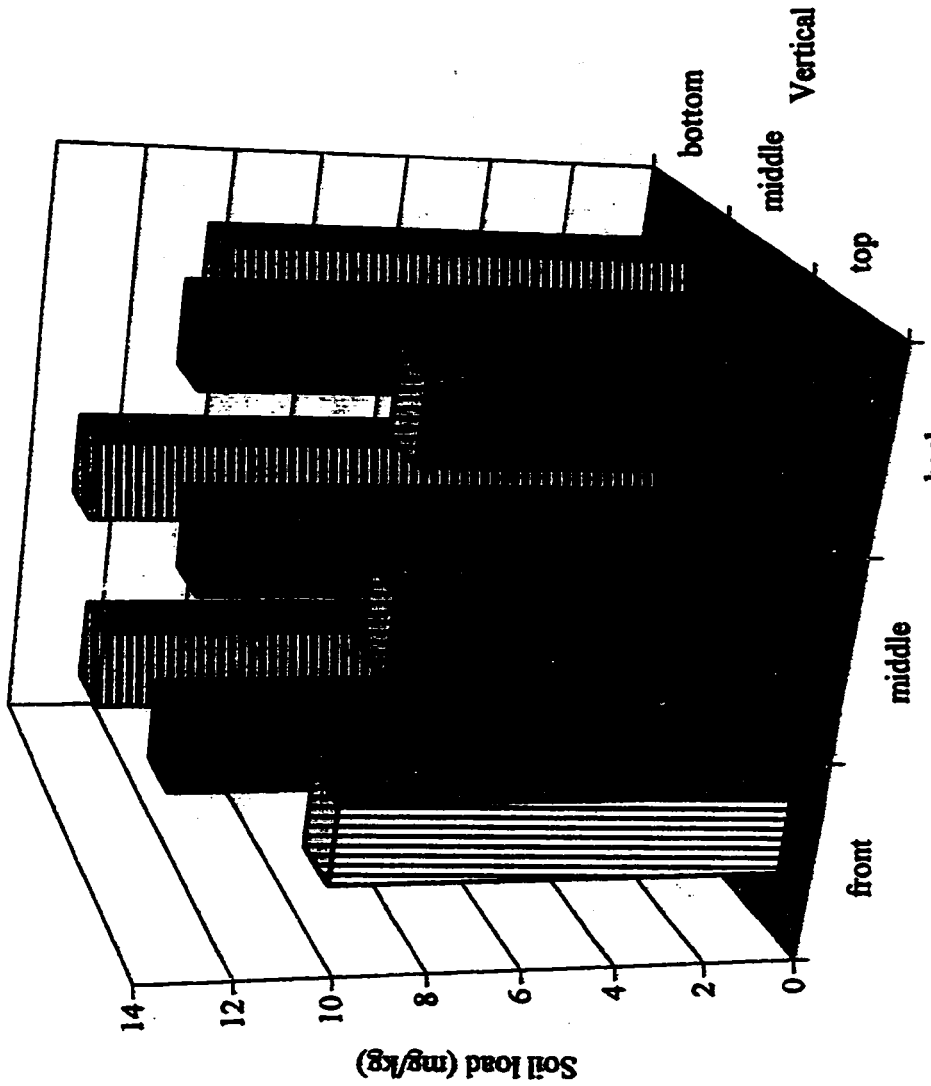

Figure 3.11. MCB single contaminant cyclic flow core

contaminant from a lower area could be sorbed as it diffuses upward. Another explanation is the movement of pollutant along the side and bottom where there is the least resistance to diffusion due to increased porosity.

3.7.3 Closure for MCB

The mass balance results for the MCB as a single contaminant for all three flow regimes is shown in a Table 3.6. The effluent mass removed per time appears to be more in the fast regime at the short time interval, a value of 0.021 mg/hr as compared to 0.0123 mg/hr in the cyclic flow. In Table 3.7, the fast and slow flow experiments were extrapolated out to the same time as the cyclic flow regime to compare effluent mass per hour rates. For the same length of time the cyclic flow leaches more contaminant, 0.0126 mg/hr as compared to 0.0086 mg/hr for fast and 0.0057 mg/hr for slow flow. The last column of Table 3.6 shows the mass accountability for the different flow regimes. The percent closure for the slow/fast flow may be poor due to: this was the first of the VOA studies and the seal on the lids may not have been adequate at that time, or other initial technical problems. The cyclic flow experiment has very good mass balance due to the high core values. As seen in Table 3.6, one cyclic core average was higher than the initial sediment load, this may be because the cores are assumed representative of the whole bed, and the initial sediment load is assumed uniform throughout the whole bed.

3.7.4 Experimental Measurements for 1,3-DCB in Single Contaminant Studies

Another lower chlorinated benzene daughter product of HCB degradation, 1,3-dichlorobenzene, was used to confirm (mono) chlorobenzene behavior in single contaminant studies. Figures 3.12, 3.13, and 3.14 follow the flow rate and the flux of

Table 3.6. MCB single contaminant mass balance

Experiment	Total time (hours)	Effluent mass (mg)	Mass/hour (mg/hr)	Average core (mg/kg)	Ave. Initial Load (mg/kg)	Remaining mass per bed (mg)	% closure
slow	87.93	0.74	0.0084				
slow	88.03	0.73	0.0083				
slow	87.93	0.73	0.0083	Incorporated in the fast run, run sequentially first time			
slow	88.03	0.68	0.0077	Incorporated in the fast run, run sequentially first time			
			0.0082				
fast	73.93	1.82	0.0246				
fast	73.92	1.37	0.0185				
fast	73.93	1.66	0.0225	3.56	10.11	5.34	50.95
fast	73.92	1.34	0.0181	2.82	10.11	4.23	41.21
			0.0209	3.19			46.08
cyclic	284.50	3.73	0.0131				
cyclic	285.00	3.13	0.0110				
cyclic	284.50	4.22	0.0148	12.25	11.90	18.38	126.58
cyclic	285.00	2.98	0.0105	10.21	11.90	15.32	102.49
			0.0123	11.23			114.54

Table 3.7. Extrapolated data

Experiment	Total time	Effluent mass	Mass/hour (mg/hr)
slow	285	1.55	0.0054
slow	285	1.05	0.0037
slow	285	1.98	0.0069
slow	285	1.97	0.0069
			0.0057
fast	285	3.73	0.0131
fast	285	3.13	0.0110
fast	285	1.66	0.0058
fast	285	1.34	0.0047
			0.0086

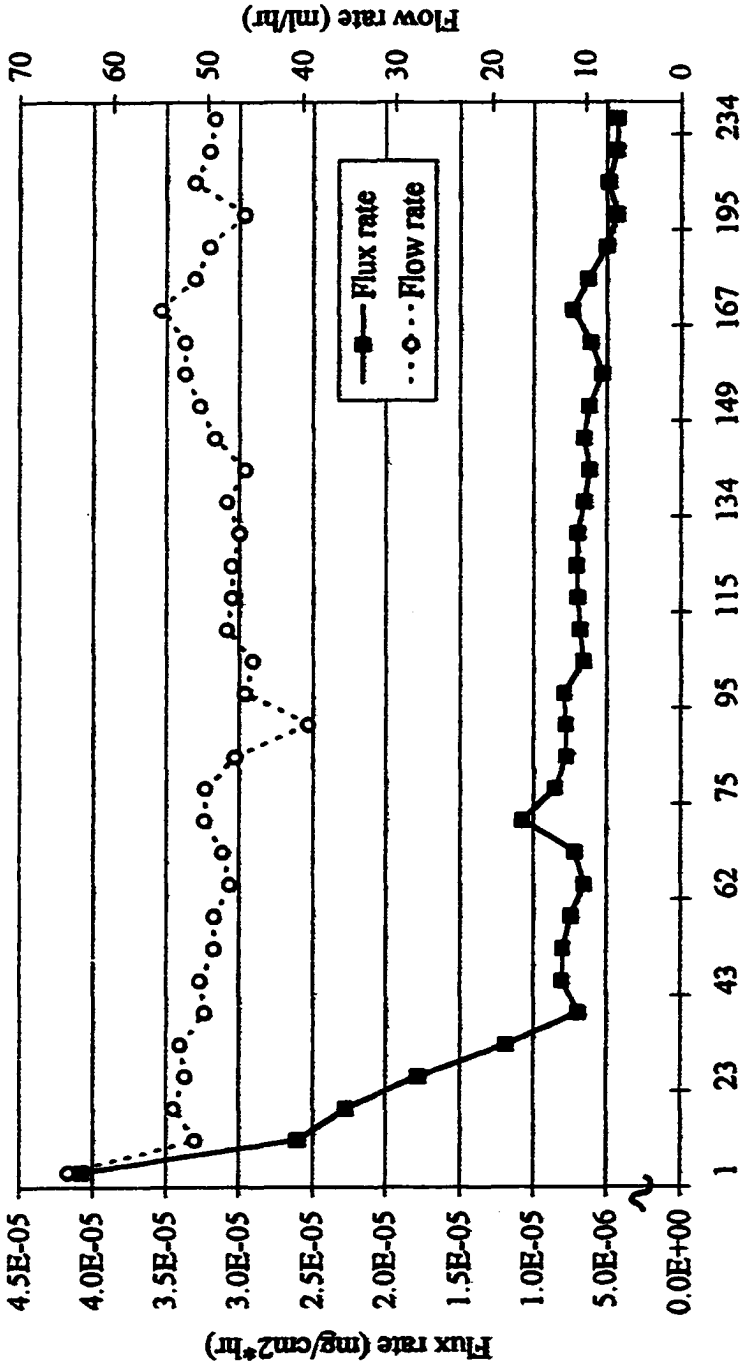

Figure 3.12. 1,3-DCB single contaminant flux under slow flow rate

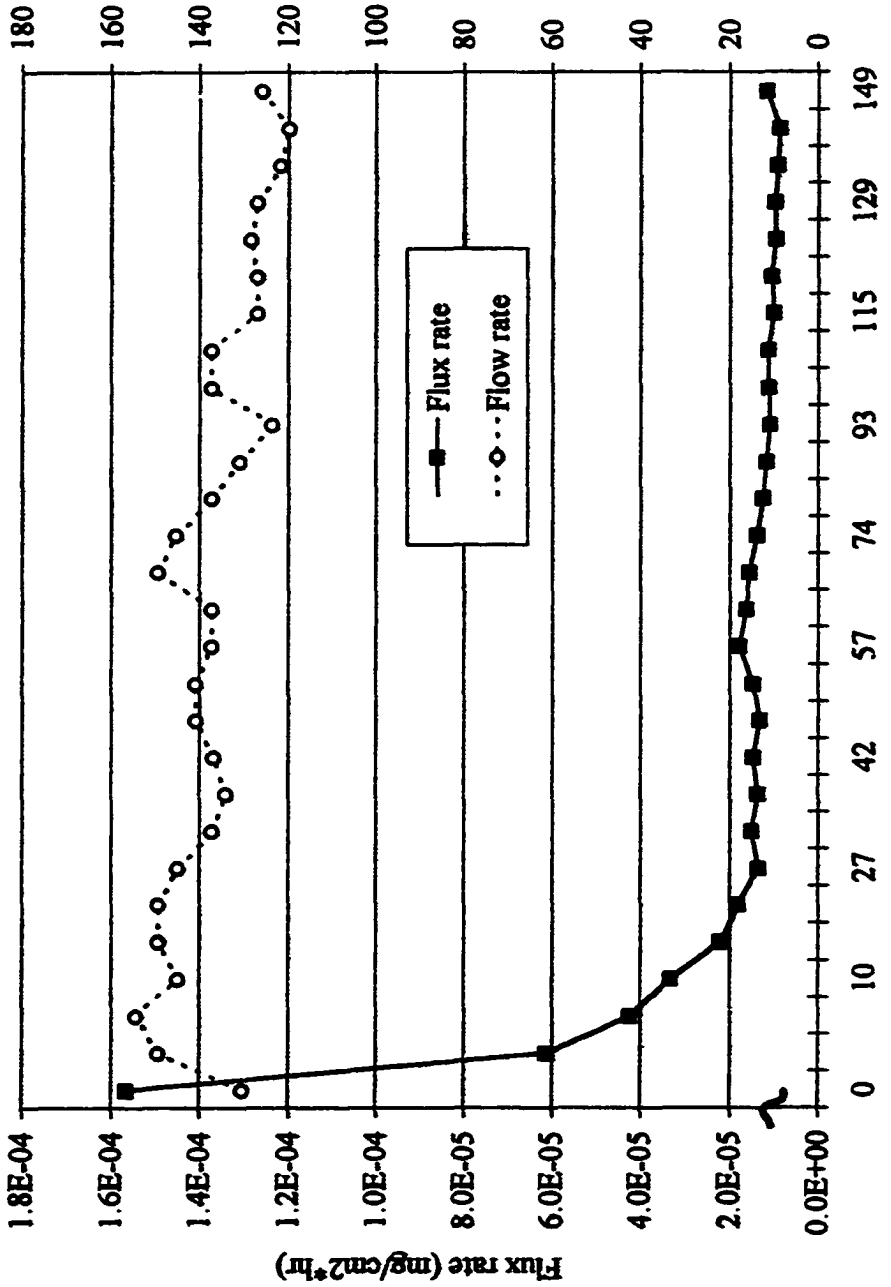

Figure 3.13. 1,3-DCB single contaminant flux under fast flow rate

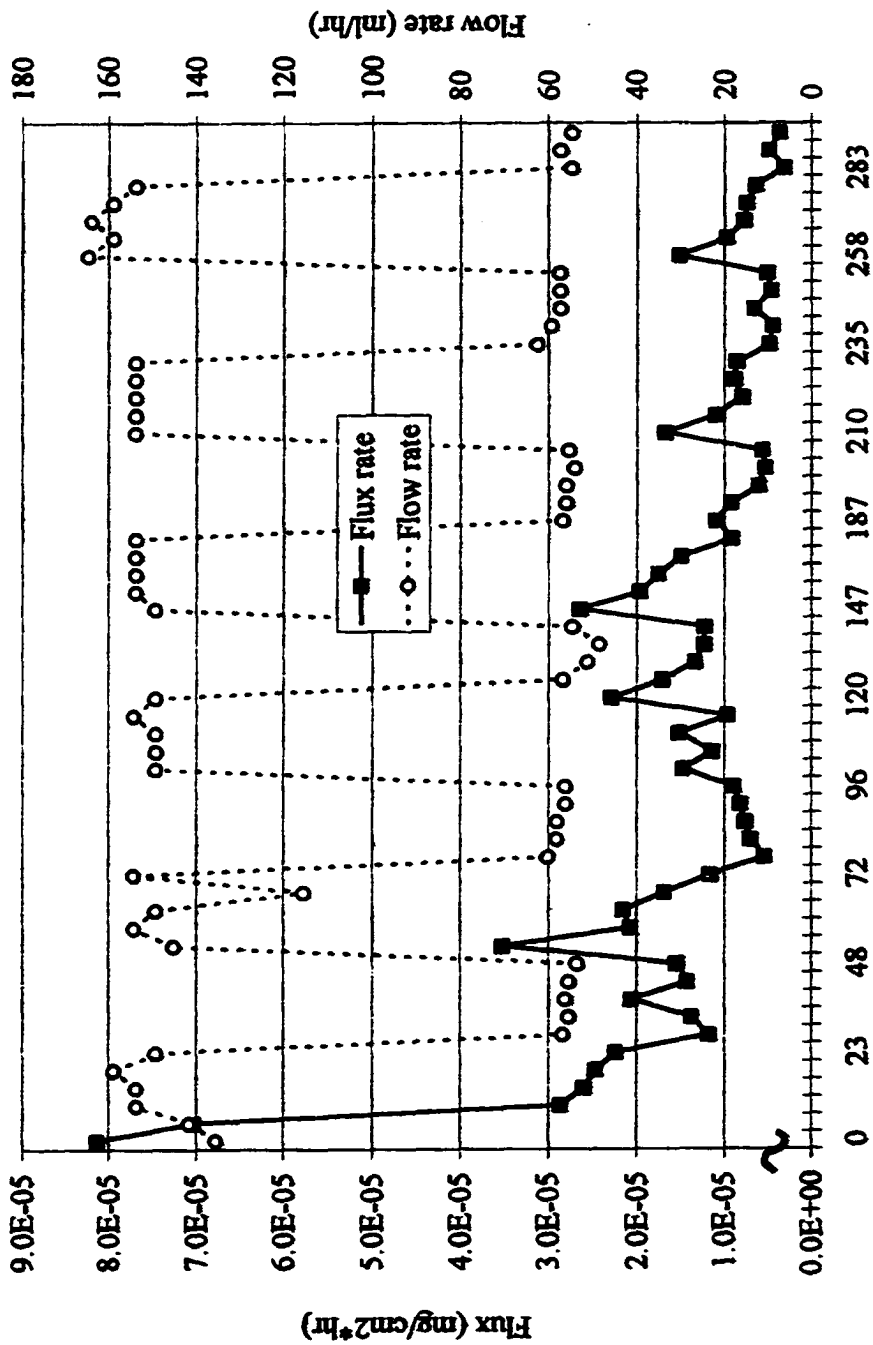

Figure 3.14. 1,3-DCB single contaminant flux under cyclic flow rate

1,3- DCB for all three regimes individually: slow, fast and cyclic. The flux versus time graphs will look very similar to the concentration versus time graphs due to the relationship shown in equation 1. Only one line is shown as the average of both beds with very little variation in the duplicates as was found with the MCB single contaminant studies. Flow rates were included to show the effect of minor variations in flow rate. As seen in the MCB single contaminant studies, the flux continues to decrease with time during continuous flow conditions as seen in the Figures 3.12, 3.13. Figure 3.14 follows the cyclic flow regime and the perturbations of flow are directly seen in increased flux values. The characteristic exponential decay can be seen in all advective enhanced leaching experiments in this study. Figure 3.15 compares all three flow rates for the 1,3-DCB single contaminant studies demonstrating the cyclic flux rate spikes higher than the fast and slow fluxes.

Of interest is the higher starting value for concentration and flux in some sediments, which may lead to a higher steady state values for both concentration and flux curves. This supports that diffusion can be faster in some sediments and slower in other sediments.

All of the previous results are single contaminants in a laboratory-contaminated sediment. To examine the mass balance, the leaching beds were cored and compared to the initial sediment contamination levels as described in the upcoming mass balance section.

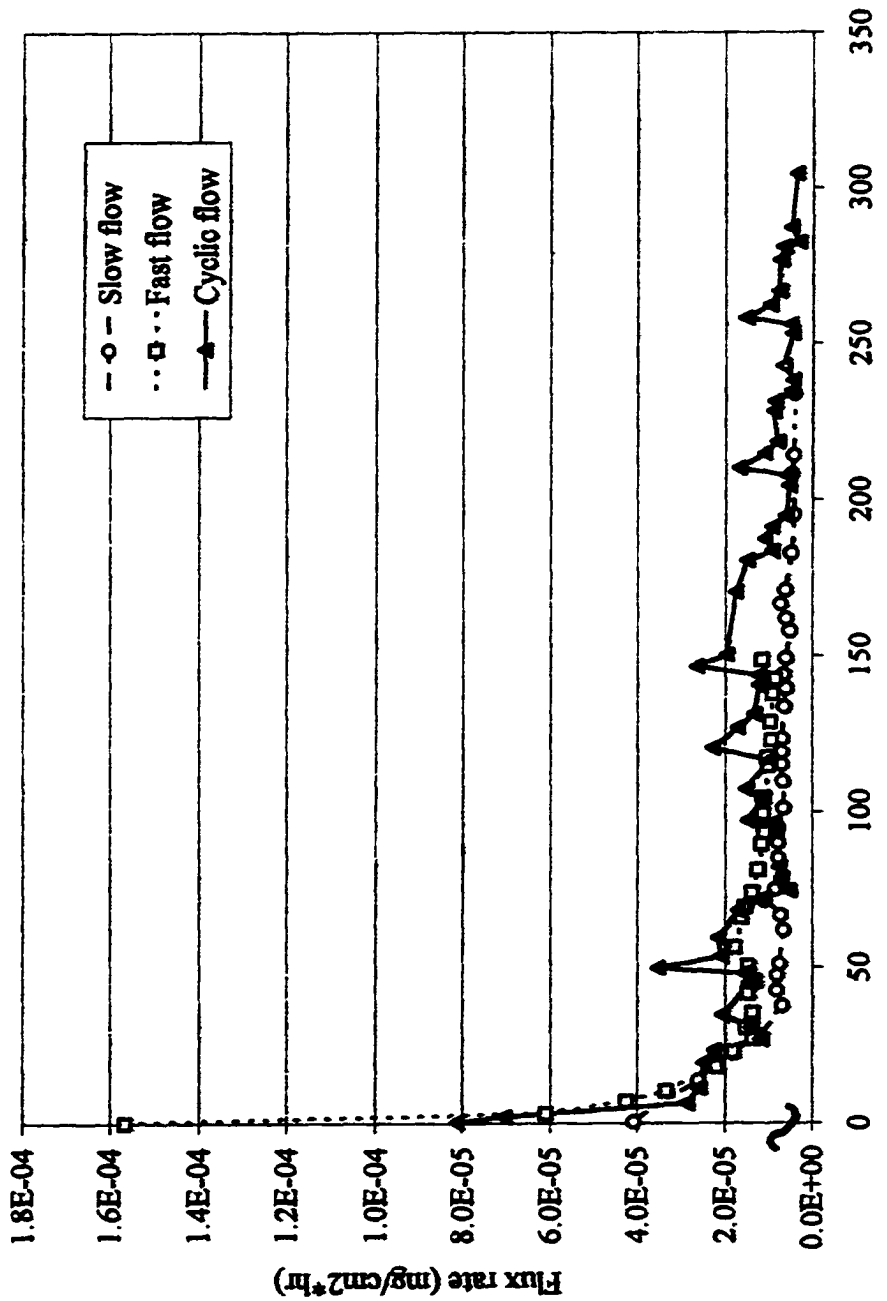

Figure 3.15. 1,3-DCB single contaminant flux comparison by flow

3.8 MASS BALANCE FOR 1,3-DCB AS SINGLE CONTAMINANT

3.8.1 Initial Contaminant Load

The initial contaminant load on the sediment was determined by taking replicate samples out of the sediment as it was loaded into the sheet flow leaching bed. The 1,3-DCB slow flow initial sediment load was 10.37 mg/kg as seen in Figure 3.16, for the 1,3-DCB fast flow the average sediment load is 12.97 mg/kg as seen in Figure 3.17. Finally, Figure 3.18 indicates the cyclic experimental initial load was 13.83 mg/kg. The desired contaminant load was 10-15 mg/kg. All the graphs show variability, which is due to the heterogeneity of the media.

3.8.2 Core Results

After the diffusion experiments were completed, the sediment was cored to determine the amount of pollutant left on the sediment. This remaining amount is termed the residual sediment load. The remaining contaminant load varied spatially inside of the leaching bed as can be seen from the core profiles. One graph is shown from each flow regime; slow, fast and cyclic, for the 1,3-DCB single contaminant studies as Figures 3.19, 3.20 and 3.21, respectively.

The slow flow experiment cores are shown in Figure 3.19. These cores do not show a clear trend. The front core has less sediment load than all the other cores. The bottom sections are expected to have a higher residual load or at least the same as the middle, which holds true for in this case. The top layer appears to have less 1,3-DCB than the other layers indicating loss of contaminant from that location.

In Figure 3.20, the back of the bed has a higher residual load in the 1,3-DCB fast flow experiment. There is lower residual load in the top layers at all three

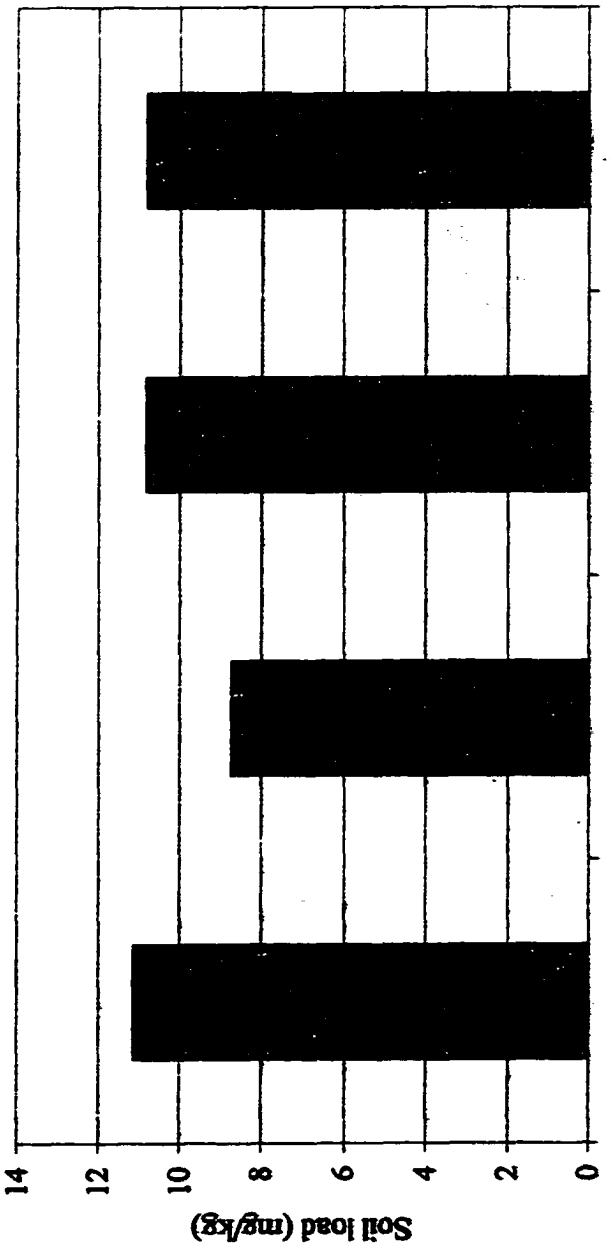

Figure 3.16. Single contaminant 1,3-DCB initial soil load for slow flow

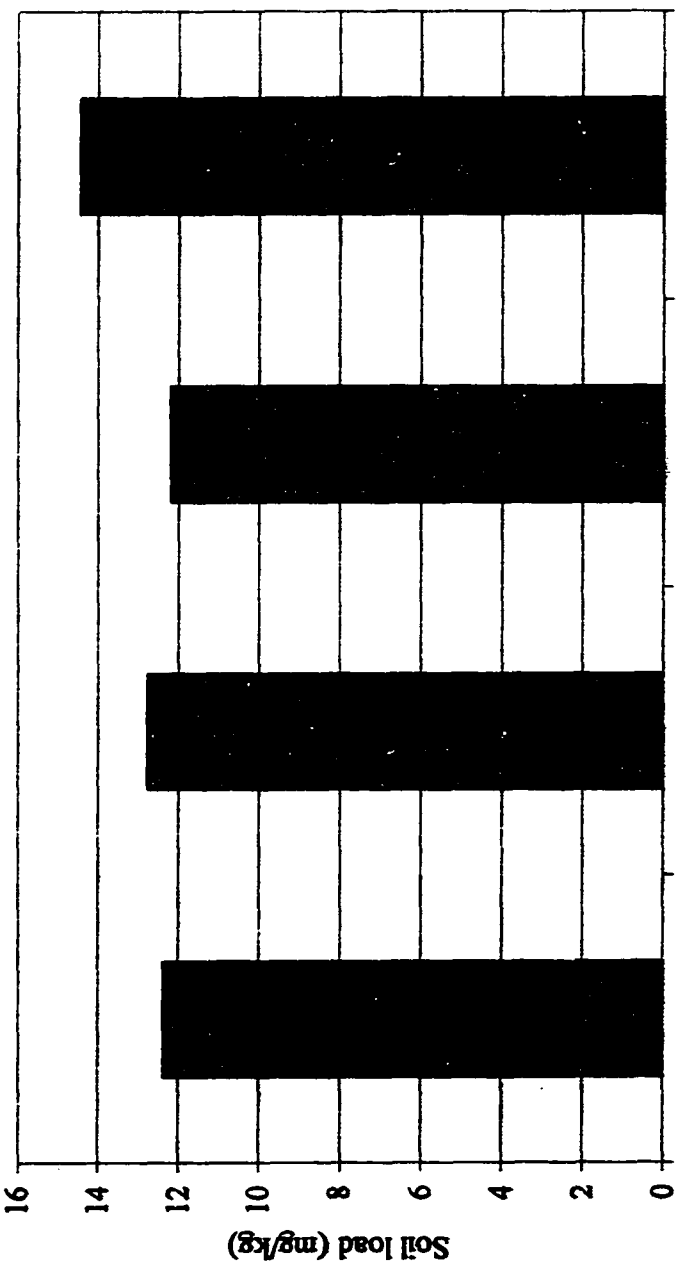

Figure 3.17. Single contaminant 1,3-DCB initial soil load for fast flow

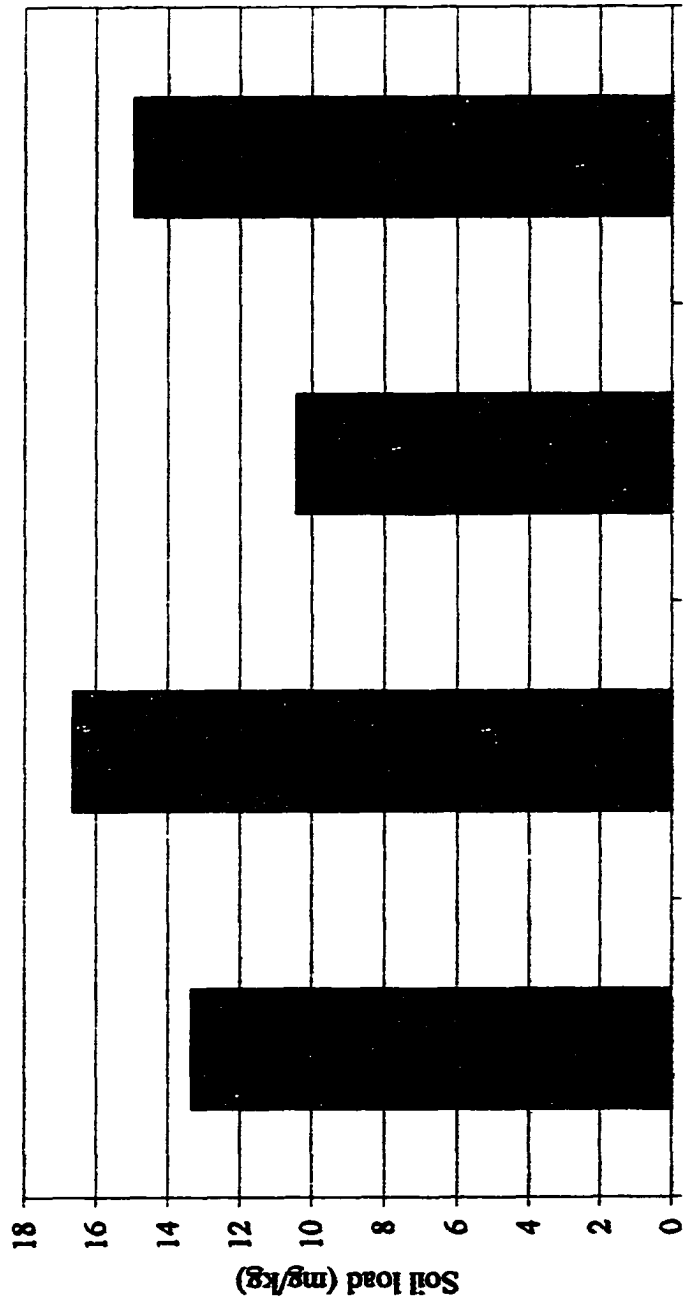

Figure 3.18. Single contaminant 1,3-DCB initial soil load for cyclic flow

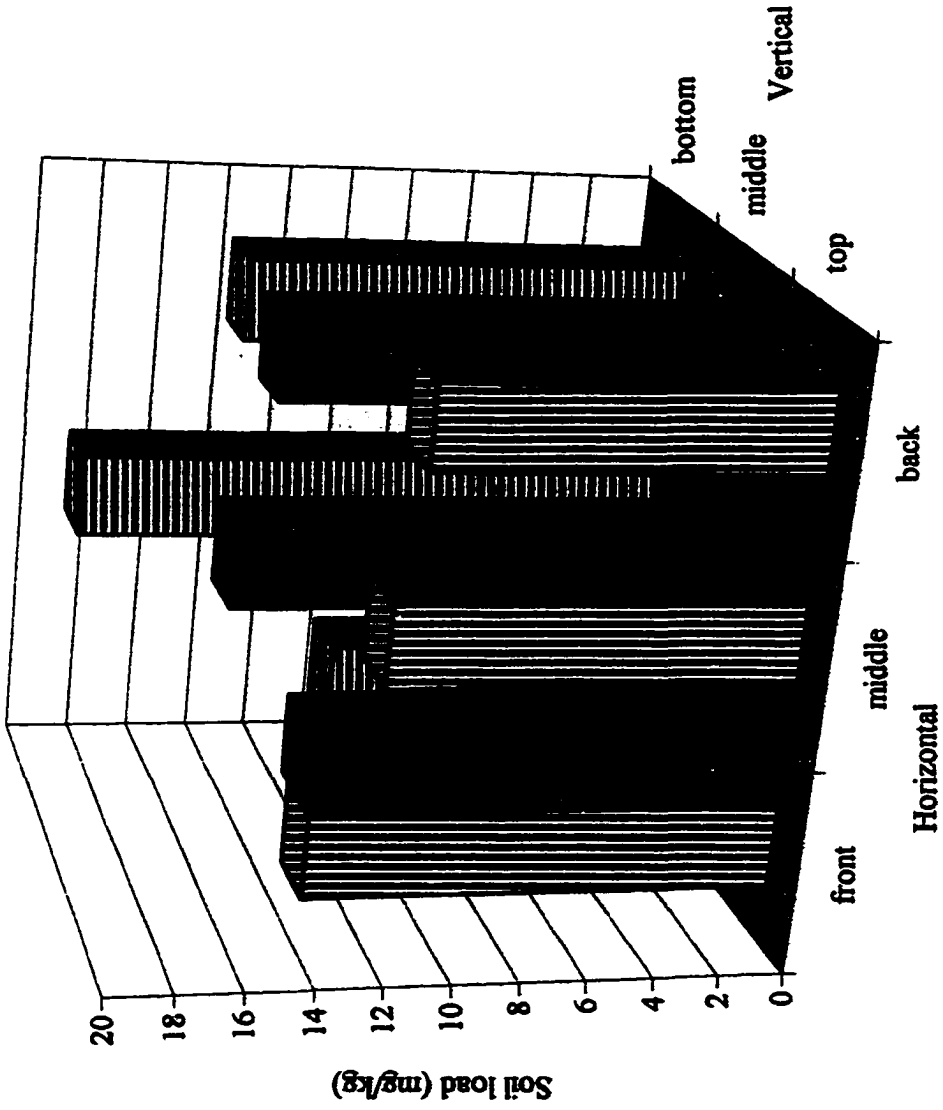

Figure 3.19. 1,3-DCB single contaminant slow flow core

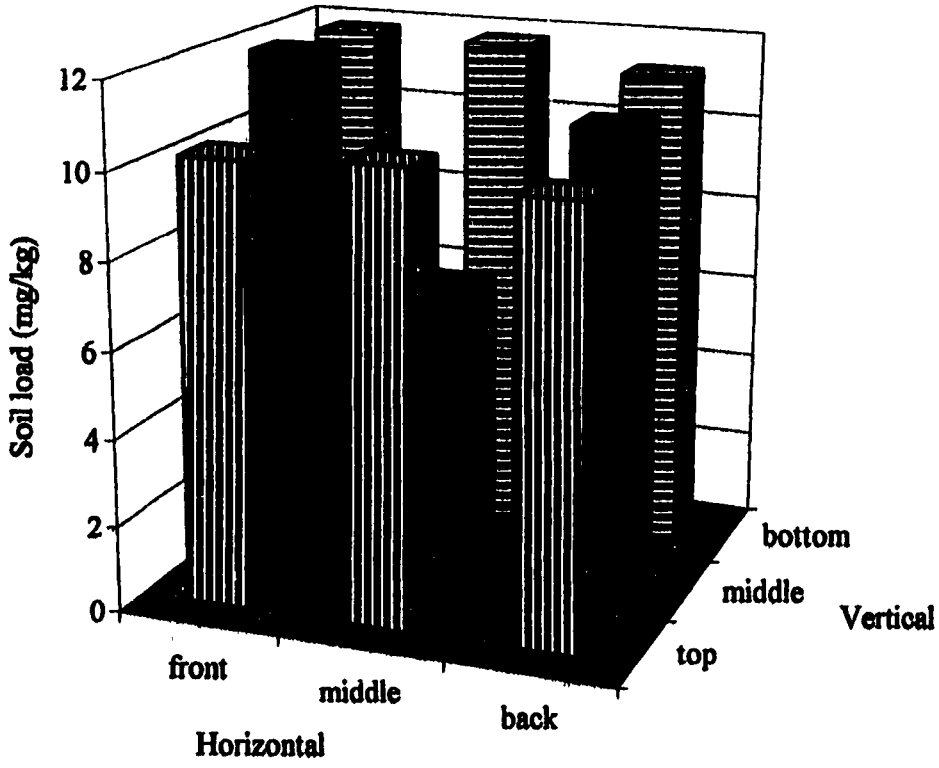

Figure 3.20. 1,3-DCB single contaminant fast flow core

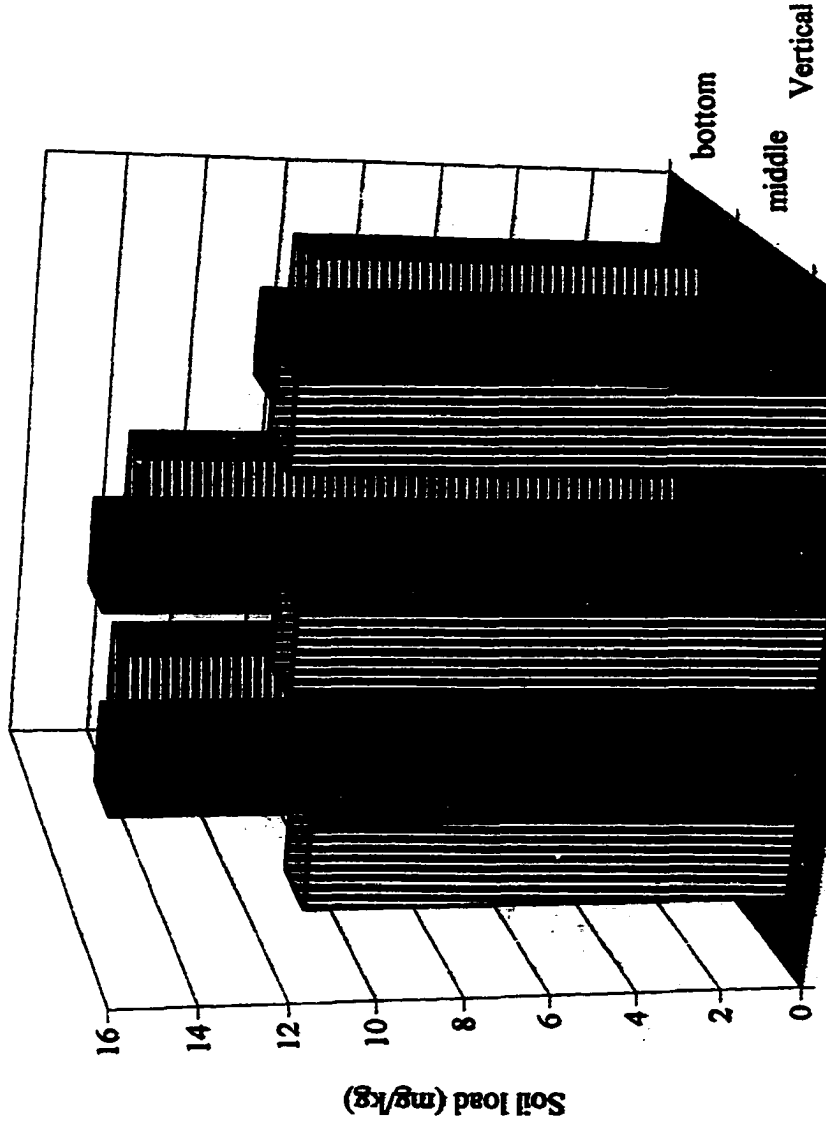

Figure 3.21. 1,3-DCB single contaminant cyclic flow core

horizontal locations in the bed indicating the pollutant 1,3-DCB has diffused out of those layers. There appears to be more residual contaminant load in the middle and bottom layers than in the top. The variation of the middle/middle core in all three figures is easily explained by sediment heterogeneity.

The last core results are presented in Figure 3.21 which is the cyclic flow for 1,3-DCB as a single contaminant. The general trend of less residual load in the top layer holds true throughout the bed. Overall, the middle has higher residual load that the bottom layer which has been true in the previous cores.

The significant observation from the coring analysis shows the front section of the bed having the least remaining sediment load. This may be due to the large driving force for diffusion at that location, where initial contact is made with the water.

3.8.3 Closure for 1,3-DCB

Table 3.8 presents the mass balance results for the 1,3-DCB as a single contaminant for all three flow regimes. The effluent mass removed was calculated by two different techniques and averaged as discussed previously in the MCB single contaminant study. The removal efficiency is shown by the mass/hour column. The cyclic experiment appears to have a lower efficiency until the short time interval of the experiment is noted. If the fast flow experiment were continued, the efficiency would drop below that of the cyclic flow as seen in the flux comparison of Figure 3.15. The percent closure is shown in the last column of Table 3.8. This series has an overall better percent closure but the variation between beds can be seen as

Table 3.8. 1,3-DCB single contaminant mass balance

Experiment	Total time (hours)	Effluent mass (mg)	Mass/hour (mg/hr)	Average core (mg/kg)	Ave. Initial Load (t=a) (mg/kg)	total soil per bed (kg)	Initial Mass per bed (mg)	Remaining mass per bed (mg)	% closure
slow (4)	234.25	0.458	0.001955	9.29	10.37	1.5	15.56	13.94	92.53
slow (4)	234.28	0.467	0.001993	18.19	10.37	1.5	15.56	27.29	178.41
slow (4)	234.25	0.49	0.002092	9.29	10.37	1.5	15.56	13.94	92.74
slow (4)	234.28	0.49	0.002092	18.19	10.37	1.5	15.56	27.29	178.56
average		0.47625	0.002033	13.74	10.37	1.5	15.555	13.935	135.5593
fast (3)	148.75	0.542	0.003644	14.78	12.97	1.5	19.46	22.17	116.74
fast (3)	148.68	0.57	0.003834	6.29	12.97	1.5	19.46	9.44	51.43
fast (3)	148.75	0.58	0.003899	14.78	12.97	1.5	19.46	22.17	116.94
fast (3)	148.68	0.61	0.004103	6.29	12.97	1.5	19.46	9.44	51.63
average		0.5755	0.00387	10.535	12.97	1.5	19.455	15.8025	84.18401
cyclic (5)	320.56	0.981	0.00306	15.01	13.83	1.5	20.75	22.52	113.26
cyclic (5)	288.53	0.934	0.003237	10.79	13.83	1.5	20.75	16.19	82.52
cyclic (5)	320.56	1.022	0.003188	15.01	13.83	1.5	20.75	22.52	113.46
cyclic (5)	288.53	0.966	0.003348	10.79	13.83	1.5	20.75	16.19	82.68
average	304.545	0.97575	0.003208	12.9	13.83	1.5	20.745	19.35	97.97903

significant. The low percent closure may be explained by sediment heterogeneity, volatilization to headspace in the SFLB, and possible loss due to sampling technique.

3.9 DISCUSSION OF SINGLE CONTAMINANT STUDIES

A comparison of all flow regimes by their flux values for 1,3-DCB is shown in Figure 3.15, which is similar to the other MCB single contaminant behavior curves in Figure 3.7. The single contaminant 1,3-DCB studies indicate the cyclic flow regime may be the most effective leaching mechanism as found in the MCB work. The graphs of MCB and 1,3-DCB for all three flow regimes indicate similar contaminant flux behavior in both experiments. The fast and slow flow regimes appear to follow the same trend of exponential decay. In both MCB and 1,3-DCB, the cyclic run demonstrates spikes of higher flux when the flow rate changes yielding a higher overall average flux rate than either the slow or fast flow. Thus, natural rainfall events in BRB may show incremental higher flux of lower chlorinated benzenes than would be expected in steady state systems. While flux is increased, it is still at relatively low levels which could be subject to phytoremediation and /or natural attenuation processes.

The cores support the removal of chlorinated benzenes from sediment due to leaching. The MCB cores show removal from the front top section during all flow regimes. The 1,3-DCB cores are not as clear but do indicate 1,3-DCB is removed from the sediment during the course of the experiment. The mass balance for the single contaminant studies show the variation between the replicates and reasonably good closure for DCB experiments.

3.10 RESULTS OF MULTIPLE CONTAMINANT STUDIES

These studies examine diffusive transport of a four contaminate mixture on laboratory contaminated sediments. The results will discuss flux rates, not concentration, since they are inherently related as seen in Equation 1 and in the single contaminant studies.

Figures 3.22, 3.23 and 3.24 compare the flux of the mixture (four chlorinated benzene contaminants, chlorobenzene (MCB), 1,3 – dichlorobenzene (1,3-DCB), 1,2 – dichlorobenzene (1,2-DCB), and 1,2,4 – trichlorobenzene (TCB)) over time for each of the flow regimes; slow, fast and cyclic. The individual component flux rates are shown to vary at all three flow regimes, slow, fast, and cyclic. Although the graphs show overall behavioral similarity, it should be noted that each compound partitions into the water phase differently due to differences in chemical properties such as K_{ow} and solubility. Of note is 1,2-DCB which appears to be very mobile under all flow conditions.

In the multi-contaminant series of experiments, the cyclic flow regime was repeated twice with similar results as seen by Figure 3.24 and 3.25. A saw tooth pattern can be seen in Figures 3.24 and 3.25 demonstrating the non-equilibrium conditions enhanced flux rates and concentrations. Graphically, a pattern of higher contaminant concentrations, and consequently higher flux rates, is indicated when the pump was cycled. The concentrations and flux rates return to steady state levels after 4-8 hours.

The next four figures are comparing the flux under different flow conditions for each contaminant. Figure 3.26 follows the MCB component of the mixture under

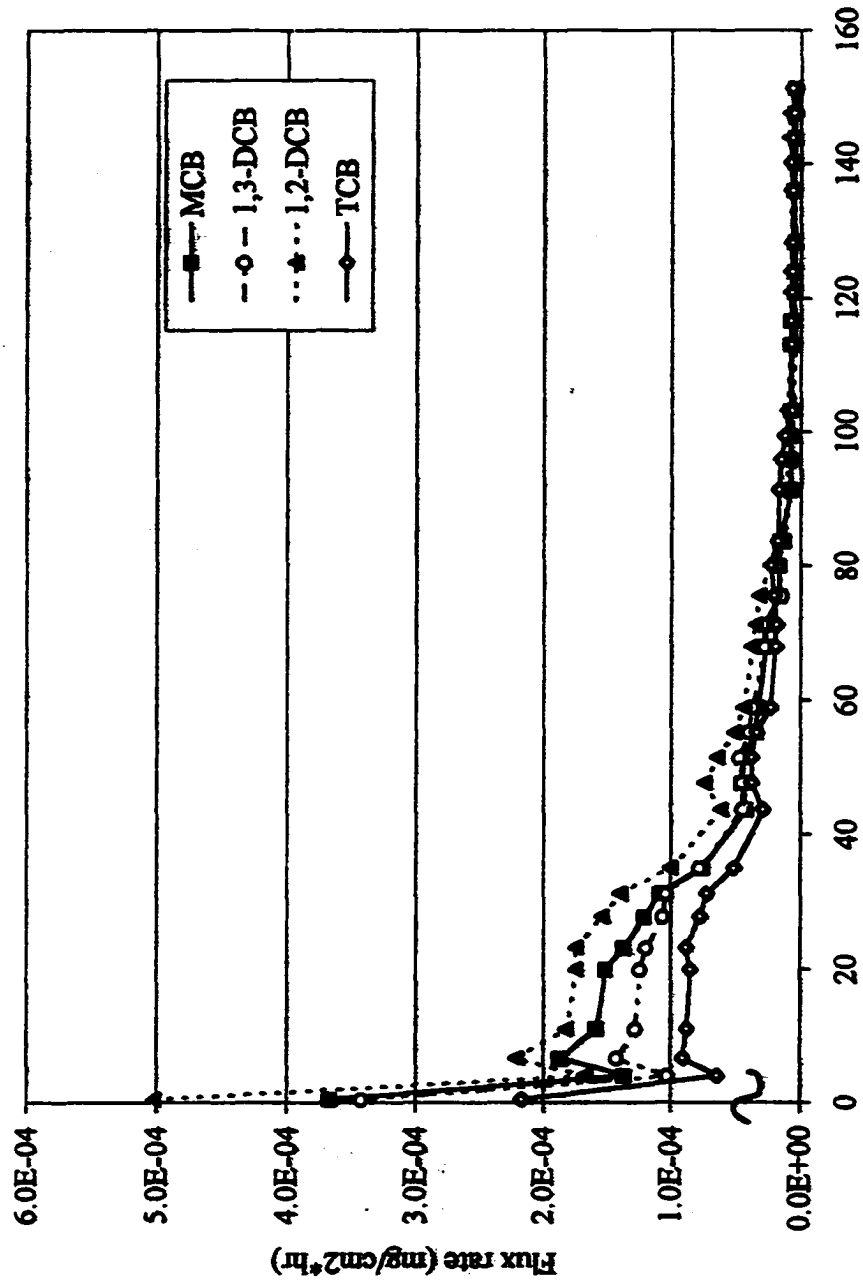

Figure 3.22 Contaminant mixture flux for slow flow

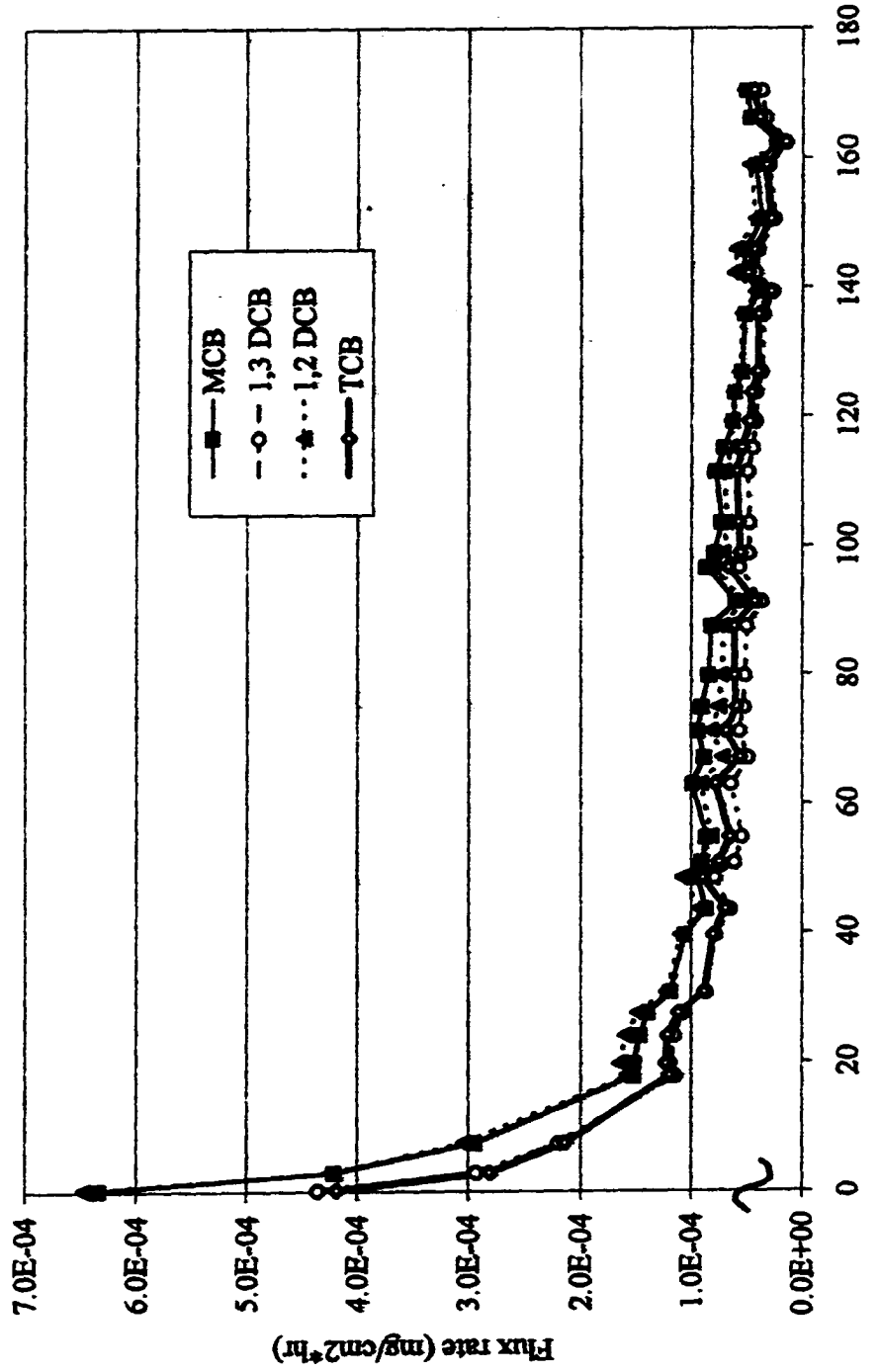

Figure 3.23. Contaminant mixture flux for fast flow

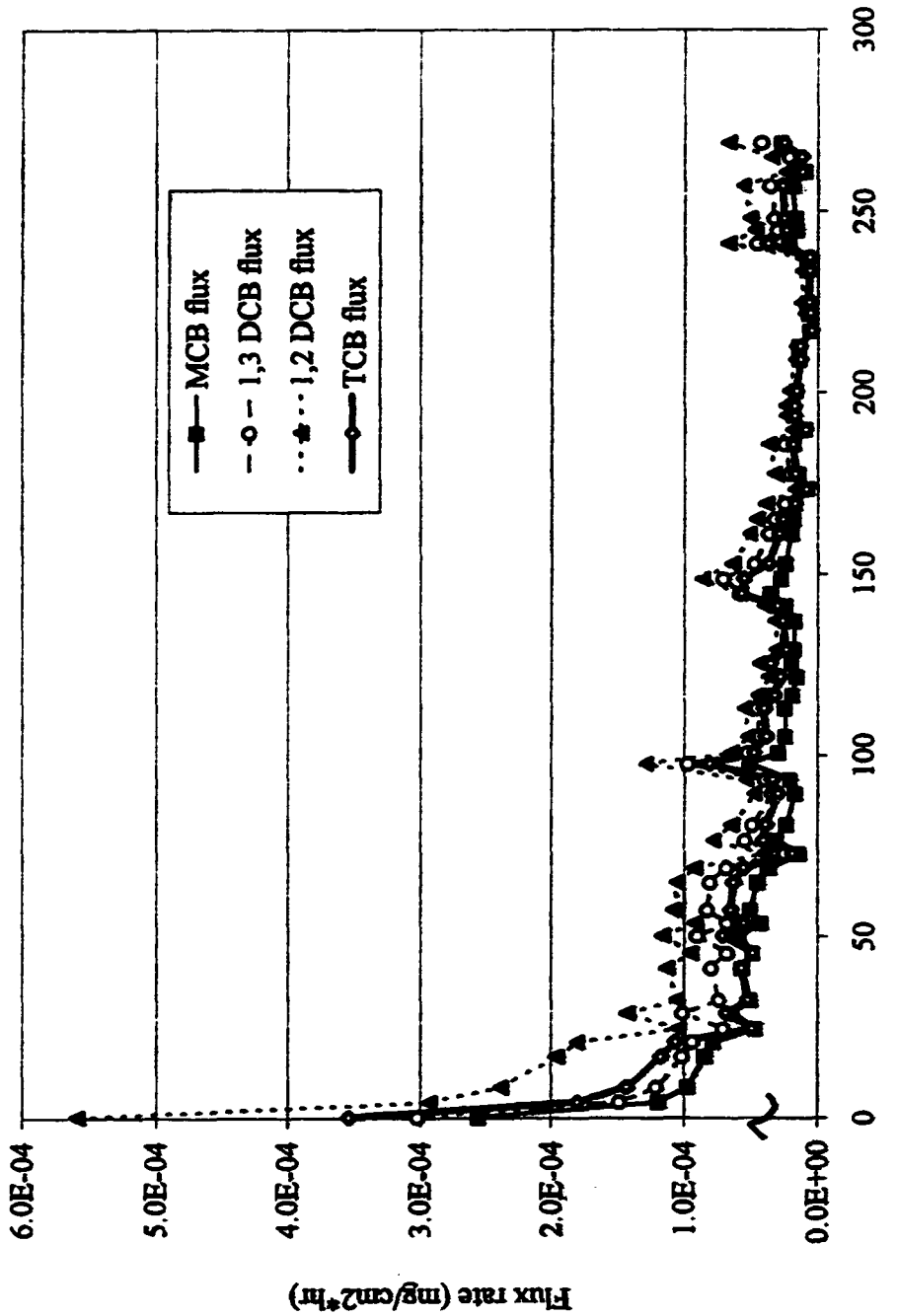

Figure 3.24. Contaminant mixture flux for cyclic flow

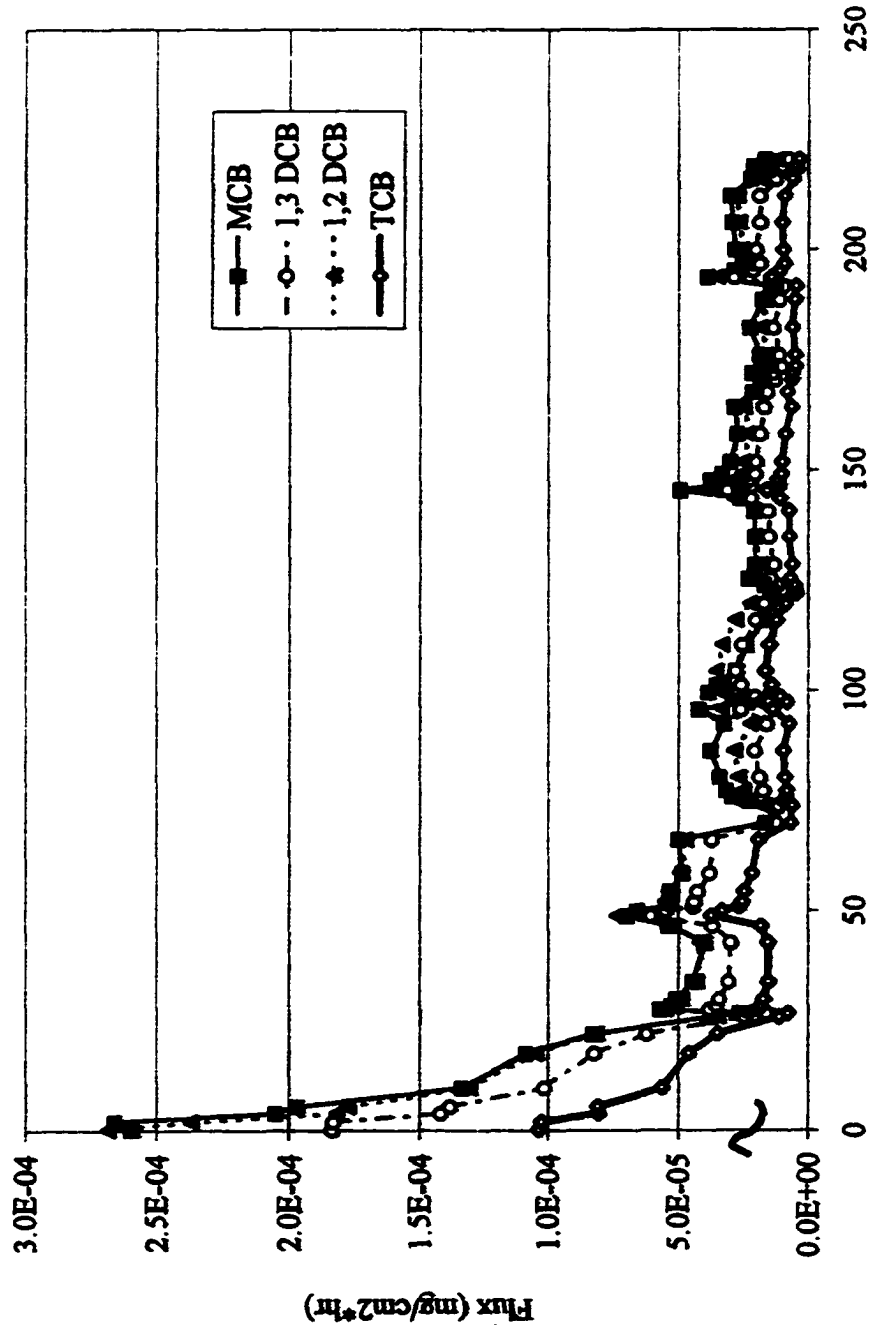

Figure 3.25. Contaminant mixture flux for repeated cyclic flow

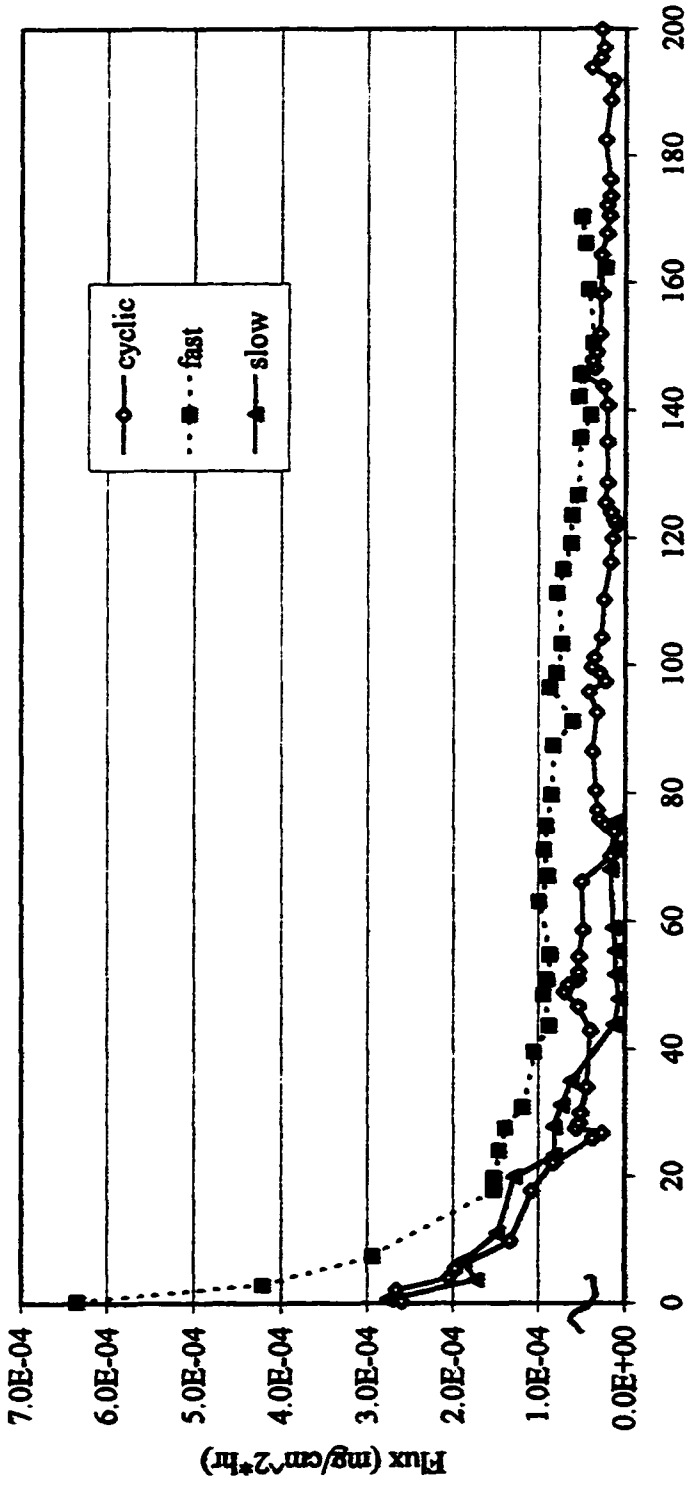

Figure 3.26. MCB in mixture flux behavior

slow, fast and cyclic flow regimes. Figure 3.27 follows the 1,3-DCB component of the mixture under slow, fast and cyclic flow regimes. The 1,2-DCB component is shown in Figure 3.28 and TCB is shown in Figure 3.29. These graphs show overall behavioral similarity, it should be noted that flux rates for each component in the mixture, under all three pumping regimes, indicated the fast flow system appears as the most efficient leaching removal, followed by cyclic rate. The diffusion modeling observed in the single contaminant studies is further evaluated via adsorption studies in the last section of the report.

3.11 MASS BALANCE FOR MULTIPLE CONTAMINANT STUDIES

3.11.1 Initial Contaminant Load

The initial contaminant load on the sediment was determined by taking replicate samples out of the sediment as it was loaded into the sheet flow leaching bed. In the slow flow experiments the initial starting contaminant load for MCB is 20.25 mg/kg, 1,3-DCB starts at 31.47 mg/kg, 1,2-DCB has initial starting concentration 35.21 mg/kg and TCB is 41.13 mg/kg as seen in Figure 3.30. Each concentration is the average of four replicates (not shown).

The next set of data examines the initial contaminant level for the fast flow experiment of all four CB components. The MCB initial load was 25.07 mg/kg, 1,3-DCB initial sediment load was 39.74 mg/kg, 1,2-DCB sediment load was 41.99 mg/kg, and TCB was 53.79 mg/kg as shown in Figure 3.31.

Finally, Figure 3.32 indicates the cyclic flow experimental initial load for MCB was 7.44 mg/kg, 1,3-DCB had initial load of 4.22 mg/kg, the 1,2 isomer was

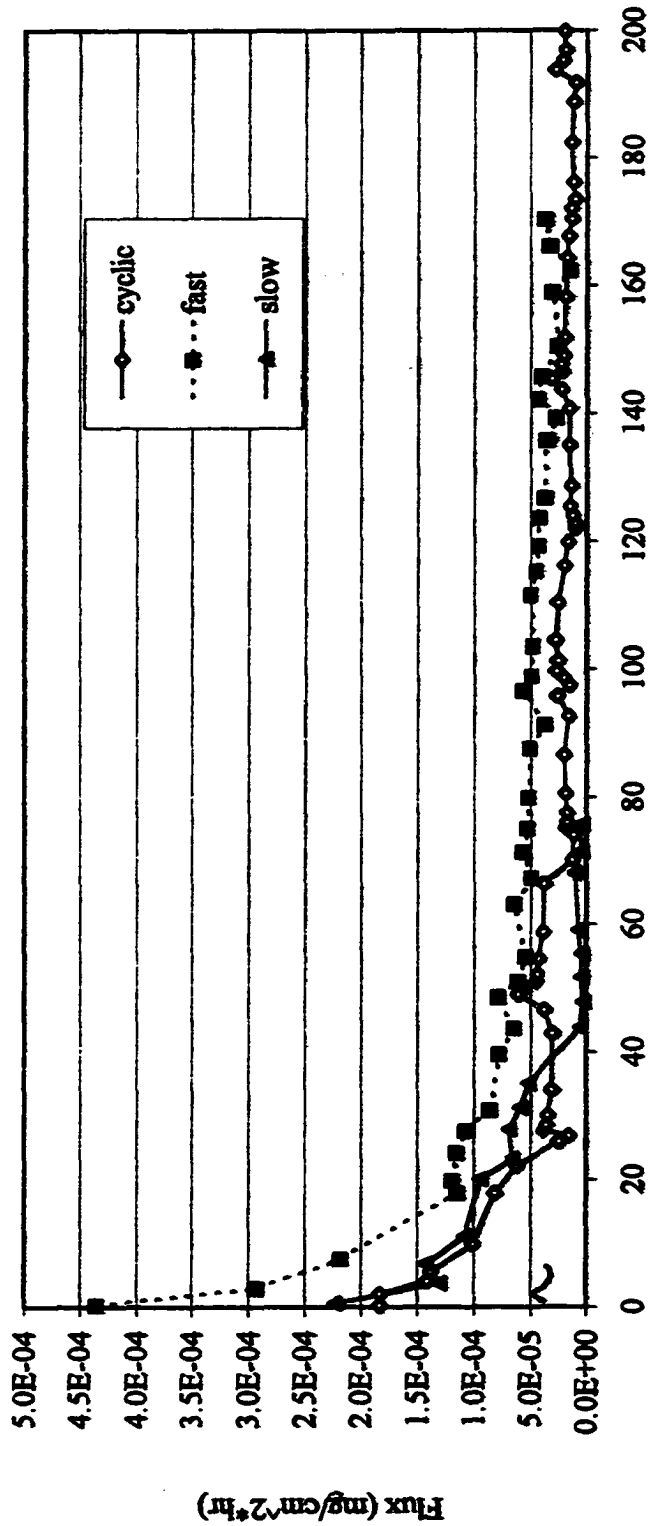

Figure 3.27. 1,3-DCB in mixture flux behavior

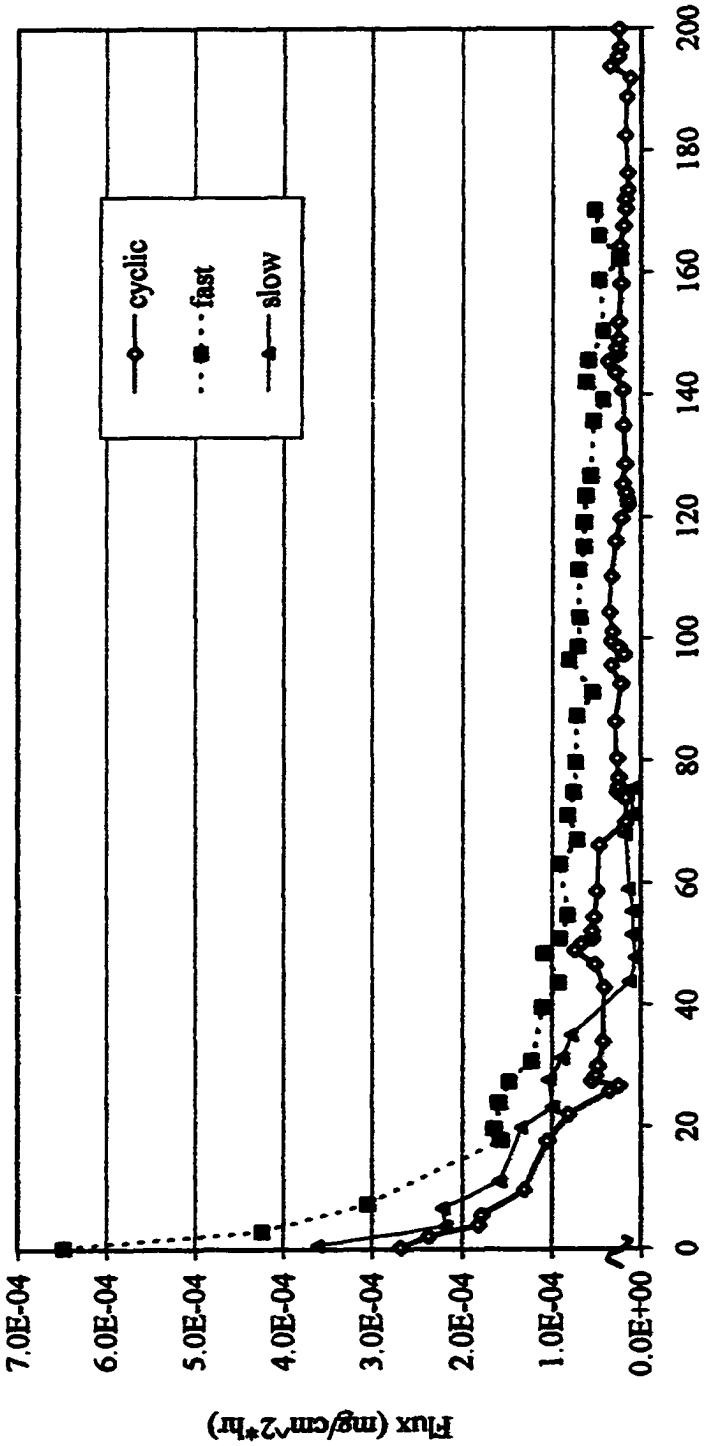

Figure 3.28. 1,2-DCB in mixture flux behavior

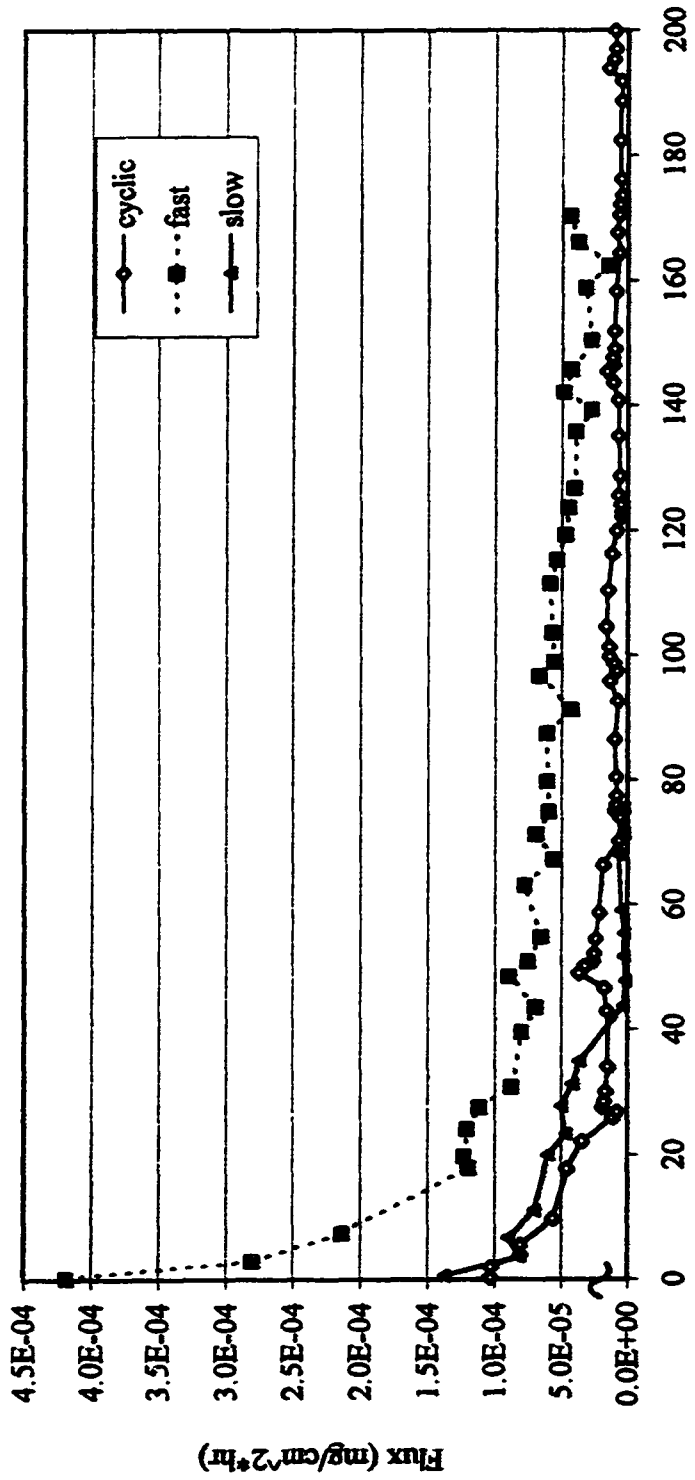

Figure 3.29. TCB in mixture flux behavior

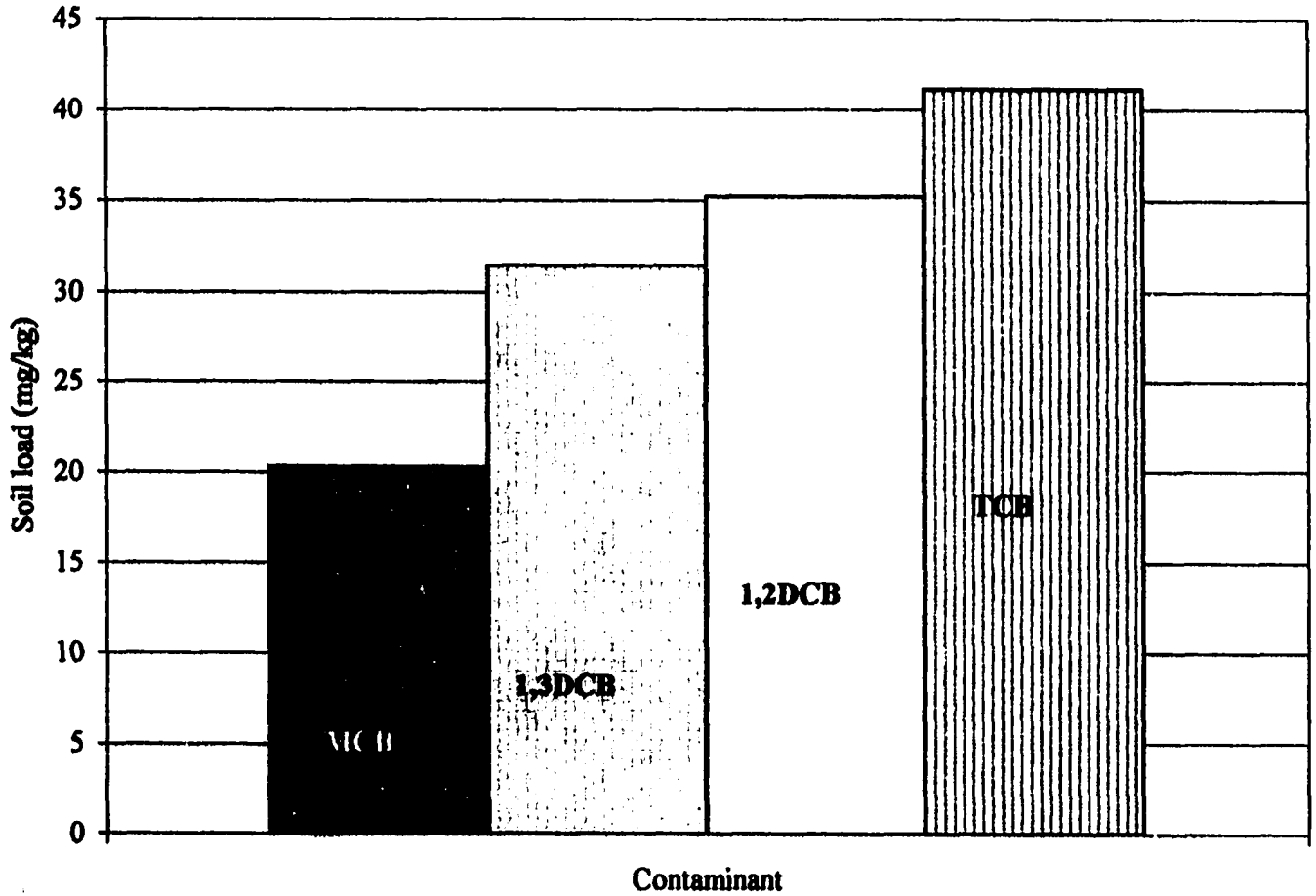

Figure 3.30 Initial mixture sediment load under slow flow

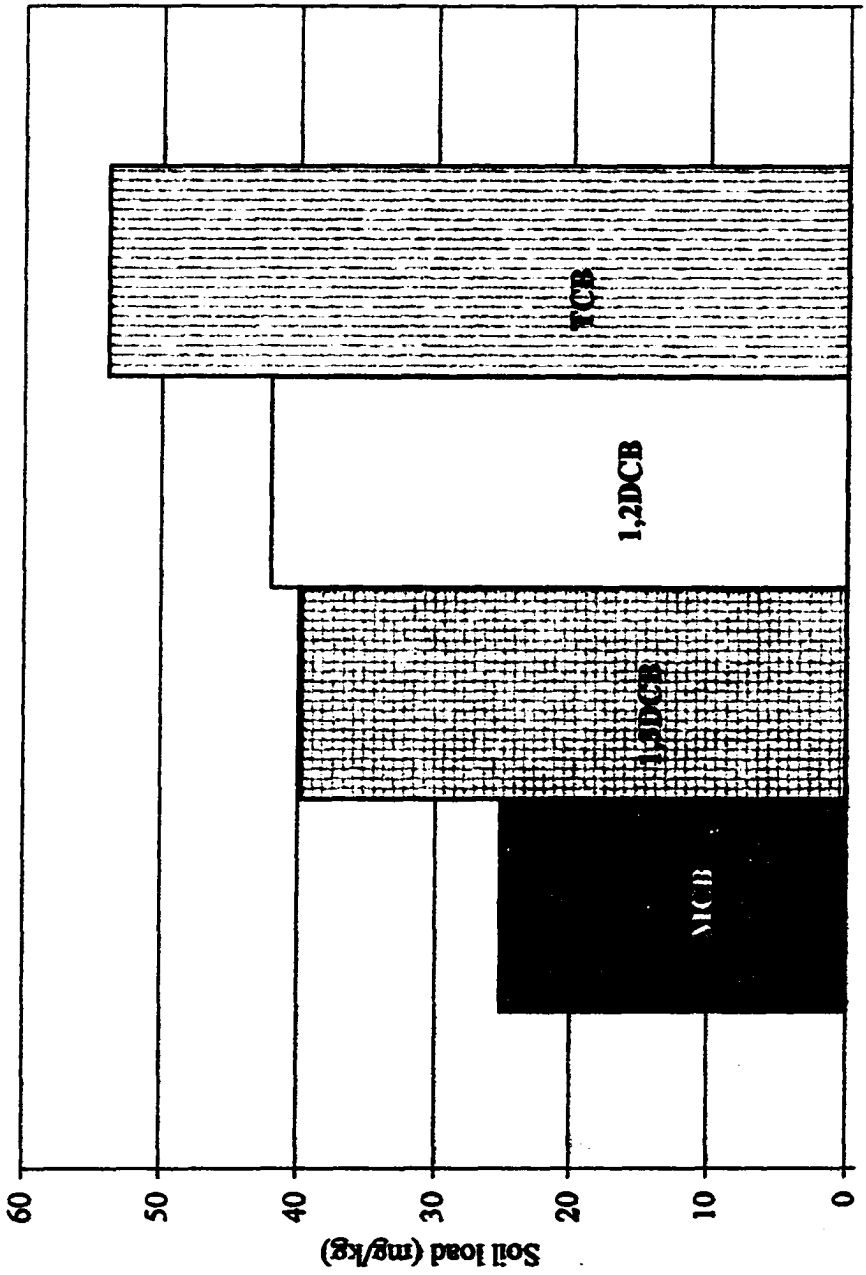

Figure 3.31 Initial mixture sediment load under fast flow

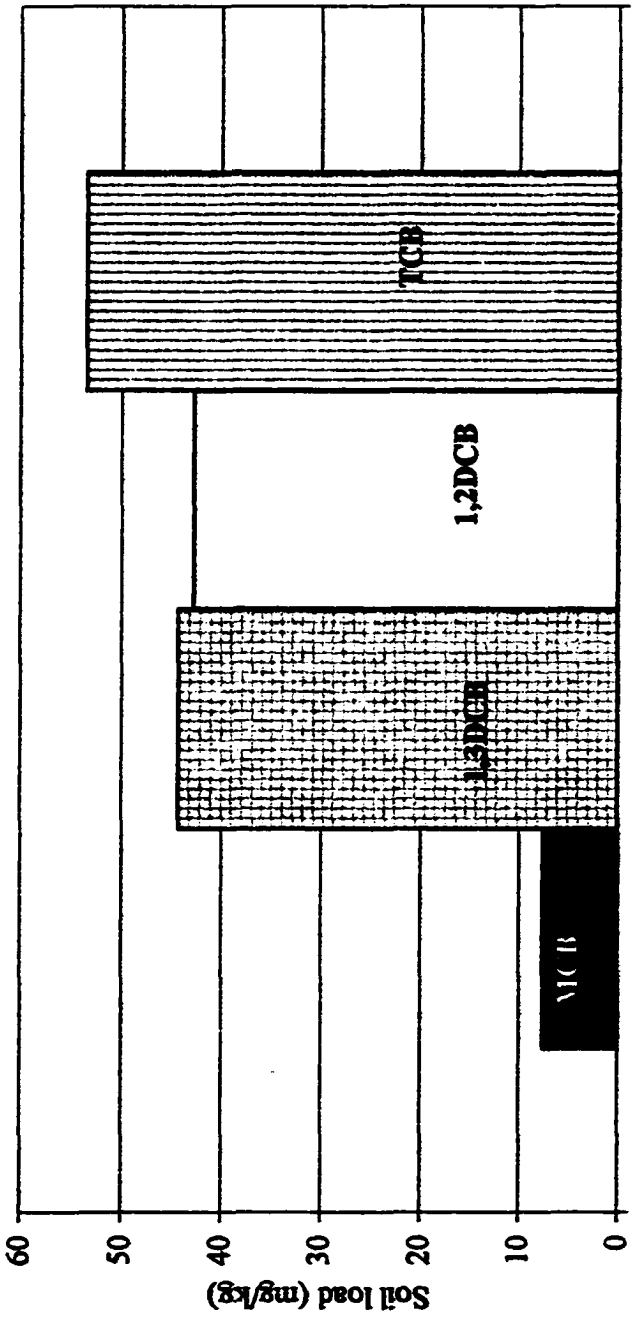

Figure 3.32 Initial mixture sediment load under cyclic flow

42.64 mg/kg and TCB started at 53.38 mg/kg. Each chlorobenzene value is the average of four replicates.

3.11.2 Core Results

After the diffusion experiments were completed, the sediment bed was cored to determine the amount of chlorobenzenes left on the sediment. This remaining amount is termed the residual sediment load. The remaining contaminant load varied spatially inside of the leaching bed as can be seen from the core profiles. Each contaminant will be examined individually under each flow regime but the graph will feature the average of both beds.

To examine the leaching effectiveness of the chlorinated benzenes the beds were cored as described previously. The four contaminants under slow flow are shown individually so their spatial variation can be seen in Figures 3.33 follows MCB, Figure 3.34 follows 1,3-DCB, Figure 3.35 for 1,2-DCB and Figure 3.36 examines TCB. All four of the components show similar removal patterns with horizontal variation being most noticeable. In Figure 3.33, the MCB results indicate the front core vertically having the least amount of residual contaminant. In the DCB isomers and TCB, Figures 3.34, 3.35, and 3.36 respectively, the middle layer has the highest remaining sediment load. Notice the trend of the front core having the lowest residual load is present in all four figures. This supports the driving force of clean water at the front of the bed.

Figures 3.37, 3.38, 3.39 and 3.40 present the results for the residual sediment load of all four CB's in the fast flow experiment. All four figures indicate the major variations in the horizontal plane, front to back. The front has the least residual and

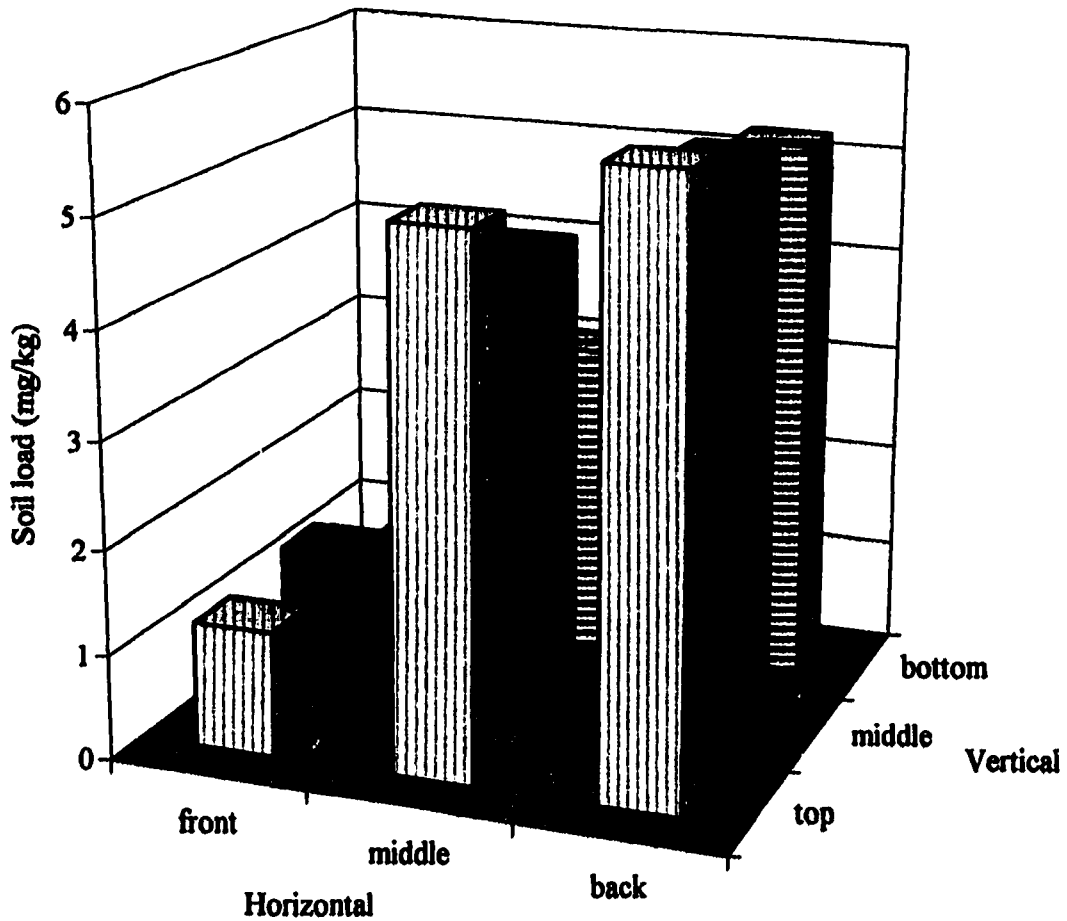

Figure 3.33. Multiple contaminant MCB slow flow core

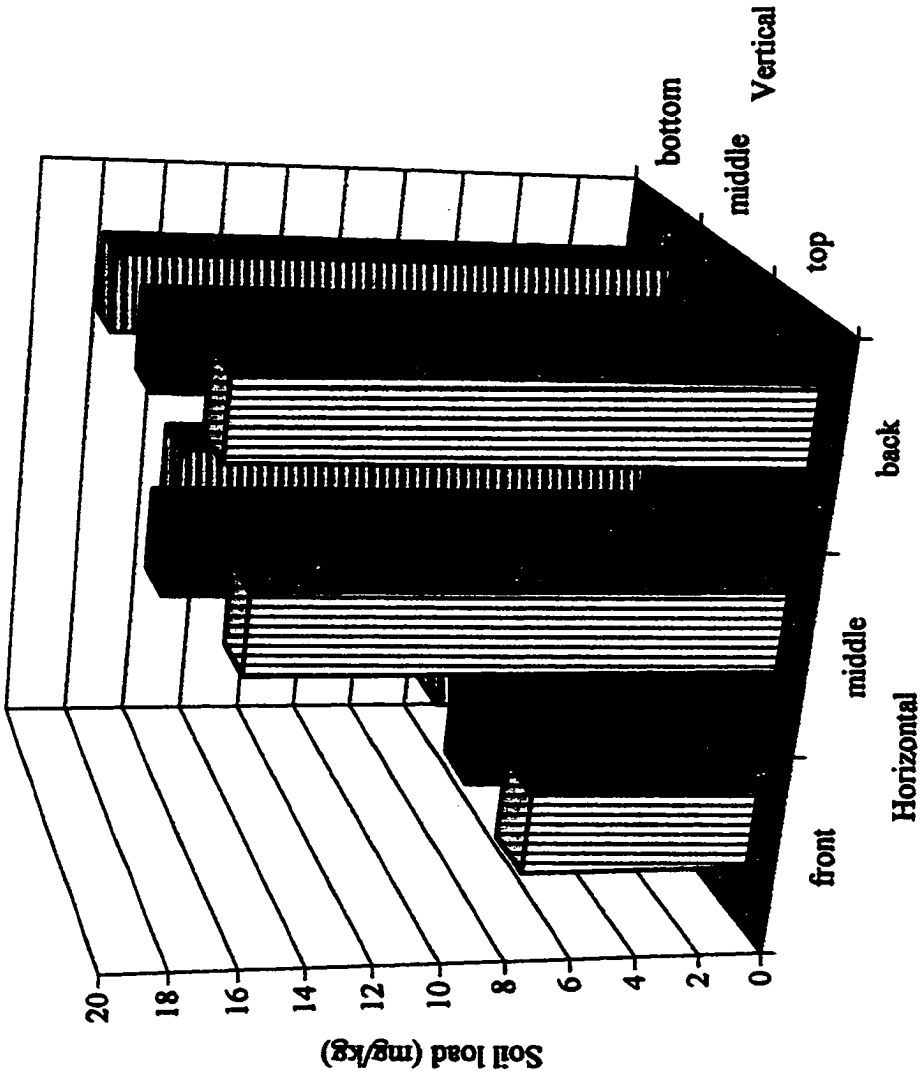

Figure 3.34. Multiple contaminant 1,3-DCB slow flow core

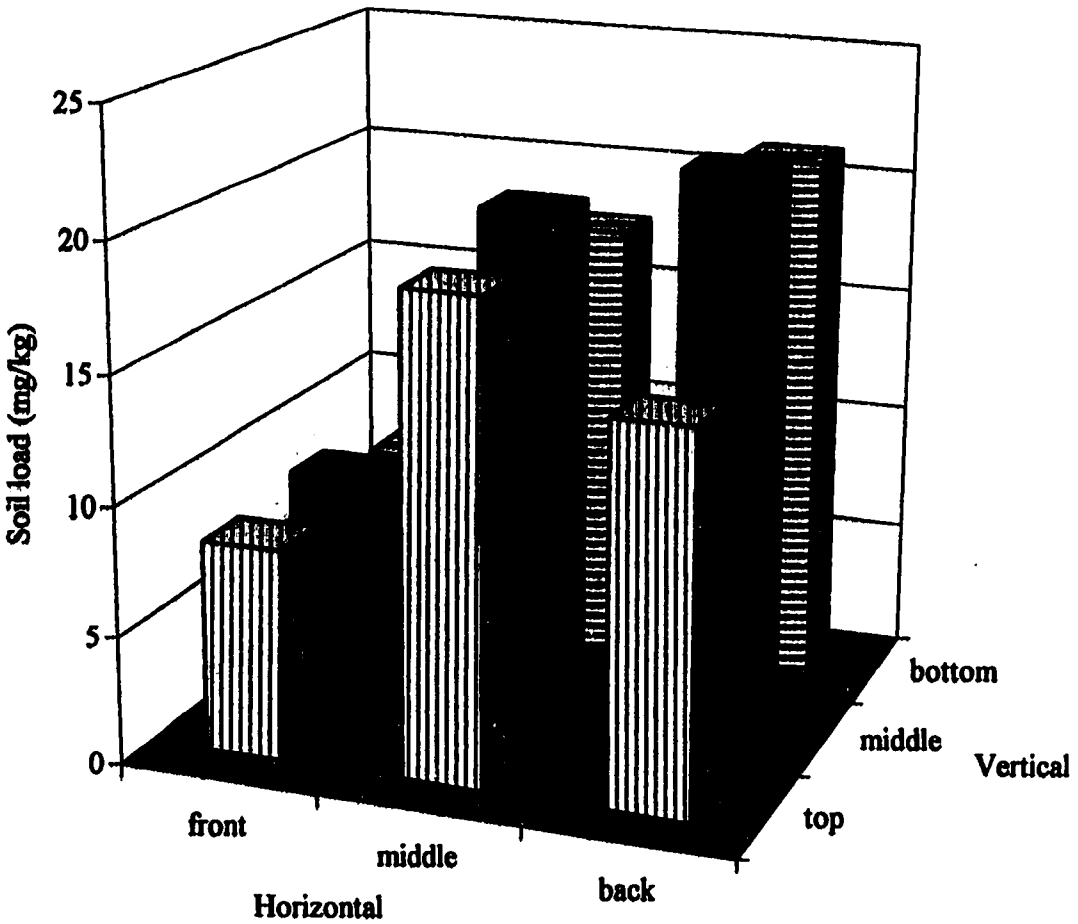

Figure 3.35. Multiple contaminant 1,2-DCB slow flow core

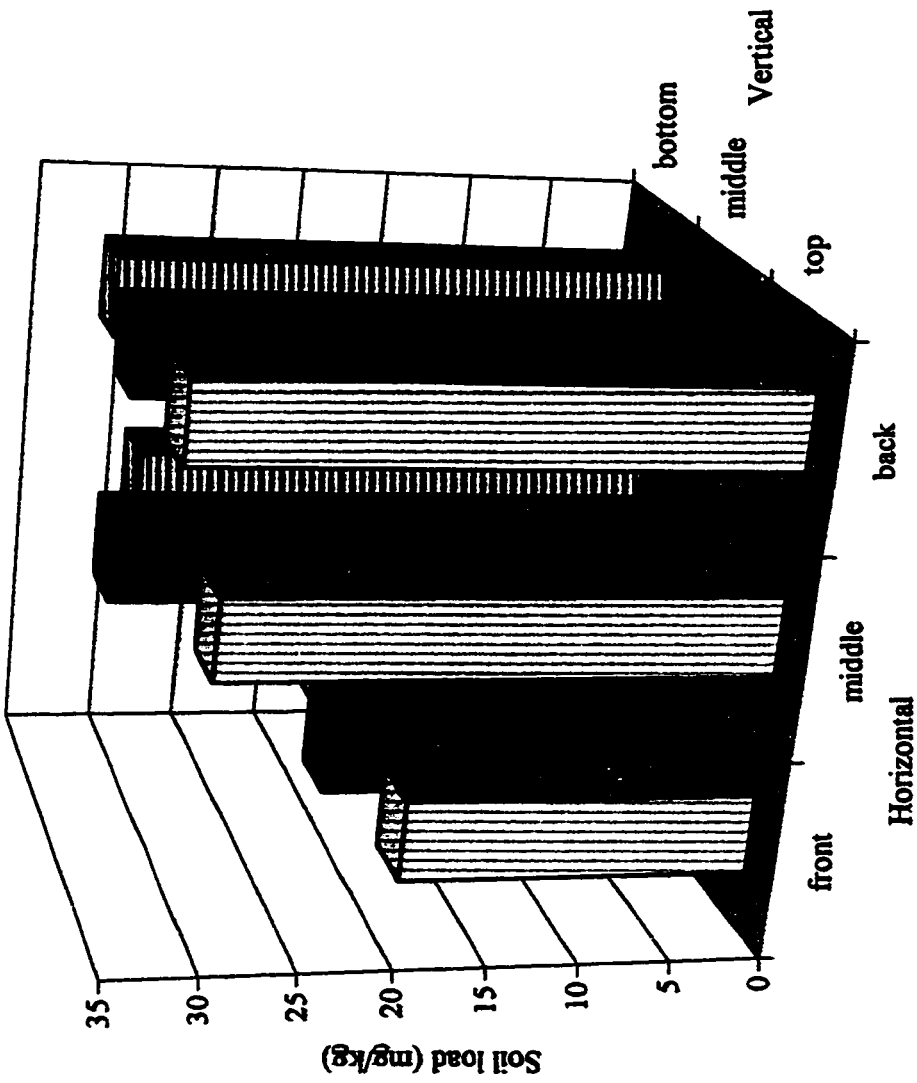

Figure 3.36. Multiple contaminant TCB slow flow core

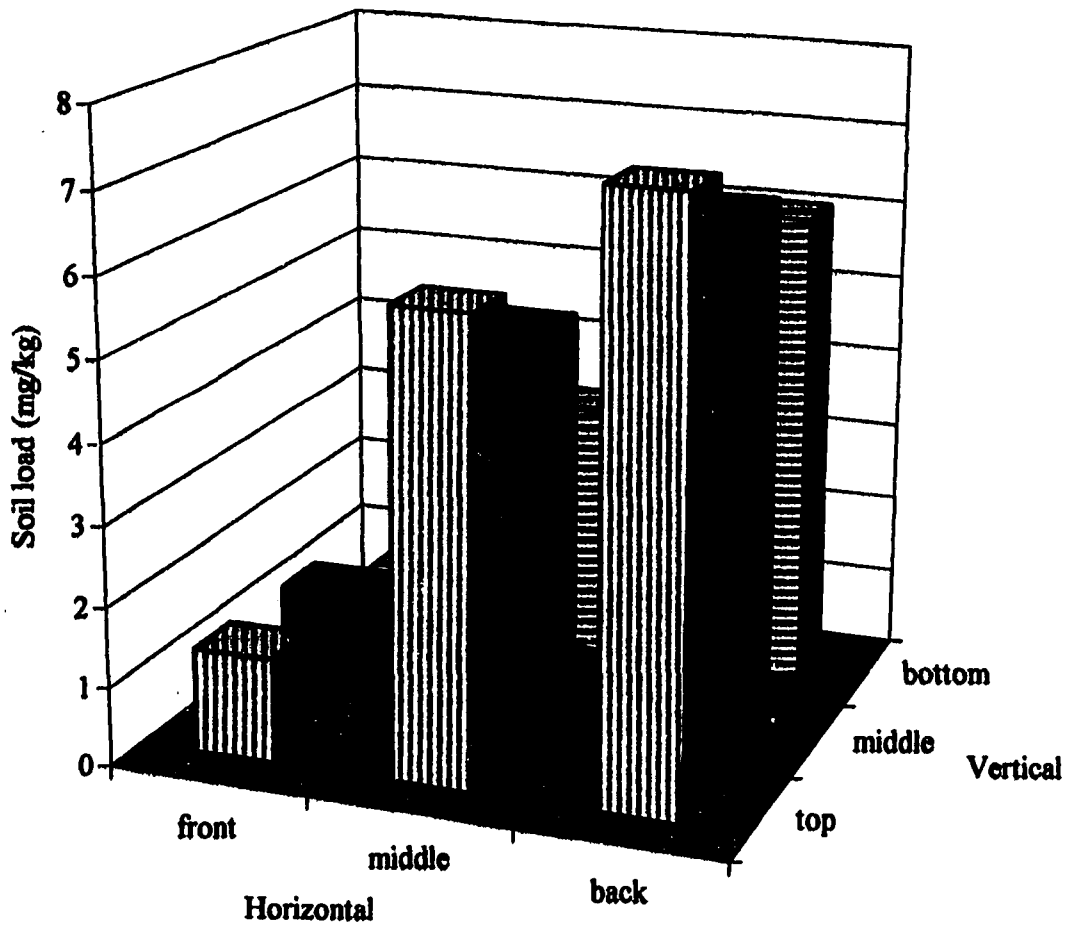

Figure 3.37. Multiple contaminant fast flow MCB core

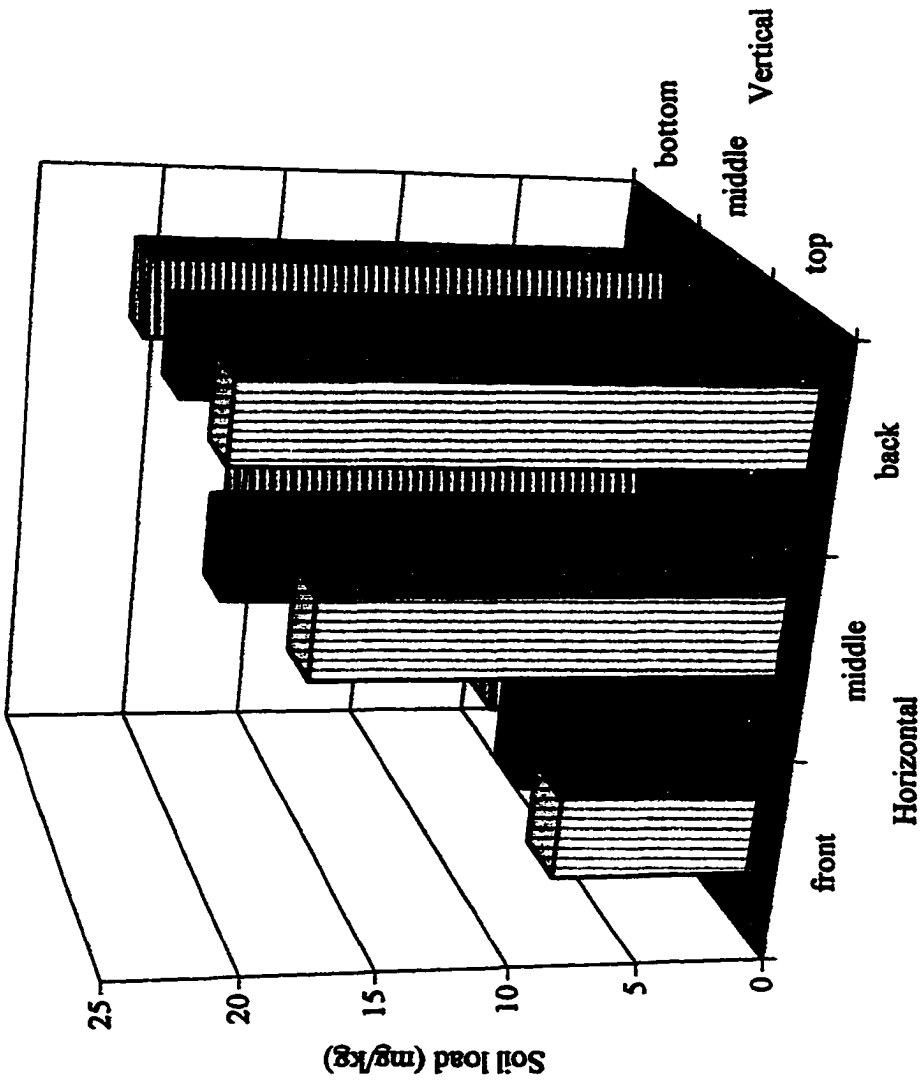

Figure 3.38 Multiple contaminant fast flow 1,3-DCB core

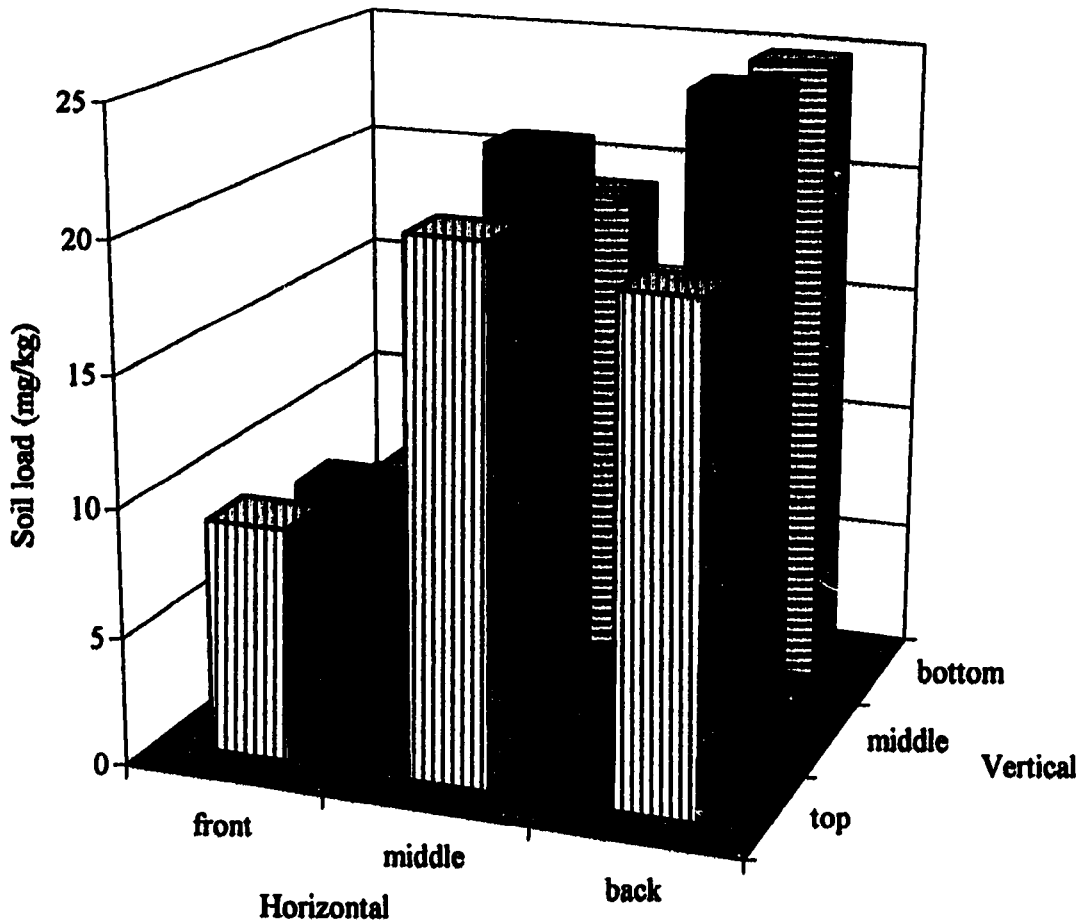

Figure 3.39. Multiple contaminant fast flow 1,2-DCB core

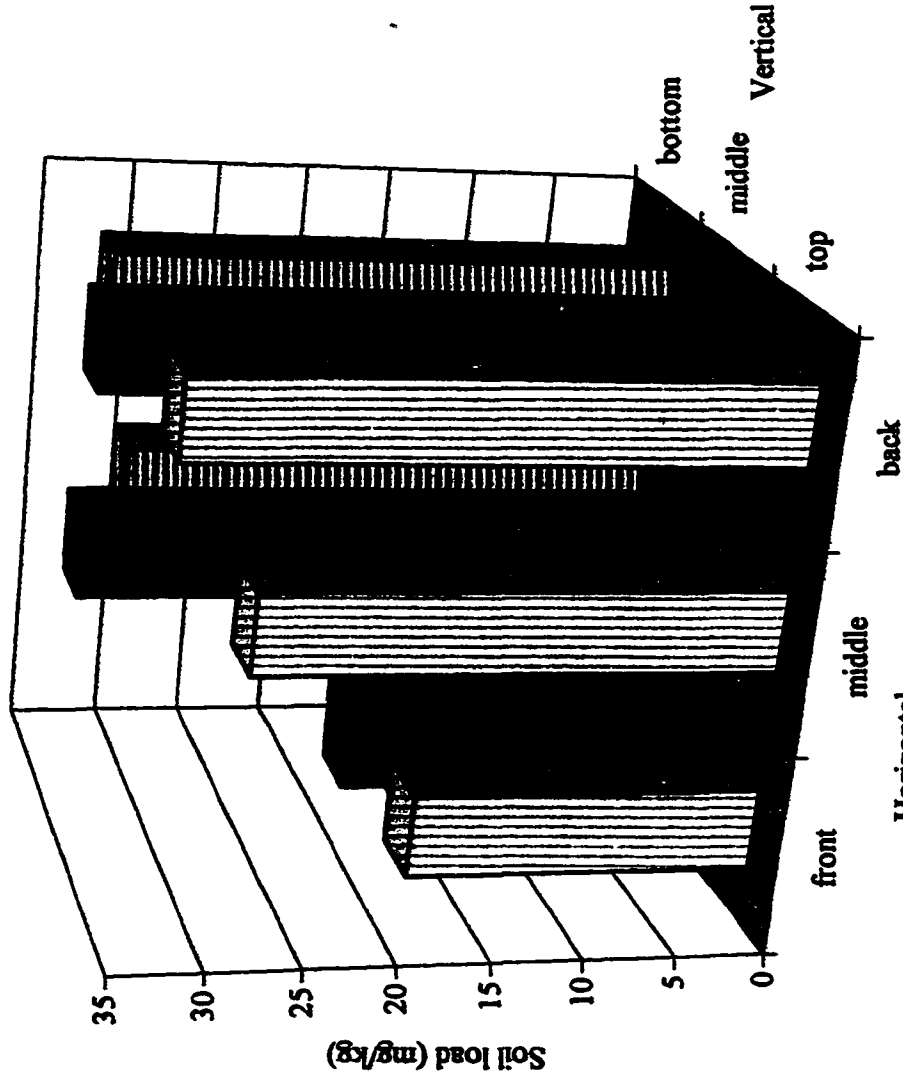

Figure 3.40. Multiple contaminant fast flow TCB core

the back has the most residual load as seen in the slow flow regime. The vertical change that was expected in not clear, in fact the MCB bottom layer has less consistently than the top as shown in Figure 3.37. The other more chlorinated constituents indicate the middle layer in the horizontal plane as having a similar residual load as the bottom layer as predicted can be seen in Figures 3.38, 3.39, and 3.40.

The core results for all four components in the multiple contaminant cyclic flow regime consistently show significant mass removal in the top layer at all locations in the leaching bed. The MCB cores indicate good removal in the top layer and some removal from front to back as shown the other cores as can be see in Figure 3.41. Figure 3.42 indicates the 1,3-DCB core looks very similar to the MCB core with the most contaminant removal in the top and front layer and residual load in the back and bottom. In Figure 3.43, the 1,2-DCB core, the removal pattern is both horizontal and vertical indicating the most loss in the layers closest to the clean water source as expected. Finally, the TCB isomer shows the same trend as the other cores in this flow regime in Figure 3.44. This removal pattern of consistently less in the top layer vertically is different from the two previous single flow rate studies where the major change was along the horizontal axis.

3.11.3 Closure for Multiple Contaminant Studies

Table 3.9 presents the mass balance results for the multiple contaminant mixture for all three flow regimes. The effluent mass removed was calculated by two different methods as discussed previously and averaged as shown. The removal efficiency is shown by the mass/hour column. At first glance, it would appear that fast

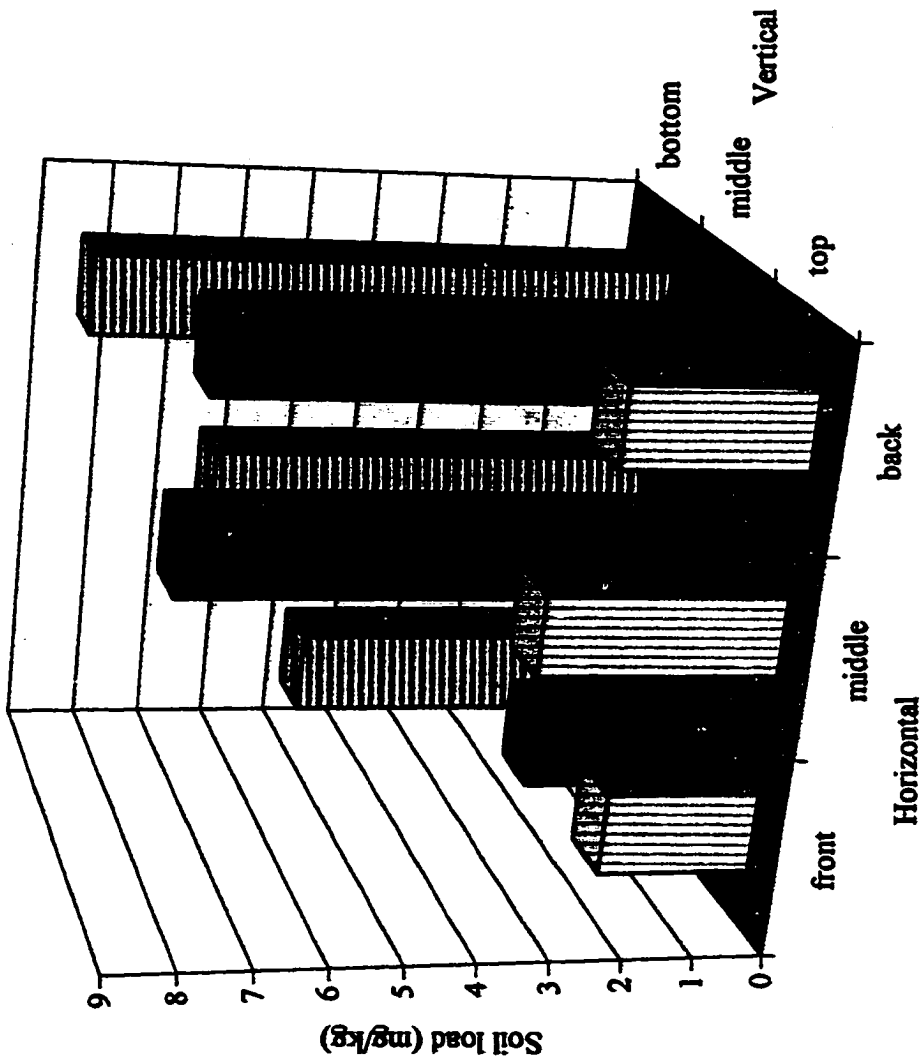

Figure 3.41. Multiple contaminant MCB cyclic core

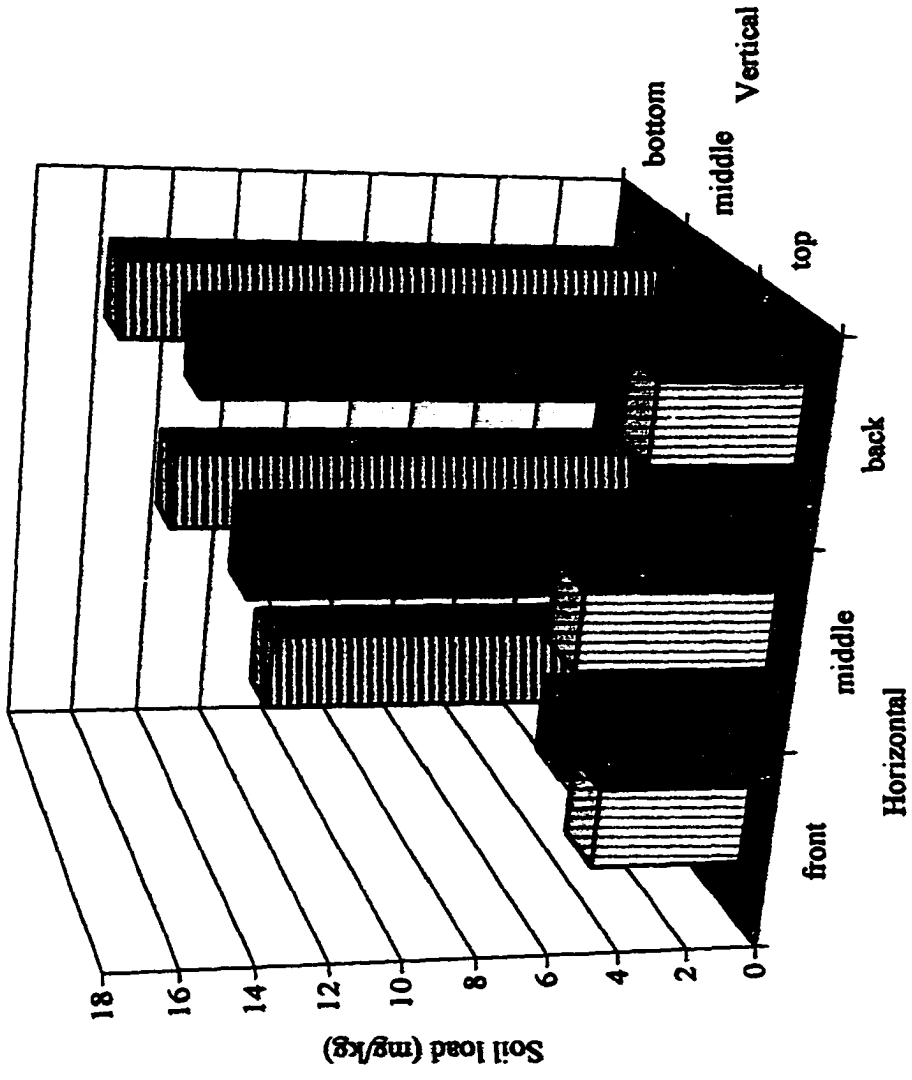

Figure 3.42. Multiple contaminant 1,3-DCB cyclic core

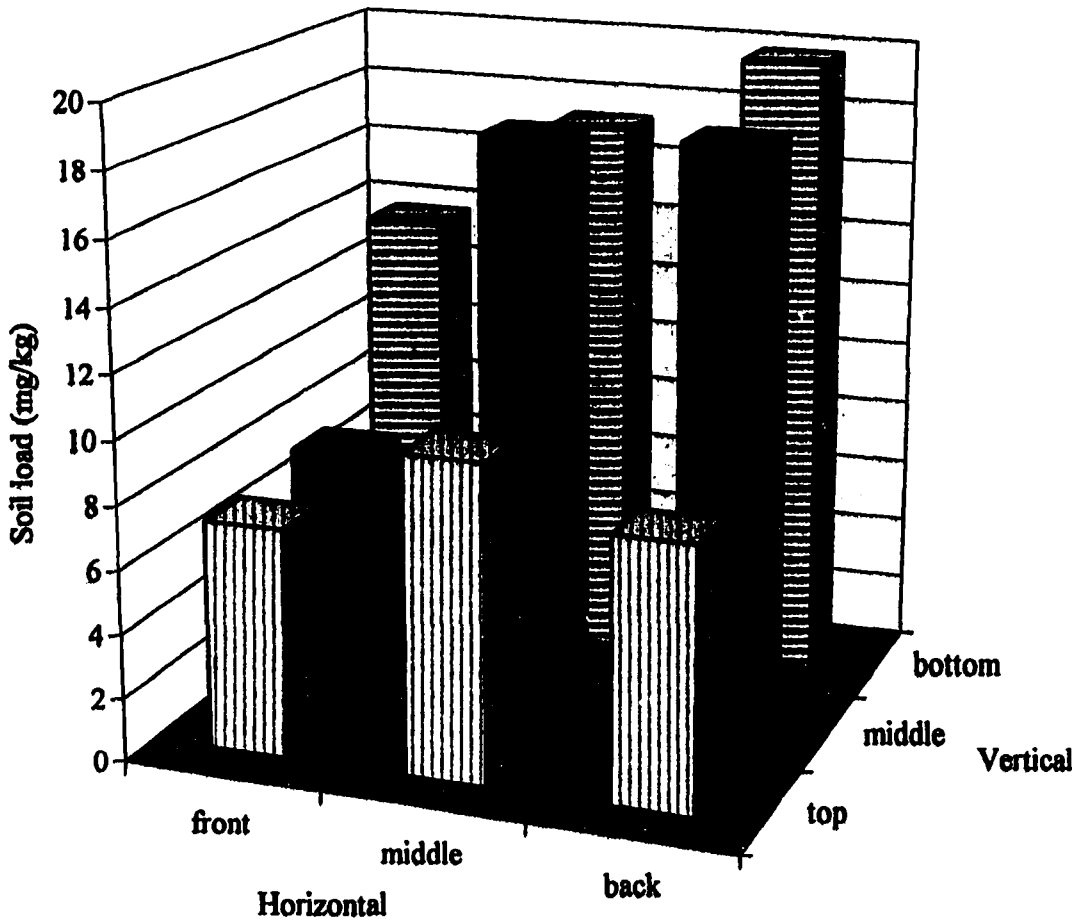

Figure 3.43. Multiple contaminant 1,2-DCB cyclic core

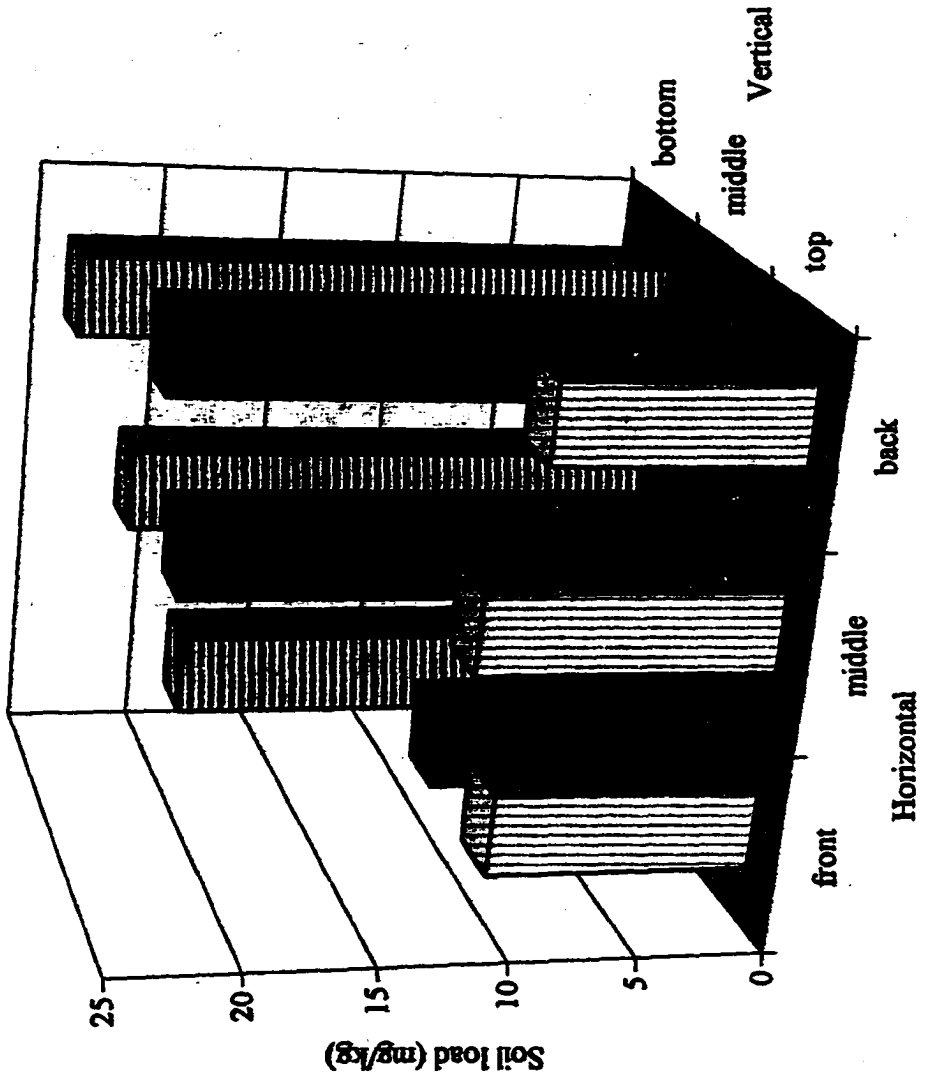

Figure 3.44. Multiple contaminant TCB cyclic core

Table 3.9. Multiple contaminant mass balance calculations

Experiment	Total time (hours)	MCB Effluent mass (mg)	1,3-DCB Effluent mass (mg)	1,2-DCB Effluent mass (mg)	TCB Effluent mass (mg)	Effluent Average mass/hr (MCB)	Effluent Average mass/hr (1,3DCB)
slow (5)	151.40	1.32	1.21	1.77	0.97	0.009	0.008
slow (5)	151.40	1.98	1.75	2.49	1.32	0.013	0.012
slow (5)	151.40	1.40	1.29	1.87	1.01	0.009	0.008
slow (5)	151.40	2.08	1.81	2.59	1.34	0.014	0.012
Average		1.69	1.51	2.18	1.16	0.011	0.010
fast (2)	170.40	4.72	2.94	4.18	3.21	0.028	0.017
fast (2)	170.40	3.49	2.43	3.51	2.67	0.020	0.014
fast (2)	170.40	2.85	1.68	1.75	0.98	0.017	0.010
fast (2)	170.40	2.85	1.60	1.71	0.92	0.017	0.009
Average		3.48	2.16	2.79	1.94	0.020	0.013
cyclic (4)	237.72	2.00	3.10	4.50	2.77	0.008	0.013
cyclic (4)	233.56	1.87	2.77	4.06	2.43	0.008	0.012
cyclic (4)	237.72	1.90	2.96	4.26	2.62	0.008	0.012
cyclic (4)	233.56	1.79	2.67	3.87	2.33	0.008	0.011
Average		1.89	2.88	4.17	2.54	0.008	0.012
cyclic (6)	221.65	1.86	1.38	1.93	0.79	0.008	0.006
cyclic (6)	219.40	2.76	1.93	2.47	0.98	0.013	0.009
cyclic (6)	221.65	1.77	1.31	1.84	0.75	0.008	0.006
cyclic (6)	219.40	2.61	1.83	2.34	0.93	0.012	0.008
Average		2.25	1.62	2.14	0.86	0.010	0.007

Table 3.9. Cont'd

Experiment	Effluent Average mass/hr (1,2DCB)	Effluent Average mass/hr (TCB)	Average MCB core (mg/kg)	Average 1,3DCB core (mg/kg)	Average 1,2DCB core (mg/kg)	Average TCB core (mg/kg)	Ave. Initial MCB Load (t=a) (mg/kg)
slow (5)	0.012	0.006	2.58	12.48	13.35	25.34	20.25
slow (5)	0.016	0.009	4.54	14.83	17.37	29.42	20.25
slow (5)	0.012	0.007	2.58	12.48	13.35	25.34	20.25
slow (5)	0.017	0.009	4.54	14.83	17.37	29.42	20.25
Average	0.014	0.008	3.56	13.66	15.36	27.38	20.25
fast (2)	0.025	0.019	2.64	12.72	13.64	25.64	25.07
fast (2)	0.021	0.016	5.64	18.44	17.69	28.73	25.07
fast (2)	0.010	0.006	2.64	12.72	13.64	25.64	25.07
fast (2)	0.010	0.005	5.64	18.44	17.69	28.73	25.07
Average	0.016	0.011	4.14	15.58	15.67	27.19	25.07
cyclic (4)	0.019	0.012	1.39	9.11	11.34	19.25	5.71
cyclic (4)	0.017	0.010	0.70	4.80	4.90	6.54	5.71
cyclic (4)	0.018	0.011	1.39	9.11	11.34	19.25	5.71
cyclic (4)	0.017	0.010	0.70	4.80	4.90	6.54	5.71
Average	0.018	0.011	1.05	6.96	8.12	12.90	5.71
cyclic (6)	0.009	0.004	2.51	4.71	8.80	11.02	7.44
cyclic (6)	0.011	0.004	7.57	14.50	17.92	22.24	7.44
cyclic (6)	0.008	0.003	2.51	4.71	8.80	11.02	7.44
cyclic (6)	0.011	0.004	7.57	14.50	17.92	22.24	7.44
Average	0.010	0.004	5.04	9.61	13.36	16.63	7.44

Table 3.9. Cont'd

Experiment	Ave. Initial 1,3DCB Load (t=a) (mg/kg)	Ave. Initial 1,2DCB Load (t=a) (mg/kg)	Ave. Initial TCB Load (t=a) (mg/kg)	% MCB closure	% 1,3DCB closure	% 1,2DCB closure	% TCB closure
slow (5)	28.52	35.64	47.79	25.61	69.88	61.14	55.05
slow (5)	28.52	35.64	47.79	43.41	84.12	80.10	64.31
slow (5)	28.52	35.64	47.79	26.00	70.14	61.42	55.13
slow (5)	28.52	35.64	47.79	43.89	84.33	80.36	64.37
Average	28.52	35.64	47.79	34.73	77.12	70.76	59.72
fast (2)	39.74	41.99	53.79	34.63	55.40	58.69	53.63
fast (2)	39.74	41.99	53.79	47.66	75.72	71.56	58.38
fast (2)	39.74	41.99	53.79	27.16	52.24	52.89	49.49
fast (2)	39.74	41.99	53.79	45.11	73.63	67.27	55.12
Average	39.74	41.99	53.79	38.64	64.25	62.60	54.15
cyclic (4)	17.87	21.25	30.91	71.45	93.83	101.21	71.22
cyclic (4)	17.87	21.25	30.91	51.17	55.79	53.71	29.03
cyclic (4)	17.87	21.25	30.91	69.81	93.06	100.11	70.74
cyclic (4)	17.87	21.25	30.91	49.77	55.23	52.80	28.69
Average	17.87	21.25	30.91	60.55	74.48	76.96	49.92
cyclic (6)	44.22	42.64	53.38	75.59	19.11	35.49	22.12
cyclic (6)	44.22	42.64	53.38	189.72	53.56	68.82	43.51
cyclic (6)	44.22	42.64	53.38	74.34	18.94	35.27	22.04
cyclic (6)	44.22	42.64	53.38	187.73	53.33	68.52	43.40
Average	44.22	42.64	53.38	131.84	36.23	52.02	32.77

flow is the most efficient but the cyclic flow efficiency is not obvious until the short time interval of the other experiments is noted. The percent closure is shown in the last column and is generally between 60 – 70 %. In this series, the variation between beds and the method of calculating mass in effluent may be significant. The average is used to look for trends in the data due to the difficulty in working with volatile compounds.

3.12 DISCUSSION FOR MULTIPLE CONTAMINANT STUDIES

The graphs of the individual components in the mixture under all three flow regimes are shown in Figures 3.45, 3.46, 3.47, and 3.48 for MCB, 1,3-DCB, 1,2-DCB and TCB. The flow regimes all appear to follow the same trend of exponential decay. The cyclic run demonstrates spikes of higher flux when the flow rate changes. When comparing the individual components by flow rate, the fast flow system appears to have a higher overall flux rate, which is the same as the single contaminant studies. One reason for this may be the higher initial concentration on the sediment in the fast flow experiments as seen in Table 3.9.

The initial sediment load is higher for all contaminants in the slow and fast flow experiments compared to the contaminant load in the cyclic experiments as seen in Table 3.9. This may explain why the cyclic flux did not appear as high as the fast flux. For all experiments a contaminant load of 10-15 mg/kg was desired but the initial sediment loading extraction results indicate some variation in contamination.

The cores support the removal of chlorinated benzenes from the sediment due to leaching. The mass balance for the multiple contaminant studies show the variation between the replicate beds in Table 3.9.

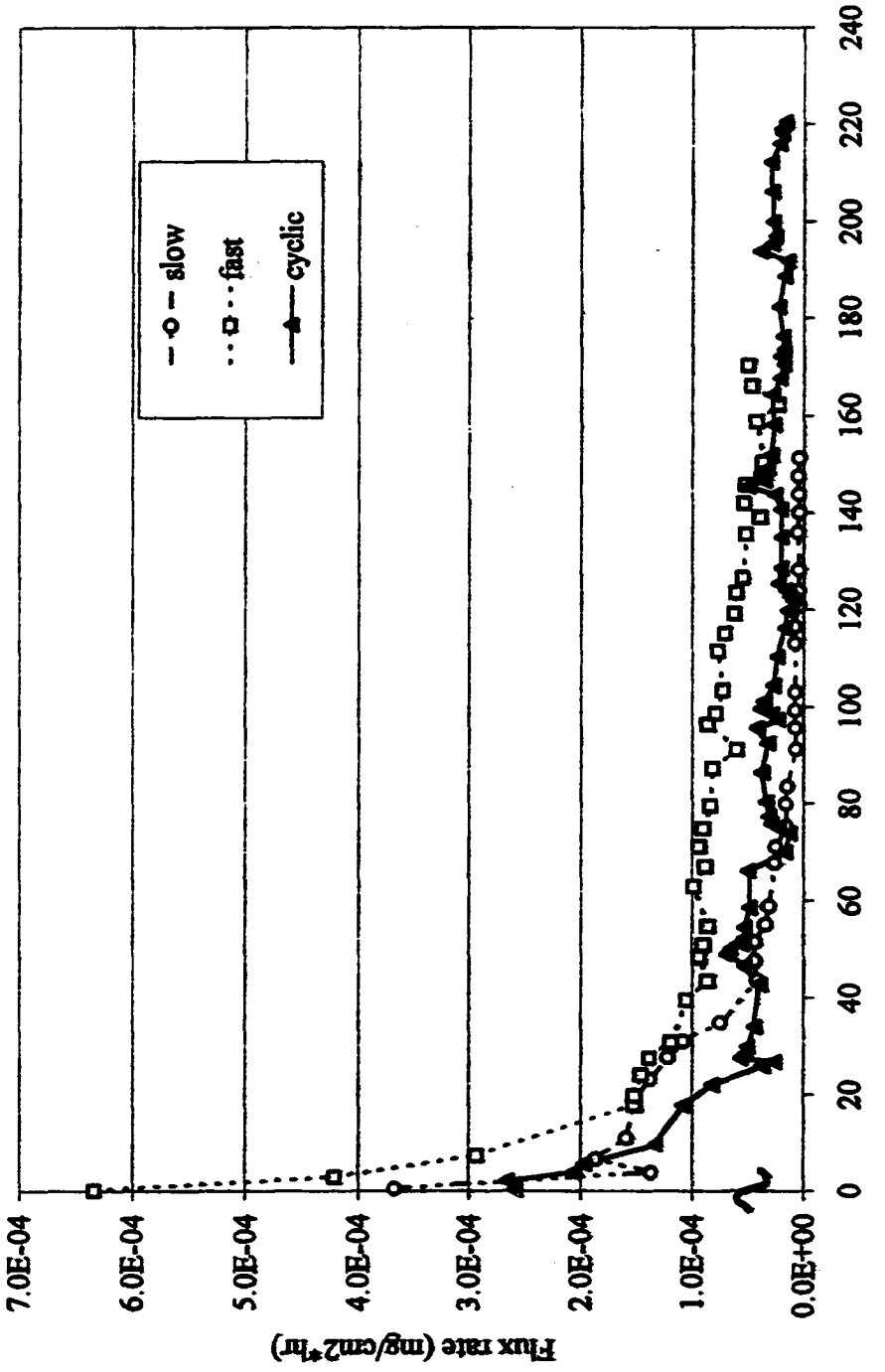

Figure 3.45. MCB in mixture comparison by flow rate

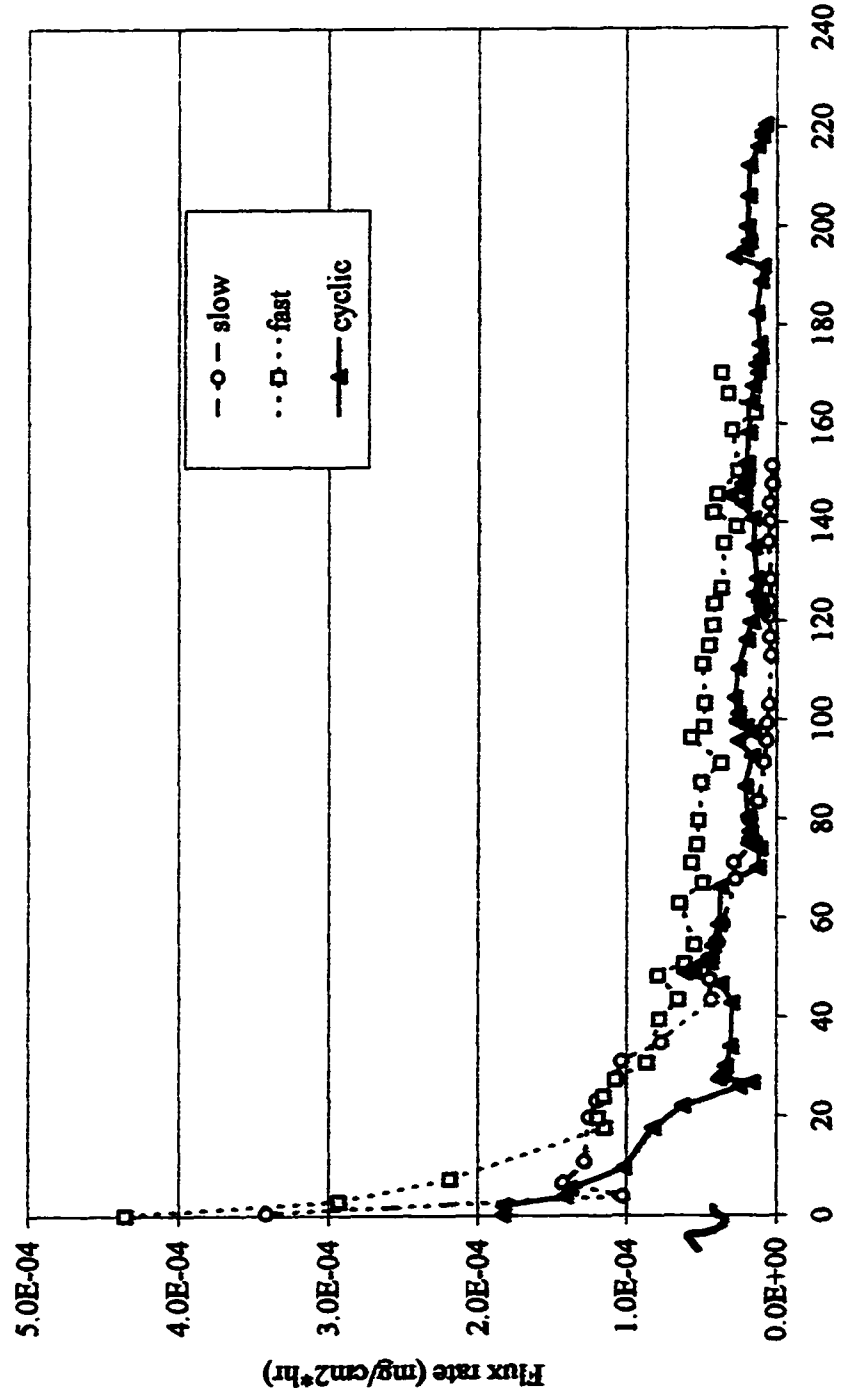

Figure 3.46. 1,3-DCB in mixture comparison by flow rate

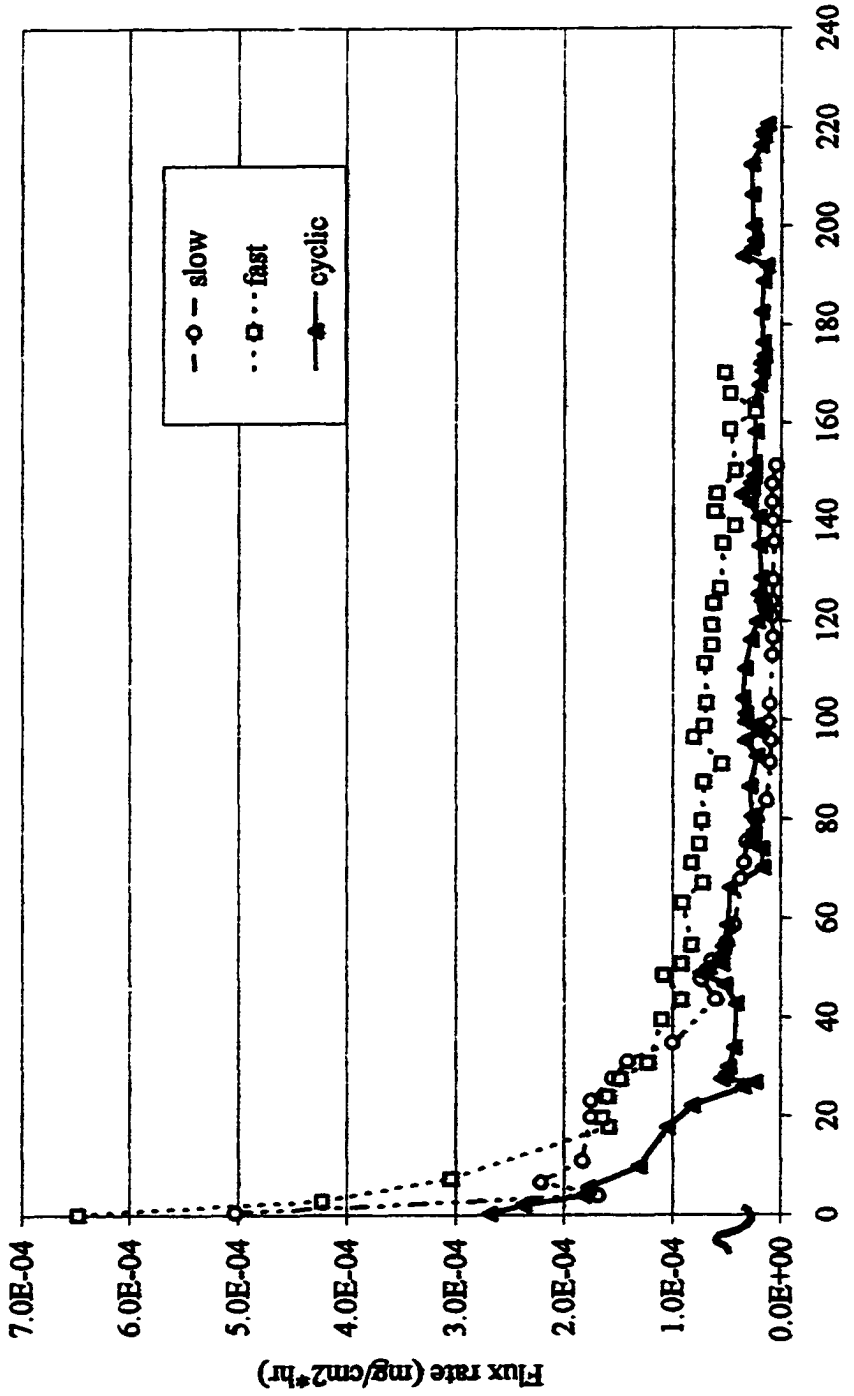

Figure 3.47 1,2-DCB in mixture comparison by flow rate

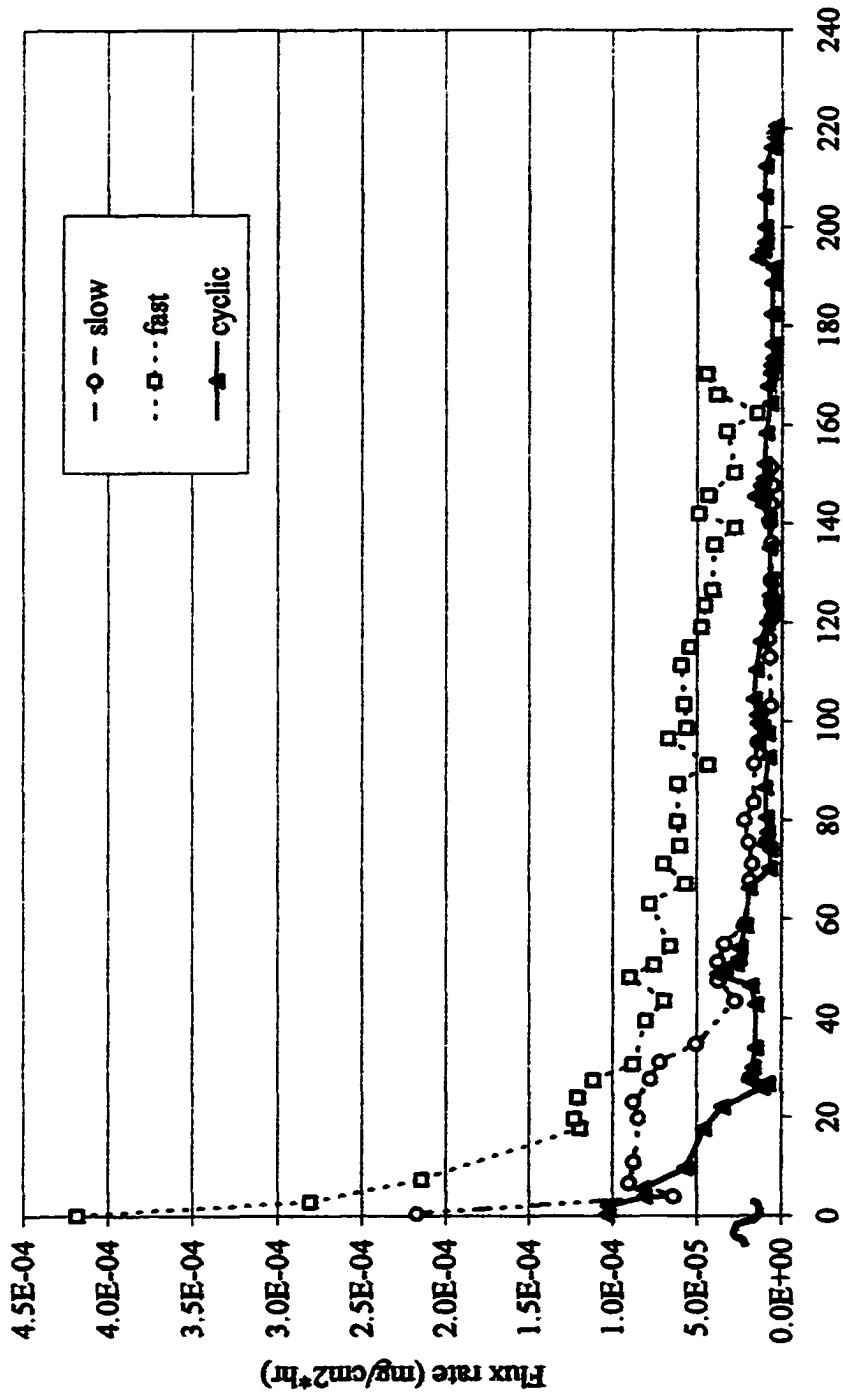

Figure 3.48 TCB in mixture comparison by flow rate

3.13 CONCLUSION

SFLB studies indicate that flux of contaminants from sediment beds can be quantified and predicted by simple diffusion models. The single contaminant studies utilizing MCB and 1,3-DCB for all three flow regimes indicate similar flux behavior for both contaminants. The fast and slow flow regimes appear to follow the same trend of exponential decay and the cyclic run demonstrates spikes of higher flux when the flow rate changes yielding a higher overall average flux rate. Thus, natural rainfall events in Baton Rouge Bayou/Devil's Swamp may show higher flux rates of lower chlorinated benzenes than would be expected in steady state systems. Even though the flux may be higher than expected, it is still at relatively low levels and can potentially be subject to phytoremediation or natural attenuation processes.

The core results support the removal of chlorinated benzenes from sediment due to leaching. The mass balance for the single contaminant studies show the variation between the replicates and reasonable closure for 1,3-DCB experiments.

Because natural systems rarely contain one pollutant, later experiments were performed utilizing four components: chlorobenzene (MCB), 1,2-dichlorobenzene, (1,2-DCB) 1,3-dichlorobenzene (1,3-DCB), and 1,2,4-trichlorobenzene (TCB). One aspect of the chlorinated benzene studies was the examining the impact of multiple contaminants on desorption and dissolution in a dynamic system as found in Baton Rouge Bayou (BRB). The individual component flux rates are shown to vary at all three flow regimes, slow, fast, and cyclic as each compound partitions into the water phase differently due to differences in chemical properties such as K_{ow} and solubility. Although the graphs show overall behavioral similarity, it should be noted that flux

rates for each component in the mixture, under all three pumping regimes, indicated the fast flow system appears as the most efficient leaching removal followed by the cyclic rate. Fast flow had the higher initial soil load which may explain the higher flux rate. All the experiments indicate the dissolution and desorption is a slow process but removal is supported by the core results. Due to the high sorptive capacity of most sediments in comparison to the water solubility of chlorinated benzenes, the solubility limit and critical loading of contaminated sediment are important concepts.

It is not clear if 1,3-DCB is more mobile in a mixture as compared to a single contaminant. These results demonstrate the behavior of compounds in mixtures is not clear and more research is needed to explore mixture phenomena. The adsorption study presented in chapter 5 attempts to assess the changes in partitioning in the previous mixture study in order to better understand dynamic effects.

3.14 REFERENCES

Caserett & Doull,'s Toxicology: The Basic Science of Poisons, Fourth Edition. 1991. Amdur, Doull, & Klaassen [Eds]. Pergamon Press, Inc. N.Y., N.Y.

Choy, Bruce and Danny D. Reible. 2000. Diffusion Models of Environmental Transport. Lewis Publishers, Boca Raton, Fl.

Constant, W.D., J.H. Pardue, R.D. DeLaune, K. Blanchard, G.A. Breitenbeck. 1995. Enhancement of *In Situ* Microbial Degradation of Chlorinated Organic Waste at the Petro Processors Superfund Site. Environmental Progress Vol. 14, No. 1, 51-60.

Deane, G., Z. Chroneer, and W. Lick. 1999. Diffusion and Sorption of Hexachlorobenzene in Sediments and Saturated Soils. Journal of Environmental Engineering, Vol. 125, No. 8., 689-696.

Mackay D., A. Di Guardo, S. Paterson, G. Kicsi, D.E. Dowan, and D.M. Kane. 1996. Assessment of Chemical Fate in the Environment Using Evaluative, Regional and Local-Scale Models: Illustrative Application to Chlorobenzene and Linear

Alkylbenzene Sulfonates. Environmental Toxicology and Chemistry vol. 15 no. 9, 1638-1648.

Schnoor, J.L. Phytoremediation. 1997. Technology Evaluation Report TE-98-01. Ground-Water Remediation Technologies Analysis Center. Pittsburgh, PA.

Schnoor, Jerald, L. 1996. Environmental Modeling: Fate and Transport of Pollutants in Water, Air and Soil. John Wiley & Sons, Inc. New York, New York.

Thibodeauz, Louis, J. 1996. Environmental Chemodynamics: Movement of Chemicals in Air, Water, and Soil. Second edition. John Wiley & Sons, Inc. New York, New York.

U.S.E.P.A. 1994. Common Chemicals Found at Superfund Sites. EPA 540/R-94/044. Office of Emergency and Remedial Response Washington, D.C.

Valsaraj, K.T., S. Verma, I. Sojitra, D.D. Reible and L.J. Thibodeaux. 1996. Diffusive Transport of Organic Colloids from Sediment Beds. Journal of Environmental Engineering Vol. 122, No. 8, 722-729.

Watts, Richard, J. 1997. Hazardous Wastes: Sources, Pathways, Receptors. John Wiley & Sons, Inc. New York, New York.

CHAPTER 4. CHLORINATED BENZENE TRANSPORT: MATHEMATICAL MODELING

4.1 INTRODUCTION

Contaminants in the soil will dissolve and desorb into the aqueous phase and migrate, eventually contaminating surface or ground waters in the process. The purpose of the models presented herein is to explore the diffusive transport processes involved in chlorinated benzene release from bed sediment in the sheet flow leaching bed (SFLB) experiments. Chapter 3 quantified flux of single and multiple contaminants under different flow conditions for the physical model of Baton Rouge Bayou/Devil's Swamp. It is envisioned that by calibrating mathematical models to experimental data these models could be to estimate pollutant release rates in similar systems. To augment natural remedies, the flux of chemicals must be quantified for microbial or plant systems to be engineered. Previous work demonstrated experimental flux data could be modeled by published solutions to the advection-dispersion equation (Chapter 2). Here, experimental data was used to calibrate previously described models (Choy and Reible, 2000) in order to determine the fitted effective diffusivity by utilizing a commercially packaged program called Mathcad® (Professional 2000). The effective diffusivity (D_e) here is a lumped parameter to describe the transport of lower chlorinated benzenes. Using a more fundamental parameter, such as tortuosity is also investigated.

4.1.1 Current Fate Modeling

Modeling chlorinated benzene transport is of interest because they are the degradation products present at Superfund sites and may be harmful to receptors. In

the equilibrium concentration (EQC) model presented by Mackay et al., (1996) (at steady state level III), there are separate simulations to show the environmental impact on fate by the medium of discharge. If chlorobenzene (CB) was discharged to air, most of it was advected away (71%) with a compartmental residence time of 3 days. If the discharge medium was water, 84% stays there with a residence time of 13 days. The longer residence time results in much higher aquatic exposure, which can be potentially impact receptors. The residence time increases to 20 days when CB is discharged solely to soil. This increased residence time may have a detrimental impact on the ecosystem and is due to the relatively slow processes of desorption and dissolution. Mackay's models underscore the progress made by contemporary modelers but these models rely on understanding and quantifying the molecular processes. This research examines diffusive transport between soil and water compartments for application in phytoremediation or natural attenuation assessment.

In a sensitivity analysis, the mass transfer coefficients "profoundly affect the source concentration in the water" (Mackay et al., 1996). Thus, in this research two different models and three different mass transfer coefficients are presented.

4.2 MATERIALS AND METHODS

4.2.1 Development of Advection Enhanced Diffusion Model

These models assume the flux of contaminants is diffusion driven upward from a finite flat source with uniform initial concentration. The experimental apparatus, the SFLB, is designed to prevent flux at the base and the bulk water concentration is used to calculate the flux. The experimental flow condition is advection at surface because water is flowing across the sediment surface. This physical situation led to two

different boundary conditions that are investigated as case 2 and case 4 from Choy and Reible's (2000) derivation.

The four diffusion models, case 4.2 and case 4.4 with three different mass transfer coefficients, (Choy and Reible, 2000) were tested to evaluate which most accurately described the experimental data. The solution for the case 2 surface flux is given below.

$$F = \frac{2 * D_e * C_o}{H_z} \sum \exp\left(\frac{-D_e}{R_f} * \alpha_n^2 * t \right) \qquad (4.1)$$

$$\text{where} \quad \alpha_n = \frac{\pi}{H_z} * \left(\frac{2n-1}{2} \right) \qquad (4.2)$$

In the previous equations, H_z is the depth of contaminated sediment, C_o is the initial pore water concentration, R_f is the retardation factor, t is time and D_e is the fitted parameter, effective diffusivity. There is no explicit mass transfer term. Choy and Reible (2000) derive the case 2 flux model for diffusion in a finite layer with uniform initial concentration, zero surface concentration, and zero flux at the base. By comparing those conditions with Figure 3.1, it can be assumed that the water flow at the surface provides a zero surface concentration. The water is in laminar flow, 2 mm in depth, across the surface of the SFLB and no advection through the soil component is assumed.

The solution for the case 4 surface flux is given as

$$F = \frac{2 * D_e * C_o}{H_z} \sum \exp\left(\frac{-D_e}{R_f} * \alpha_n^2 * t \right) * \sin^2 (\alpha_n * H_z) \qquad (4.3)$$

$$\text{where} \quad \alpha_n \tan (\alpha_n * H_z) = \{k_s / D_e\} \qquad (4.4)$$

All the variables have been defined in the previous model except k_a. The laminar flow boundary layer theory yields a surface mass transfer coefficient, k_a, based on Reynolds and Schmidt numbers (equation 1.14) given in Choy and Reible (2000). The case 4 model is derived for uniform initial concentration and zero flux at the base but it assumes mass transfer at the surface. Again looking at Figure 3.1, the mass transfer at the surface condition more appropriately describes the physical situation: flow across the surface of the SFLB. The stainless steel provides for zero flux at the base and uniform initial concentration is attempted by laboratory contamination as discussed in Chapter 3.

The mass transfer coefficient, k_a, was modified to compare the impact of different mass transfer coefficients in equation 4.3. One modification utilized a soil mass transfer coefficient derived from Thoma (1994) to verify negligible water side resistance with

$$K_{thoma} = 1.165\,[Q * D_w^2/H^2 * L * W]^{1/3} \qquad (4.5)$$

where Q is the volumetric flow rate, D_w is the diffusivity of the compound in water, H is the height of the water layer, L is the length of the water layer and W is the width of the water layer. The other substitution for k_a was to use the volumetric flow rate (Q) over the surface area (A) of flux, Q/A to account for changes in transport due to flow rate.

4.2.2 Model Analysis

Mathcad 2000 Professional® computer software was utilized for higher math functions. Some parameters used in model are calculated from literature values using Mathcad®, are given in Table 4.1. The fitting of these solutions yielded an " average

Table 4.1. Model inputs for Mathcad

Parameter	Symbol	Value	Reference
Porosity	ε	0.53	Lab determined
Molecular diffusivity	D_m	9.09×10^{-6} cm^2/s (MCB) 8.33×10^{-6} cm^2/s (DCB) 7.57×10^{-6} cm^2/s (TCB)	Thibodeaux, 1996
Effective diffusivity	De	$D_w * \varepsilon^{4/3}$	Welty et. al., 1984 Thibodeaux, 1996
Length bed	L	50 cm	Lab determined
Volumetric flow rate	Q	50 to 150 ml/hr	Lab determined Varied by experiment
Initial soil load	W	10-15 mg/kg	Lab measured
Bulk density	ρ_b	1.05 - 1.08	Lab determined
Particle density	ρ_p	2.47 – 2.74	Lab determined
Retardation factor	R_f	$\varepsilon + \rho_b * K_d$	Watts, 1997 Choy & Reible, 2000
Water side resistance	k	$0.664 * Re^{0.5} * Sc^{1/3} * (De/Hz)$	Choy & Reible, 2000
Partition coefficient	K_d	$K_{oc} * f_{oc}$	Lab determined Watts, 1997
Area of bed	A	258.054 cm^2	Lab determined
Width of bed	w	5.08 cm	Lab determined
Height of soil	Hz	3 cm	Lab determined
Octanol/water partition coefficient	Log K_{ow}	2.71-2.98 (MCB) 3.38-3.60 (1,3DCB) 3.38-3.55 (1,2DCB) 4.10 (TCB)	Watts, 1997 Watts, 1997 Watts, 1997 Thibodeaux, 1996
Organic carbon partition coefficient	Log K_{oc}	2.46 (MCB), 3.09 (1,3DCB) 3.12 (1,2DCB) 3.69 (TCB)	Thibodeaux, 1996 Watts, 1997 Watts, 1997 Thibodeaux, 1996
Fraction organic carbon	f_{oc}	0.00213	Watts, 1997

fitted effective diffusivity" either based on literature K_d, (litKd) or on experimentally determined K_d (expKd) to calculate the retardation factor. Because the experimentally determined partition coefficient (expKd) was very close to the literature estimated partition coefficient (litKd), only the data from the literature based K_d will be presented. The sum squared error (SSE) is determined by the difference at each point:

$$SSE = \Sigma (\text{model flux} - \text{experimental flux})^2 \qquad (4.6)$$

The root mean squared error (RMSE) is calculated from the SSE by:

$$RMSE = (SSE/n\text{-}1)^{.5} \qquad (4.7)$$

The RMSE indicates approximately how much each point deviates from the model. By manually minimizing the sum of squared errors, Mathcad® is able to iteratively calculate an average effective diffusivity for the best fit of the experimental data. The best fit for the models was determined by the smallest value for the RMSE. Mathcad® can also linearize the data and model to return a Pearson's correlation coefficient to investigate the best fit of model to data.

Each of the models from Choy and Reible were run utilizing two sets of input parameters; literature based and experimental. Literature values for K_d, the partition coefficient, are used for the average fitted effective diffusivity for both the case 2 and the case 4 models. Both models, case 2 and case 4, were run again utilizing the experimentally determined partition coefficient, yielding another fitted average effective diffusivity. This means each model had multiple simulations run for each bed: case 2 litKd, case 2 expKd, case 4 litKd with boundary layer theory Kq, case 4 litKd with Kthoma, case 4 litKd with K= Q/A, case 4 expKd with boundary layer theory Kq, case 4 litKd with Kthoma, case 4 litKd with K= Q/A. There was no

significant difference between the models fitted from the input of experimental K_d or literature K_d, therefore the four flux model solutions with literature K_d will be shown as case 2, case 4(Kq), case 4 (Kthoma), and case 4 (Q/A). The results section will present the models as lines and the experimental flux data will be shown as individual points.

4.2.3 System Predictors

The benefit in using models is to have a predictor for determining either flux from the sediments to the overlying water or the probable concentrations to which receptors may be exposed. This research examines two parameters as predictors, the effective diffusivity and the tortuosity. As mentioned in the previous chapter, there were three different flow regimes to be examined; fast flow = 150 ml/hr, slow flow = 50 ml/hr and cyclic flow which indicated 24 hours of fast flow followed by 24 hours of slow flow in 24 hour cycles. The four models were fitted to the fast flow regime and an average fitted effective diffusivity determined utilizing all runs, both single and multiple contaminants. Utilizing the relationship

$$D_e = D_w^* (\varepsilon / \tau) \qquad (4.8)$$

where D_w is the diffusivity of the pure compound in water, ε is the porosity and τ is the tortuosity, the model derived effective diffusivity can be used to determine the actual tortuosity. Tortuosity is a more fundamental parameter describing the experimental system. Because the mixture under fast flow regime had the best fit to model solutions, the average tortuosity for the experimental system was determined using that data. The tortuosity is intrinsically related to the soil and the SFLB apparatus and therefore may be utilized as a system constant for predicting flux. The

average tortuosity was calculated to yield the sample standard deviation in order to evaluate the tortuosity as a system descriptor. To test the validity of (plus or minus one standard deviation) the mean tortuosity for predicting mass transport in the changing flow rate situation, the case 4 (Q/A) solution was compared to all the slow and cyclic experimental data.

Recall that the effective diffusivity is a fitted parameter obtained by minimizing the sum squared error. Using the fitted average effective diffusivity from the respective models, the tortuosity was back calculated for each contaminant in the fast flow condition. The tortuosities from all the simulations were averaged and the standard deviation determined to yield the possible range of tortuosities which describe this SFLB system. The high and low tortuosity (plus and minus one standard deviation of mean) were used to predict the expected flux rates from the slow and cyclic flow regimes in order to validate the use of tortuosity as a system descriptor.

Another approach to validation of these models was to determine the average "average fitted effective diffusivity" and standard deviation so a range of effective diffusivities could describe this SFLB system. Once the mean and standard deviation were calculated, the high and low effective diffusivities (plus / minus 1 standard deviation of the mean) were substituted back into the case 4 (Q/A) model to predict a range of expected fluxes under cyclic and slow flow conditions.

4.3 MODELING RESULTS

Experimental flux data was fitted to previously published flux models (Choy and Reible, 2000) in order to determine the average fitted effective diffusivity. These models are intended to describe diffusion in a finite layer with uniform initial

concentration, and zero flux at the base. The difference between the case 2 and case 4 models is that case 2 assumes zero surface concentration whereas the case 4 model assumes mass transfer at the surface. The case 4 model is run with three different mass transfer coefficients as described previously. The transport mechanisms are adequately described by the model because the data fits the trend as seen by the root mean squared error (RMSE) and the correlation coefficient.

All of the fast flow experimental runs with the corresponding model fits are follow in Figure 4.1 for the single contaminant MCB. All the models fit the data well visually but are hard to differentiate between each other. Figure 4.2 compares the fast flow regime experimental flux compared to the model derived fluxes for 1,3-DCB as a single contaminant. All the models can be seen and appear to fit the experimental flux data with no significant difference.

The next set of data examinse the models fitted to individual compounds in a multiple contaminant mixture under fast flow conditions. Figure 4.3 presents the four diffusion models and experimental flux data for MCB in a mixture of four chlorinated benzenes. The fitted models are so similar that differentiation is difficult but all of the models fit the experimental data very well visual. In Figure 4.4, the models are fit to the experimental data of the 1,3-DCB component of the mixture. The models are not significantly different from each other and provide a reasonable approximation of the flux. Figure 4.5 the 1,2- DCB component of the mix is shown along with the fitted models. All the fitted models appear to slightly overestimate the experimental flux rates. The last component of the mixture, TCB, is shown in Figure 4.6 with the corresponding fitted models.

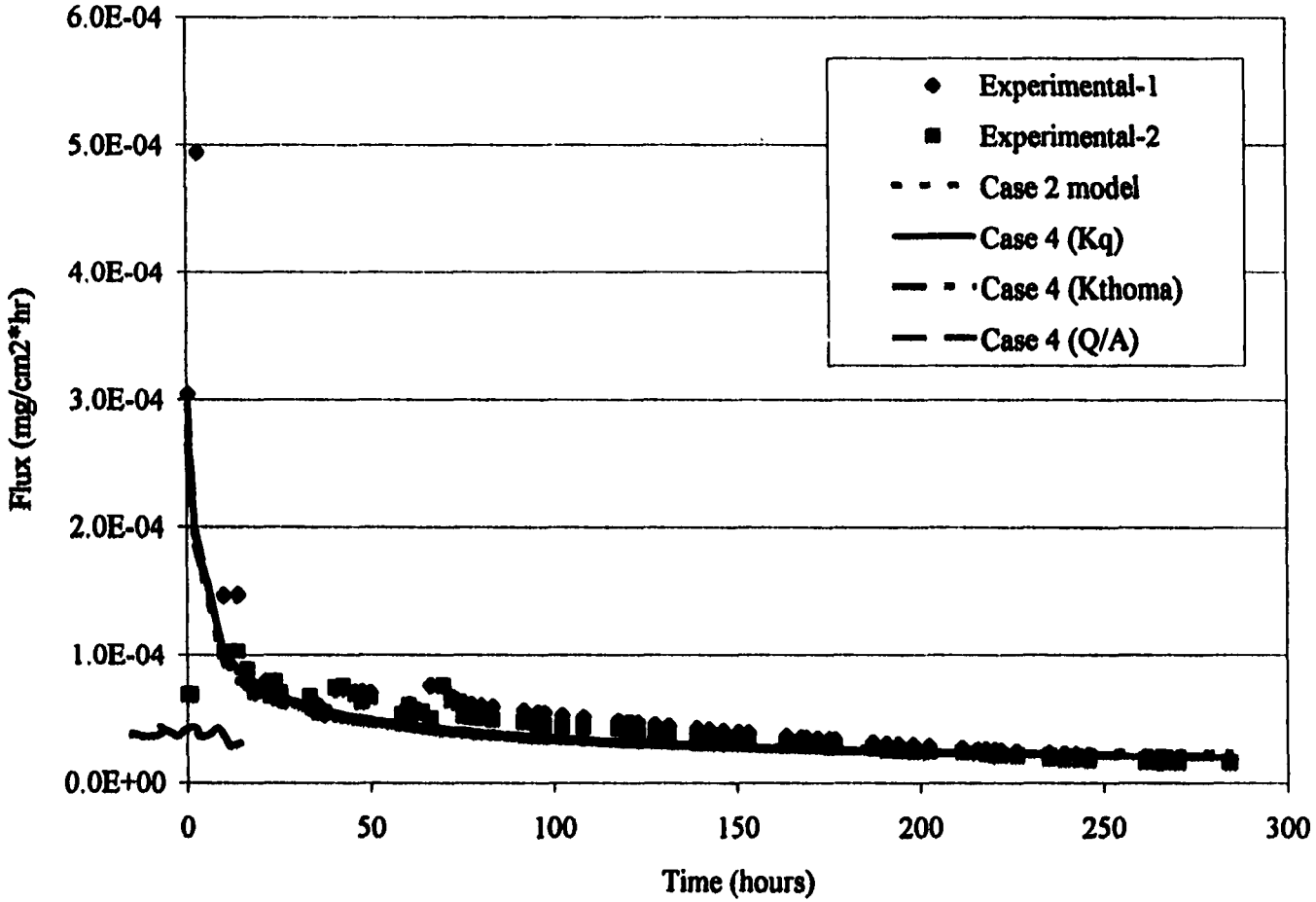

Figure 4.1. MCB single contaminant fast flow fit models and data

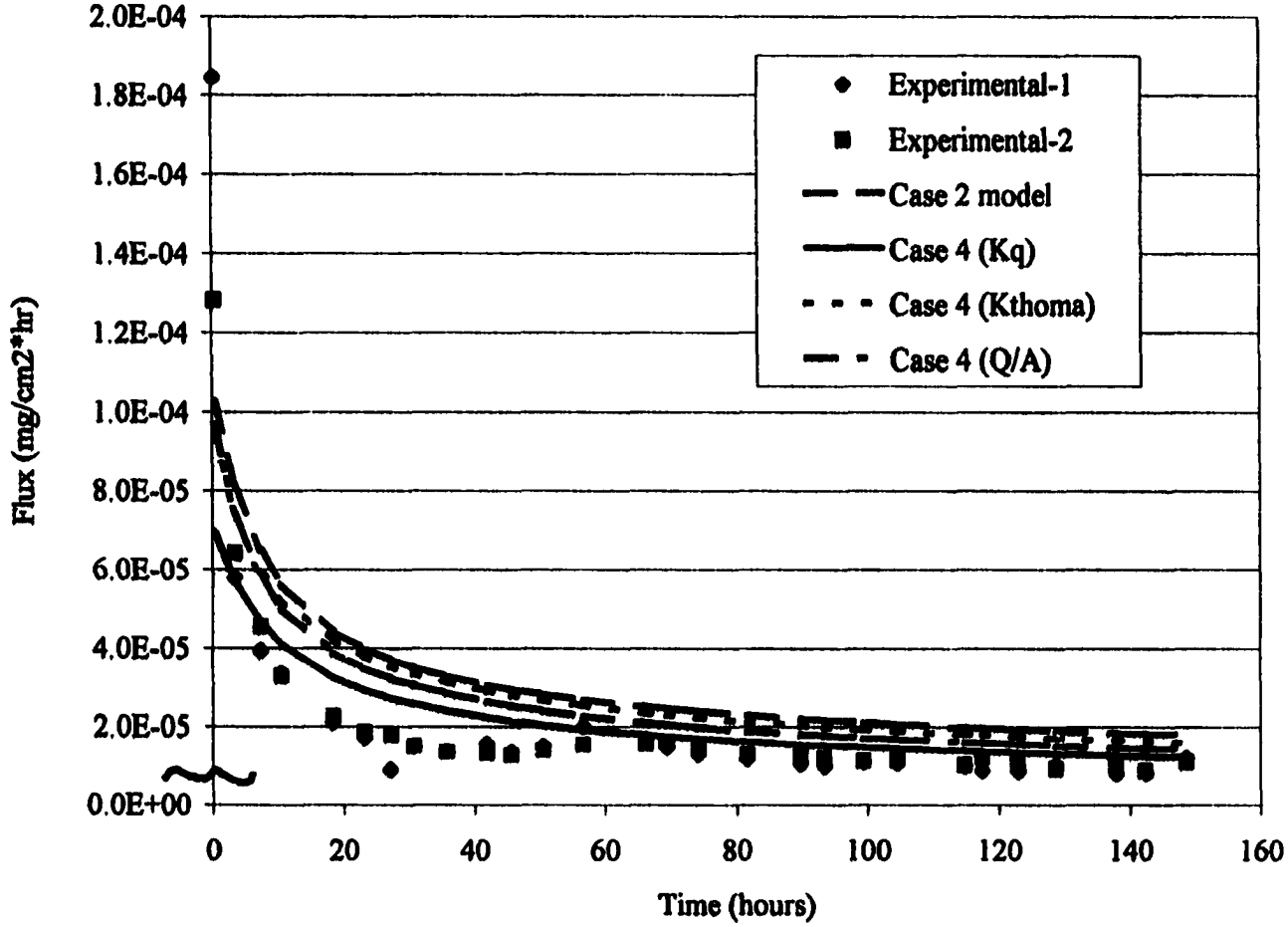

Figure 4.2. 1,3-DCB single contaminant fast flow fit models and data

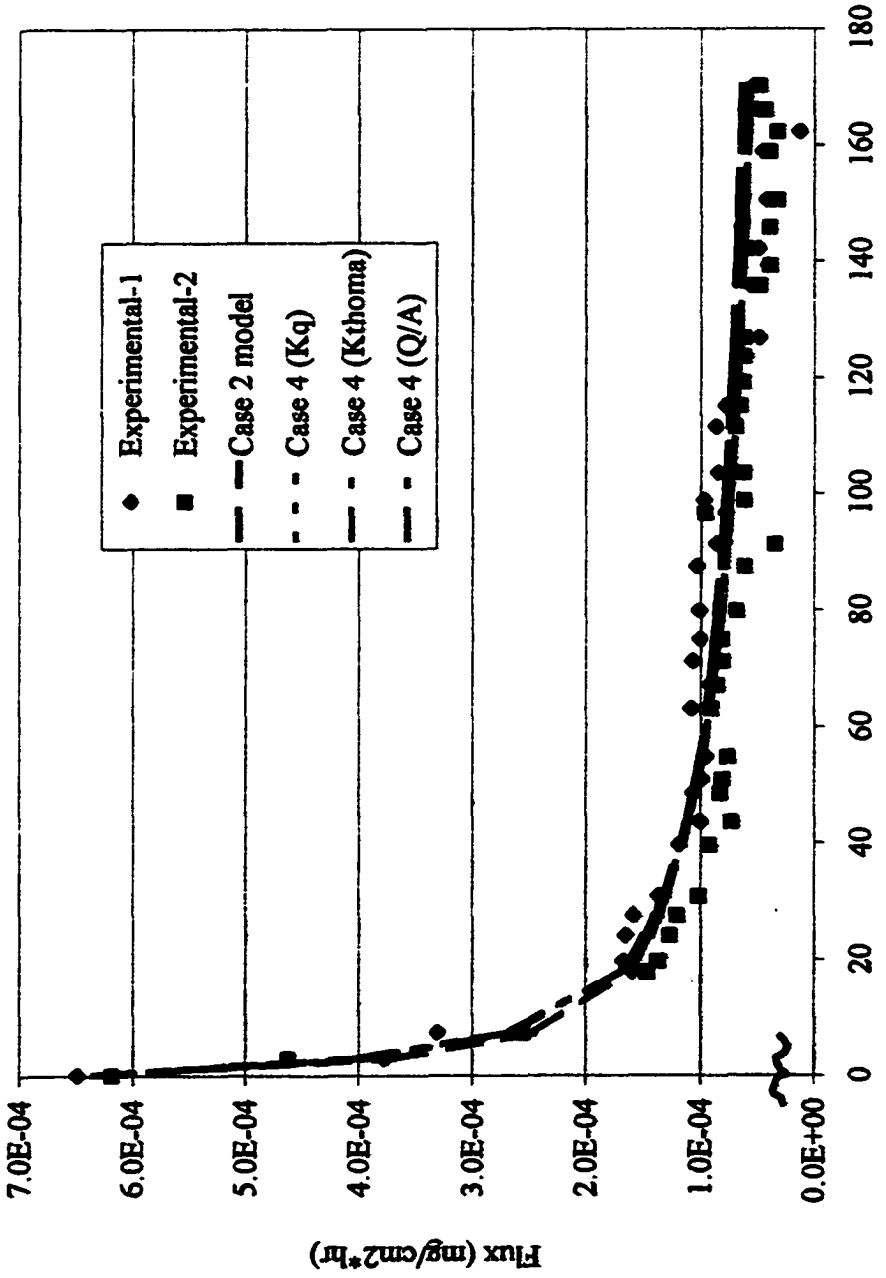

Figure 4.3. MCB in mix fast flow fit models and data

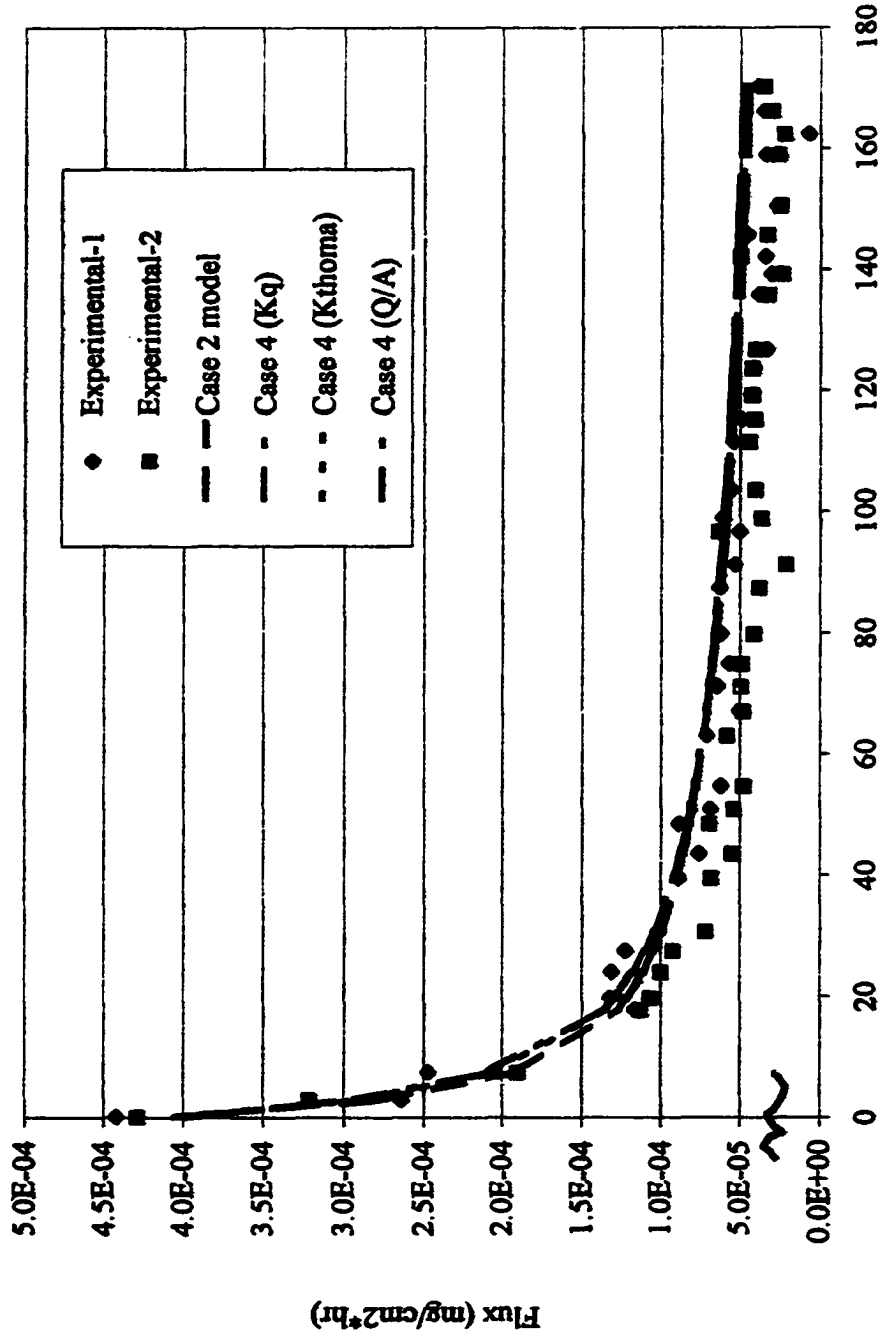

Figure 4.4. 1,3DCB in mix fast flow fit models and data

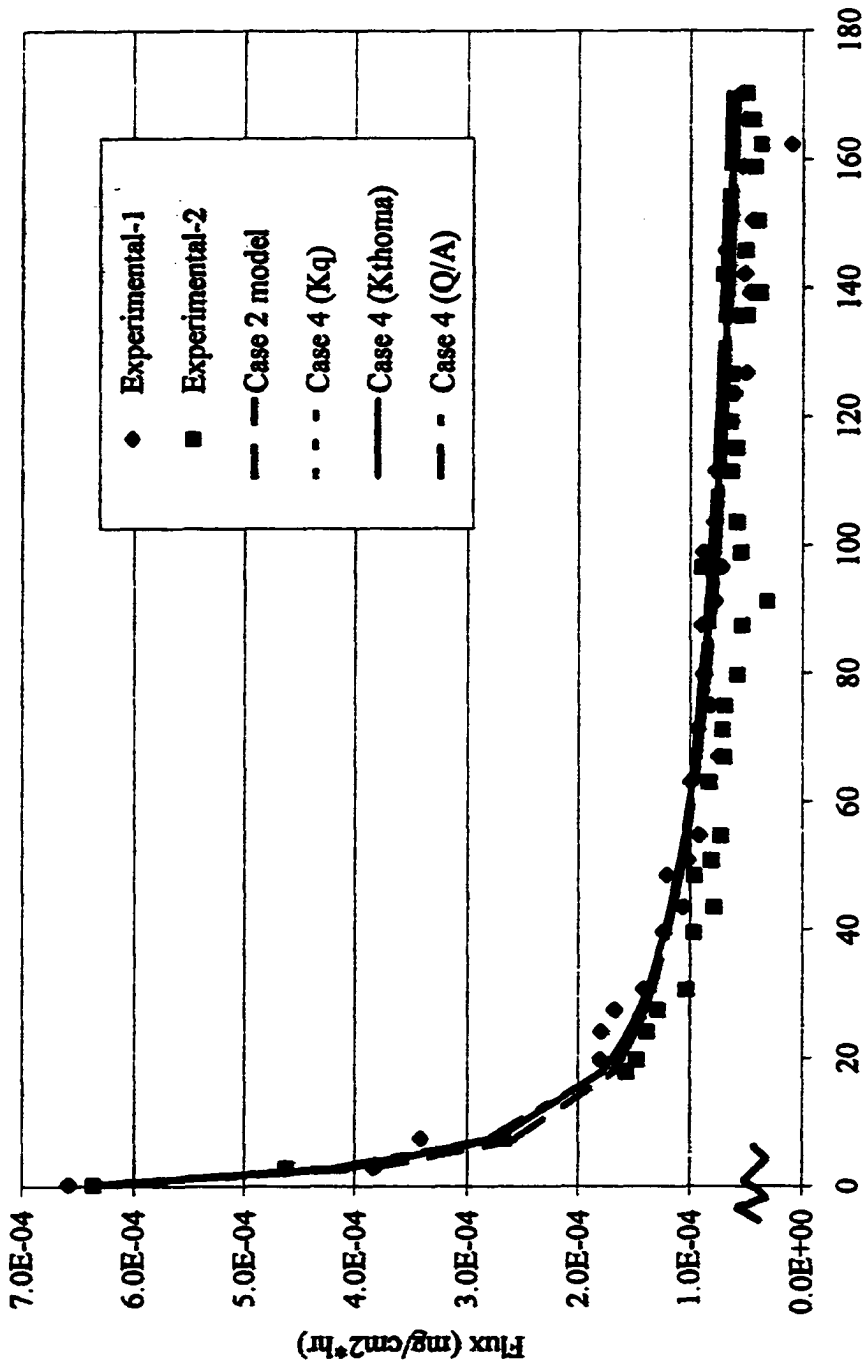

Figure 4.5. 1,2-DCB in mix fast flow fit models and data

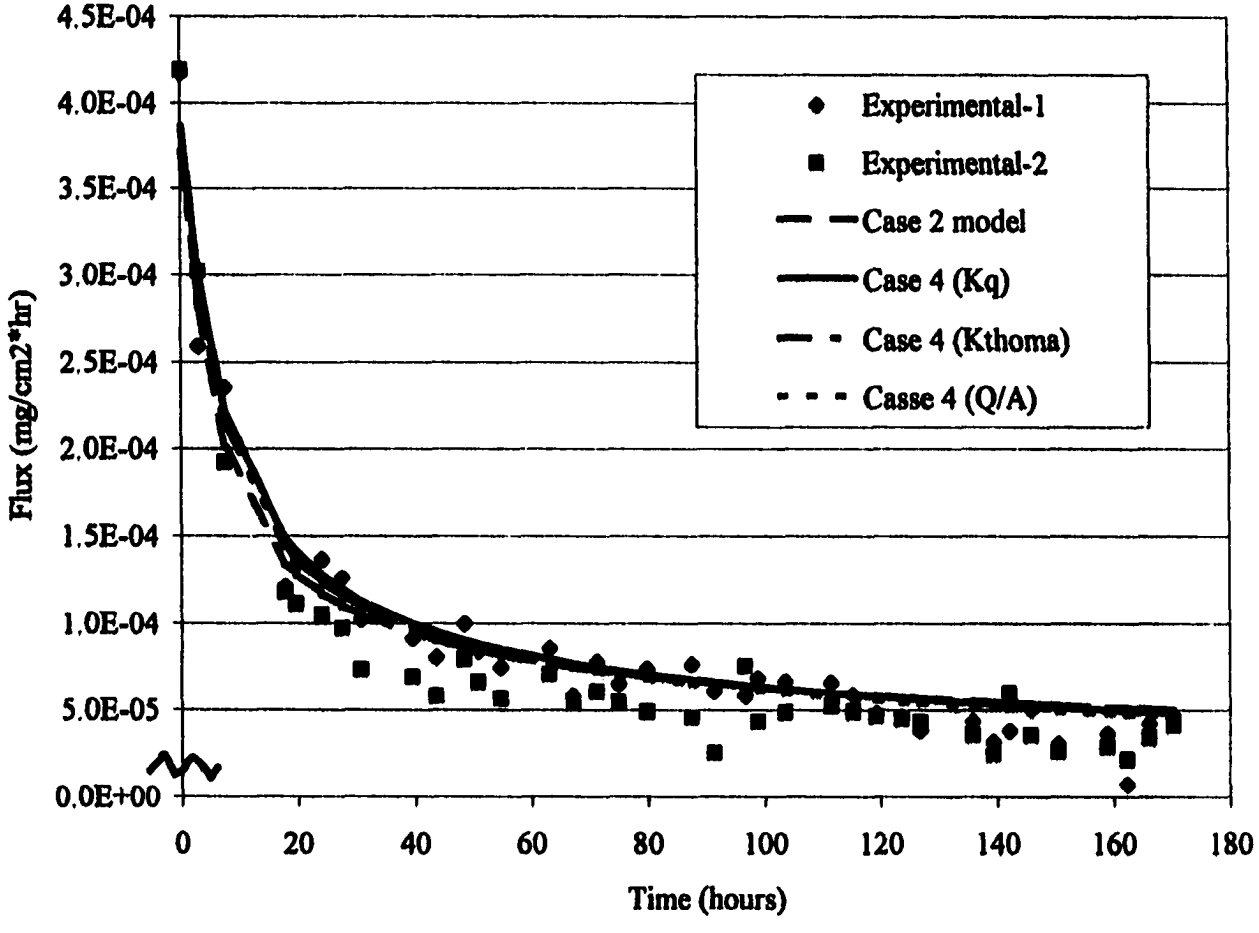

Figure 4.6. TCB in mix fast flow fit models and data

By visual examination, all fast flow experiments appear to be adequately modeled by either case 2 or the different case 4 diffusion models. The models iteratively calculate the average effective diffusivity to fit the flux curve to the experimental flux data by minimizing the sum of squared errors, but this does not allow for weighting of the transient or steady state as may be desired. The fitted average effective diffusivity for each flux curve will be presented in tabular form next.

Table 4.2 presents the correlation coefficient, RMSE, calculated tortuosity, (eqn 4.3) and the fitted average effective diffusivity for all four model simulations. As expected, the slowest diffusivity will have the highest tortuosity. A comparison of the correlation coefficients and RMSEs indicate the models can adequately predict the transport of these contaminants. All the fast flow simulations in Table 4.2 were used to determine a predictive average tortuosity, tau, and a predictive average effective diffusivity, mu. The predictive average tortuosity, tau, was determined to be 13.27 with sigma equal to 6.92. The predictive average effective diffusivity, mu was equal to 46.55 E^{-8} cm^2/s with sigma calculated to be 28.58 E^{-8} cm^2/s. These two parameters are now tested for predicting flux rates in the two other flow conditions, slow and cyclic.

4.3.1 Tau as System Descriptor: Slow Flow

Figure 4.7 is the first in the series utilizing tortuosity, tau to predict contaminant transport under slow flow conditions. Figure 4.7 demonstrates the high tau fits the flux curves for MCB as a single contaminant very well. Figure 4.8 demonstrates the high and low tau predictive flux curves for 1,3-DCB as a single

Table 4.2. Summary for calculation of average De and tau for system descriptors

Single MCB fast	Fit De (10^-8 cm^2/s)		RMSE (mg/cm^2*hr)	Tau	Correlation coefficient, r	Single 1,3-DCB fast	Fit De (10^-8 cm^2/s)		RMSE (mg/cm^2*hr)	Tau	Correlation coefficient, r
Case 2	20.00	+/- 0.22	2.20E-05	24.36	0.862	Case 2	31.75	+/- 0.25	1.81E-05	14.06	0.895
Case 4, Kq	30.90	+/- 0.28	1.62E-05	15.77	0.891	Case 4, Kq	23.10	+/- 0.18	7.77E-05	19.32	0.961
Case 4, Kth	35.85	+/- 0.22	1.53E-05	13.59	0.895	Case 4, Kth	40.00	+/- 0.19	1.73E-05	11.16	0.993
Case 4, Q/A	30.10	+/- 0.20	1.57E-05	16.21	0.878	Case 4, Q/A	31.10	+/- 0.22	1.16E-05	14.36	0.909
Mixture MCB fast	**Fit De (10^-8 cm^2/s)**		**RMSE (mg/cm^2*hr)**	**Tau**	**Correlation coefficient, r**	**Mixture 1,3-DCB fast**	**Fit De (10^-8 cm^2/s)**		**RMSE (mg/cm^2*hr)**	**Tau**	**Correlation coefficient, r**
Case 2	17.05	+/-0.23	1.92E-05	28.58	0.990	Case 2	28.95	+/- 0.18	1.72E-05	15.43	0.995
Case 4, Kq	23.55	+/-0.15	1.38E-05	20.69	0.995	Case 4, Kq	39.64	+/- 0.15	1.63E-05	11.26	0.995
Case 4, Kth	25.06	+/-0.18	1.52E-05	19.44	0.994	Case 4, Kth	42.02	+/- 0.19	1.71E-05	10.63	0.995
Case 4, Q/A	23.19	+/-0.15	1.35E-05	21.01	0.995	Case 4, Q/A	38.80	+/- 0.14	1.59E-05	11.51	0.995
Mixture 1,2-DCB fast	**Fit De (10^-8 cm^2/s)**		**RMSE (mg/cm^2*hr)**	**Tau**	**Correlation coefficient, r**	**Mixture TCB fast**	**Fit De (10^-8 cm^2/s)**		**RMSE (mg/cm^2*hr)**	**Tau**	**Correlation coefficient, r**
Case 2	46.28	+/-0.15	2.00E-05	9.65	0.993	Case 2	77.81	+/-0.18	1.52E-05	5.21	0.992
Case 4, Ka	63.95	+/-0.18	1.48E-05	6.98	0.996	Case 4, Ka	109.75	+/-0.15	1.67E-05	3.70	0.990
Case 4, Kth	67.70	+/-0.18	1.65E-05	6.60	0.996	Case 4, Kth	111.30	+/-0.12	1.67E-05	3.65	0.990
Case 4, Q/A	62.56	+/-0.15	1.42E-05	7.14	0.997	Case 4, Q/A	102.50	+/-0.20	1.61E-05	3.96	0.989

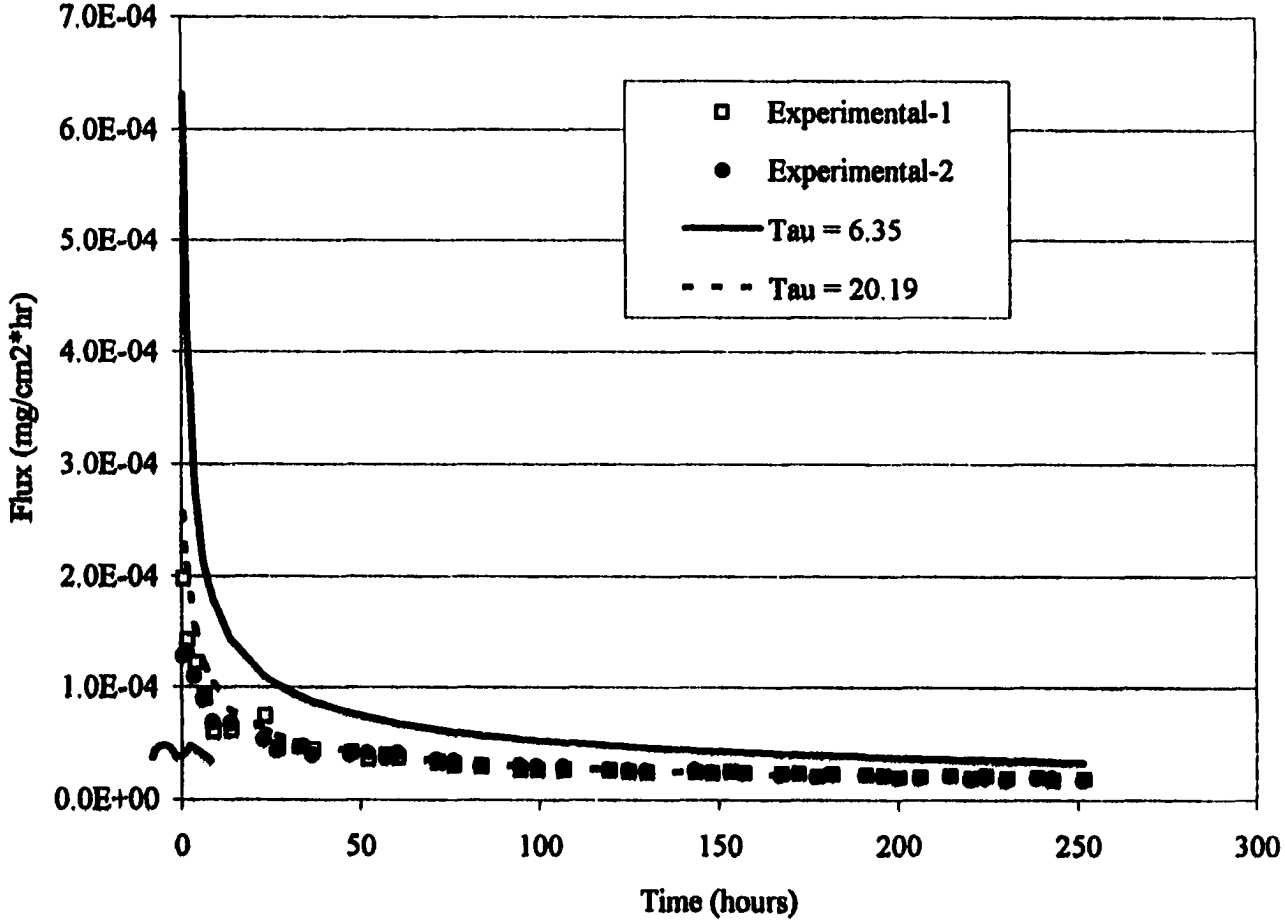

Figure 4.7 Tortuousity as system predictor for MCB single slow flow

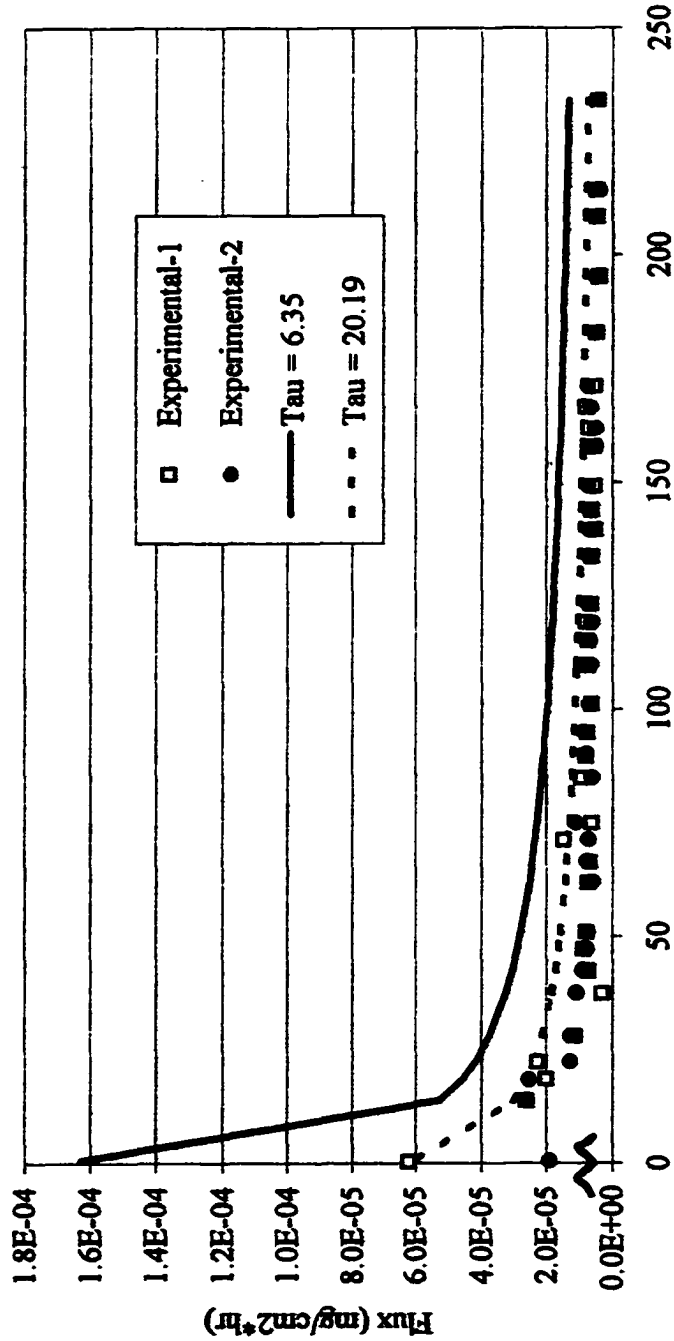

Figure 4.8. Tortuousity as system predictor for 1,3-DCB single contaminant slow flow

contaminant, although both over predicted the experimental flux. It can be seen that there were some problems with the flow rate causing variations in the flux rate at the beginning of the slow flow mixture experiment. This variation in flow will be seen in all four compounds as they all have the same flow rate. Figure 4.9 compares the experimental flux rates bracketed by the high and low tau model flux rates for MCB in the mixture. The high and low tau flux curves are shown with the experimental data for the mixture components 1,3-DCB and 1,2-DCB in Figure 4.10 and 4.11, respectively. Of the mixture series, only the TCB data is remotely predicted by the high and low tau parameter as a predictor as seen in Figure 4.12. The pump problem is blamed for the model over estimation of contaminant flux under the slow condition. In the slow flow regime, the best fit would be expected by the high side of the overall range of tau values.

4.3.2 Tau as System Descriptor: Cyclic Flow

The following series demonstrates how well the models can predict the experimental flux rates under cyclic flow conditions by using the mean plus and minus one standard deviation. Figure 4.13 examining the range of tau to adequately predict flux for the single contaminant MCB cyclic flow experimental data. The single contaminant 1,3-DCB is more closely predicted by the highest tau value as seen in Figure 4.14. The component MCB in the mixture is well modeled by the range of tau values bracketed in Figure 4.15. In Figure 4.16, the 1,3-DCB component is adequately modeled as can be seen by points both above and below the range predicted by tau. Of this series, the parameter tau does an excellent job of predicting the flux of the 1,2-DCB isomer is the mixture as seen in Figure 4.17.

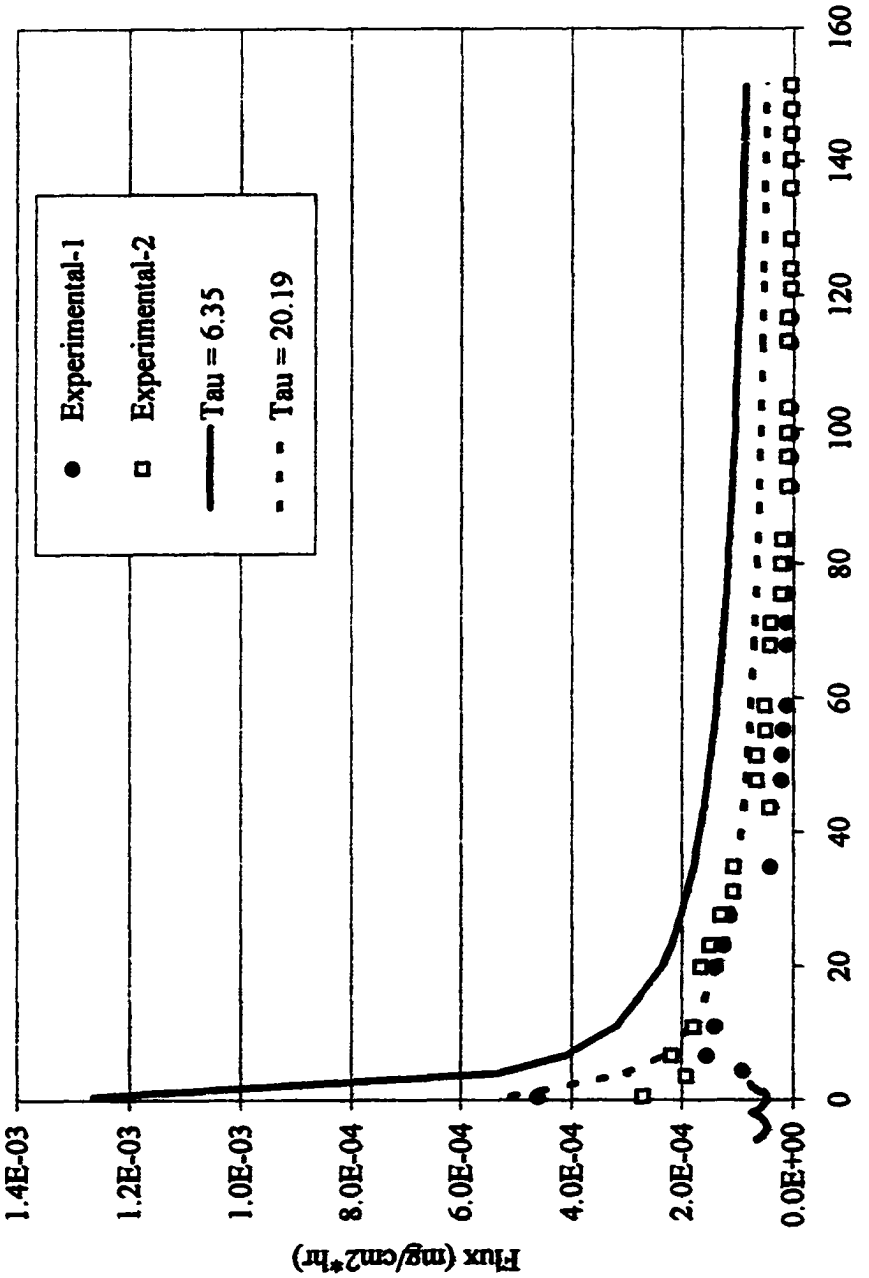

Figure 4.9. Tortuousity as system predictor for MCB in mix under slow flow

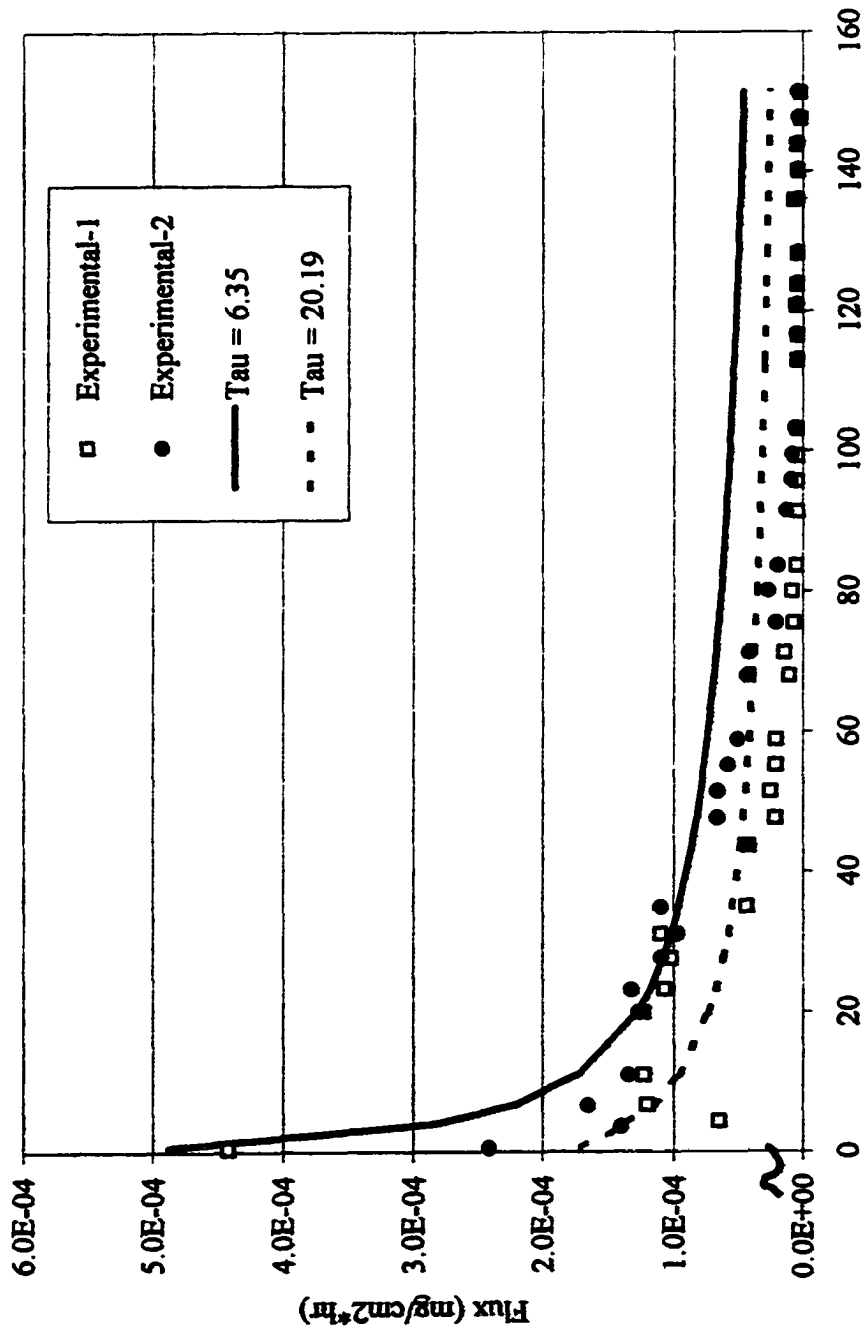

Figure 4.10. Tortuousity as system predictor for 1,3-DCB in mix under slow flow

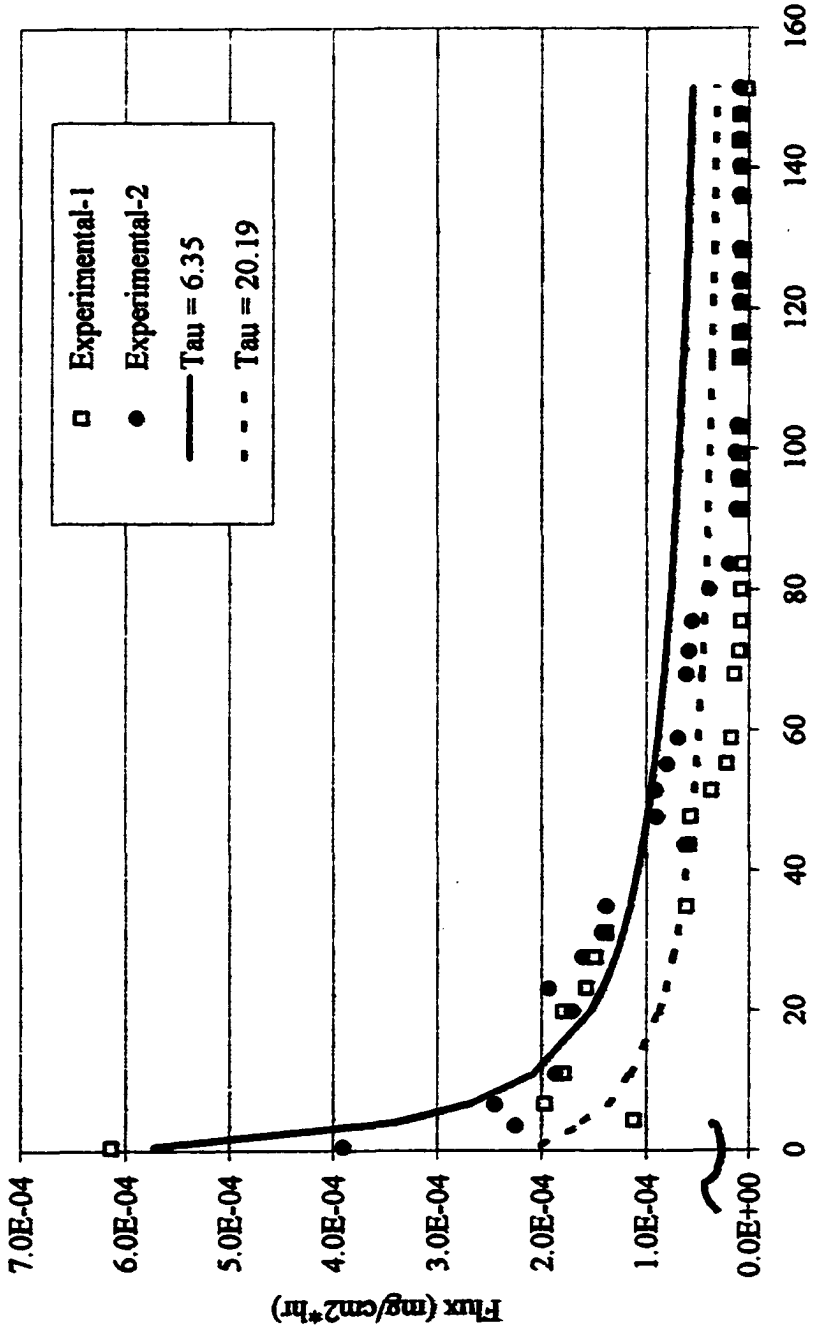

Figure 4.11. Tortuousity as system predictor for 1,2-DCB in mix under slow flow

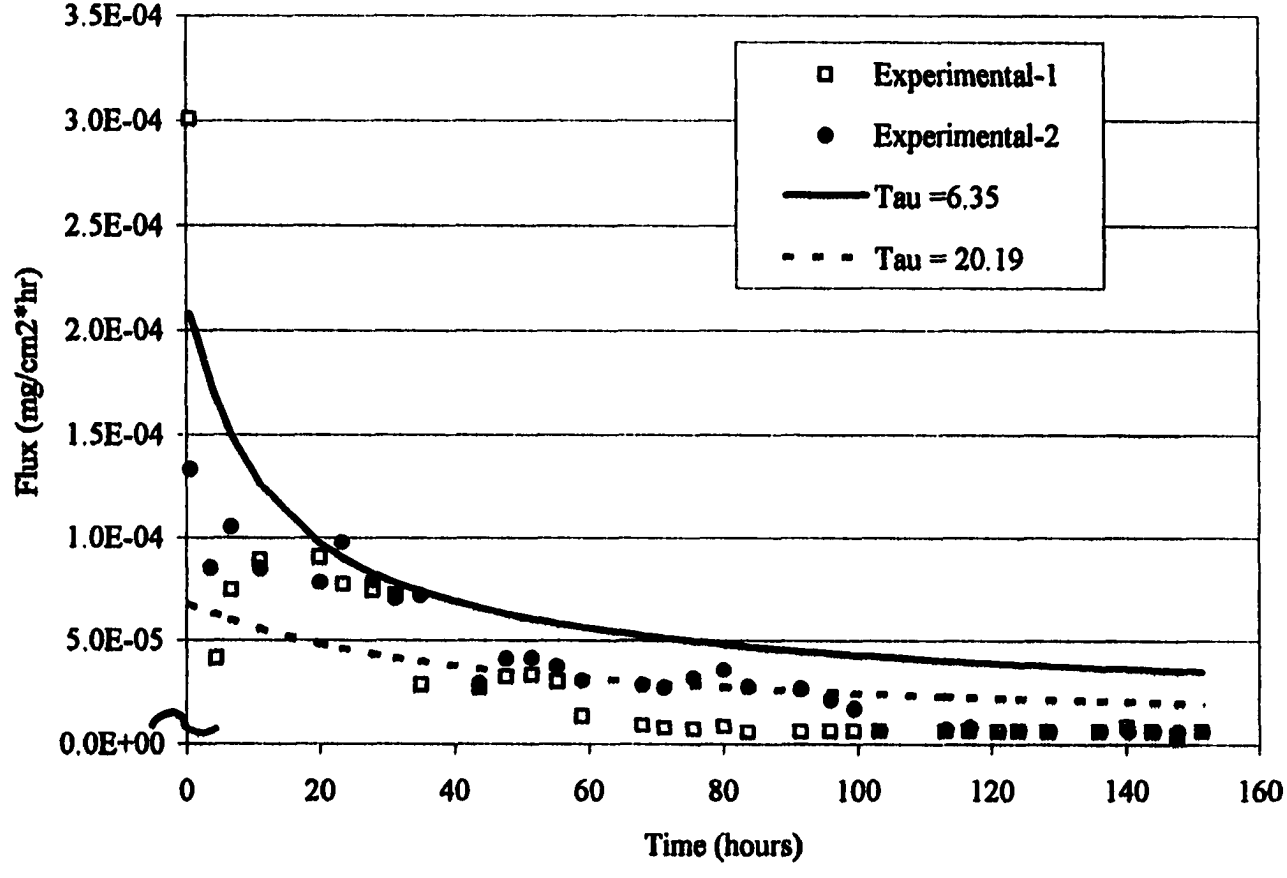

Figure 4.12. Tortuousity as system predictor for TCB in mix under slow flow

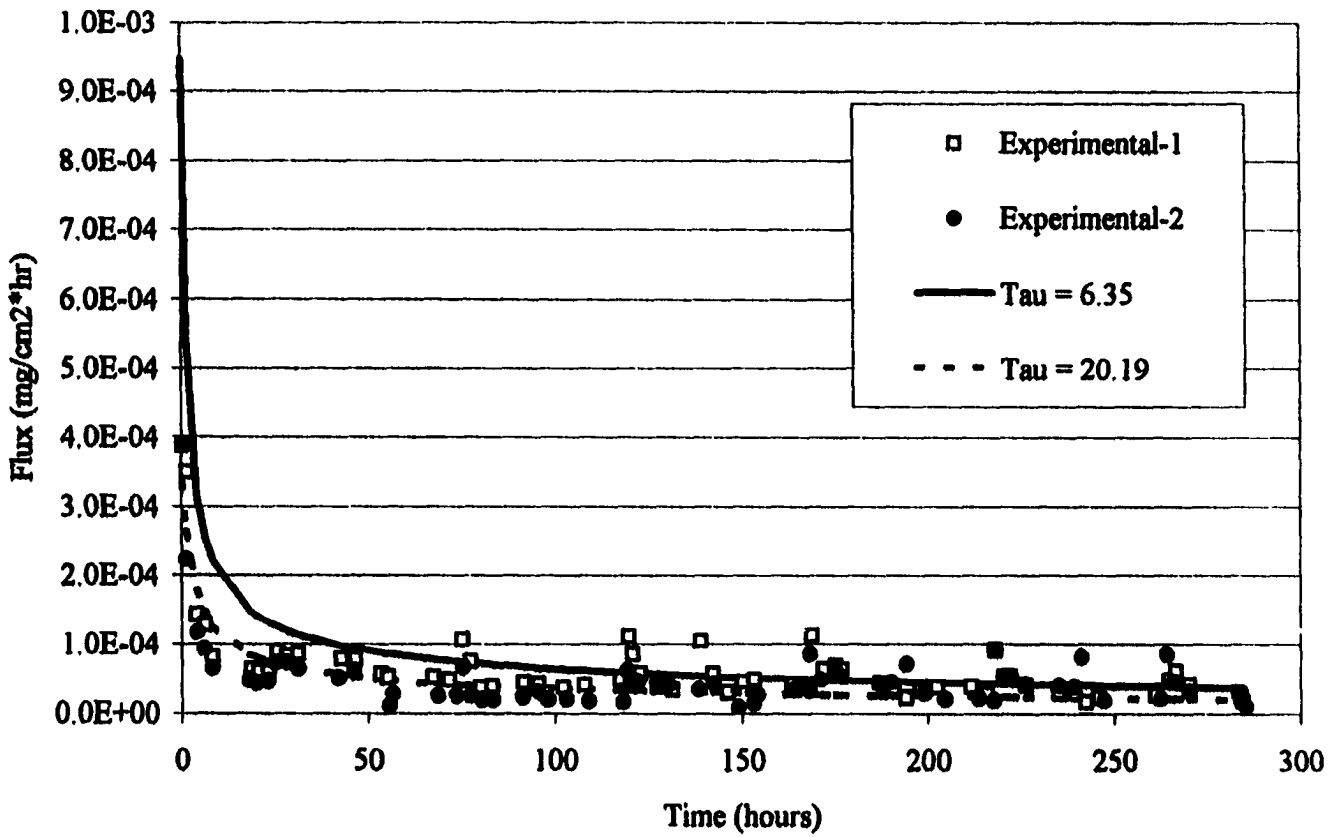

Figure 4.13. Tortuosity as system predictor for MCB single contaminant cyclic flow

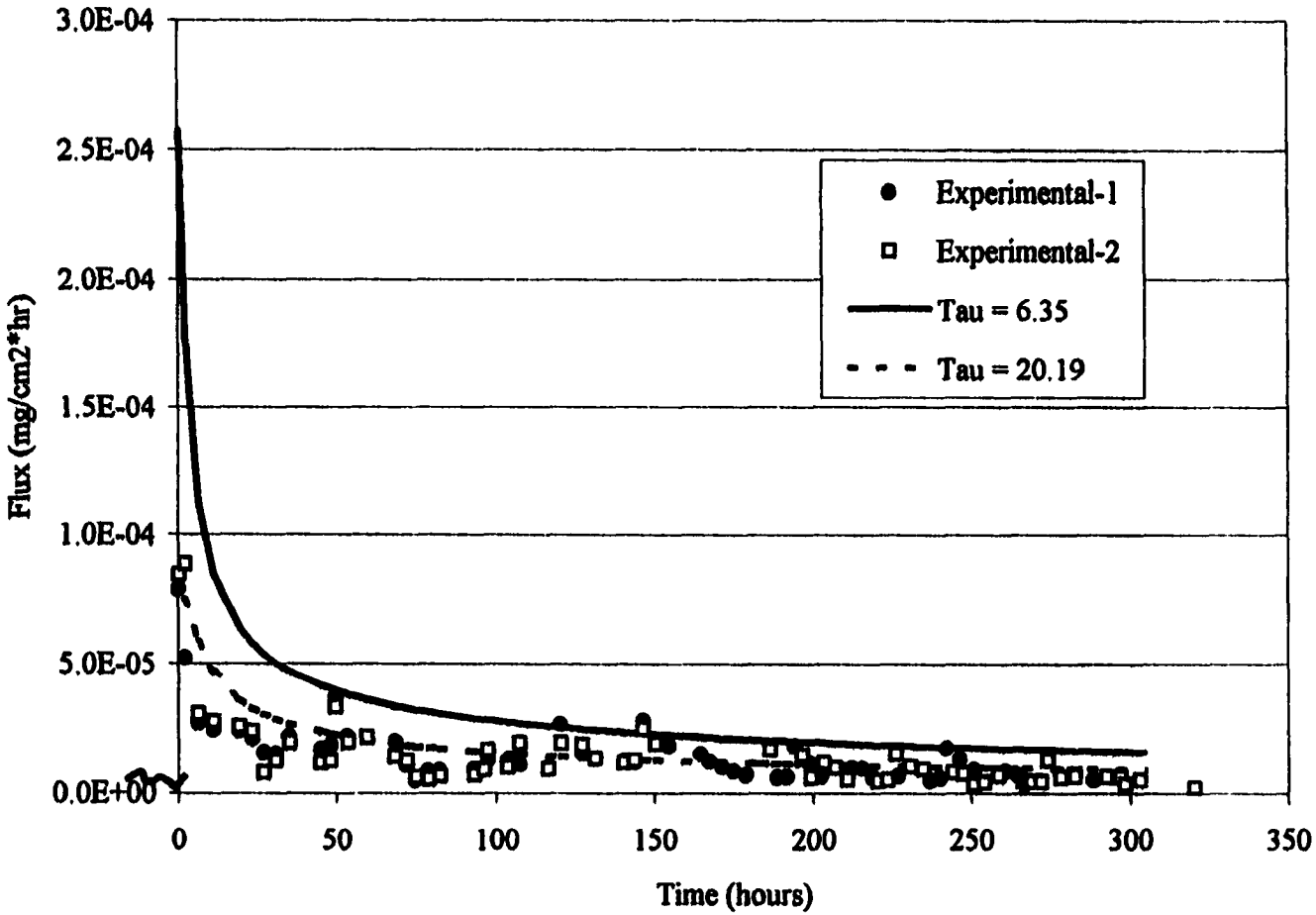

Figure 4.14. Tau as system predictor for 1,3-DCB single contaminant cyclic flow

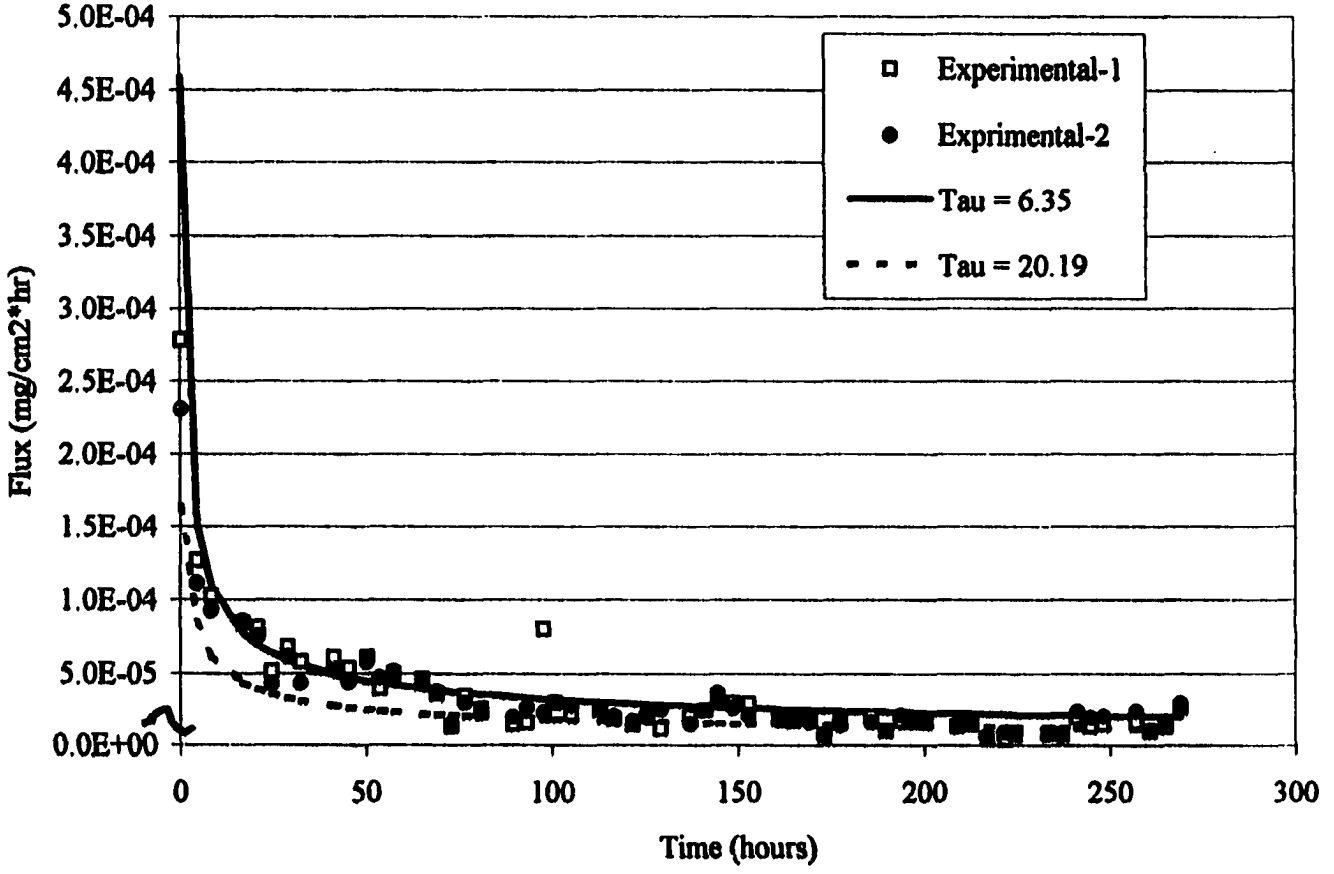

Figure 4.15. Tortuousity as system predictor for MCB in mix under cyclic flow

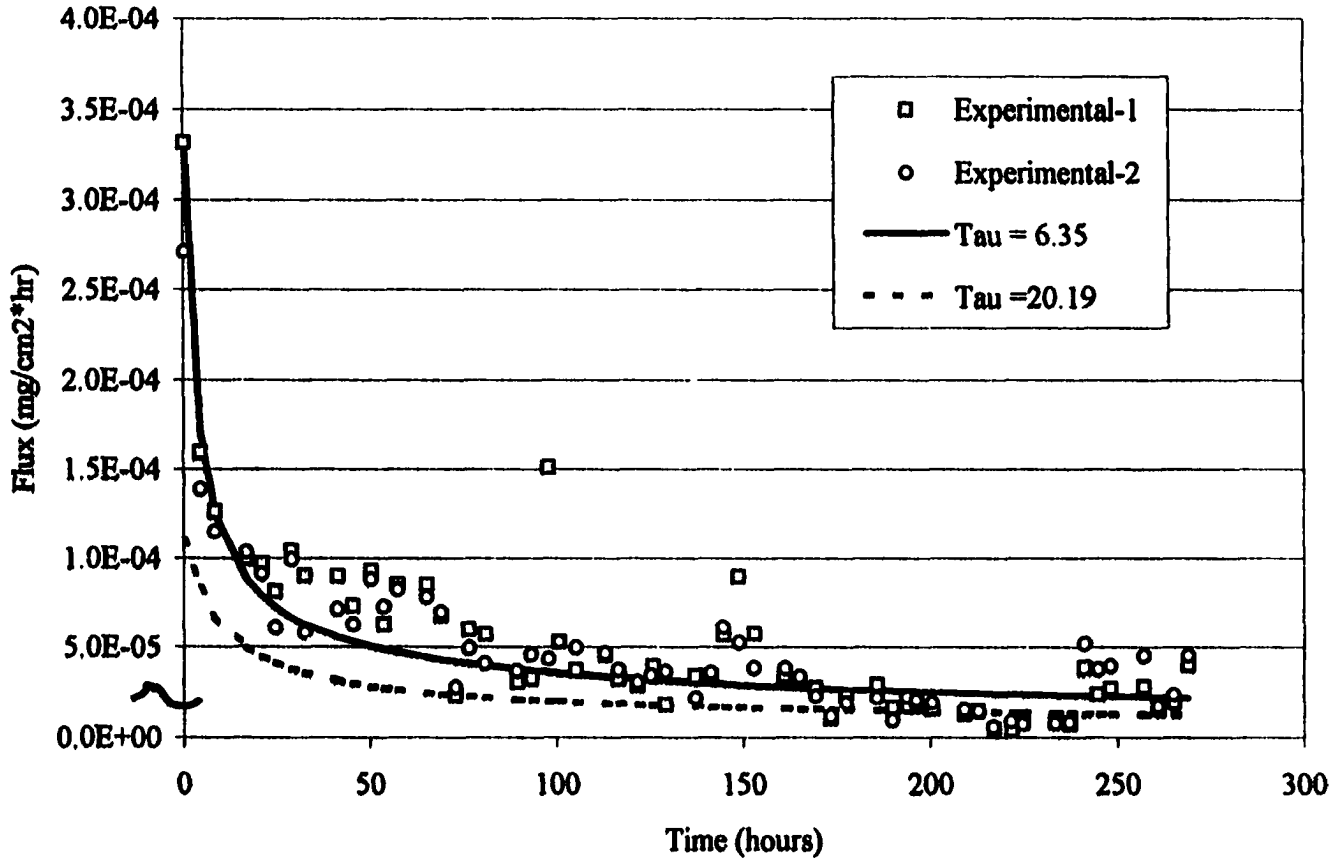

Figure 4.16. Tortuousity as system predictor for 1,3-DCB in mix under cyclic flow

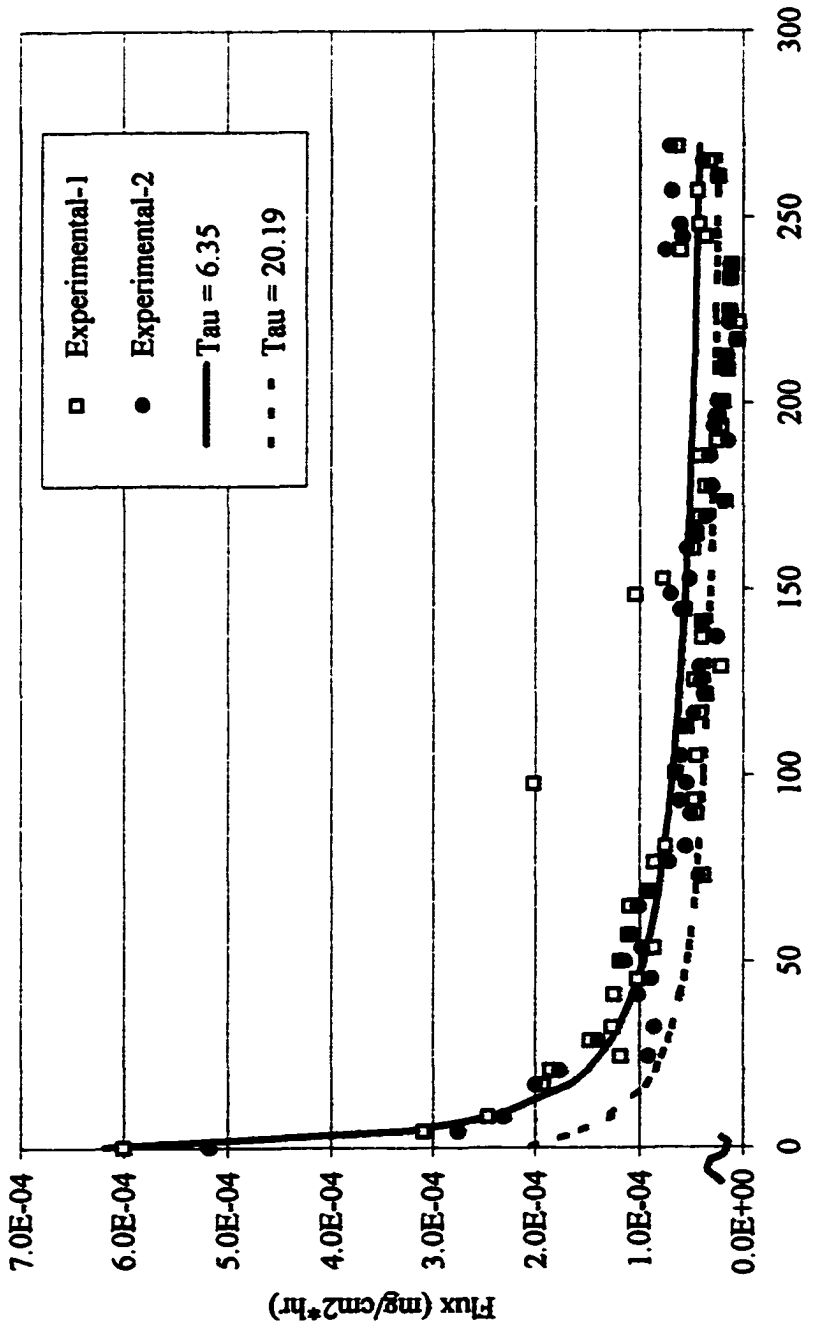

Figure 4.17. Tortuousity as system predictor for 1,2-DCB in mix under cyclic flow

Figure 4.18 indicates the TCB experimental flux is predominately under estimated using the range of predictive tau.

Table 4.3 presents the graphic results in tabular form to aid in understanding the differences between the modeled results. By using equation 4.4, the effective diffusivity is calculated based on the two tau values and is presented for both slow and cyclic flow regimes. The RMSE indicates how well the new predicted flux fits the experimental flux. Comparing Table 4.3 to Table 4.2, the predicted models are in the same order of magnitude as the original fitted models based on the RMSE. The correlation coefficients are similar also indicating tau can be used as a system descriptor to model contaminant transport.

4.3.3 Effective Diffusivity (mu) as System Predictor: Slow Flow

The next series of graphs utilized mu, the predicted average fitted effective diffusivity determined from the fast flow regime (plus or minus one standard deviation of the mean, mu) to show the predicted range of flux rates for slow flow. Figure 4.19 and 4.20 demonstrate the lower effective diffusivities are better predictors of single component transport for MCB and 1,3-DCB respectively. Recall that there were pump problems for remainder of the predictive models for mixture components in the slow flow series. Figure 4.21 presents the flux rates predicted by high and low effective diffusivities (mu plus and minus one standard deviation) for MCB in the mixture. The behavior of 1,3-DCB and 1,2-DCB in the multiple contaminant mixture is very similar as seen in Figures 4.22 and 4.23. It is believed that these two isomers would be well predicted if the pump could have adequately pumped such slow flow rates.

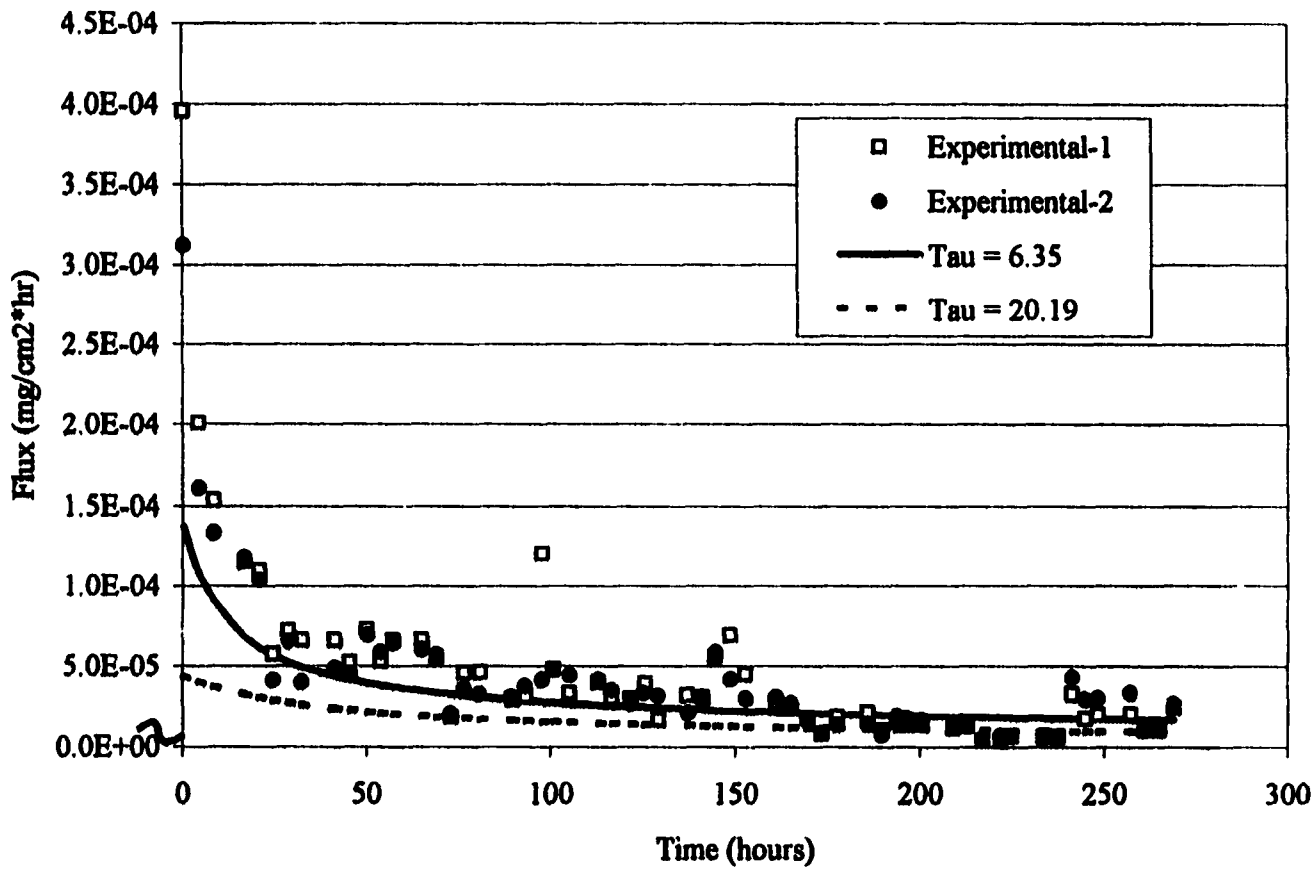

Figure 4.18. Tortuousity as system predictor for TCB in mix under cyclic flow

Table 4.3. Model comparison with tortuosity, tau, as predictor

	Tau = 6.35			Tau = 20.19		
Slow flow	De (10 -7 cm2/s)	RMSE (mg/cm2*hr)	Correlation coefficient	De (10 -7 cm2/s)	RMSE (mg/cm2*hr)	Correlation coefficient
MCB-single	7.673	9.70E-05	0.968	2.413	2.11E-05	0.991
1,3DCB-single	7.031	2.63E-05	0.923	2.211	6.17E-06	0.959
MCB in mix	7.673	2.02E-04	0.906	2.413	5.75E-05	0.932
1,3DCB in mix	7.031	5.91E-05	0.927	2.211	4.04E-05	0.921
1,2DCB in mix	7.031	5.64E-05	0.941	2.211	6.72E-05	0.935
TCB in mix	6.390	3.55E-05	0.905	2.010	3.20E-05	0.892

	Tau = 6.35			Tau = 20.19		
Cyclic flow	De (10 -7 cm2/s)	RMSE (mg/cm2*hr)	Correlation coefficient	De (10 -7 cm2/s)	RMSE (mg/cm2*hr)	Correlation coefficient
MCB-single	7.673	9.10E-05	0.934	2.413	2.62E-05	0.904
1,3DCB-single	7.031	3.49E-05	0.906	2.211	8.25E-06	0.874
MCB in mix	7.673	2.93E-05	0.942	2.413	2.20E-05	0.970
1,3DCB in mix	7.031	1.93E-05	0.922	2.211	4.12E-05	0.917
1,2DCB in mix	7.031	2.49E-05	0.965	2.211	6.36E-05	0.954
TCB in mix	6.390	3.59E-05	0.936	2.010	5.51E-05	0.851

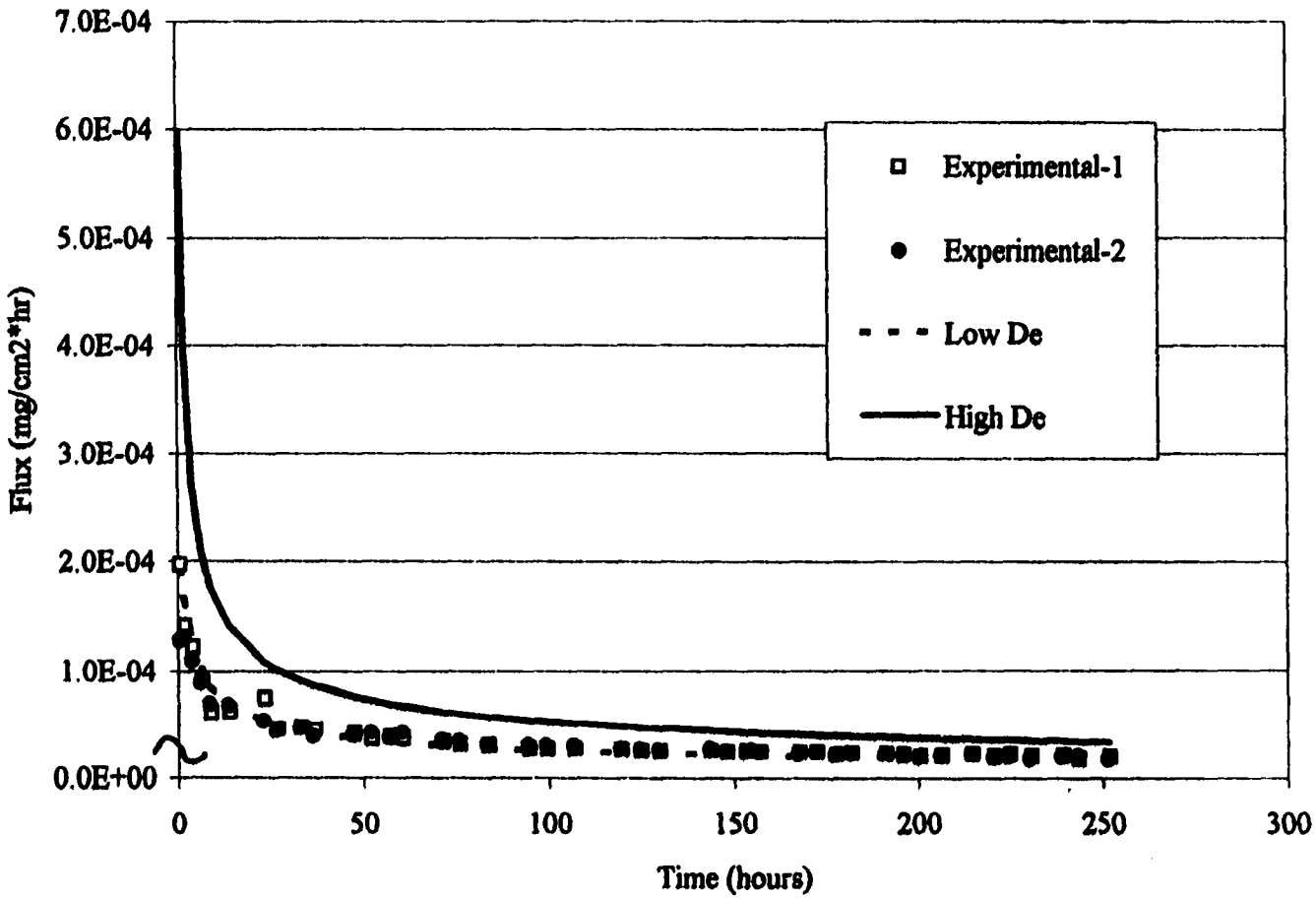

Figure 4.19. Effective diffusivity as system predictor MCB single contaminant slow flow

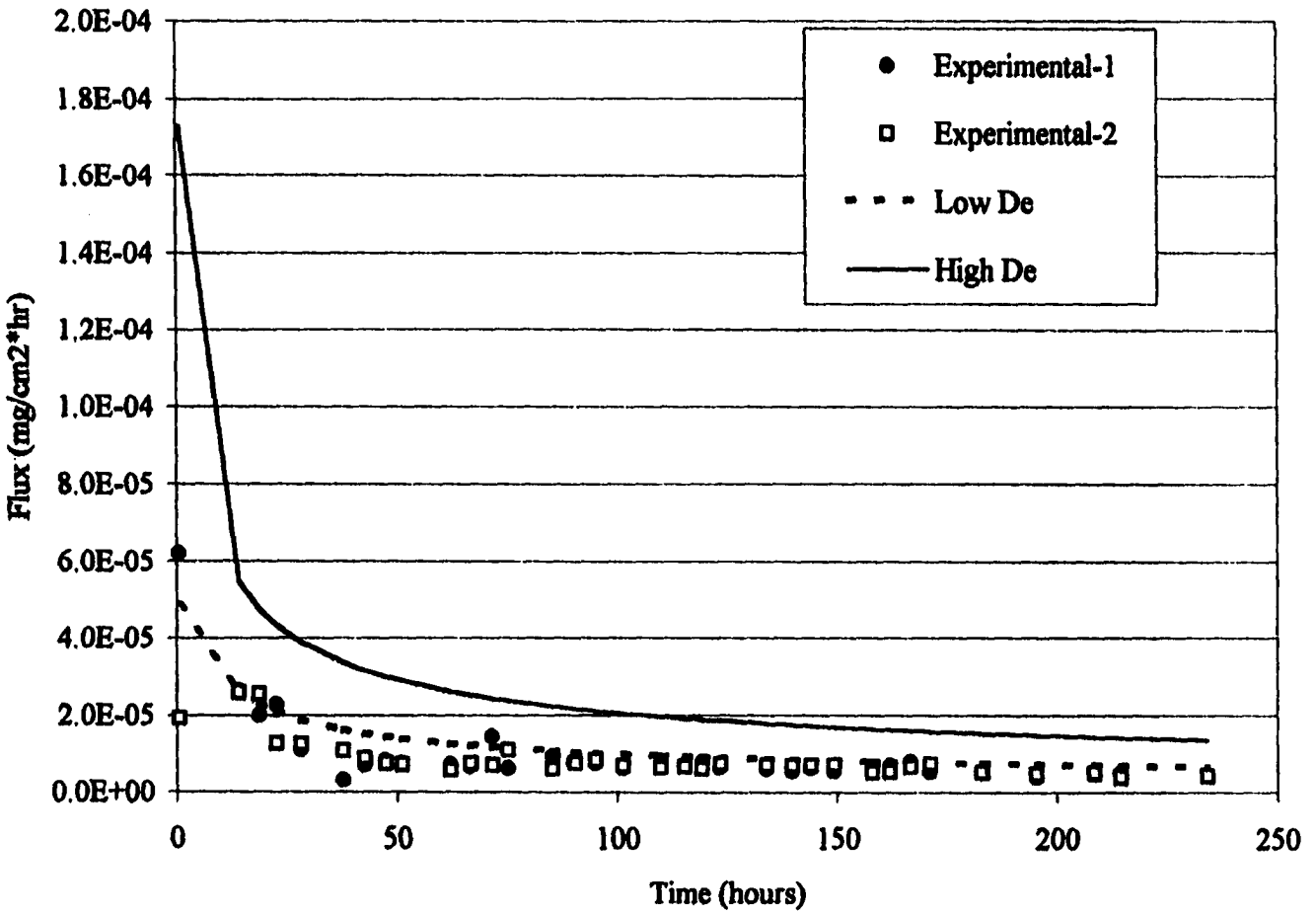

Figure 4.20. Effective diffusivity as system predictor for 1,3-DCB single contaminant slow flow

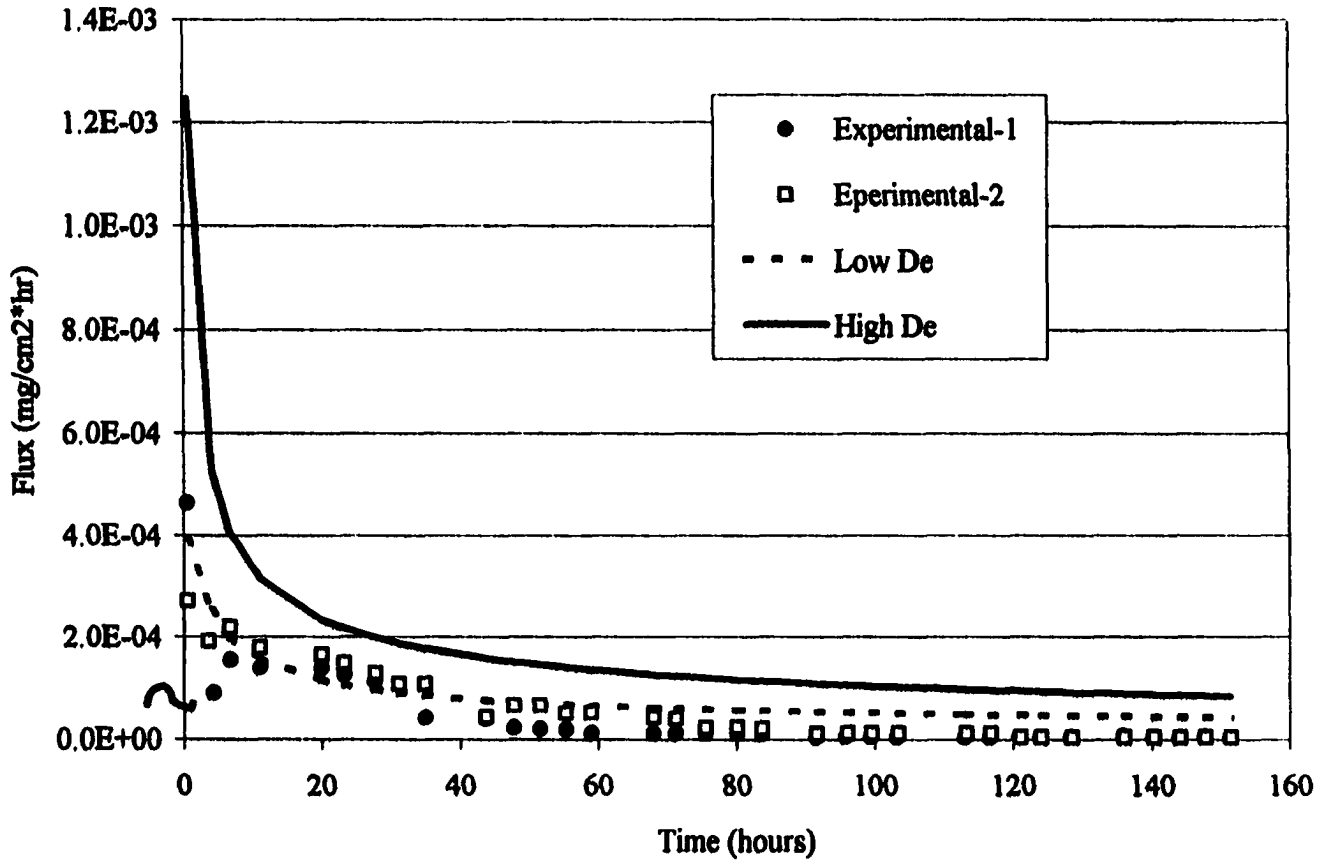

Figure 4.21. Effective diffusivity as system predictor for MCB in mix slow flow

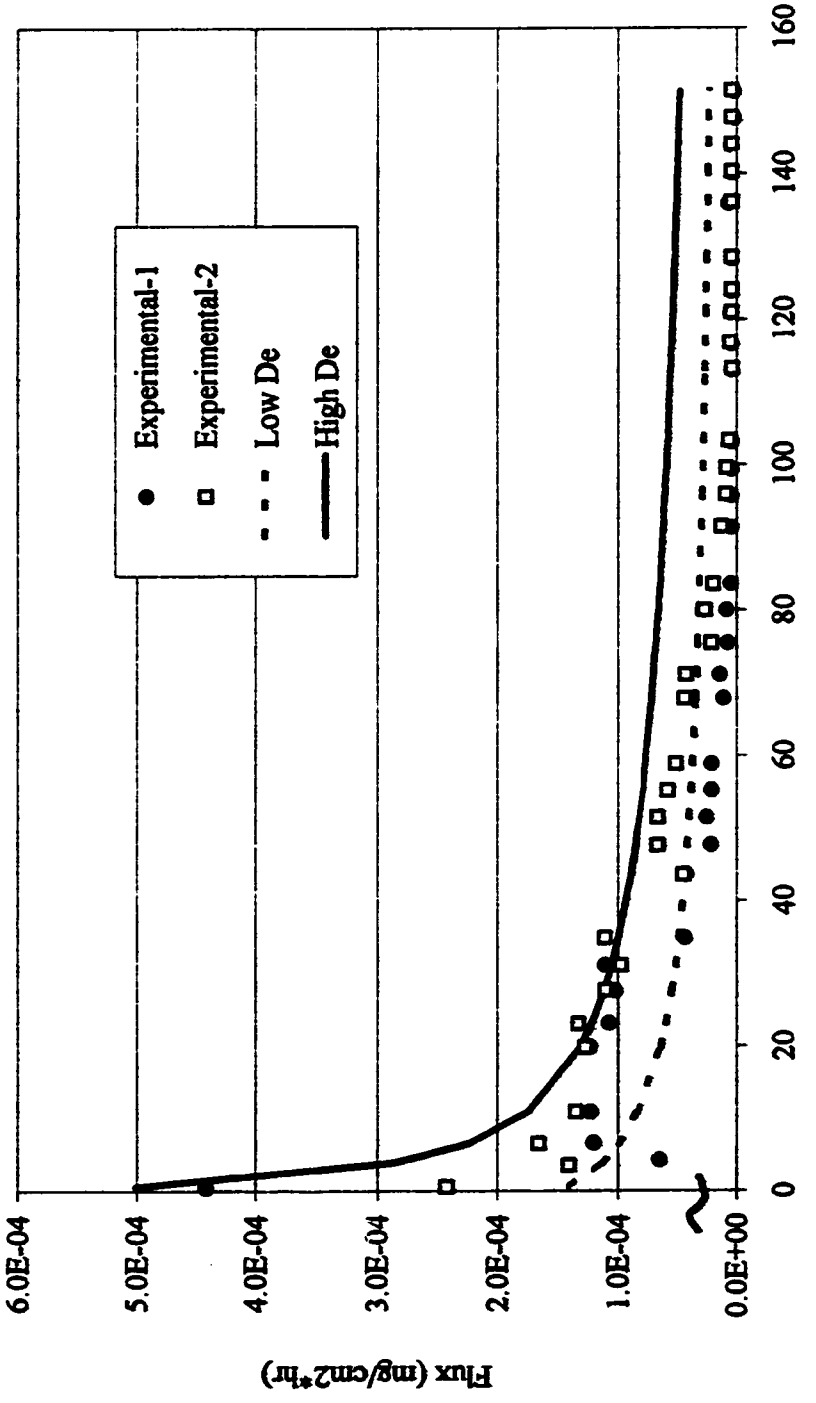

Figure 4.22. Effective diffucivity as system predictor for 1,3-DCB in mix slow flow

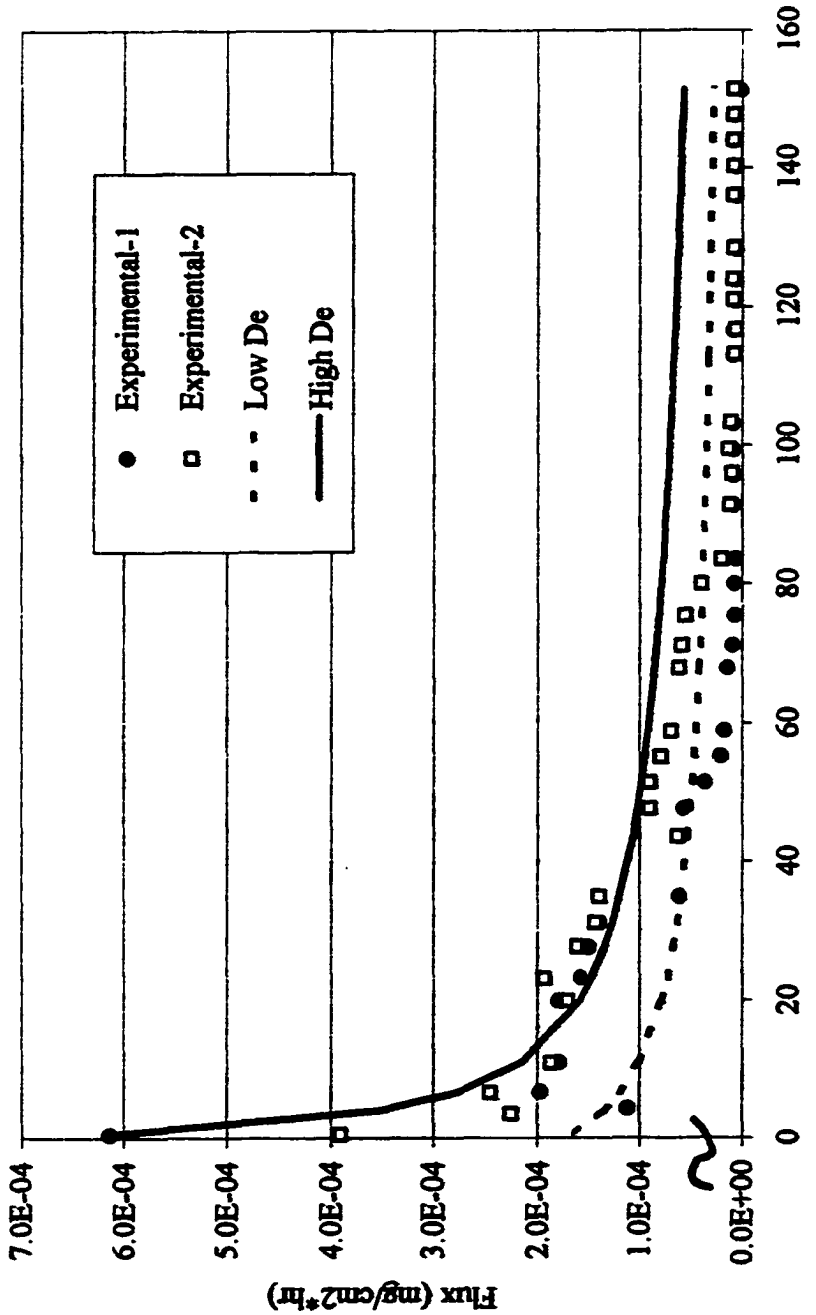

Figure 4.23. Effective diffusivity as system predictor for 1,2-DCB slow flow

The flux rates for the TCB component of the mixture are presented along with the values predicted by the range of mu in Figure 4.24.

4.3.4 Effective Diffusivity (mu) as System Predictor: Cyclic Flow

Figure 4.25 begins the series examining the range of diffusivities (mu plus and minus one standard deviation) as predictors for the contaminant flux rates under the cyclic flow regime. Figure 4.25 presents the range of values predicted by the effective diffusivities for the single contaminant MCB. In Figure 4.26 the flux rates of single 1,3-DCB is predominately overestimated by the range of predictive effective diffusivities. The effective diffusivity does an excellent job of predicting the mixture component MCB as seen in Figure 4.27. In Figure 4.28, the predictive models generally underestimated the experimental flux rates for 1,3-DCB in the mixture. The component 1,2-DCB experimental flux is bracketed as well as could be expected for predictive parameters in Figure 4.29. Figure 4.30 demonstrates the range of flux rates predicted for TCB in the mixture under the cyclic flow regime.

Table 4.4 presents the graphic results in tabular form to aid in understanding the differences between the modeled results. By using equation 4.4, a new tortuosity is calculated based on the two effective diffusivity values and is presented for both slow and cyclic flow regimes. The RMSE indicates how well the new predicted flux fits the experimental flux. Comparing Table 4.4 to Table 4.2, the predicted models are in the same order of magnitude as the original fitted models based on the RMSE. The correlation coefficients are similar also indicating the effective diffusivity can be used as a system descriptor to describe and predict contaminant transport for a given system.

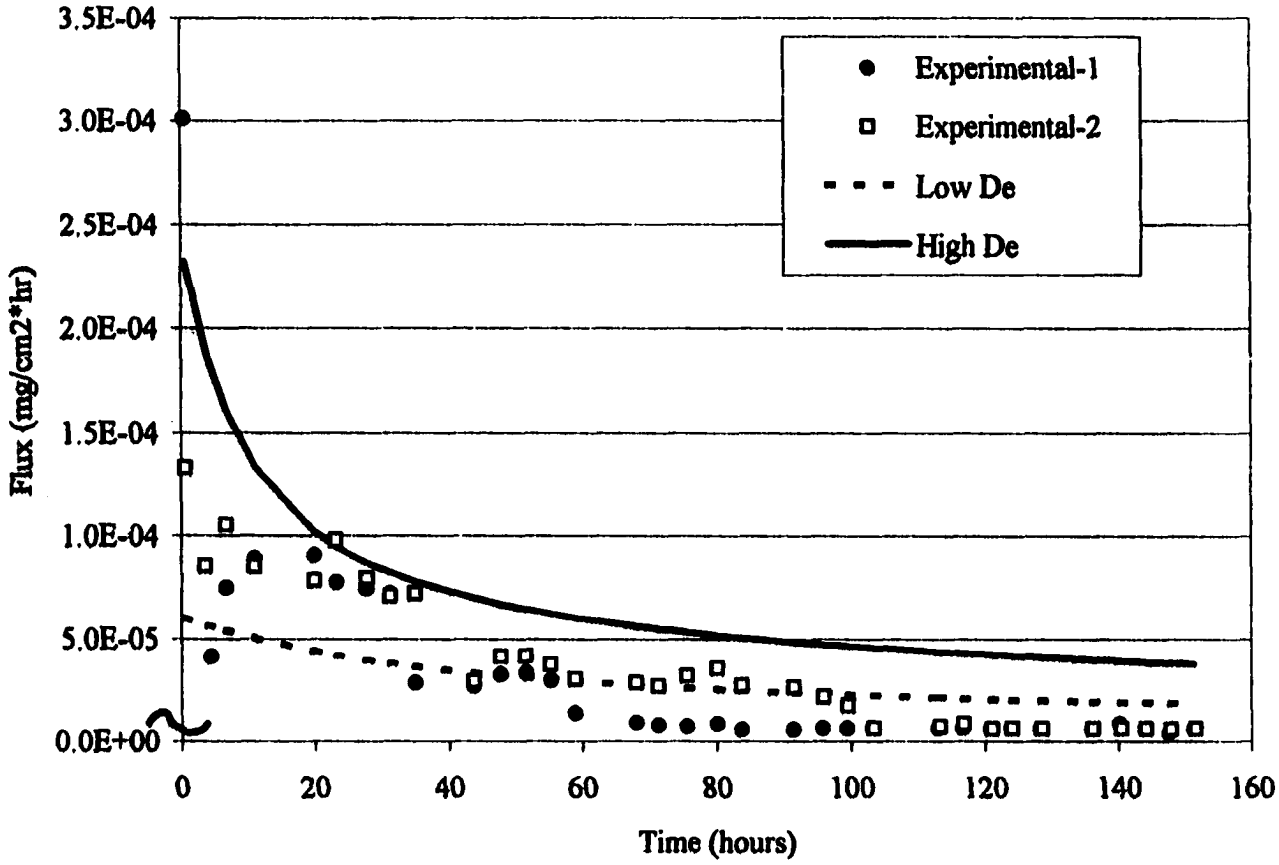

Figure 4.24. Effective diffusivity as system predictor for TCB in mix slow flow

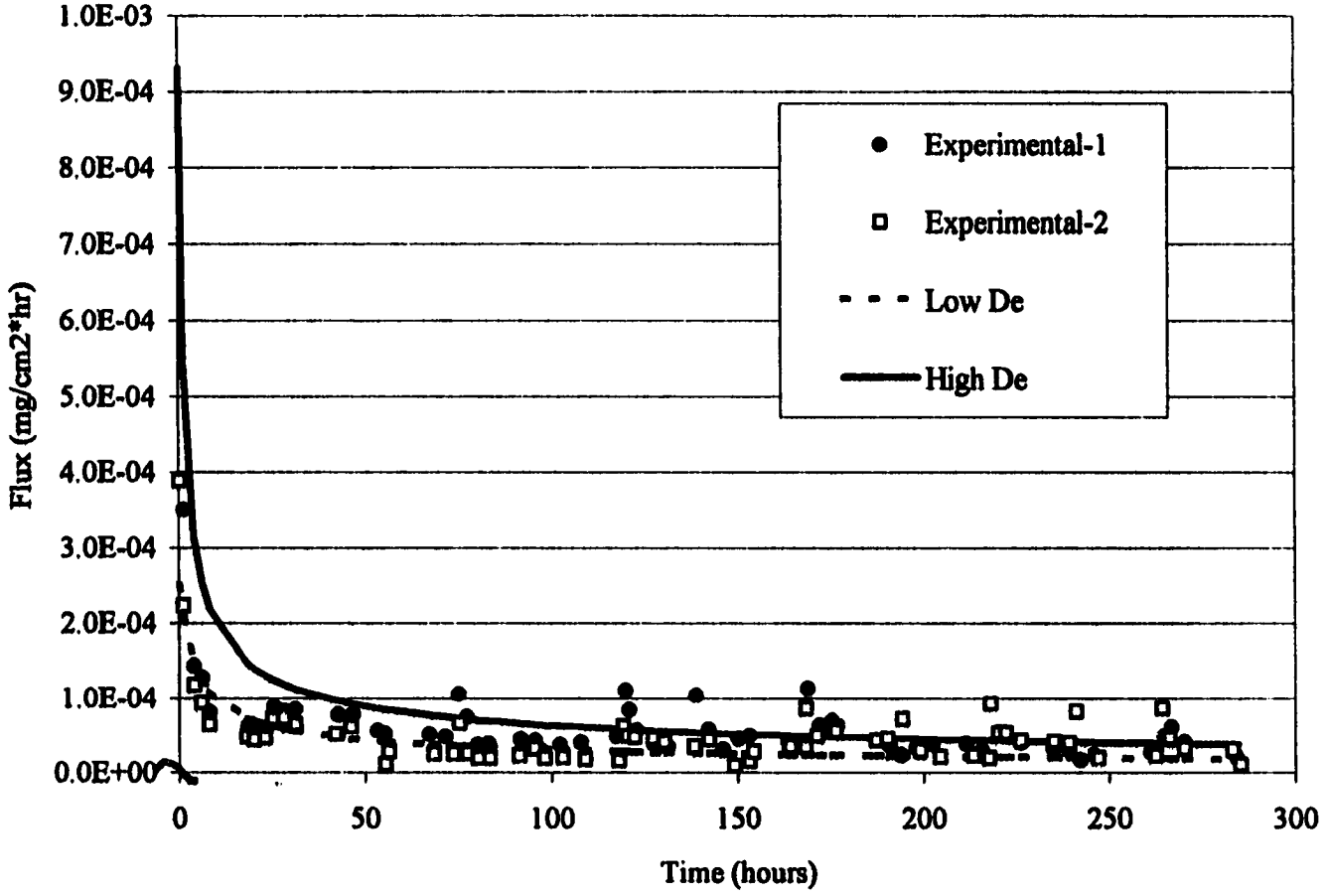

Figure 4.25. Effective diffusivity as system predictor MCB single contaminant cyclic flow

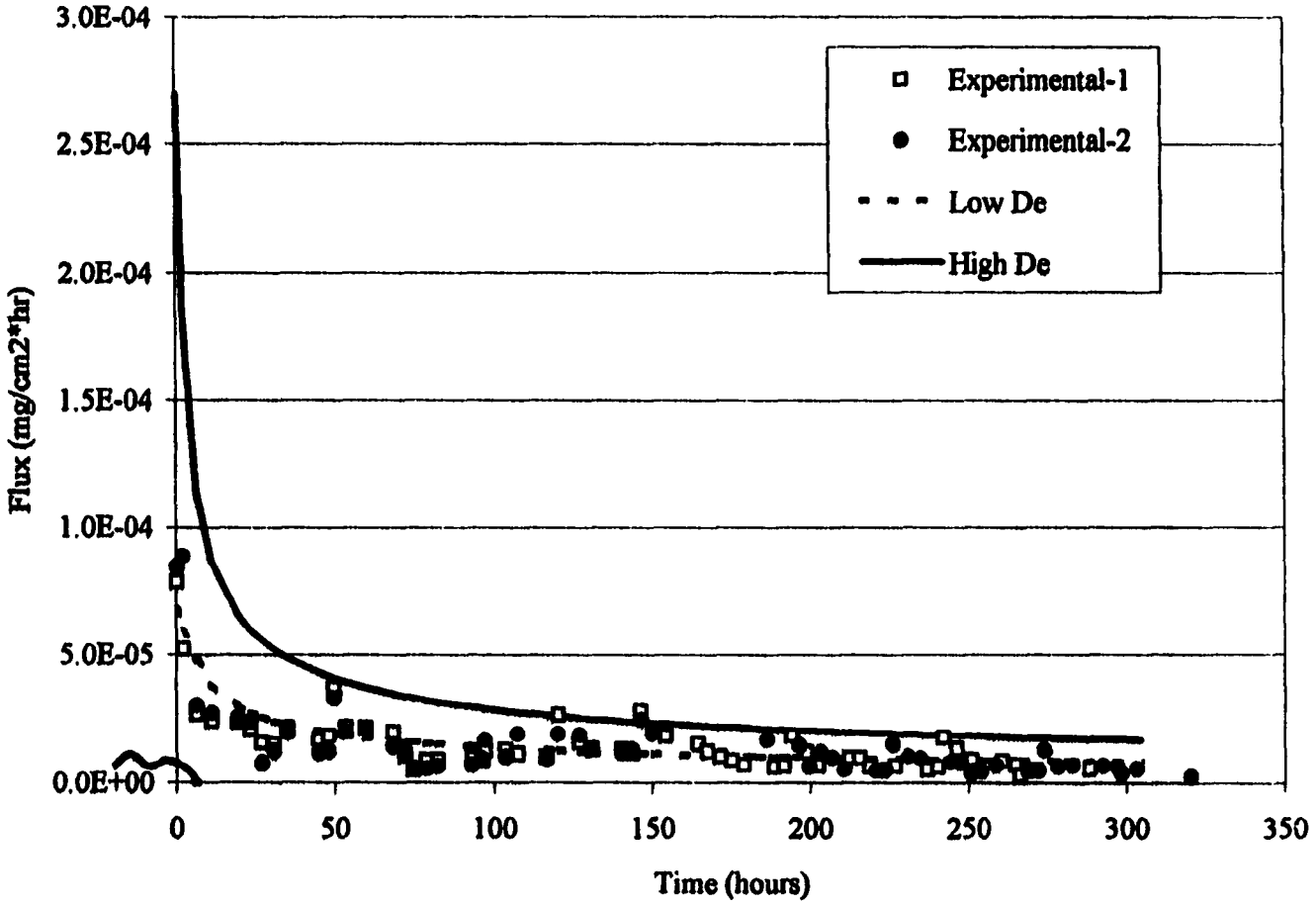

Figure 4.26. Effective diffusivity as system predictor for 1,3-DCB single contaminant cyclic flow

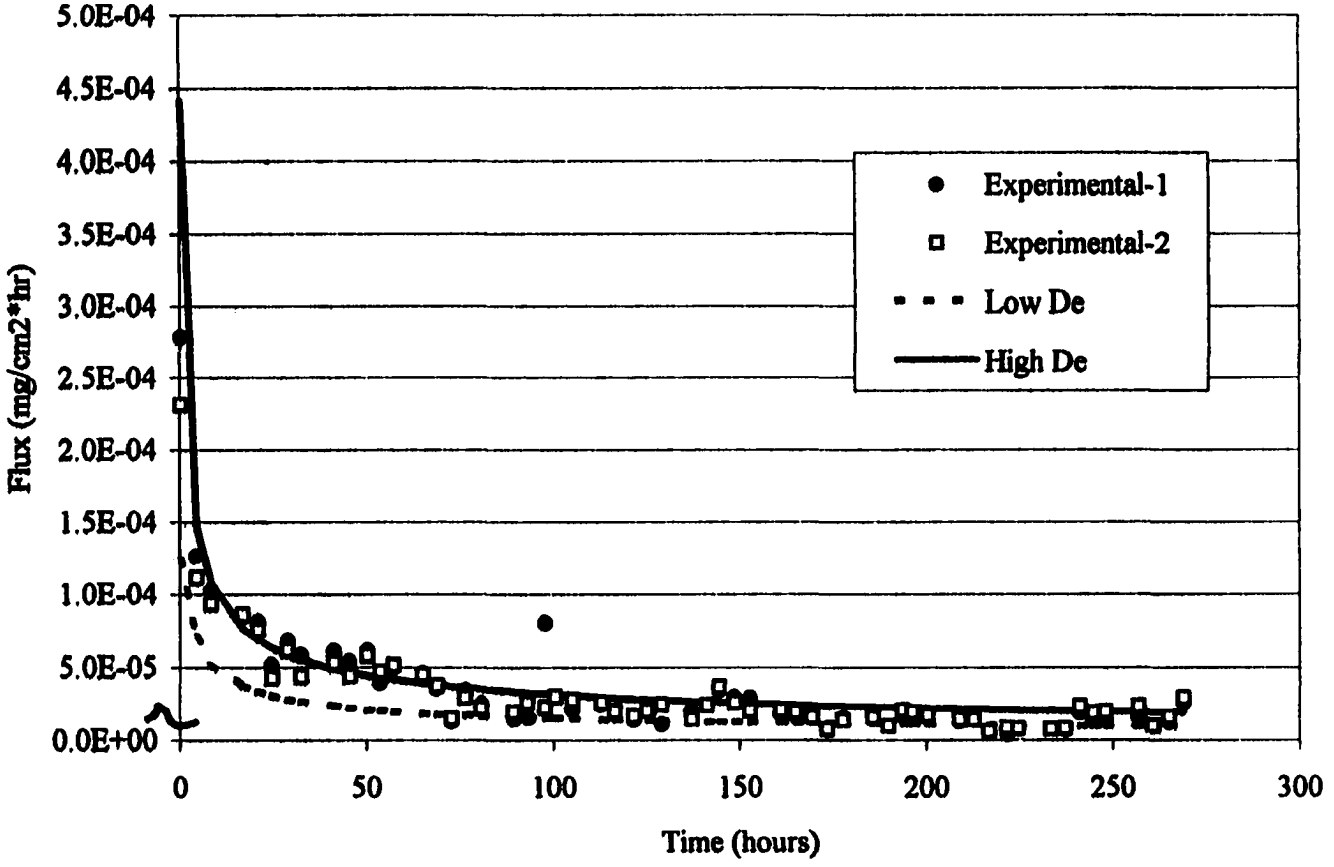

Figure 4.27. Effective diffusivity as system predictor for MCB in mix cyclic flow

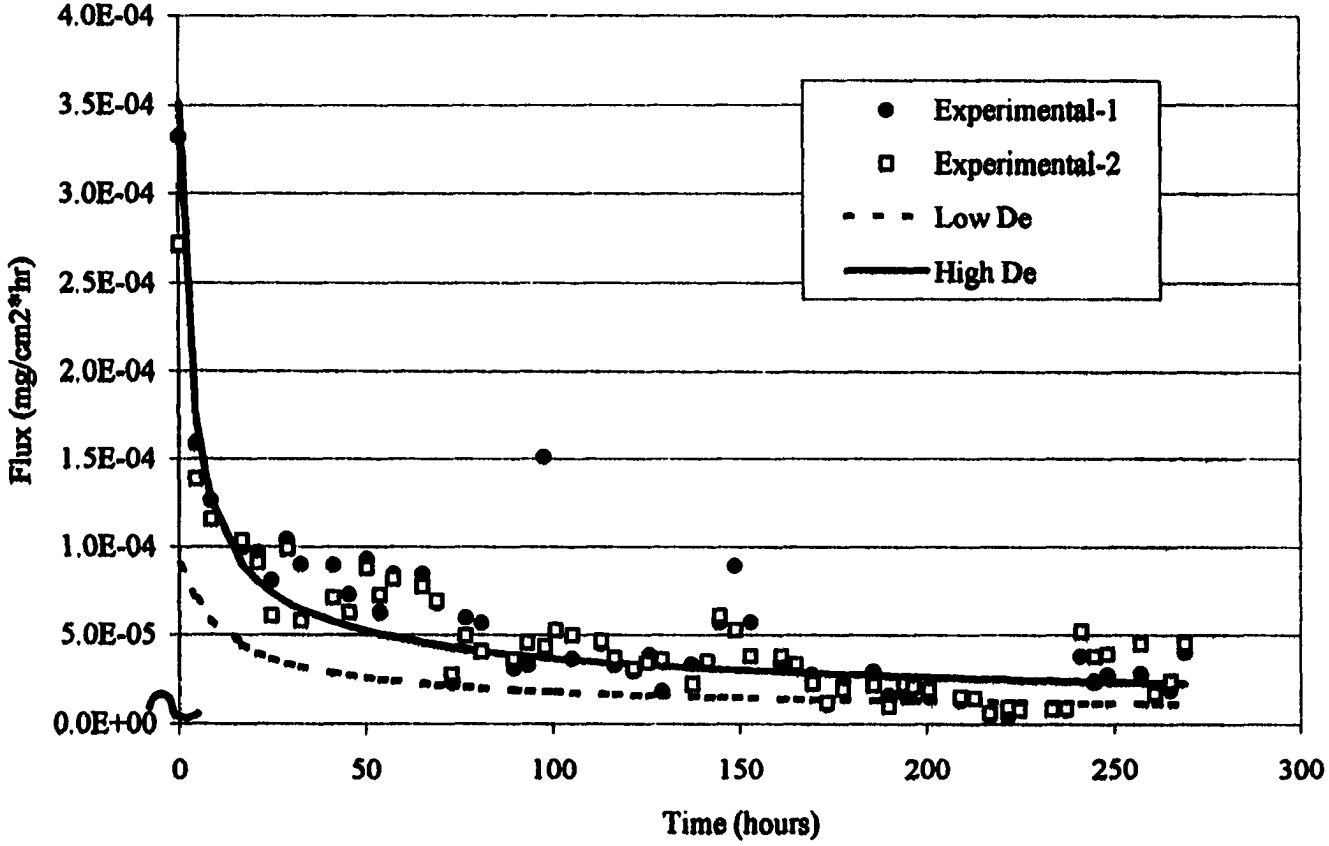

Figure 4.28. Effective diffusivity as system predictor for 1,3-DCB in mix cyclic flow

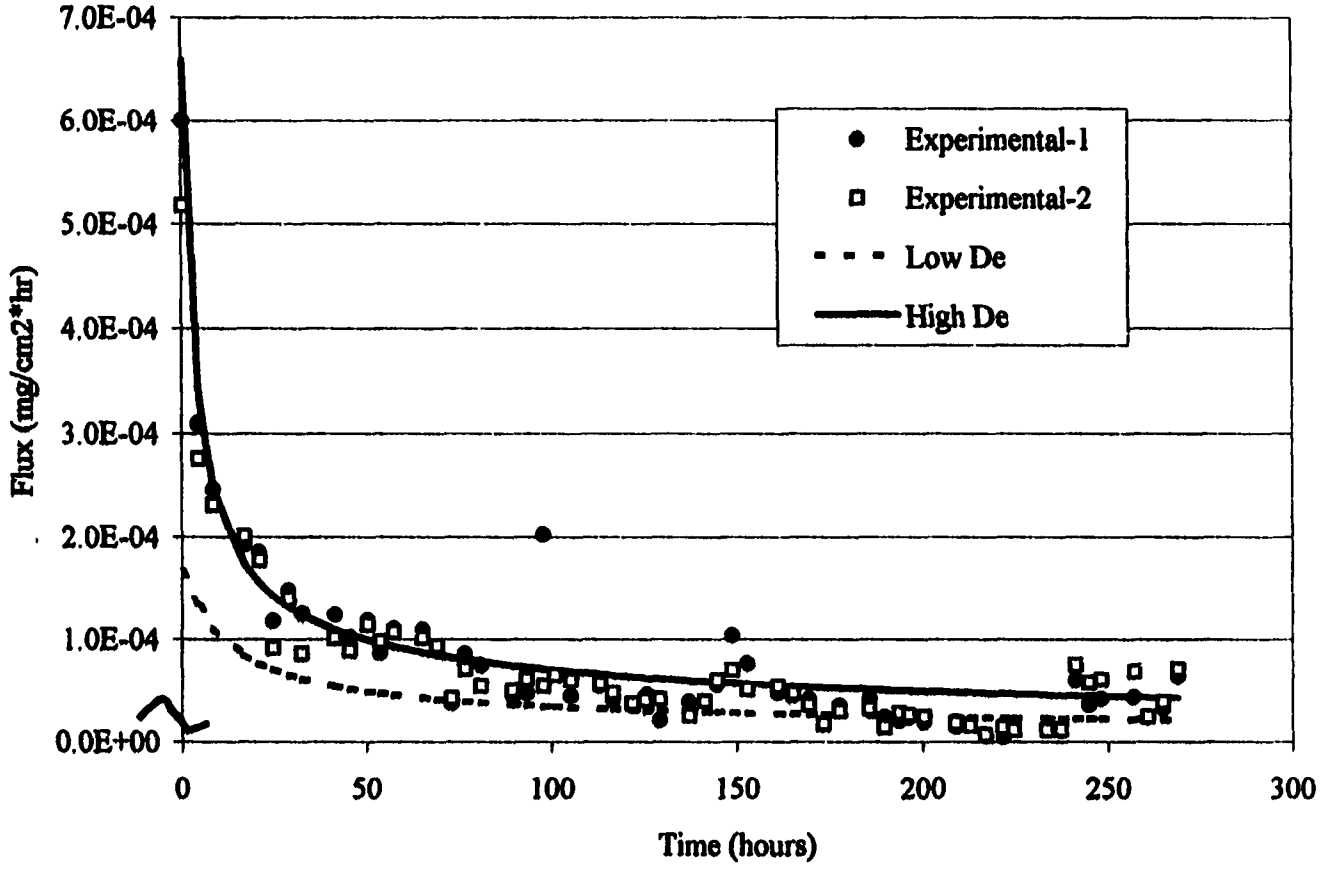

Figure 4.29. Effective diffusivity as system predictor for 1,2-DCB in mix cyclic flow

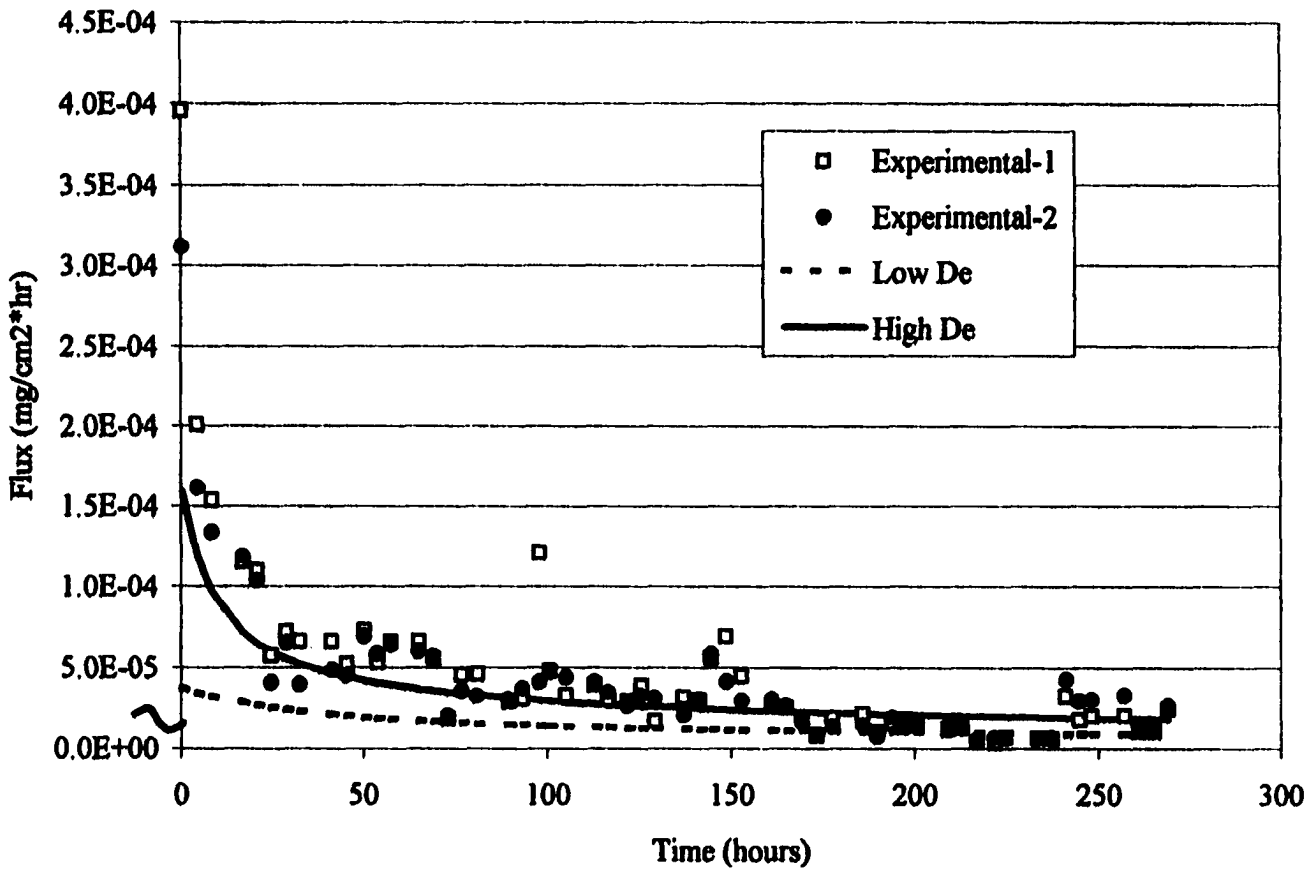

Figure 4.30. Effective diffusivity as system predictor for TCB in mix cyclic flow

Table 4.4. Model comparison with effective diffusivity, mu, as predictor

	mu = 17.967E-8 cm2/s			mu = 75.127E-8 cm2/s		
Slow flow	Tau	RMSE (mg/cm2*hr)	Correlation coefficient	Tau	RMSE (mg/cm2*hr)	Correlation coefficient
MCB-single	27.118	8.70E-06	0.993	6.485	9.12E-05	0.971
1,3DCB-single	24.850	4.10E-06	0.959	5.943	2.80E-05	0.922
MCB in mix	27.118	4.12E-05	0.937	6.485	1.98E-04	0.906
1,3DCB in mix	24.850	4.55E-05	0.919	5.943	6.14E-05	0.929
1,2DCB in mix	24.850	7.45E-05	0.932	5.943	6.08E-05	0.941
TCB in mix	22.583	3.37E-05	0.891	5.401	4.02E-05	0.907

	mu = 17.967E-8 cm2/s			mu = 75.127E-8 cm2/s		
Cyclic flow	Tau	RMSE (mg/cm2*hr)	Correlation coefficient	Tau	RMSE (mg/cm2*hr)	Correlation coefficient
MCB-single	27.118	3.23E-05	0.885	6.485	8.87E-05	0.934
1,3DCB-single	24.850	6.83E-06	0.871	5.943	3.67E-05	0.906
MCB in mix	27.118	2.59E-05	0.971	6.485	2.71E-05	0.944
1,3DCB in mix	24.850	4.47E-05	0.911	5.943	1.95E-05	0.922
1,2DCB in mix	24.850	7.05E-05	0.946	5.943	2.79E-05	0.964
TCB in mix	22.583	5.68E-05	0.844	5.401	3.25E-05	0.946

4.4 CONCLUSION

SFLB mathematical modeling studies indicate that flux of contaminants from sediment beds can be quantified and predicted by simple diffusion models. Notice the previously discussed exponential shape is clearly present in the fast flow experiments and the models fit the experimental data adequately as seen by visual observation. Under this flow rate, any of the models can be employed to predict the diffusive transport of chlorobenzenes from the surface sediments. There was no significant difference in the different models to adequately predict the diffusive flux of contaminants from surface sediments. The slow and cyclic flow could be reasonably predicted with the system descriptors of average tortuosity, tau, and an average effective diffusivity, mu. Due to the more fundamental nature of tortuosity, it is suggested that calibrated models could provide a simple system descriptor for predicting chemical flux rates.

Generally, all the models appear identical in the steady state region. Visually, the models appear to over estimate the flux of contaminants in the slow flow, which may be an artifact of the minimization procedure in Mathcad® and technical problems with the pump. These models iteratively calculate the average effective diffusivity by minimizing the error between the model flux from the experimental flux but the program does not allow one to adjust the weight given to transient or steady state situations.

The RMSE along with the correlation coefficient indicate the flux from sediments can be estimated by inputting literature values in models as opposed to determining them. The predictive tortuosities are higher than predicted by the porosity

to the 4/3 power and may be more representative of the multiple processes in the experimental soil system. The RMSE and correlation coefficient demonstrates there is no significant difference between the model cases and very little difference was seen between the use of experimentally determined parameters or literature based approximations (data not shown). Published diffusion models can be calibrated to adequately describe contaminant movement. An effort is being made to determine if multiple contaminants at a site may behave differently than the same components individually but the data here is inconclusive.

Although there was no significant difference between the boundary condition of mass transfer at the surface and the boundary condition of zero surface concentration, the physical process appears to modeled best by the mass transfer coefficient equal to the flow rate over the area. Most importantly, it was demonstrated that these models can be effective with minimal experimental determination of input parameters (bulk density, particle density and soil load).

Due to the high sorptive capacity of most sediments in comparison to the water solubility of chlorinated benzenes, the solubility limit and contaminant loading of sediment are important concepts for understanding transport of chemicals in the environment. The mass transport can be quantified by two possible parameters; 1) a water-side mass transfer coefficient and 2) a soil-side mass transfer coefficient. The model assumed there was no water - side resistance which is supported by the fit of the presented models. The total resistance is presumed on the sediment side.

In this research, local equilibrium was assumed and the diffusion models of Choy and Reible adequately described the behavior of chlorinated benzenes in

SFLB's. The results support the use of equilibrium partitioning models (Choy and Reible, 2000) for chlorinated benzenes at the PPI site.

4.5 REFERENCES

Choy, B. and D. D. Reible. 2000. Diffusion Models of Environmental Transport. Lewis Publishers, Boca Raton, Fl.

Mackay D., A. Di Guardo, S. Paterson, G. Kicsi, D.E. Dowan, and D.M. Kane. 1996. Assessment of Chemical Fate in the Environment Using Evaluative, Regional and Local-Scale Models: Illustrative Application to Chlorobenzene and Linear Alkylbenzene Sulfonates. Environmental Toxicology and Chemistry vol. 15 no. 9, 1638-1648.

Mathcad 2000 Professional. MathSoft, Inc. Cambridge, Massachesetts.

Thoma , G. J.. 1994. Studies on diffusive transport of hydrophobic organic chemicals in bed sediments: A Dissertation. Department of Chemical Engineering, Louisiana State University, Baton Rouge, Louisiana.

CHAPTER 5. CHLOROBENZENE ADSORPTION STUDIES

5.1 INTRODUCTION

Results from the sheet flow leaching bed experiments indicate variability due to the different sediments used. While similar sediment samples were given to LSU each time the request for more surface sediment was filled, differences were found in the sediments as noted earlier in Table 3.5 (previous chapter). Although this may explain the variation in behavior of the compounds due to the different nature of the sediments, it also gives a good overall view of the heterogeneity of the Petro-Processors site (PPI). The advantage of modeling is to make predictions for large areas based on limited information.

The muted spikes in cyclic flow flux rates relative to slow and fast flow flux observed in the multiple component systems lead to examining K_d as a reflection of this interaction. Adsorption isotherms were determined for two lower chlorinated benzenes, chlorobenzene (MCB) and 1,3-diclorobenzene (1,3 DCB), individually and for the four component mixture (chlorobenzene, 1,3-dichlorobenzene, 1,2-dichlorobenzene, and 1,2,4-trichlorobenzene) in order to evaluate the impact of single vs. multiple components on transport. There appeared to be two "types" of sediments from the site and therefore adsorption experiments were performed on both sediment "types" called "silty sand" and "clayey sand". The objective of these experiments was to determine K_d, the sediment/water partition coefficient, for individual vs. multiple component systems on the two site sediment types. The K_d was determined by the slope of the isotherm trend line with the intercept set to zero in Microsoft Excel®.

These values were used in the model derivations of effective diffusivity, D_e, because adsorption is assumed reversible under laboratory-contaminated conditions.

5.2 MATERIALS AND METHODS

5.2.1 Sediment Collection

All surface sediments were originally from the site but contaminated in the laboratory. Sediment was taken from the Petro Processors site near the Baton Rouge Bayou. It was received in sealed five gallon buckets. All sediment material for the chlorinated benzene studies were kept sealed until prepared. Multiple chlorinated benzene sediment samples came from PPI site and were collected by PPI personnel. All buckets were labeled with location and date, sealed on site, delivered to LSU by NPC Services, Inc. or LSU staff.

5.2.2 Sediment Preparation

Following appropriate safety measures, buckets were unsealed, large twigs and debris was removed by hand by pouring the sediment into a tray. Generally, each bucket was prepared sequentially. Initial preparation was the placement of sediment inside a hood to air dry in flat Nalgene trays (18" X 24" size). During the drying process, the large clumps were broken and debris was removed. In order to ensure relatively consistent particle size, the dry sediment was run through a grinder, and sieved through a US std. sieve size # 10 to remove hard clumps, rocks, and small pieces of debris.

5.2.3 Experimental Procedure

Approximately 5 grams of surface sediment was weighed into 30 ml centrifuge tubes. Each tube was filled with the appropriate chlorinated benzene solution to a

concave bubble prior to sealing with Teflon lined lids. The tubes were placed on a gyrotary shaker at 250 rpm for 4 days prior to centrifugation. The centrifugation was at 9,000 rpm for 25 minutes at room temperature. The supernatant was removed by pipet and analyzed by GC/MS to determine the amount remaining in the water phase. To determine the amount sorbed on to the solid phase, the remaining material in the centrifuge tube was extracted by sonication for 30 minutes with methanol as the solvent. The tubes were centrifuged again for 15 minutes at 9,000 rpm to separate the sediment – methanol mixture. The supernatant was removed and analyzed by GC/MS. All samples are maintained at 4°C in VOA vials until analyzed.

5.2.4 Contaminant Loaded Water

Dilution solutions of 0.5 ppm, 1 ppm, 5 ppm, 50 ppm and 100 ppm (mg/L) of the desired chlorinated benzene (MCB, 1,3-DCB, 1,2-DCB, TCB) were prepared from stock solutions of 1000 ppm chlorinated benzene in methanol. The original methanol stock was made by weighing of the chlorinated benzene using a gas tight GC syringe into a volumetric flask nearly filled with methanol. Solutions were immediately transferred to VOA vials and stored at 4°C until analyzed. The solutions were made and diluted at the start of each sorption experiment. Care was taken at all times to minimize volatilization of the chlorobenzenes.

5.3 DATA ANALYSIS

The effluent samples were analyzed with a Hewlett Packard 5890 gas chromatograph (GC) equipped with a Hewlett Packard 5971 mass spectrometer detector (MS). The GC/MS system was run by HPChemStation software and utilized a PTA-30 autosampler. Due to the nature of volatile organics, a Tekmar liquid solid

sample concentrator (LSC-2) purge and trap was utilized with a purge flow of 40 ml/min. The GC run time was 27 minutes with injector and detector temperatures of 180 ^{0}C. In accordance with EPA 8260A method parameters, the initial temperature is 45 ^{0}C for 2 minutes then ramp to 110 ^{0}C at a rate of 6 ^{0}C per minute followed by a ramp of 12 ^{0}C per minute to a final temperature of 210 ^{0}C, which is held for 5 minutes. The column was a Phenomenex ZB-624 30 m length by 0.25mm diameter. The flow rate to the MS was 1.0 ml/min with an initial 4 minutes solvent delay. Standards of known concentrations are prepared and run before samples for every GC/MS operation. The concentration values of the standards were determined by the expected value of the sample. All standard curves had a coefficient of variance above 0.96.

5.3.1 Data Management

Graphing and calculations of amount remaining on sediment were performed utilizing the Microsoft Excel® spreadsheet software in Microsoft Office® 2000. Spreadsheets were constructed to calculate the quantity of contaminant remaining in the water and the amount sorbed onto the sediment from the reported concentrations. Graphs and tables were constructed from these spreadsheets and will be shown in the results section below. The resulting graphs show the amount of chlorobenzene remaining in the water after coming to equilibrium on the X-axis. The Y-axis indicates the amount determined to be on the sediment after sonication extraction.

5.4 RESULTS FOR SINGLE CONTAMINANT STUDIES

Results will be shown for two different sediment types, clayey sand and silty sand, as characterized from the site samples. The K_d value is the slope of the linear

regression line. For single contaminant MCB, the sediment/water partition coefficient is 1.164 L/kg for clayey sand and 1.58 L/kg for the silty sand as seen from Figure 5.1. Although the behavior appears to be very similar in the two sediments, more water would be needed to remove MCB from the silty sand sediment type than the clayey sand sediment type. From Figures 5.2, the K_d values for 1,3-DCB are 1.85 L/kg and 2.81 L/kg for the clayey sand and silty sand respectively, indicating a similar trend of a higher K_d for silty sand for both contaminants.

5.5 RESULTS FOR MULTIPLE CONTAMINANT STUDIES

For simplicity the K_d values for all four components of the mixture on the clayey sand will be presented first in Figure 5.3. For MCB the slope was determined to be 0.745 L/kg, which is termed the K_d. The slope of 1,3-DCB can be seen to be 2.59 L/kg, 1,2-DCB had a slope of 3.27 L/kg while TCB had a K_d of 6.54 L/kg. This indicates that each component will partition relative to its own chemical properties (MW, K_{ow}, solubility, etc) as seen in the plots of flux rates in the previous chapter. The K_d values for the silty sand are taken from Figure 5.4 as follows: MCB is 1.16 L/kg, 1,3-DCB is 2.37 L/kg, 1,2-DCB had a slope of 1.46 L/kg, and the TCB had a value of 3.59 L/kg. Again, the behavior is similar with TCB having the highest K_d and MCB having the lowest. To facilitate discussion these values are presented in tabular form in Table 5.1.

5.6 DISCUSSION OF RESULTS

As seen in the table of K_d values, the single component K_d values for the silty sediment are similar to the K_d values for the clayey sand, with MCB less than 1,3-

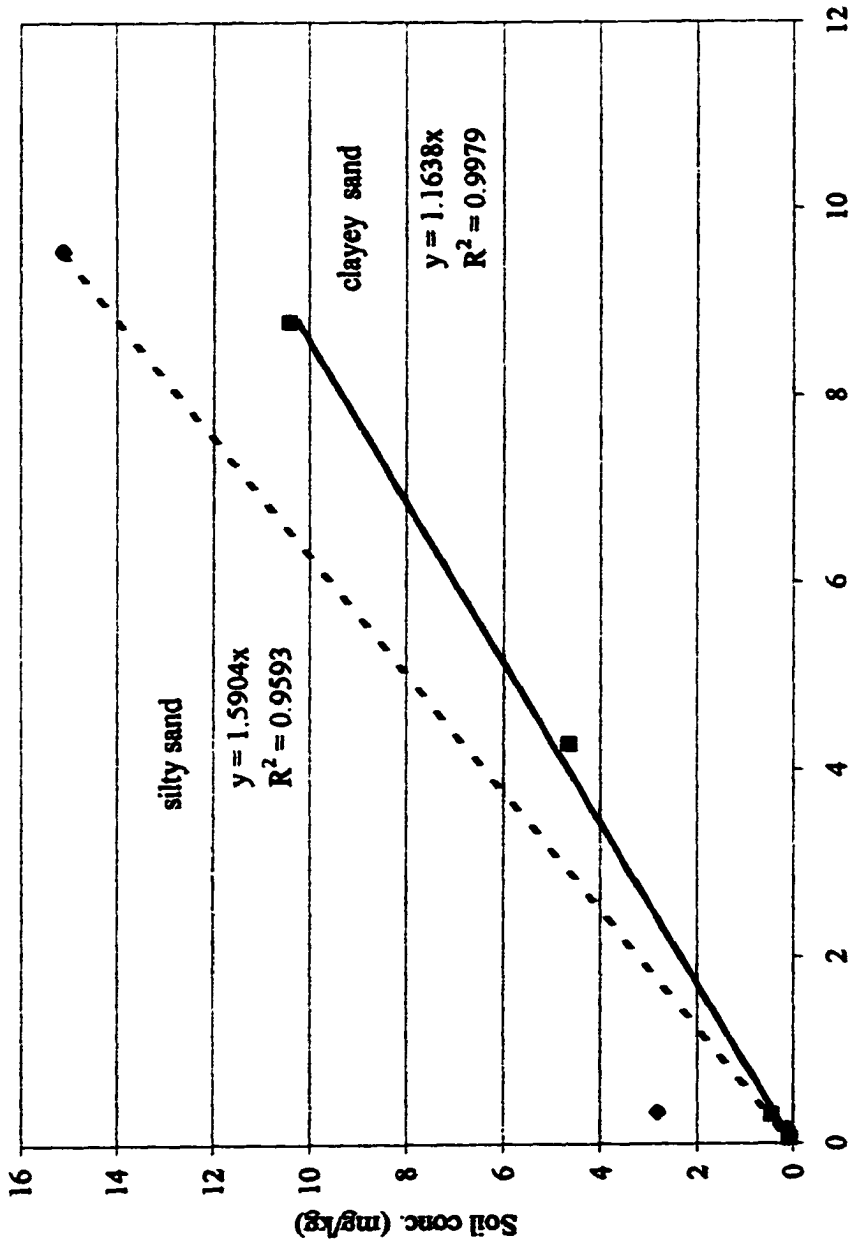

Figure 5.1. MCB single contaminant adsorption on two sediments

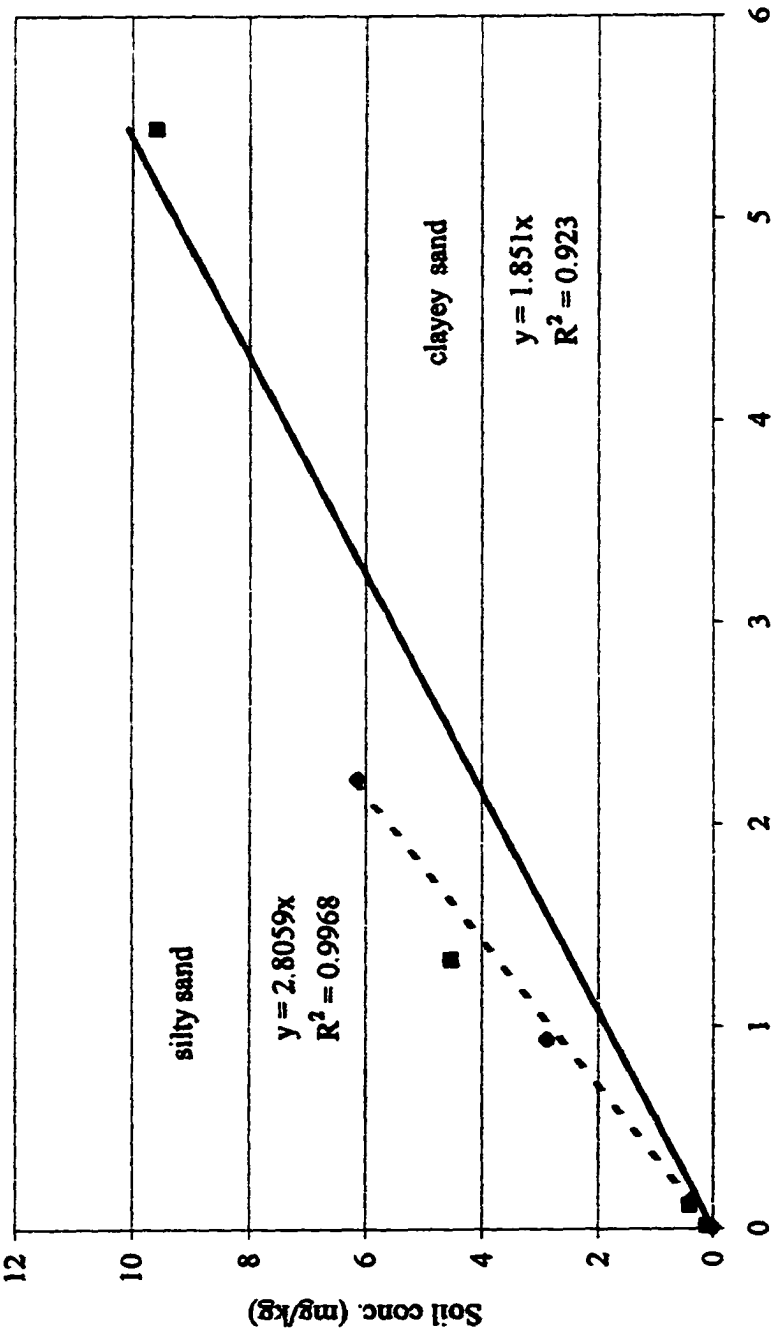

Figure 5.2. 1,3-DCB single contaminant adsorption on two sediments

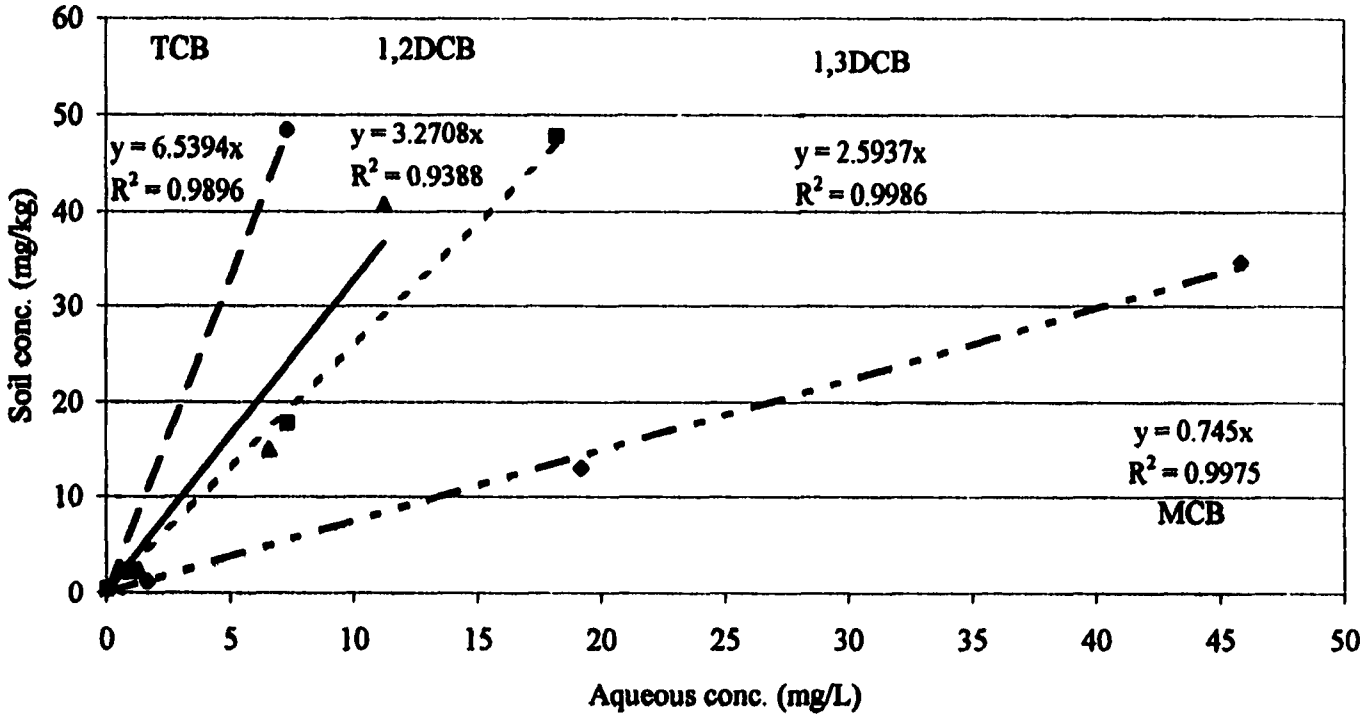

Figure 5.3. Contaminant mixture adsorption on clayey sand

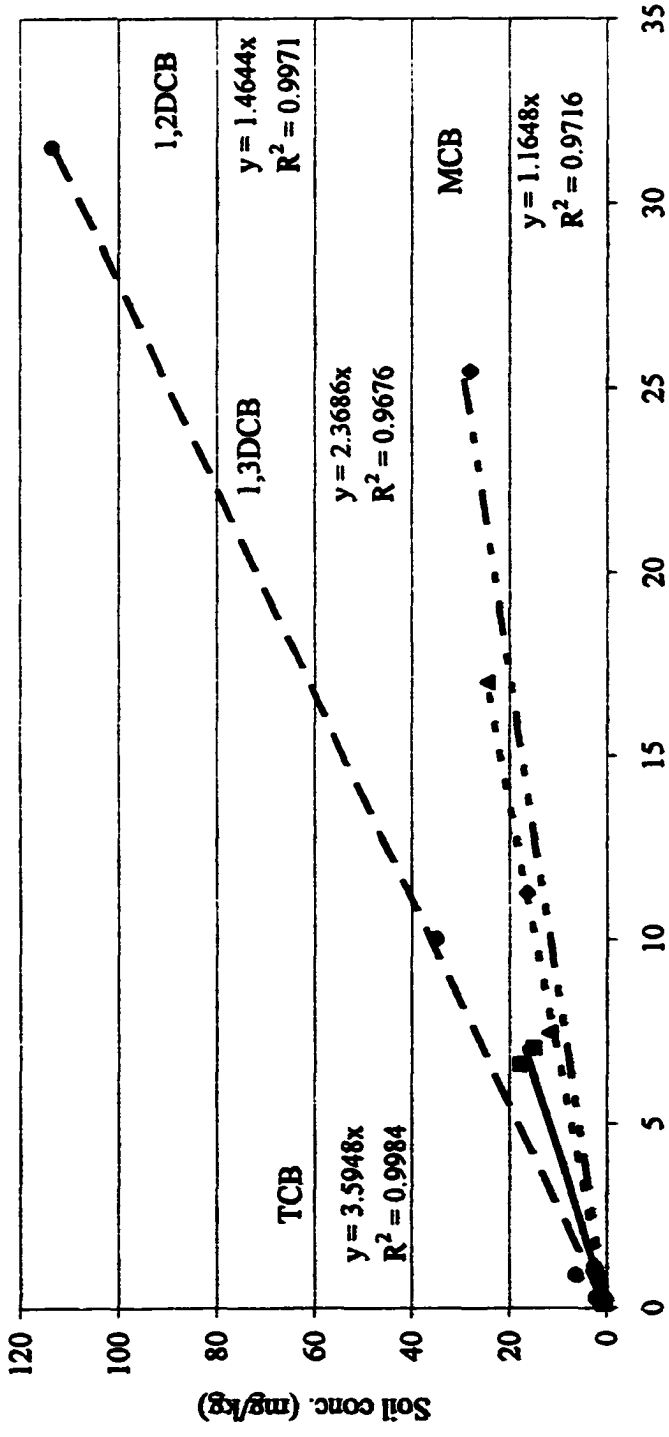

Figure 5.4. Contaminant mixture adsorption on silty sand

Table 5.1. Chlorinated benzene adsorption results

SINGLE COMPONENT			MULTIPLE COMPONENT		
Clayey	Kd value (L/kg)	R^2	Clayey	Kd value (L/kg)	R^2
MCB	1.16	0.87	MCB	0.74	1.00
DCB	1.85	0.92	1,3 DCB	2.59	1.00
			1,2 DCB	3.27	0.94
			TCB	6.54	0.99
Silty	Kd value (L/kg)	R^2	Silty	Kd value (L/kg)	R^2
MCB	1.58	1.00	MCB	1.16	0.97
DCB	2.81	1.00	1,3 DCB	2.37	1.00
			1,2 DCB	1.46	0.97
			TCB	3.59	1.00

DCB. The similarity is expected as these are from the same site but indicate the variation present in the research sediment samples. The comparison of the individual to the multiple components for MCB indicates a lower K_d for the multiple component system. In other words, the MCB was more mobile, as less water per mass was required to move the same amount of contaminant. The 1,3-DCB single component K_d value is lower than the multiple component K_d in the clayey sand sediment but not in the silty sediment. In the silty sediment, the soil water partition coefficient, K_d, value is lower for compounds in the mixture than for the single component. The other sediment does not appear to follow a clear trend, but the linear fit was not as good for the clay single component as with the other experiments as it was the first in the series of experiments. Unfortunately, experimental error could be a factor as it was extremely difficult to avoid air bubbles in the centrifuge tubes. The predicted behavior was the MCB K_d should be lower than the 1,3-DCB K_d because the lower K_{ow} as seen in the Tables 3.1 and 3.2 (previous chapter). This trend of MCB desorbing and being more mobile than 1,3-DCB is seen in both sediment types and under single and multiple compound mixtures.

In Table 5.1 the multiple component mixture has lower K_d values when compared to the single component K_d's, with the exception of 1,3-DCB. Table 5.1 may indicate multiple compounds present together change sorption behavior when compared to single compound sorption behavior. The trend of increasing sorption with increasingly chlorinated compounds is predominately supported. It appears that contaminants may sorb differently, if similar contaminants are present in the bulk water, as found in the mixture, thus changing the mobility of contaminants. This

change in mobility may explain why flux peaks were attenuated in earlier cyclic experiments. Laboratory and mathematical models provide both a quantitative and qualitative tool for understanding transport processes.

It should be noted the supernatant was not filtered for fear of volatilizing contaminants in the sample, therefore colloids and colloid-sorbed contaminants may have also been present affecting transport of contaminants. Colloids can be very important in transport (Valsaraj et al., 1996; Deane et al., 1999) and may explain some of the differences in sorptive behavior between sediments and their change in behavior as colloids are removed.

The importance of the partition coefficient cannot be underestimated in modeling as stated by Mackay et al., (1996). The soil water partition coefficient should be determined for the site and the compounds in question. Its steady state importance stems from the retardation factor in the diffusion models. In the short-term transient behavior, the K_d is used to calculate the initial concentration which is dominant in the first term of the diffusion model. Very little is known about the transport behavior of multiple compound mixtures and the results here are not clear.

5.7 RECOMMENDATIONS FROM ADSORPTION STUDIES

The importance of the partition coefficient, K_d, was stated previously, therefore efforts should focus on perfecting a system to alleviate problems related to volatilization of chlorinated benzenes. Centrifuge tubes frequently developed air bubbles if left on the shaker too long. The use of centrifuge tubes were unbreakable but required another transfer step which may contribute to volatile losses. Parafilm was used to aid in containment of volatiles but may also contribute to losses due to

sorption. The glass VOA vials if used as the experimental apparatus may break inside of the centrifuge at high rpms, although they exhibited less possibility of air bubbles.

The variation in sediment samples was visible and may have caused variation in the flux and adsorption results. Therefore, more emphasis on soil characteristics, i.e., the impact of organic matter and particle size could potentially explain the different partitioning seen in these sediments. Both the particle density and porosity, along with K_d determine the retardation factor, which was the term of interest for the models presented previously.

The paltry literature available discussing transport of multiple compounds when they are present with other similar compounds dictates more research in this area is necessary. This research proposes that multiple component systems behave differently from single component systems, but more replicates with statistical analyses is needed to verify this conclusion. However, it has been shown that multi-component K_d's are different in some cases than the K_d's in single components and thus to effectively model actual systems, multiple contaminants in a mixture must be taken into account. The lack of a clear trend in comparison of the single to multiple component K_d's, while differences remain, may be due to changes in soil loading and variations in soil properties.

5.8 REFERENCES

Deane, G., Z. Chroneer, and W. Lick. 1999. Diffusion and Sorption of Hexachlorobenzene in Sediments and Saturated Soils. Journal of Environmental Engineering, Vol. 125, No. 8., 689-696.

Mackay D., A. Di Guardo, S. Paterson, G. Kicsi, D.E. Dowan, and D.M. Kane. 1996. Assessment of Chemical Fate in the Environment Using Evaluative, Regional and Local-Scale Models: Illustrative Application to Chlorobenzene and Linear

Alkylbenzene Sulfonates. Environmental Toxicology and Chemistry vol. 15 no. 9, 1638-1648.

Valsaraj, K.T., S. Verma, I. Sojitra, D.D. Reible and L.J. Thibodeaux. 1996. Diffusive Transport of Organic Colloids from Sediment Beds. Journal of Environmental Engineering Vol. 122, No. 8, 722-729.

CHAPTER 6. CONCLUSIONS AND RECOMMENDATIONS

6.1 INTRODUCTION

Both physical and mathematical model studies are aimed toward understanding the fundamental principals of chemical transport and understanding which properties of the chemical and the site are critical descriptors. Mathematical and laboratory models quantifying these dynamic systems in surface soils and sediments are scarce in the literature. The advantage of mathematical modeling is that with limited data, predictions can be made regarding pollutant concentrations in the field. The presented laboratory and mathematical modeling effort is needed to quantify the pollutant concentrations leaching from soil and sediments to the overlying water for assessment of risk. The success of bioremediation and monitored natural attenuation is dependent on the aqueous phase contaminant concentration for uptake by biota. The aqueous phase concentration is dependent on the desorption of the chemical off the soil particle and its dissolution into the fluid phase. In order to more realistically explore how the dynamic situations affect transport of chemicals, actual flux rates were calculated from overlying water concentrations and used to calibrate and validate the models presented in Choy and Reible (2000) for two different chemicals: 2,4,6-trinitrotoluene and lower chlorinated benzenes.

6.2 CONCLUSIONS

6.2.1 Conclusions for Nitroaromatic Low Concentration Studies

A model for contaminant flux was desired for use in the riffle bed reactor system. The riffle bed reactor system would expose plants to TNT concentrations leached from contaminated soil or sediment. The purpose of the semi-infinite diffusion

model was to examine the quiescent diffusive flux and characterize it by the effective diffusivity. The error function solution to the advection dispersion equation appears to adequately model the flux under static conditions as expected. The flux decreased by the characteristic exponential curve during constant flow conditions. This preliminary work lead to exploring variation in flow conditions, which would be more realistic in practice, and was proposed to enhance flux. Analysis of experimental data indicated the flux decreased exponentially when the flow rate was held constant but spikes in the bulk concentration, and therefore the flux, accompanied spikes in flow rate.

6.2.2 Conclusions for Nitroaromatic High Concentration Studies

When the TNT soil load was high (above 5000 ppm), the asymptotic decrease in concentration was not seen. The aqueous concentration was close to the solubility limit therefore a constant flux would be expected. The pulsing of contaminant concentration may be used to induce higher rates of transformation as long as toxic responses by the biological system can be ameliorated, if not prevented. The simple diffusion model could not adequately describe the flux because the water side resistance was not included into that model. One of the challenges of finding appropriate physical models is to remain within the boundary conditions of the mathematical solutions. This laboratory and modeling effort was to approximate the concentration of TNT for plant uptake under the proposed riffle bed system.

6.2.3 Conclusions for Advective Enhanced Leaching TNT Studies

In preliminary riffle bed experiments using the SFLB under continuous constant flow, the model derived for those boundary conditions fit with an R^2 of 0.82. The model flux appears to deviate from the experimental flux in the transient

condition (short term) and fit better in the steady state condition. The average fitted effective diffusivity from the published diffusion model was lower than expected and may be due to the increased resistance in the bed. This increased soil resistance may be due to a desorption resistant fraction of contaminant proposed by others. The steady state flux would be the benchmark flux to match leaching concentrations into the plant reactors. The pulsing flow system was proposed to increase flux rates, thereby increasing the extraction efficiency and potentially maximizing biological transformation rates. Analysis of results indicated an increase in flux with flow perturbation and although local equilibrium was re-established quickly, the diffusion models were unable to fit the data if no flow rate was present (due to the collapse of the flux equation when the volumetric flow rate, Q, is equal to zero). This study quantified the flux of TNT and demonstrated that the flux may increase at least one order of magnitude under pulsing conditions.

6.2.4 Conclusions for Chlorinated Benzene Transport: Laboratory Model

In the chlorinated benzene studies, the goal was to quantify chemical flux for natural attenuation at the PPI site. The purpose of the laboratory model was to simulate flux of contaminants into Baton Rouge Bayou and Devil's Swamp to assess the buffering potential of plant uptake and phytoremediation. Sediment properties were both estimated from literature correlations and determined in the lab. Estimates of chemical properties based on literature were used to determine model input parameters.

The comparison of flux rates across all three flow regimes demonstrated the impact of different flow rates had on flux. The cyclic flow regime was hypothesized to

be a more efficient way to leach contaminants out of the sediment due to periodic deviations from equilibrium conditions. In the single contaminant studies, the cyclic flux appeared visually greater than flux at the slow or fast flow rate. In both MCB and DCB, the cyclic run demonstrated spikes of higher flux when the flow rate changed yielding a higher overall average flux rate than either the slow or fast flow. This observation supports the pulsed pumping to improve contaminant recovery (U.S.E.P.A., 1990).

For the single component chlorinated benzene experiments, a contaminant load of 10-15 mg/kg was desired but the initial sediment loading extraction results indicated some variation in contamination. The analysis of cores supported the removal of chlorinated benzenes from the sediment due to leaching. The mass balances for each contaminant in each study showed the variation between the replicate beds. The top layer appeared to have less MCB or DCB than the other layers indicating loss of contaminant from the top horizon in the single contaminant studies.

The visual inspection of flux rates from the multiple component mixture indicated fast flow regime was the most effective for leaching, i.e., had the highest flux rates. As shown in the previous experimental figures, low concentration contaminated soil diffuses chemicals to the overlying water with concentration decreasing with time. Switching from continuous to pulsed flow was shown to improve contaminate recovery because the non-pumping time allows local equilibrium to be reached (U.S.E.P.A., 1990). When the pump is off or the flow rate is decreased, the chemicals have more time to diffuse out of less permeable zones until equilibrium

is again established. This was seen experimentally as a spike in the flux, due to the wave of contaminated water flowing across the SFLB.

The significant observation from the multiple component studies was that the front section of the bed had the least remaining sediment load. Results of all four compounds indicated the major variation of residual sediment load in the horizontal plane, front to back. The front core had the lowest residual load and the back core had the most residual load, which differs from the single contaminant studies. This observation supports the view that the driving force of clean water acts strongly at the front of the bed and may diminish due to the competition of contaminants. The difference in core depletion between the single contaminant studies and multiple contaminant mixture may be due to differences in mixture chemical behavior.

6.2.5 Conclusions for Chlorinated Benzene Transport: Mathematical Model

The flux of chlorinated benzene from the sediment to the water was the parameter used for the models to calculate the fitted average effective diffusivity. The average fitted D_e was one way to quantify and compare the movement of pollutants under different conditions. Both cases of the advection enhanced model fit the experimental results, based on the correlation coefficient and the RMSE, indicating these models could be calibrated to describe transport in the SFLB. The models assumed there was no water side resistance, but negligible water side resistance was confirmed by the use of the soil side mass transfer coefficient from Thoma (1994). Based on the transfer coefficients presented here, the resistance is predominantly on the sediment side.

The use of tortuosity and effective diffusivity to be system descriptors was examined. The models were calibrated with the fast flow data and validated by the predicting the flux for slow and cyclic flow. Overall, both tortuosity and effective diffusivity were reasonable descriptors, but the tortuosity is a more fundamental parameter and is easier to implement. The root mean squared error (RMSE) values and indicated an adequate fit of models using the system descriptors of tortuosity and effective diffusivity (τ and μ) to predict the experimental flux. The correlation coefficient ranged from 0.80 to 0.996.

Understanding how variations in flow affect transport processes can be advantageous in a riffle bed system, or engineered plant contact reactors. More work is needed for modeling of highly unstable systems but the preliminary results indicate the local equilibrium is established with in a few hours. This fact supports the validity of the local equilibrium assumption in this mathematical modeling exercise. The changing flow regimes reflects the impact that rainfall events and seasonal flooding can have on contaminant transport processes.

Deane et al.(1999) reasons that if sorption times are comparable to transport times, then the assumption of local chemical equilibrium is not valid. Models assuming rapid chemical sorption equilibrium did not fit as well as models assuming intra particle diffusion and non-equilibrium sorption processes. Mcgroddy and Farrington (1995) found that equilibrium-partitioning models were good descriptors of PCB congener partitioning in both in situ and desorption studies, but PAH compounds were not well described by equilibrium partitioning models. The authors suggest the hysteresis is not due to physical or chemical alterations but instead to factors unique to

PAH compounds. This research supports the use of equilibrium partitioning models (Choy and Reible, 2000) for TNT under quiescent conditions. The models from Choy and Reible (2000) adequately described the behavior of lower chlorinated benzenes in SFLB's representing 150' of Baton Rouge Bayou.

6.3 RECOMMENDATIONS

The soil and sediment characterization results show the variation in the sediment samples, which is an indicator of the homogeneity of the site itself. Because of variation in the soil and sediment concentrations and characteristics, more replicates are suggested in the experimental design so statistical analyses can determine how much variation is in the flux measurements. Soil properties need to be determined for each set of experiments using that particular soil or sediment. The chlorinated benzene modeling study used average soil values and may have introduced some error into the fit of the models although the majority fit adequately based on sum squared error (SSE). The TNT models used parameters determined by other researchers (particularly K_d) and this may have introduced error, as the soil properties are known to change with depth as well as location. The f_{oc} model input was the average for all soils but each batch should be characterized to more precisely determine the impact of organic material, as mentioned previously regarding soil characteristics. The f_{oc} is an important descriptor of the sorbent and has significant impact on K_d. K_d is an important parameter because the model is sensitive the retardation factor, whose dominant term is K_d. Since initial concentration in pore water is calculated by W/K_d, and it is the pore water concentration that is the driving force for transport thereby

demonstrating the importance of K_d again. Initial pore water concentration is not in the exponent term so C_o has a high impact on model.

Although, the contaminated chlorinated benzene sediments were developed in the laboratory to range between 10-15 mg/kg, the analysis of initial sediment loading results indicated the contamination procedure was highly variable. This variation may also be due to the several different sediments obtained from the site. The higher starting value for concentration and flux in some sediments, which may lead to higher steady state values for both concentration and flux curves, which consequently affects model output.

The experimental apparatus should be scaled up so the depth profiles would not be influenced by artifacts introduced from the sides and bottom. The lost of contaminants from the bottom layer of the SFLB is believed to represent this artifact. The TNT static beaker experiments had a clearer trend of depletions from the top layers due to the longer diffusion path provided. Mass balances need to be utilized, although the variation of contaminant levels in site soil was problematic as seen in the advective enhanced TNT study.

Volatilization of the contaminants was a significant concern; but modifications to the apparatus may have attenuated this problem fairly well in single 1,3-DCB and the mixture studies. The percent closure for the MCB single contaminant studies may be poor due to this being the first of the VOA studies and the seal on the lids may not have been adequate at that time, or other initial technical problems.

6.4 REFERENCES

Choy, B. and D. D. Reible. 2000. Diffusion Models of Environmental Transport. Lewis Publishers, Boca Raton, Fl.

Deane, G., Z. Chroneer, and W. Lick. 1999. Diffusion and sorption of Hexachlorobenzene in sediments and saturated soils. Journal of Environmental Engineering, Vol. 125, No. 8., 689-696.

Thoma , G. J.. 1994. Studies on diffusive transport of hydrophobic organic chemicals in bed sediments: A Dissertation. Department of Chemical Engineering, Louisiana State University, Baton Rouge, Louisiana.

McGroddy S.E., and J.W. Farrington. 1995. Sediment porewater partitioning of polycyclic aromatic hydrocarbons in three cores from Boston Harbor, Massachusetts. Environmental Science & Technology Vol. 29, No. 6, 1542-1550.

U.S.E.P.A. 1990. Basics of Pump-andTreat Ground-Water Remediation Technology, EPA-600/8-90/003. Mercer, J.W., D.C. Skipp and D.Giffin. Robert S. Kerr. Environmental Research Laboratory, Ada, OK.

VITA

Marti Charleen Blad was born in South Bend, Indiana, on September 29, 1964. She received her high school diploma in May of 1981 from Washington High School in South Bend, Indiana. After some personal exploration, Marti graduated *Magna Cum Laude* and earned The George and Juanda Bick Award in Environmental Science in May 1990 from St. Mary's College in Notre Dame, Indiana, with a bachelor of science in biology. After working at the University of Notre Dame for two years, Marti started her master of science degree requirements in environmental toxicology at Louisiana State University in August of 1992. Upon completion in December 1994, She has been working toward her doctoral degree in Civil and Environmental Engineering. The degree of Doctor of Philosophy will be conferred in August 2001.

DOCTORAL EXAMINATION AND DISSERTATION REPORT

Candidate: Marti Charleen Blad

Major Field: Civil Engineering

Title of Dissertation: Mass Transfer of 2,4,6-Trinitrotoluene and Lower Chlorinated Benzenes from Sediment into Water

Approved:

Major Professor and Chairman

Dean of the Graduate School

EXAMINING COMMITTEE:

Date of Examination:

2/21/2001